Determination of epithelial growth factor receptor mutations in circulatory tumour cells from non-small cell lung cancer patients isolated using a novel microfluidic device.

PhD by Thesis

NKEIRUKA O OGIDI

University of Hull

CENTRE OF BIOMEDICAL SCIENCES
Hull York Medical School

July, 2022

Abstract

Patients with epidermal growth factor receptor (EGFR) sensitizing mutations in non small cell lung cancer (NSCLC) receive benefit from Tyrosine Kinase inhibitors. Accurate selection of patients before treatment is highly dependent on precise molecular diagnosis of EGFR mutations. Presently in the clinic, the diagnostic samples routinely used tumour biopsy and/or cell free DNA (cfDNA), are not sufficiently effective for precise diagnosis. Circulatory tumour cells (CTC) in blood have been explored successfully as alternative and complementary diagnostic markers to the current clinical tools. However, utility in the clinics has been hampered by the relatively low concentration of CTC in blood, and the lack of robust technologies that are adaptable for routine use. The present study describes the design and optimization of an immunomagnetic based microfluidic device (Lung card version II) that isolates CTC expressing the epithelial cell adhesion molecule (EpCAM) from blood with high capture efficiency and purity. The device is a 2-part system comprising a disposable chip that is simple in design and a reusable microfluidic unit that contains a mobile magnetic arm. The simple design and work-flow process of the device ensures cost efficiency for scalability and, ultimately, use in the clinic. The device was initially validated for its capability to isolate EpCAM positive cells. Results from spiking carboxylfluorescein succinimidyl ester stained EpCAM positive cells in media/blood showed a capture efficiency of ≥ 65% and a purity ≥ 97% from a 13ml sample in 50 minutes. The isolated CTC from NSCLC patients (n=38) were analysed for mRNA markers specific to malignant cells and were characterized for EGFR mutations following PCR and next generation sequencing. The mutational status of CTC was compared to that obtained from matched, tumour biopsy, samples. Significantly more mutations (*P=0.0173*) were detected in CTC enriched samples than the matched biopsy. Interestingly, mutations were detected in only 4 biopsy samples and the mutations detected in the biopsy were only concordant with results from CTC enriched samples for 1 patient. Exon 19 deletion was the most frequent mutation detected (86.7%) with rare mutations such as: L792P, C797S, H509R also been detected in CTC, and the present study reports the detection of K708R mutation in NSCLC for the first time. The clinical outcomes of patients who were positive for EGFR mutation from CTC, but had been placed on therapies based on mutation results from tissue biopsy were evaluated in this study. The results showed that no significant progression free survival (PFS) benefit was attained when comparing treatment response between patients whose CTC possessed an EGFR mutation and patients whose CTC possessed no EGFR mutation *(10 months vs26 months p value-0.3420 HR- 0.76 95% CI- 0.2498-2.319)*. In summary the results from this study showed that the microfluidic device captured CTC with efficiency equal to other immuno-affinity based devices but had better purity rates and throughput and also that the device can be utilized for CTC processing for downstream analysis. Results from this current study further demonstrated the clinical potential of CTC+NGS matrix for the detection of EGFR mutations and the prospective impact it would have for precision oncology in NSCLC are discussed.

List of contents

Table of Figures

List of Tables

Abbreviations

ALK	Anaplastic lymphoma kinase
AKT 5	Protein kinase B
AKT	Murine thymoma viral oncogene homolog 1
ATP	Adenosine triphosphate
BSA	Bovine serum albumin
BRAF	RAF murine sarcoma viral oncogene homolog
CME	Clathrin mediated endocytosis
CfDNA	Cell free DNA
CTC	Circulatory tumour cells
CtDNA	Circulatory tumour DNA
CCGA	Cell cycle growth aberration
DAPI	4’6-Diamidino-2-phenylindole
DEPTOR DEP	Domain containing mTOR interacting protein
DDR_2	Discodion domain receptor tyrosine kinase
DMSO	Dimethyl sulfoxide
DNA	Deoxyribonucleic acid
EGF	Epidermal growth factor
EGFR	Epidermal growth factor receptor
EMT	Epithelial-mesenchymal transition
EPCAM	Epithelial cell adhesion molecule
$ERBBB_{1/}$ $ERBBB_2$	Human epidermal growth factor receptor 1,2,3,4
EURATAC	The European Tarceva versus chemotherapy
ERK	Extracellular signal-regulated kinase
FACS	Fluorescence activated cell sorting
FBS	Foetal bovine serum
FGFR	Fibroblastic growth factor receptor
FISH	Fluorescence *insitu* hybridization
G	Gram
GAP	GTPase activating protein
GDP	Guanosine diphosphate
GEF	Guanosine exchange factor
GRB2	Growth factor receptor-bound protein 2
GTP	Guanosine triphosphate
h/hrs	Hour/hours
HR	Hazard ratio
KRAS	Kirsten Sarcoma viral oncogene
Litre	Litre
JAK	Janus kinase
IPASS	Iressa Pan-Asia study
LUAD	Lung Adenocarcinoma
LUS	Lung squamous cell carcinoma
MAPK	Mitogen-activated protein kinase

MET	Met proto-oncogene tyrosine kinase
mRNA	Messenger RNA
miRNA	Micro RNA
mTOR	Mammalian target of rapamycin
MUT	Mutation
NCME	Non-clathrin mediated endocytosis
NEJ002	North-east Japan 002 study
NGS	Next generation sequencing
ND	Not done
NR	Not reported
NSCLC	Non-small cell lung cancee
OR	Overall response
ORR	Objective response rates
OS	Overall survival
PBS	Phosphate buffered saline
PCR	Polymerase chain reaction
PD	Progressive disease
PFS	Progression free survival
PI3K	Phosphoinositide-3-kinase
PTEN	Phosphatase and tensin homolog
PR	Partial respons
RAS	Rat sarcoma
RET 5	“rearranged during transfection” protooncogene
RECIST	Response evaluation criteria in solid tumors
RNA	Ribonucleic acid
RNAi	RNA interference
Rpm	Revolutions per minute
RPMI	Roswell park memorial institute medium
RR	Response rate
RTK	Receptor tyrosine kinase
SD	Standard deviation
SCLC	Small cell lung cancer
STAT 5	Signal transducer and activator of transcription
TKI	Tyrosine kinase inhibitor
WSTOG	West Japan Thoracic Oncology Group.

Covid 19 Impact statement

The Covid 19 pandemic impacted my studies in the following ways. At the beginning of the pandemic/lockdown. I was back home in Nigeria on secondment under the sponsorship of an EU/Marie Curie grant work and due to the national lockdown, I was unable to return to UK to continue my research. I had to apply for suspension of my studies from May to August 2020. And with the start up time, I effectively lost a total of 6 months of laboratory work, which decreased the number of patients recruited for my research. Even when lockdown was relaxed the hospitals in Hull took many months to return to normal operation. The pandemic also affected my attendance at all the conferences I hoped to attend as they were cancelled. I regret not having the opportunity to present my work and receive critical feedback.

ACKNOWLEDGEMENTS

I would like to acknowledge the following people, who made this research possible. First and foremost, my supervisors Professor John Greenman and Professor Michael Lind for their motivation, encouragement and support. I would also like to thank Dr Hannah Moody, for teaching me most of the experiments required for this project. I am thankful to Dr Leigh Madden for help with flow cytometry experiments. I am also grateful to Dr Alex Iles for help with chip design and manufacture and the team at StabVida (Portugal) for their help in optimizing the Magnetic Actuator programme and analysis of Next generation sequencing. My gratitude extends to EU/Marie Curie foundation and Yorkshire Cancer Research charity for funding some of the work in this thesis. I am also thankful to the clinical staff in the Oncology unit Castle Hill Hospital for help with sample collection over the years and of course the patients who permitted me to use their tissue. I would like to thank my friends; Peju Bolanle, Dr Abimbade, Dr Remi for their motivation and encouragement. Finally, I would like to express my gratitude to my parents, my children and siblings for their patience, encouragement and tremendous understanding over the years.

Authors Declaration

I confirm that this work is original and that if any passage(s) or diagram(s) have been copied from academic papers, books, the internet or any other sources these are clearly identified by the use of quotation marks and the reference(s) is fully cited. I certify that, other than where indicated, this is my own work and does not breach the regulations of HYMS, the University of Hull or the University of York regarding plagiarism or academic conduct in examinations. I have read the HYMS Code of Practice on Academic Misconduct, and state that this piece of work is my own and does not contain any unacknowledged work from any other sources.

I confirm that any patient information obtained to produce this piece of work has been appropriately anonymised.

Chapter 1

Introduction

1.0 Introduction

1.1 Epidemiology of lung cancer

Lung malignancies are the leading cause of death attributed to cancer. They accounted, for about 18% of the 9.8million cancer related deaths in 2020 (Sung et al 2021). Mortality statistics, from global surveillance of cancer 5 years following diagnosis show that, only about 30% of patients with lung cancer are alive 5 years after diagnosis. This report attributed the low survival rates in lung cancer mainly to the fact that diagnosis is at a relatively late stage, there is rapid spread of this form of malignancy to adjacent organs and acquired resistance to available therapeutics (Allemani et al 2015; Siegel et al 2021). Based on its histopathological features, lung cancer is divided broadly into two types (1) Non-small cell lung cancer (NSCLC), which accounts for about 85% of cases and (2) Small cell lung cancer (SCLC), accounting for the remaining 15% (Alberg et al 2007: Durendez-Saez et al 2017). Work in this thesis focuses on NSCLC.

1.2 Non-small cell lung cancer subtypes

Based on its histopathological features, NSCLC is classified broadly into 3 types. The classification of NSCLC is linked to the anatomical location from which the cancer cells originate (**Figure 1.1**) and the type of cells that make up the histology. The three main histopathological identified subtypes of NSCLC are: (1) Lung adenocarcinoma (LUAD) these accounts for about 50% of all NSCLC cases. LUAD emanates from the periphery of the lungs usually from small bronchi, bronchioles and alveolar epithelial cells (**Figure 1.1**). The types of cells that make up its histology are cuboidal, type II pneumocytes, columnar, mucinous and non-mucinous Clara cells. Cells of LUAD histology can have any of the following growth patterns: acinar, micropapillary, papillary or solid (**Figure 1.2**) (Ho et al 2015); (2) Lung squamous cell carcinoma (LUSC) which accounts for about 45% of all NSCLC emanates from major bronchi and thus are centrally located (**Figure 1.1**). The type of cells that make up the histology of LUSC are typically squamous cells that may be keratinized and, on a few occasions, will contain intracellular bridges (**Figure 1.3**) (Ho et al 2015); and (3) Large cell lung carcinoma accounts for only 3% of all NSCLC cases and arises in the periphery of the lungs (**Figure 1.1**), which is characterized by large necrotic cells that are nest-like in appearance. The types of cells that make up this sutype of histology are polygonal in shape comprising of pleomorphic and vesicular nuclei. Rare NSCLC subtypes include

adenosquamous, pleomorphic spindle cell and giant cell carcinoma, these subtypes together account for less than 2% of NSCLC (Travis et al 2015; Zheng, 2016).

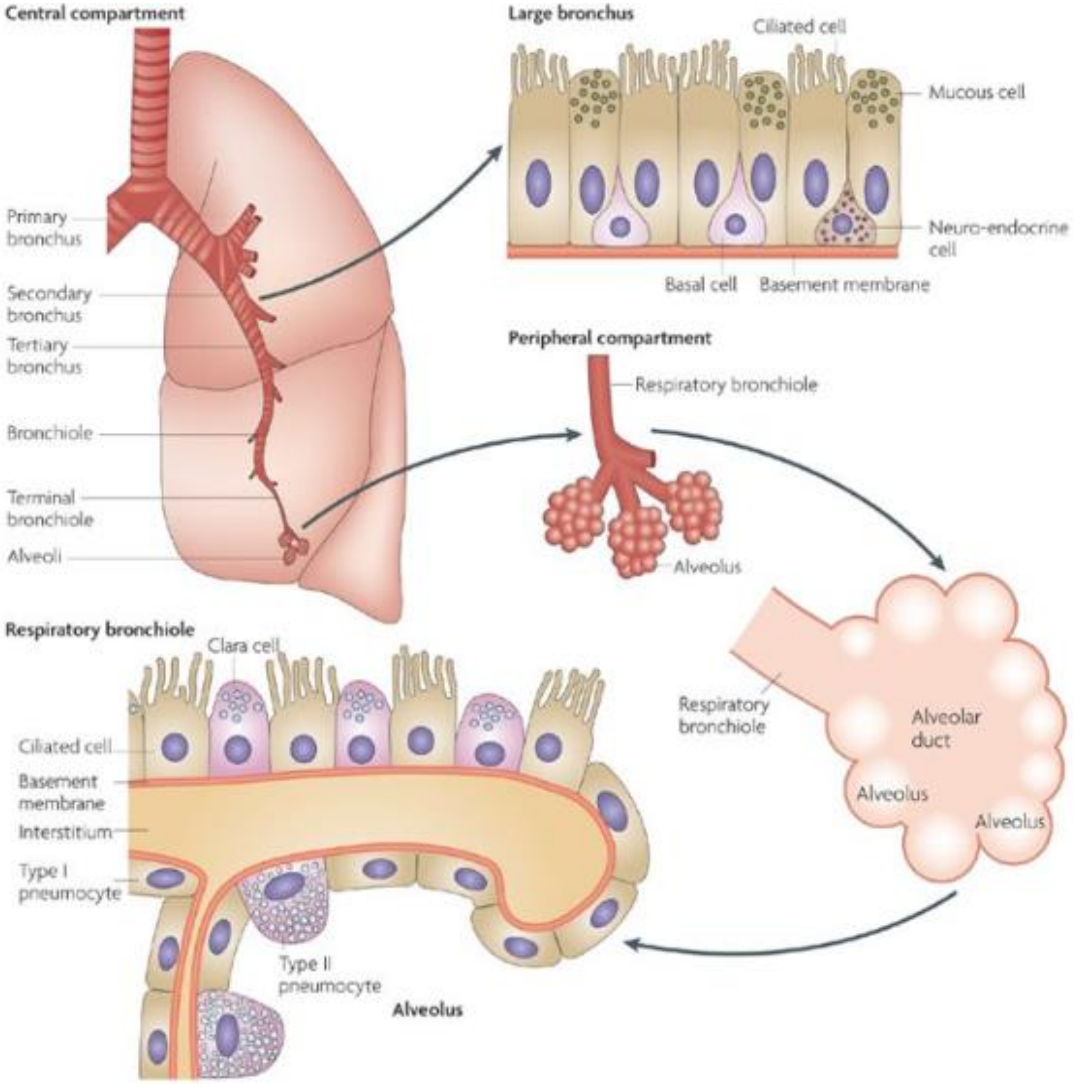

Figure 1.1: Anatomy, Physiology and Histology of the lungs. Sun et al (2007)

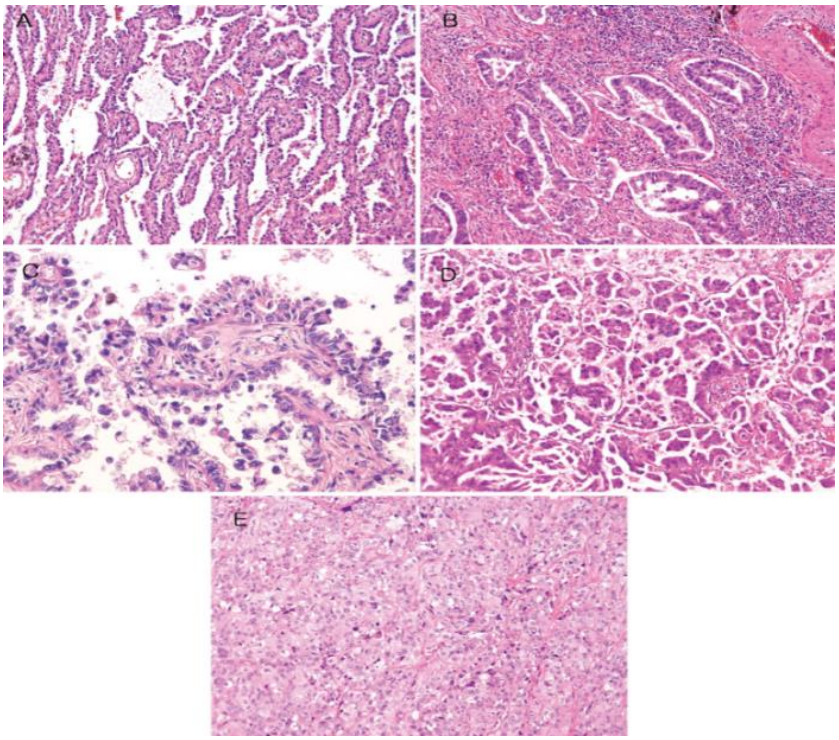

Figure 1.2: Histopathological characteristics of lung adenocarcinoma (Haematoxylin and Eosin stain ×100 magnification**)** (A) Lepidic subtype (B) Acinar subtype (C) Papillary subtype (D) Micropapillary ((E) Solid subtype. Travis et al (2015).

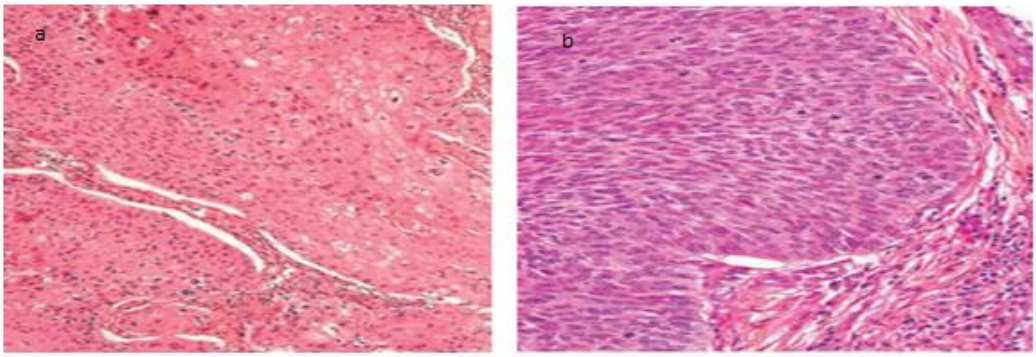

Figure 1.3: Squamous cell carcinoma, **(a)** well differentiated with keratinization and keratin pearls (Haematoxylin and Eosin stain × 100 magnification). **(b)**-Basaloid, this tumor consists of lobules of small uniform cells with peripheral palisading and a high rate of mitosis. Travis et al (2015).

The histopathology of the two main subtypes of NSCLC (LUAD& LUSC) is influenced by many different factors. Several reports, on the epidemiology of lung cancer by histologic type have associated the LUSC subtype with tobacco smoking and the LUAD subtype with non- smoking factors such as; hormones, viral infections and genetics (Sun et al 2007; Travis et al 2015; Kadara & Scheet 2016; Barta et al 2019). Cancer causing agents in tobacco (**Table 1.1)** target both the central and peripheral airway pathways to induce (i) rapid uncontrollable growth of cells (ii) aberrant cell progression

(iii) down regulation of apoptotic process via: the promotion of double stranded DNA breaks, oxidative changes in DNA and mutations of key cellular processes (iv) whole chromosome loss and gains and (v) geno toxicity. All of these can combine to change the normal histology of the lungs (Kadara & Scheet 2016; Barta et al 2019).

Table 1.1: Carcinogens in cigarettes

Carcinogen types	Compounds examples
Polycyclic aromatic hydrocarbons	Benzo(pyrene), Benzo Flurothane, Di benzanthancene, 5 Methylchrysenes,
Azaarenes	Di benz acidene
N-Nitrosamines	N-Nitro Diethylene, 4- Methyl nitrosamine-1,
Miscellaneous Organic compound	1, 3 butadiene
Inorganic compounds	Nickel, Chronium, Cadmium, Arsenic, Hydrazine

Field& Winters (2012)

1.3 Non-smoking Factors

Non-smoking factors (**Table 1.2)** such as: ionizing radiation, exposure to carcinogenic chemicals/ elements, and some occupational and manufacturing processes have been suggested to be key contributors to the histology of the LUAD subtype (Travis et al 2015; Dublin & Griffin, 2020). Mechanisms- by which these non-smoking factors fuel the histopathology of LUAD are the same as described for smoking factors above. Other non- smoking factors suggested to fuel the histopathology of LUAD are hormones, viral infections, chronic obstructive pulmonary disease (COPD) and an individual's inherited genome.

Table 1.2: Non-smoking causes of NSCLC

Activity	Forms
Ionizing Radiation	Alpha emitters (Radon 222 & Plutonium 239, gamma rays & X-rays)
Carcinogenic chemicals	Arsenic, Berylium, Cadmium, Nickel, Chronium, Bichloro methyl ether, Sulphur, Coal tar, Soot, Diesel, Engine exhaust
Occupation/Manufacturing process	Coal gas, Coke production, Iron &Steel founding, Aluminium production, Paint & rubber manufacturing, Asbestos and Fibres
Hormones	Oestrogen
Virus	Human Papilloma virus (HPV) Merkel cell polymovirus (McPyV), Episten Barr Virus (EBV) Jaagsiekte Sheep Retrovirus (JSRV), John Cunningham Virus (JCV)
Genetics	T790M, P848L and V843I mutations in Epithelial Growth Factor Receptor (EGFR)

Barta et al (2019)

1.3.1 Hormones

Hormones, such as oestrogen have been implicated in the pathology of LUAD. Oestrogen receptors (ERα and ERβ)), are expressed on healthy lung tissue as well as cancer ridden lung tissue. Kawai et al (2005), evaluated oestrogen receptor expression in 132 resected NSCLC tumours. This group reported the appearance of α oestrogen in the cytoplasm of 73% of the tissue analysed using immunological staining techniques and reported β oestrogen receptor expression in the nucleus of 53% of the patients. They reported that patients with oestrogen receptors expression were associated with poorer survival ($P<0.001$). Wu et al (2005), in an evaluation of oestrogen receptors of surgically resected tumours from 301 patients with NSCLC, reported that ERβ is the predominant oestrogen receptor expressed among non- smokers particularly females. Purported mechanisms, by which oestrogen may foster NSCLC are (1) stimulation of proliferation of lung cells of the lungs via oestrogen receptor mediated cell signalling, which may involve its interaction with the epithelial growth factor receptor (EGFR) pathways (2) oestrogen's ability to change the biochemical breakdown of carcinogens e.g. polycyclic aromatic hydrocarbons (PAH), thus fostering carcinogenesis (3) oestrogens acting as direct carcinogens after biochemical breakdown to catechol oestrogens creating mutagenic adducts and (4) the oestrogen gradient generated by malignant cells and tumour associated macrophages in the tumour micro environment which can cause the f ibroblast to express a number of other tumour promoting growth factors e.g. epithelial growth factor (EGF), α and β transforming growth factor (TGFα and TGFβ) (Hsu et al 2017; Smida et al 2020; Mukherjee et al 2021).

1.3.2 Chronic obstructive pulmonary disease

Previous history of COPD has been linked to lung cancer. Brenner et al (2012) in a definitive study evaluated the risk of developing lung cancer after having COPD using data obtained from seventeen studies from the international lung cancer consortium between the years 1984-2011 involving 24,607 patients and 81,829 controls from Europe and North America. This group using a Cox proportional hazard model adjusted for sex, age and cumulative tobacco smoking reported that patients with a history of emphysema, bronchitis, tuberculosis and pneumonia had a 2.44-fold (95% CI) elevated risk of having a lung cancer. The mechanisms outlined below have been proposed as facilitators of lung cancer pathology in patients with COPD (1) modulation of the tumour micro environment towards pro-malignancy and (2) stimulation of lung repair

processes which may stimulate epithelial to mesenchymal transition a hall mark of carcinogenesis (Barta et al 2019).

1.3.3 Viruses

Viruses that have been identified to date that have a role in the pathogenesis of NSCLC: are Human papilloma virus (HPV 16/18), Merkel cell polymovirus (McPyV), Epstein Barr Virus (EBV), Jaagsiekte Sheep Retrovirus (JSRV) and John Cunningham Virus (JCV). These viruses and their proteins have been demonstrated in both pre-clinical and clinical studies to be over expressed in lung cancer tissue in comparison to lung tissue from healthy individuals (White & Khallil 2005; Gheit et al 2012; Kato et al 2012; Behdarvaad et al 2017; Sinagra et al 2017; de Olivera et al 2018; Grey et al 2019; Yeh et al 2019). The suggested mechanisms by which these viruses may influence the pathophysiology of lung cancer is via penetration into lung cells through interaction with cell surface receptors such as heparin sulphate proteoglycans (HSPG), CD 21 on B cells or epithelial cells and hyaluronidase-2 (Hy2) and sulphated glycosaminoglycans. Upon penetration into lung cells these viruses trigger cellular events that foster cancer pathology e.g., HPV16/18 penetrates lung cells via interaction with HSPG through its oncoproteins E6 and/or E7, then amplifies angiogenesis by increasing the expression of hypoxia inducible factor 1α (HIF 1α), vascular endothelial growth factor (VEGF) and interleukin 8 (IL-8) (Zhang et al 2014; Hu et al 2020). Secondly, viral infection promotes p53 degradation by binding to LxxLL motif of the cellular ubiquitin ligase resulting in chromosomal instability which facilitates the conversion of HPV infected cells into cancerous cells (Wu et al 2011). Finally, HPV infection induces dysregulated cell proliferation by degradation of retinoblastoma suppressor protein (pRB) which leads to the disassociation of E2F/pRB histone deacylase complex and cells becoming resistant to apoptosis (Wu et al 2005).

1.3.4 Genetic factors

A family history of lung cancer has been suggested to increase the risk of having lung cancer. Matakidou et al (2005), conducted a systematic review of the relationship between family history and risk of lung cancer on 28 case-control, 17 cohort and seven twin studies reporting that first degree relatives of patients with lung cancer are also at an increased risk of having cancer (RR-1.84, 95%CI:1.64-2.05). Similar results were obtained from epidemiological analyses by Ding et al (2018) and Canon-Albright et al

(2019) who conducted surveillance studies evaluating the relative risk of an individual for lung cancer based on their family history. Lan et al (2012), in a genome wide association analysis study to identify common genetic variants that contribute to lung cancer susceptibility identified the following susceptibility loci on these chromosomes; 10q25.2, 6q22.2, 5p15.33, 3q2.8 and17q24.3 in women of Asian origin who had never smoked. Furthermore, germline mutations such as: V843I, P848L, R766H and T790M in the EGFR gene have also been associated with familial lung adenocarcinoma (Sequist et al 2006; Ohutska et al 2011; Oxnard et al 2012; van Nosel et al 2013; Prim et al 2014).

1.4 Driver mutations in NSCLC

Aside from smoking and non-smoking factors described above. "Driver mutations'' (**Figure 1.4**) have also been identified as key facilitators of the histopathology of NSCLC (Riley et al 2006; Levy et al 2012; Sigsmund et al 2018; Chevallier et al 2021). "Driver mutations" can be described as genetic aberrations that play central roles in the initiation, progression and maintenance of tumour growth. Various groups using multiplexed polymerization chain reaction (PCR), fluorescence *in situ* hybridization (FISH) and sequencing techniques involving: whole genome, transcriptome and exome analysis of more than 3,000 lung tumour samples have identified the following mutations in NSCLC; EGFR (10-30%), KRAS (15-30%), FGFRI(20%), HER2(2-5%), PIK3CA (2-5%), ALK (3-5%), BRAF(1-3%) ROSI (1%) MEK1 (1%) RET (1%), NRAS (1%) AKTI (<1%) (Pao et al 2004; Riley et al 2006; Bleeker et al 2008; Ding et al, 2008; Lee at al 2010; Kwak et al 2010; Dut et al 2011; Bergethon et al 2012; Takeuchi et al, 2012; Guo et al 2019) .

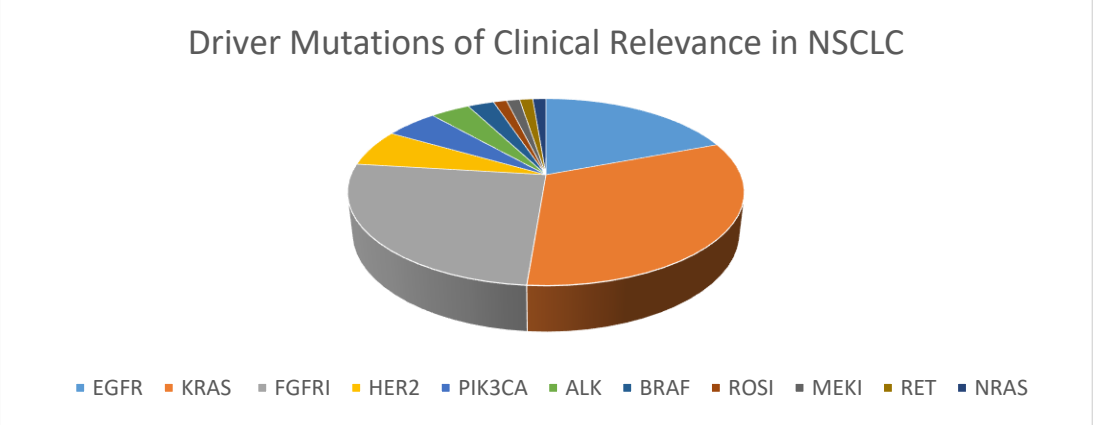

Figure 1.4: Incidence of driver mutations in NSCLC represented with a pie chart: Riley et al (2006); Guo et al (2019).

The "driver mutations'' mentioned above are mostly found in genes encoding catalytic receptor tyrosine kinases which function in cellular signalling pathways responsible for cell growth, movement and angiogenesis (**Table 1.3**, Riley et al 2006). Receptor tyrosine kinases are central to the initiation and regulation of cellular signalling pathways with key molecules being: RAS, PI3K, mTOR RTK/Ras/MAPK, PI3K-PKB (Akt) -β-Smad, and AK- STAT (**Table 1.4**). The mechanisms by which these proteins initiate and regulate signalling pathways almost always involve the transfer of phosphate groups from ATP by receptor tyrosine kinase domains to specific target proteins that activate growth signalling pathways **(Figure 1.5)**. Overexpression, mutations, insertions, fusions and gene arrangements of these enzymatic proteins will lead to aberrant cellular signalling leading to uncontrolled cellular growth which is characteristic of cancer (Levy et al, 2012; Chevallier et al 2021). Knowledge of these "driver mutations'' in NSCLC has opened up a window of opportunity for therapeutics in NSCLC especially as regards metastatic NSCLC. One such molecular event that has been exploited and proven effective as a drug target is the epidermal growth factor receptor (EGFR).

Table 1.3: Brief description of receptor tyrosine kinase implicated in NSCLC pathology

Receptor Tyrosine Kinase (RTK)	**Description**
EGFR	Epidermal growth factor receptor: binding of a ligand (EGF) to its extracellular membrane triggers dimerization of its receptor, autophosphorylation of tyrosine residue and transfer of phosphate groups to proteins that initiate the signalling pathways for cell proliferation and growth.
HER 2	Erbb$_2$: receptor tyrosine kinase 2 is a member of the epithelial growth factor receptor. It initiates signalling pathways responsible for cell proliferation and opposition to apoptosis.
DDR$_2$	Discodin domain receptor is also known as an adhesion receptor. This receptor binds and is activated by collagen, plays key roles in the regulation of cell growth, differentiation and metabolism.
ALK	Anaplastic lymphoma receptor tyrosine kinase is a member of the insulin receptor super family and is generally considered an orphan receptor as it can activate RAS-MEK-ERK, JAK-STAT3 and P13K-AKT pathways without ligand activation.
ROS 1	ROS proto-oncogene 1 receptor tyrosine kinase belongs to the insulin receptor super family. It is involved in initiation and regulation of pathways such as: JAK-STAT, RAS/MEK/ERK, P13K/AKT responsible for cell growth, and survival.
RET	RET proto-oncogene is an oncogene that encodes for member of the cadherin super family of receptor tyrosine kinases. Binding of neurotrophic ligand co receptor complexes to this RTK causes dimerization of its extracellular membrane, then autophophorylation of its tyrosine residues this leads to activation of RAS/MAPK, P13K/AKT and JNK. Cell signlling pathways

MET	Mesenchymal epithelial transcription factor is an oncogene that encodes for the RTK hepatocyte growth factor receptor (HGFR). Upon ligand activation of HGFR dimerization of its extracellular membrane and autophosphorylation of its tyrosine residues initiation of RAS/MEK/ERK pathway for cell proliferation is activated.
FGFR1	Fibroblast growth factor receptor I is a member of the fibroblast growth factor receptor. It triggers the RAS/MEK/ERK and P13K/AKT signalling pathways necessary for cell differentiation, angiogenesis and cell proliferation

Levy et al, 2012; Chevallier et al 2021

Table 1.4: Brief description of components of signaling pathways implicated in NSCLC pathology

Component	Description
KRAS	This protein belongs to the RAS gene family. It encodes for the proteins in the GTPase family. GTPase are enzymes that regulate RAS the initiator of the RAS/RAF/MEK signalling pathway
BRAF	Is a proto-oncogene that codes for a SER-Thr kinase protein a downstream effector protein that phosphorylate MEK and activates ERK in the RAS/RAF/ERK signalling pathway
P1K3CA	This gene encodes for PIIOα isoform the catalytic sub unit of the lipid kinase protein P13K which reproduces phosphatidyl inositol-3 phosphate a key mediator of PI3K/AKT signalling pathway.

Guo et al (2019)

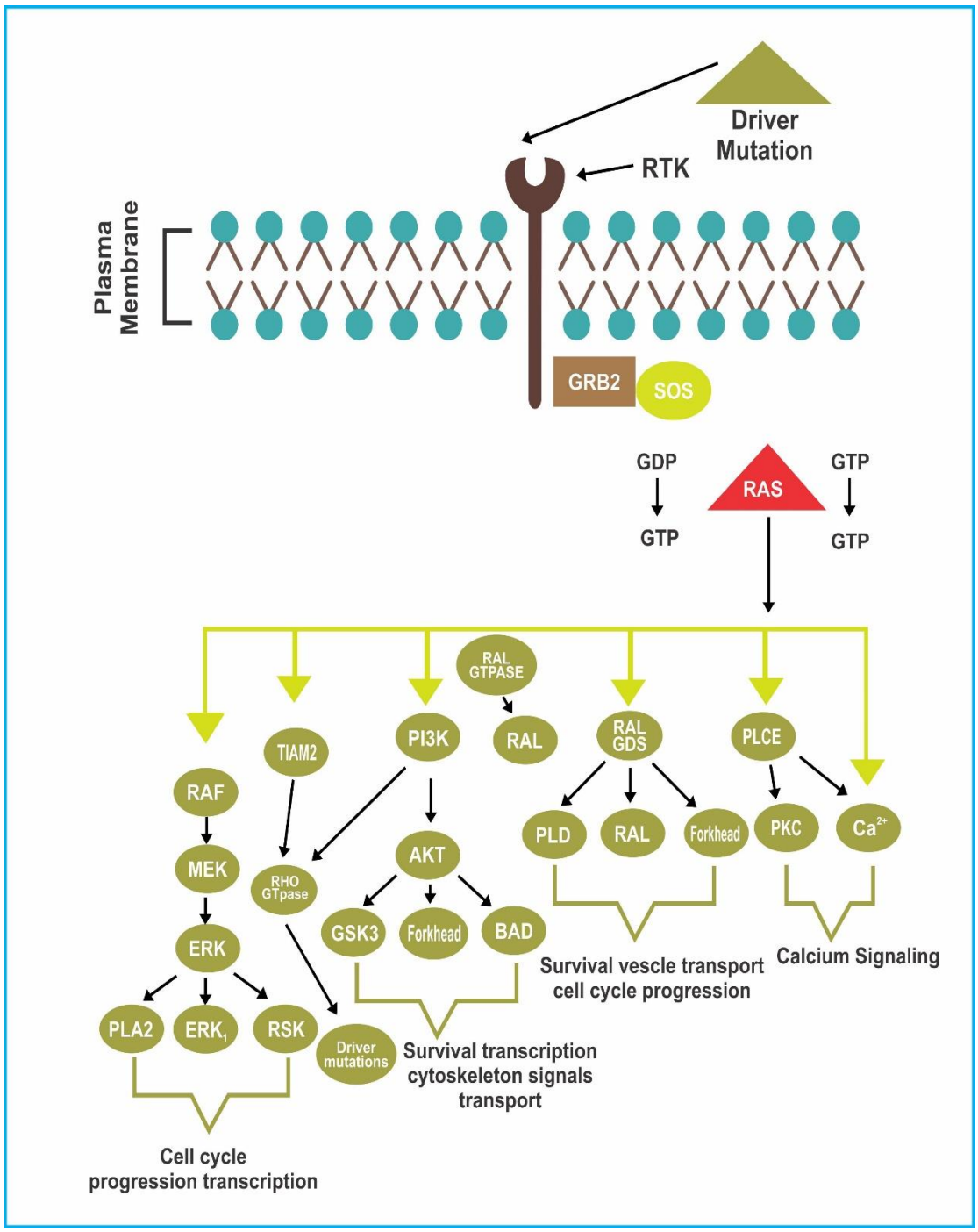

Figure 1.5: Cellular signalling pathways influenced by RTK and GTPase. Mutations result in uninhibited growth of cells, unregulated apoptosis and increased angiogenesis. Adapted from Du & Lovly (2018) and drawn using Adobe illustrator.

1.5 Epithelial Growth Factor Receptor (EGFR)

1.5.1 Structure

EGFR is a protein about 170 kiloDalton (kDa) in size that is encoded on the short arm q22 of chromosome 7. It occupies about 110 Kb of DNA and spans 28 exons. EGFR belongs to the ErBB family of cell surface tyrosine kinases that include the following: HER1 (EGFR/ErBB1), HER2 (NEU, ErBB2), HER3 (ErBB3) and HER4 (ErBB4). This family of kinases is capable of forming homo and heterodimers with one another and can form up to 28 combinations (Wee & Wang, 2017). Structurally (**Figure 1.6**) EGFR comprises of 3 parts:

Extracellular ligand binding and dimerization domain- This zone spans exons 1-16 region and it is made up of a total of 621 amino acids. This zone is further divided into four domains; Domain I- spans exons 1-4 and takes part in ligand binding. Domain II- spans exon 5-7 is capable of forming homo or hetero dimers with analogous domain of family members. Domain III- spans exons 8-12 and also takes part in ligand binding. Domain IV- spans exon 13-16 and is capable of forming disulphide bonds with domain II and has links to the transmembrane zone of the receptor (Rosokoski, 2014).

Transmembrane domain- This zone is a long hydrophobic single membrane structure that links the intracellular domain to the extracellular domain it comprises of 23 amino acids, that spans exon 17. Its contribution to the physiological role of EGFR is still not clear. However, results from different studies involving truncation of extracellular ligand binding, induction of mutation in transmembrane zone have suggested that the transmembrane zone plays a role in receptor activation of EGFR (Cymer & Schneider, 2010).

The intracellular domain- this zone is 542 amino acids long and it comprises a flexible juxta membrane segment made up of 40 amino acids, a tyrosine kinase domain comprising of amino acids 690-953 that spans exon 18-24 and the C terminal tail comprising of amino acids 954-1136 spanning exon 25-28. The tyrosine kinase domain is further divided into two lobes a β sheet structure called an N lobe and an α helical structure called a C lobe. An ATP binding site is located between the two lobes (Wee & Wang, 2017).

The structure of EGFR aligns well with its physiological role of regulation of cell survival, proliferation and differentiation. Its physiological roles are made possible through molecular mechanisms that involve ligand stimulation of the extracellular membrane with consequent catalytic activation of the tyrosine kinase domain that triggers phosphorylation of target proteins resulting in the activation of several intracellular signalling cascades that trigger pathways necessary for cell proliferation, apoptosis and differentiation (Olayioye et al 2000; Du et al 2021). The regulatory role of EGFR in key cellular activities is explained below.

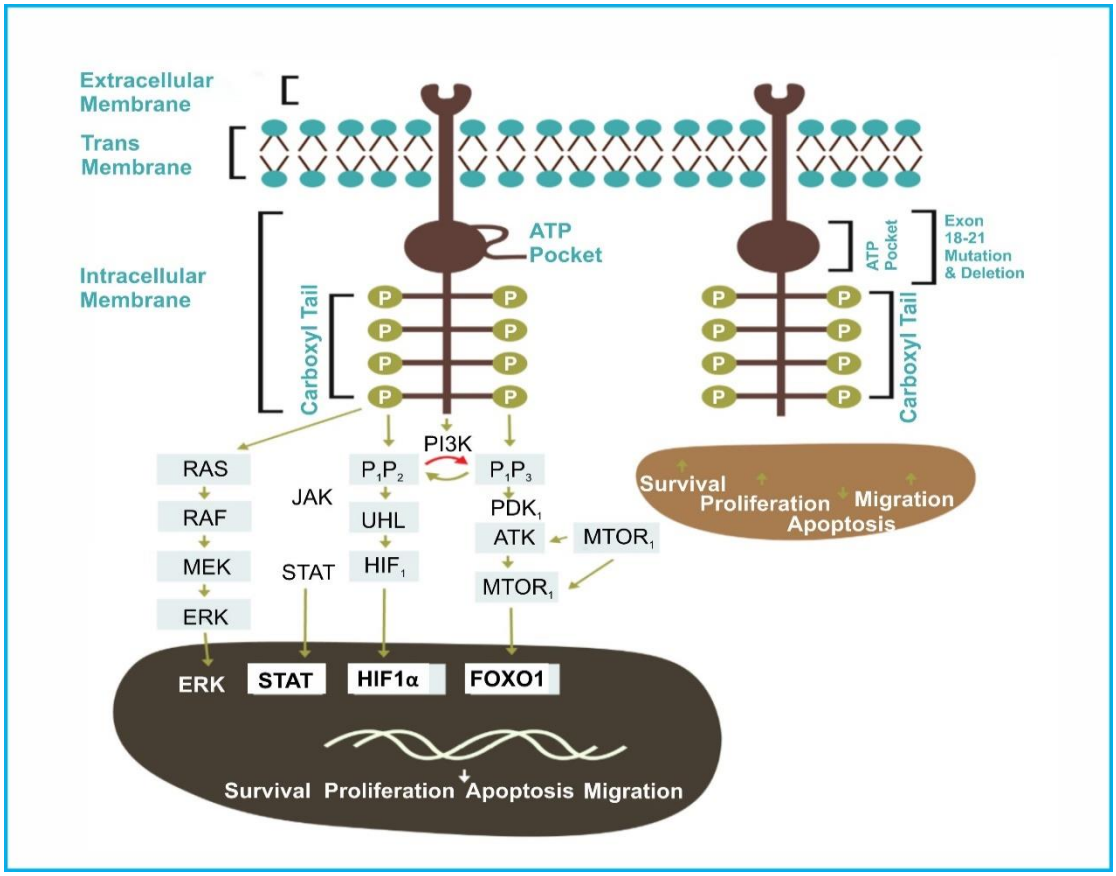

Figure 1.6: EGFR showing normal and defective receptor. The transmembrane links the tyrosine kinase domain to the extracellular domain. The tyrosine kinase domain comprises of a carboxyl tail with tyrosine residues and an ATP pocket. A defective receptor with mutations and or deletions in exon 18-21 of the tyrosine kinase domain results in uncontrolled proliferation and resistance to apoptosis. Adapted from Du & Lovly (2018) drawn using Adobe illustrator.

1.5.2 Ligand binding/dimerization

When not stimulated the EGFR is in an auto-inhibited non dimerized state. In this state domain II of the extracellular membrane is enclosed into domain IV via disulphide bonds. Binding of ligands such as epithelial growth factor (EGF), transforming growth factor α (TGF-α), heparin binding EGF (Hb-EGF), amphiregulin, epiregulin, betacellulin and neuroregulin 2 to domains I and III fosters a domain reorganisation such that the dimerization arm of domain II is exposed in an extended conformation. Exposure of the dimerization arm of domain II results in communication of the juxtamembrane with the kinase domain. Communication of the juxtamembrane with the kinase domain involves the interaction of the N lobe of one receptor to the C lobe of another receptor (this process is termed receptor mediated dimerization). These interactions result in stability of EGFR dimerization and trans-autophosphorylation of the kinase domain (Enders et al 2014; Du et al 2021).

1.5.3 EGFR trans auto-phosphorylation

The tyrosine kinase domain remains in an auto-inhibited state until receptor dimerization triggered by ligand binding to extracellular membrane. Receptor dimerization and structural rearrangement in the cytoplasm causes auto-phosphorylation of the tyrosine kinase domain. On activation of the tyrosine kinase domain, the activation loop (ATP binding site) opens, this allows for transfer of phosphates from ATP to tyrosines on the receptor molecules. There is also transfer of phosphates from ATP to tyrosine residues in some cellular proteins involved in signal transduction (Sigsmund et al 2018). Furthermore, the phosphorylated tyrosine residues serve as docking sites for proteins bearing phospho-tyrosine binding residues e.g. Src homology 2 (SH2) and a phospho-tyrosine binding domain (PBT). Other docking sites on the phosphorylated tyrosine residues are SH3 (binds proline rich proteins), 14-3.3 (binds phosphoserine), bromo (binds acetylated lysine and PH domain). Docking of proteins to phosphorylated tyrosine residues on EGFR leads to recruitment, assembly, membrane translocation and activation of key players/ proteins involved in initiating signalling pathways necessary for cellular survival, growth, proliferation, differentiation and angiogenesis (Wee & Wang, 2017).

1.6 EGFR in Cellular Signalling

1.6.1 RAS/ERK/MAPK Pathway

After receptor trans-phosphorylation, Protein initiators of the RAS/ERK/MAPK pathways dock onto phosphorylated tyrosine residues on EGFR (**Figure 1.6**). These proteins are the growth factor receptor binding protein (GRB2) and the SRC homology and collagen (SHC) protein. The ability of these proteins to dock onto phosphorylated tyrosine residues on EGFR has been linked to the presence of SH2 and PTB domain present in them. These domains have an affinity for phosphorylated residues such as: Y1068, Y1086, Y1145 and Y1173. Once binding occurs the SH2 domains on GRB2 bind to the son of sevenless1 (SOS1) protein via its proline rich carboxyl terminal (Schlessinger, 2000). The SOS1 protein is a guanine nucleotide exchange factor for the enzyme RAS small guanine triphosphatase (GTPase). The GTPase enzyme activates RAS by inducing the exchange of GTP to GDP. Activated RAS interacts with RAF-1 via its GTP binding domain. Interaction of RAF-1 with RAS leads to membrane translocation of RAF and to its phosphorylation at its SER338 and TYR 341 residues. Phosphorylated RAF acts as a binding site for MEK1/2. MEK (mitogen activated protein kinase kinase (MAPKK) is a dual specific kinase (tyrosine and threoinine/serine) that activates ERK1/2 by phosphorylating its threonine-glu and tyrosine motif in the ERK1/2 activation loop. The activated ERK1/2 phosphorylates multiple substrates to initiate various biological responses e.g. phosphorylation of the pro apoptotic protein, regulation of pyrimidine synthesis, chromatin remodelling, ribosome synthesis and protein translocation (Du & Lovly, 2018).

1.6.2 PI3K-AKT-MTOR Pathway

The PI3K-AKT-MTOR signalling cascade regulates metabolism, proliferation, cell size, survival and motility. The class 1 PI3K protein is a major initiator of this signalling pathway via EGFR. The class 1 PI3K are of two sub classes; sub class1a (PI3Kα, PI3Kβ & PI3Kδ) sub classIb (PI3Kγ). The subclass1a group of PI3K proteins are activated by RTK while the subclass1b are activated by G protein coupled receptors. Activation of the PI3K protein of the subclass Ia group is through binding of its P85 subunit to adaptor proteins such as GAB1 (GRRB2 associated binder) and CBL (Sigsmund et al 2018). Following binding, the adaptor proteins bind to EGFR via the interaction of their proline rich domain with GRB2 SH3 domain. Phosphorylation of GRB2 is then transferred to PI3K thereby causing its activation. Furthermore, activation of PI3K is

also made possible by binding of RAS protein to its P110 catalytic domain. This leads to phosphorylation of the 3OH group of the membrane lipid phosphatidylinositol-4-5-biphosphate (PIP2) (Du et al 2021). Phosphorylation of PIP2 generates phosphatidylinositol-3, 4-5 triphosphate (PIP3). The PIP3 generated acts as a secondary messenger and it links the lipid kinase activity of PI3K to key proteins in signalling cascades e.g., AKT. AKT binds to PIP3 via its PH (Pleckstrin homology) domain and once tethered at the plasma membrane AKT alters a number of signaling processes, e.g. it functions in an anti-apoptotic manner by directly phosphorylating and inhibiting BAD. AKT also inhibits the catalytic activity of caspase 9 by phosphorylating the molecule at amino acid S196. It also inhibits the activity of FOX1 by phosphorylating T32 and S25 residues (Schlessinger, 2000). Furthermore, AKT phosphorylates and inhibits the protein TSC2; TSC2 is an inhibitor of MTOR. The subsequent activation of MTOR results in increased synthesis of growth promoting factors such as cyclin D1, hypoxia inducible factor 1 and VEGF (Wee & Wang, 2017)

1.6.3 PLCγ-1-PKC Pathway

PLCγ-1 is activated by binding directly to activated EGFR through its SH2 domain. Following binding to EGFR it is translocated to the plasma membrane. The PLCγ-1 protein can also be recruited to the plasma membrane via its PH domain by binding to PIP3 derived from PI3K in response to EGFR activation. The activated PLCγ-1 hydrolyses into free intracellular 1, 4 5 triphosphate (IP3) and diacyl glycerol (DAG). IP3 and DAG are important cellular messengers. IP3 binds to IP3 receptors at the endoplasmic reticulum to induce intracellular calcium release. The calcium released shunts into the DAG pathway. Calcium and DAG then collectively activates protein kinase C (PKC). The activated PKC interacts with cellular substrates/proteins such as EGFR, RAF1, H-RAS, P21, GSK-3β, RHOA, BAD BCL-2. These interactions cause cell growth, receptor desensitization, transcription regulation, modulation of membrane structure and immune response (Du et al 2021).

1.6.4 JAK-STAT pathway

Activation of the EGFR induces transfer of TYR 701 for phosphorylation of STAT protein and the integration of STAT 1 and STAT 3 to JAK 1 and JAK 2. The complex

formed is transported into the cell nucleus and results in the stimulation of matrix metalloproteinase activity which is responsible for cell migration (Schlessinger 2000). The phosphorylation of EGFR and the resultant initiation of multiple cellular signaling mechanisms responsible for cell growth, differentiation and survival induced by ligand binding to the extracellular membrane of EGFR is regulated within narrow limits. Paradoxically, ligand binding induces the cellular machinery that regulates the magnitude, quality and duration of signals that it initiates (Olaoye, 2000; Schlessinger, 2000).

1.6.5 Regulation of EGFR Signaling

Ligand binding results in the assembling of an endocytic machinery that regulates the magnitude, quality and duration of the signals generated by the activation of the catalytic tyrosine kinase domains. The endocytic mechanisms involved in the regulation of signals are of two major types clathrin mediated endocytosis (CME) and non-clathrin mediated endocytosis (NCE) (Bakker et al, 2017).

1.6.5.1 Clathrin mediated endocytosis regulation of EGFR signaling

Clathrin mediated endocytosis regulation of EGFR signalling is triggered by low ligand availability and it involves mainly receptor recycling and on very few occasions receptor degradation. At low ligand concentrations, phosphorylation of EGFR leads to the recruitment of the following proteins adaptor protein 2 and GTPase dynamin. The adaptor protein 2 assembles clathrin coated pits ensuring that the pits are of the right vesicle size essential for receptor clustering redistribution. Accumulation of receptors in the clathrin coated pits fosters cross phosphorylation thereby optimizing receptor phosphorylation. The GTPase dynamin protein regulates the assembly time for the clathrin coated pits this regulation fosters productive signalling, as the clathrin coated pits are assembled only when needed. Furthermore, phosphorylation of the β2 sub unit of the adaptor protein 2 by EGFR occurs simultaneously with the assembly of clathrin coated pits. This results in the internalization of EGFR into the endocytic pathway. In the endocytic pathway, receptors with reduced signalling potential due to low ligand binding are recycled in endocytic vesicles that contain the protein GTPase RABII (Capuani et al 2015).

1.6.5.2 Non-clathrin mediated endocytosis regulation of EGFR signaling

Non-clathrin mediated endocytosis- this cellular machinery is triggered by high ligand concentration and it is important for dampening EGFR signalling and acts as a modulator of excessive EGFR signalling. The key mechanism by which dampening of EGFR signalling is achieved is via lysosomal degradation of high signalling EGFR. At high ligand concentrations phosphorylation of the tyrosine kinase domain of EGFR leads to the recruitment of CBL and the adaptor protein GRB2. CBL attaches to the GRB2, the GRB2 protein docks onto the phosphorylated EGFR causing ubiquitylation of EGFR. The ubiquitylated EGFR is recognized by the ubiquitin dependent adaptors of the endosomal sorting complexes required for transport (ESCRT). The ubiquitylated EGFR is then transferred into intraluminal vesicle of endosomes. Transfer of ubiquitylated EGFR to the endosomes involves the removal of signalling tail of EGFR from the cytosol, this results in termination of the downstream signalling cascade and degradation of EGFR in the lysosomes (Conte & Sigsmund, 2016; Bakker et al 2017). Activation and down regulation of EGFR signalling must be regulated within narrow limits so that cellular activities can be maintained at equilibrium. Any disruption or deviation from normal regulatory mechanism will result in uninhibited cellular mechanisms such as aberrant cell proliferation and cell migration which are hallmarks of cancer.

1.7 Oncogenic EGFR

1.7.1 EGFR over expression and genetic amplification in NSCLC

Several studies evaluating EGFR expression on biopsy samples from patients with NSCLC report that between 40-80% of lung cancer tumours express EGFR, with higher expression rates observed in lung squamous cell cancer (Selvaggi et al 2004; Nakamura et al 2006; Shivaligsamwy et al 2018). Prospective studies- to evaluate the association of EGFR expression with survival and prognosis in NSCLC report that EGFR overexpression is associated with disease progression, metastasis and shorter overall survival (Selvaggi et al 2004). Mere overexpression of EGFR I.e an increase in local concentration of the receptor, is not sufficient to transform normal cells to oncogenic cells, overexpression has to translate into amplified signal transduction. Amplified signal transduction is made possible by ligand binding to the increased number of receptors. Other triggers are transcriptional/translational enhancement of the receptors

by mutant proteins and aberrations in normal regulatory mechanism (Du & Lovly 2018).

1.7.2 Gain of function mutations

Mutations in the extracellular domain and tyrosine kinase domain of EGFR have been associated with the pathogenesis of NSCLC. Ji et al (2006), evaluated the presence of mutations on the extra cellular domain of 179 NSCLC tumour biopsy samples of patients using a combination of techniques including; fluorescence *in situ* hybridization (FISH), quantitative real time PCR and immunostaining. This group reported that mutations in the extracellular domain was only observed in patients with squamous cell carcinoma and only 5% of patients with squamous cell carcinoma had a distinct mutation on the extracellular domain of the EGFR. The mutation is an inframe deletion of exons 2-7 (EGFR variant III). Furthermore, this group evaluated the role of the mutation in tumour maintenance and initiation by designing transgenic mice with the mutation. The results from their experiments suggest that the EGFR vIII mutant leads to continuous and amplified downstream signal transduction and activation of AKT and ERK 1/2 signalling pathway, which results in cells that are resistant to apoptosis.

Shigematsu et al (2005a) carried out a sequence analysis of the entire tyrosine kinase domain of EGFR using genomic DNA (gDNA) obtained from 96 biopsy samples from patients with NSCLC. Results from this investigation showed that mutations associated with the tyrosine kinase domain in NSCLC are located within exon 18-21. Furthermore, this group- in a much larger study validated their initial results of mutations in exon 18-21 of tyrosine kinase domain in NSCLC evaluated the frequency of these mutations using gDNA obtained from a total of 617 biopsy samples; from centres in Australia, North America and Asia. Control samples used for this study was gDNA obtained from 524 matched normal lung tissue and 243 biopsy samples obtained from patients with other epithelial tumours such as: bladder, breast and colorectal and gall bladder. The results from this study show that mutations in the tyrosine kinase domain of EGFR were detected in 130 of the 617 biopsy samples. Of the 130 patients with the mutation 30% were of Asian origin. More females appear to have the mutation (42% versus 14%). Additionally, the mutation appeared to be more prominent amongst never smokers than smokers (51%vs 10%) and the mutations were most common in patients with the adenocarcinoma. Surprisingly, mutations located in exon 18-21 of the tyrosine kinase

domain in patients with NSCLC were not observed in the other epithelial tumors. Similar results were obtained from other groups too (Lynch et al 2004; Shigematsu et al 2005b; Wang & Wang, 2014; Yang et al 2022).

Mutations in the tyrosine kinase domain of EGFR are found in the kinase activation loop, around the nucleotide binding pocket close to the ATP cleft. Mutations located in exon 18-21 results in structural modifications near the ATP cleft this results in the magnification of the catalytic activity and auto-phosphorylation of the tyrosine kinase domain following its activation by ligands. The heightened activity of EGFR results in amplified and continuous activation of AKT and STAT pathways these pathways foster cell proliferation and resistance to cell death. About 90% of mutations located in exon 18-21 are either in frame deletions in exon 19 mostly E746-A750 or point mutations on exon 21 where leucine exchanges for arginine on position 858 (Riley et al 2006). **See Table 1.5** for other mutations that have been reported. Knowledge of key mechanisms by which aberrant EGFR signalling initiate and maintain tumourigenesis resulted to research for molecules that will specifically target EGFR perhaps attenuate signalling and alleviate any of the hallmarks of cancer. One of the molecules designed to target EGFR specifically is the tyrosine kinase inhibitors (TKI). The application of TKI in the management of patients with NSCLC resulted in significant improvement in progression free survival (PFS) and objective response rates (ORR) when compared to platinum-based chemotherapy. However, these improvements in clinical outcomes was only observed in a sub-group of patients those with EGFR mutations WJTOG3405 (2010), NEJ002 (2010), OPTIMAL (2011), EURTAC (2012), ENSURE (2015). These findings opened up the possibility of molecular markers being predictors of treatment outcome.

Table 1.5: List of common mutations on exon 18-21 on tyrosine kinase domain of EGFR associated with NSCLC

Exon	Mutations and/or deletions associated with the exon
18	G719C, G7119C, V689M, N700D, E709K, E709Q, S720P
19	E746-A750, E746-T751, E746-A750(ins RP), E746-T751(InsA/v), E746-T751(ins VA). E746-S752(Ins A/v), L747-E749 (A750P), L747-A750(ins P/S), L747-T751(ins p/s), L747-752 (P753) , L741-S752(insQ), L747-P753, S752-1759, D761Y
20	V765A, T783A, D770_N771, (ins NPG), D770_N771(ins SVQ), D770_N771(InS G), N771T, V769L, S7681, T790M
21	L858R, N826S, A839T, K846R, L861Q

Lynch et al 2004; Chung et al 2012; Oxnard et al 2013; Keam et al 2014; Yang et al 2015; Kobayashi et al 2016; Passaro et al 2018

1.8 TKI in clinic

1.8.1 TKI in clinical trials

Tyrosine kinase inhibitors: geftinib and erlotinib were designed without prior knowledge of the existence of somatic mutations in exon 18-21 of the tyrosine kinase domain of EGFR. As at that time what was proposed as the possible contribution of EGFR to oncogenesis was amplified and continuous signalling of the tyrosine kinase domain possibly due to EGFR overexpression or gene amplification. The approval of TKI for the management of patients with progressive NSCLC following failure of chemotherapy by the USA food and drug administration (FDA) was due to results from clinical trials such as; the randomized double-blind phase II multicentre trials of Iressa Dose Evaluation of gefitinib in Advanced Lung Cancer (IDEAL I &II) (2003). This clinical trial involved the assessment of clinical outcomes following treatment with 250mg or 500mg of continuous oral gefitinib in more than 400 patients previously treated with chemotherapy. Data from this trial showed an improvement in lung cancer symptoms 69.2% (250mg/dl) and 85.2% (500mg/dl), an objective response rate of 9-19% and a median survival of 6-8 months. Furthermore, the Canada clinical trials group Br 21 (Shepard et al 2005) in a randomized, placebo controlled double blind study evaluated the clinical outcome of a total of 731 patients placed on either erlotinib or placebo following failure of first line chemotherapy. A total of 488 patients were placed on erlotinib and 243 patients were on the placebo. The results from this trial showed a response rate of 8.9% for the group on erlotinib and a response rate of less than 1 % for the placebo group. The median duration of response reported from this study was 7.9 months for the group on erlotinib and 3.9 months for the group on placebo ($P \leq 0.001$). An overall survival of 6.7 months was reported for the group on erlotinib and 4.7

months for the group on placebo. Despite the moderate success of TKI in terms of improved clinical outcomes from the trials discussed above scientists and clinicians remained sceptical about the use of TKI in the management of NSCLC as some trials had reported minimal/no significant benefit. Thatcher et al (2005), in a randomized phase III placebo controlled multicentre study (Iressa Survival Evaluation in Lung Cancer (ISEL)), evaluated the effect of gefitinib plus supportive care as second- or third-line treatment on survival in 1,692 patients with locally advanced or metastatic NSCLC following treatment failure with chemotherapy. A total of 1,129 patients were placed on geftinib plus supportive care and 563 were placed on placebo plus supportive care. After a median follow up of 7.2 months survival did not differ significantly between the two groups. The group on geftinib plus supportive care had a median survival of 5.6 months, while the group on placebo plus supportive care had a median survival of 5.1 months. Furthermore, randomized phase III trials such as INTACT I &II (2004), TRIBUTE (2005) and TALENT (2007) that evaluated the effect of TKI in combination with chemotherapy also reported no significant advantage in terms of overall survival, tumour response and time to progression in the group of patients on combination TKI with chemotherapy, when compared to the group of patients on chemotherapy alone. However, what was striking about all these clinical trials was that a group of patients with certain clinicopathological features had significantly longer overall survival and better response rates. The clinicopathological features associated with superior objective response rates and longer overall survival were female gender, never/ former smokers, Asian ethnicity and the adenocarcinoma histology type.

1.8.2 Mechanism of TKI

TKI, although designed to specifically target EGFR, its mechanism of action was not well understood. The correlation of clinical response of patients to gefitinib and level of EGFR expression and/or gene amplifications was not clear because the level of EGFR expression or gene amplification in patients appeared not to have any effect on response to TKI. The report of superior response in patients with a particular type of clinicopathological feature led to investigations involving nucleotide sequence analysis of tumour samples from patients known to have a superior response to TKI. Lynch et al (2004) investigated mutations in the EGFR gene of tumour biopsy samples from nine patients who had shown superior response to gefitnib in the ISEL clinical trials. The controls used in this study were matched, non-cancerous, lung cancer tissue from the 9

patients responsive to gefitinib and tissue biopsy samples from 7 patients with no response to gefitinib. The patients who had responded to gefitinib had the following clinicopathological characteristics (I) they were mostly women (II) they were never smokers (III) they had the adenocarcinoma histology. Mutations in exon 19 and 21 of the tyrosine kinase domain were observed in eight of tumour samples while no mutations were observed in matched non-cancerous lung tissue nor from tissue samples from patients who had no response to gefitinib. Results from this study suggested that these mutations had arisen somatically during tumour formation. The mutants identified were in frame deletions in exon 19 removing amino acids 746-750 (n=4), and amino acid substitutions in exon 21 substitution of leucine for arginine on codon 858 L858R (n=2), amino acid substitution of leucine for glutamine on codon 861 L861Q (n=1). Furthermore, this group also evaluated the potential mechanism by which these mutants detected could cause tumorigenesis using cell culture models of the mutant type's analysed i.e L747-P753 deletion on exon 19, L858R mutation on exon 21 and wild type EGFR. This group observed that in the absence of ligand activation the tyrosine kinase domain was auto inhibited. However, on ligand stimulation by EGF activation/autophosphorylation of the tyrosine kinase domain of the EGFR was three times more than what was observed by the wild type. This was evaluated by the quantification of autophosphorylation of the tyrosine residue 1068. Additionally, this group also analysed the effect of normal regulatory mechanisms of EGFR receptor signalling on these cellular models. They reported continuous activation / autophosphorylation of the mutant tyrosine kinase domain 3 hours after initiation of normal regulatory mechanisms. However, activation was inhibited in the wild type following initiation of regulatory mechanisms. This group also evaluated the sensitivity of cell models of the mutations to gefitinib. Their results show that EGF induced autophosphorylation of the cell models of mutation was completely inhibited at a concentration of 0.2μm, while for the wildtype cell models it took a much higher concentration (2.0μM) of gefitinib for complete inhibition to occur. This group proposed that mutations in the kinase domain of the EGFR may be more sensitive to TKI because these mutations are situated near the ATP cleft and cause repositioning of critical residues, thereby stabilizing/promoting constant autophosphorylation and cellular signalling. Gefitinib is an aminolinoquinazoline compound that binds reversibly to the ATP cleft and mutations near the ATP cleft stabilizes binding of gefitinib thereby resulting in the inhibition of autophosphorylation. The results from

this group led to the redesign of clinical trials involving TKI taking into consideration clinicopathological features of the patient and presence of EGFR mutations before patient selection.

The IRESSA Pan-Asia study (Mok et al 2005) was the first to identify that clinicopathological features and mutation in the EGFR gene may be a strong predictor of better response to gefitinib in patients with advanced NSCLC. In this phase III open label study only patients who never smoked with pulmonary adenocarcinoma were recruited for this study. The patients recruited were randomized to either receive gefitinib or standard chemotherapy (Carboplatin plus paclitaxel). Overall median survival was better in the group on gefitinib when compared to the group on carboplatin plus paclitaxel (18.6 months vs. 17.3 months). A better objective response rate was also observed in patients on gefitinib 43.0% vs. 32.2%. However, the presence of EGFR mutations resulted in superior response rates to gefitinib. Patients with EGFR mutations treated with TKI had objective response rates of 71.2% as against 43.0% observed in patients with EGFR mutations on carboplatin plus paclitaxel. The median progression free survival was also better for patients with EGFR mutation on TKI when compared to patients with EGFR mutation on carboplatin plus paclitaxel (9.5 months versus 6.3 months). The EGFR mutations identified in this study were exon 19 deletions (53.6%), exon 21 mutation L858R (42.5%) exon 20 mutations T790M (4.2%). Based on these findings' earlier studies such as: Br21, IDEAL I&II, INTACT I & II and Tribute (**Table 1.6**) that had failed to identify the predictive and prognostic value of EGFR mutations were re-assessed and patients re-stratified based on clinicopathological features and their tumour samples were retrospectively analysed to evaluate EGFR mutations and to correlate any association with response to TKI. Additionally, subsequent studies including: WJTOG3405 (2010), NEJ002 (2010), OPTIMAL (2011), EURTAC (2012), ENSURE (2015), Lux-Lung 5 (2013), Lux-Lung 6 (2014) comparing efficacy of TKI with standard chemotherapy did stratify patients based on knowledge of EGFR mutations and their clinicopathological characteristics. Data from these studies showed that EGFR mutations were strong predictors of better response to TKI (**Table 1.6)**. The results from these clinical trials revolutionized management of patients with NSCLC from "one drug fits all" into individualized therapies. The latter involves knowledge of patients' molecular or genomic characteristics before selection of therapy. Although, the use of TKI for the management of patients with metastatic NSCLC has resulted in

better clinical outcomes, the benefits appeared to be short-lived as about 50% of patients with advanced NSCLC, on first generation TKI, developed resistance 9-12 months following commencement of therapy (Capuzzo 2015; Romanidou et al 2016). Resistance to first generation TKI necessitated drug discovery of new TKI that would circumvent resistant clones. The various generations of TKI currently in use in the clinic are discussed in the next section.

Table 1.6: Summary of key trials evaluating response of patients with EGFR mutations to TKI and/or chemotherapy

Study	**IDEAL I&II**	**INTACT I&II**	**NEJ002**	**IPASS**
Date	2005	2005	2010	2009/2011
Study type	Retrospective	Retrospective	Phase III prospective trial	Phase III prospective trial
Description	Molecular analysis of the IDEAL trials, patients on gefitinib 250mg/d or 500mg/d	Molecular analysis of the INTACT trials. patients on gefitinib& chemotherapy	Randomized open label study EGFR mut patients on gefitinib 250mg, / vs. carboplatin/paclitaxel	Randomized open label study. EGFR mut patients on gefitinib 250mg, / vs carboplatin/paclitaxel
Population	79 (14=EGFR mutation vs 65=WT)	220(23=EGFR mutation 197=WT)	230=EGFR Mut	434(261=EGFR mut173=EGFR WT)
ORR (%)/ *P* value	46 vs 10 *P≤0.005*	72 vs 55	73.7 vs 30.7 (pt on gefitinb vs chemo) *P≤0.001*	71.2vs47.3 *P≤0.001* (pt on gefitinib vs chemo for EGFR mut)
PFS (Months)	4 vs 2	NR vs 6	10.8 vs 5.4 (pt on gefitinib vs chemo) 11.5 vs 10.8 (exon 19 del vs L858R) 2.2 vs 11.4 (other mut vs exon19del/L858R on gefitinib) 5.9 vs 5.4 (other mut vs exon19del& L858R on chemo)	9.5 vs 6.3 (gefitinib vs chemo for EGFR mut)
HR/P value	N/A		0.3 *P≤0.001*	0.48 *P≤0.0001*
OS (months	No impact	15 vs 9	27.7 vs 26.6 (pt on gefitinb vs chemo) 30.5 vs 23.6 (exon 19 del vs L858R) 11.9 vs 29.3 (other mut vs exon19del/L858R on gefitinib) 22.8 vs28.0 (other mut vs exon19del/L858R on chemo)	21.6 vs 21.9 (gefitinib vs chemo for EGFR mut)
HR/*P* value	N/A		0.89	1
Mutations, response rate (%)	Exon 19 deletions L858R exon 21 mutations exon 20-V769L, D770_N771 (ins NPG		117=exon 19 del 97=L858R Other mut= G719X, L861Q RR-82.8 vs 67.3 (ex 19 del vs L858R) 20 vs 76 (other mut vs exon19del& L858R on gefitinib) 20 vs 32 (other mut vs exon19del & L858R on chemo)	140=exon 19 del 111=L858R exon 21 mut RR to gefitinib 84.8vs 60.9 (ex 19vs L858R)

Study	Lux Lung 6	WJTOG3405	Optimal	EUROTAC
Date	2014	2010/2014	2011/2015	2012
Study type	Phase III prospective trials	Phase III Prospective trial	Phase III prospective trial	Phase III prospective trial
Description	Randomized open label study. Comparing overall survival results of EGFR mut patients on afatinib (40mg/d vs cisplatin gemicitabine	Randomized open label study EGFR mut patients on gefitinib 250mg, / or cisplatin/docetaxel	Randomized open label study. EGFR mut patients on erlotinib 150mg, / vs carboplatin/gemcitabine	Randomized open label study. EGFR mut patients on erlotinib150mg, / vs platinum doublet
Population	364= EGFR mut	177=EGFR Mut	154=EGFR mut	173=EGFR mut
ORR (%)/ *P* value	66.9v s23 (pt on afatinib vs chemo) *P≤0.0001*	62.1 vs 32.2 (pt on gefitinb vs chemo) *P≤0.001*	83 vs 36 (pt on erlotinib vs chemo) *P≤0.001*	58vs 23 (pt on erlotinib vs chemo) *P≤0.001*
PFS (Months)	11.0 vs5.6 (pt on afatinib vs chemo)	9.2 vs 6.3 (gefitinb vs chemo) 9.0 vs 9.6 (Exon 19 del vs L858R)	13.1 vs 4.6 (pt on gefitinib vs chemo)	9.7 vs 5.2 (pt on erloitinib vs chemo 11.0 vs 8.4 (exon 19 del vs L858R)11.0 vs 4.6 (exon 19 del on erlob vs chemo) 8.4 vs 6.0 (L858R on erlo vs chemo)
HR/ *P* value	0.28 *P≤0.0001*	0.49 *P≤0.001*	0.16 *P≤0.001*	0.37 *P≤0.001*
OS (months	23.1vs23.5 (pt on afatinib vs chemo) 31.4 vs 18.4 (exon 19 del on afatinib vs chemo) 19.6 vs 24.3 (L858R afatinib vs chemo)	34.8 vs 37.3 (geftinib vs chemo for EGFR mut)	22.8 vs27.2	19.3vs 19.5
HR/ *P* value	0.93 P=0.61	1.25	1.19	1.04
Mutations response rate (%)	exon 19 del, 138=L858R 40 =other mutations T790M, G719X, S768I, L861Q	87=exon 19 del 85= L858R	82=exon 19 del 72= L858R	115=exon 19 del 58=L858R exon 21 mut RR 64vs 18 (Exon 19 del vs L858R)

1.9 First, second and third generation TKI in the clinic

Irrespective of the success of first generation TKI (geftinib and erlotinib) in improving clinical outcomes in NSCLC patients with EGFR mutation. About 50-60% patients with an EGFR mutation (particularly exon 19 deletion and L858R mutation) previously responsive to first generation TKI develop a resistance to TKI during treatment (Takeda and Nakegwa, 2019). Resistance mechanisms commonly associated with resistance to first generation TKI are (1) T790M, a point mutation in exon 20, codon 790, where methionine is substituted for threonine, (2) MET amplification, (3) over expression of hepatocyte growth factor, (4) activation of insulin like growth factor I receptor, (5) transformation to squamous cell carcinoma, and (6) development of D716Y or L747S mutations (Camidge et al 2014).

Second generation TKI: afatinib and dacomitinib were designed to bind irreversibly with the ATP pockets of the tyrosine kinase domain of both EGFR and other ErBB family members. The irreversible binding of these TKI to the ATP pocket was hypothesized to prevent steric hindrance by T790M mutation at the ATP pocket that inhibits the activity of first generation TKI. Additionally, its activity against multiple receptors was hypothesized to result in extended inhibition of receptor tyrosine kinase activity. Pre-clinical studies on NSCLC cell lines (NCI-H1975a) with L858R/T790M mutation showed that Afatinib killed cell lines harbouring this mutation and suppressed EGFR signalling (Kwak et al 2005). Clinical studies (LUX-Lung 7 & ARCHER 1050) comparing afatinib and dacomitinib respectively with first generation TKI report that patients with an EGFR mutation placed on afatinib or dacomitinib had longer progression free survival (PFS) compared with patients placed on gefitinib with an EGFR mutation. LUX-Lung7 open label phase IIb trial reported a PFS of 11.0 months and 10.9 months (HR=0.73 $P=0.017$) for patients placed on afatinib and gefitinib respectively. Whilst the ARCHER 1050 open label phase III study reported a PFS of 14.7 months and 9.2 months (HR=0.59 $P<0.0001$) for dacomitinib and geftinib respectively. The results from these clinical studies suggested that second generation TKI are superior to first generation TKI in terms of PFS. The potential of second generation TKI to kill T790M bearing cell lines, demonstrated in pre-clinical studies, was not translated to the clinic as about 40-50% of patients on afatinib become resistant to the drug after a median time of 14 months with most of this resistance being attributed to T790M mutations (Wu et al 2016; Yu et al 2017).

Third generation TKI osimertinib, a mono-anilino pyrimidine compound that binds irreversibly with cysteine 797 residue in the ATP pocket, has been reported in clinical studies to be beneficial for patients with EGFR sensitizing mutations and the EGFR resistant mutation T790M. Mok et al (2017) conducted a randomized international open label phase III trial comparing clinical outcomes from EGFR mutation positive NSCLC patients placed on osimertinib versus patients placed on platinum+pemetrexed. The characteristics of patients recruited for this study were: patients who had previously been exposed to first generation TKI but had disease progression and had acquired a T790M mutation. The results showed that median PFS was significantly longer for patients with osimertinib when compared to patients with platinum+pemetrexed, 10.1 months vs. 4.4 months (HR= 0.30, 95% CI, 0.25-0.40, *P<0.001*). Overall response rate was significantly better with the group on osimertinib in comparison to the group with platinum+pemetrexed 71% (95% CI 65-76) vs. 31% (95% CI 24-40). Soria et al (2018), in a double-blind phase III trial study (FLAURA trial) compared the efficacy of osimertinib to first generation TKI in treatment naïve patients with EGFR mutations (exon 19 deletion or L858R mutation). PFS was the clinical outcome assessed. The results from this study showed that patients on osimertinib had a significant PFS when compared to patients on first line TKI (18.9 months vs 10.2 months HR-0.46 95%CI 0.37-0.57 *P<0.001*). The results from FLAURA trial suggested that osimertinib was beneficial to patients with T790M mutation and was superior to first generation TKI. Results from these studies resulted in the adoption of osimertinib as first line drug in patients with an EGFR mutation with metastatic NSCLC. Although osimertinib has been adopted as first line drug in patients with an EGFR mutation with metastatic cancer, around 30% of patients with metastatic NSCLC carrying an EGFR mutation receive no benefit from its use because of the type of EGFR mutation they harbour e.g., a C797S mutation has been reported to cause resistant to osimertinib (Thress et al 2015).

1.10 EGFR mutations and response to TKI

1.10.1 Common EGFR mutations associated with NSCLC and response to TKI

The focus of most studies evaluating EGFR mutation response to TKI have been exon 19 deletion; mostly 15 nucleotide deletions from nucleotide 2481-2495 or 2482-2496 eliminating codon 746-750, and point mutations of codon 858 on exon 21 where leucine exchanges for arginine L858R (Jackman et al 2006; Riley et al 2006; Maemondo et al 2010; Mitsudomi et al 2010; Zhou et al 2011; Janne et al 2012; Wu et al 2015). These mutations account for about 80-90% of all EGFR associated mutations in NSCLC (Castellanos et al 2016). Although, both mutations have been reported to have good response to TKI when compared to other EGFR mutations. Exon 19 deletions have been reported to have better treatment response, longer time to progression and overall survival than the L858R mutations with first generation TKI **(Table 1.6**). Jackman et al (2006) in a single centre prospective study evaluated response to erlotinib or gefitinib in 36 patients with either the exon 19 deletion or L858R mutation genotype and reported a response rate of 73% for patients with exon 19 deletion and 50% for patients with the L858R mutation. This group also reported better overall survival of 38 months vs. 17 months in patients with exon 19 deletions compared to L858R mutations. Similar results were obtained in the CALGB 30406 Phase II trial. The CALGB 30406 trials reported 83% vs.40% treatment response rates for exon 19 deletions vs L858R mutations. PFS (months) was reported as 15.7 vs. 12.6. Overall survival (months), of 31.3 vs. 29.8 was also reported. Patients with L858R mutation appear to have better clinical outcomes with second generation TKI when compared to their response with first generation TKI. Paz-Ares et al (2017), in a phase IIb randomized study compared the efficacy of first generation TKI to efficacy of afatinib in treatment naive patients with EGFR mutation (exon 19 deletion and L858R mutation) and reported that patients with the L858R mutation on afatinib had a superior response when compared to patients with the mutation on first generation TKI overall survival of patients with the L858R mutation on afatinib vs. gfitinib was 25.0 vs. 21.2 months (HR 0.91 95% CI 0.62-1.36 *P=0.6583*) respectively.

1.10.2 Uncommon EGFR mutations associated with NSCLC

The response of uncommon mutations to TKI is highly varied and less well understood. Uncommon mutations are sometimes associated with smoking status and old age, but the association is not strong. They are a distinct and highly heterogeneous sub group of NSCLC and account for approximately 10% of all EGFR mutated patients (Russo et al 2019; Attilli et al 2022).

1.10.2.1 Exon 18 Mutations

Mutations in exon 18 account for about 60-70% of uncommon mutations and have been reported as single point mutations, mixed mutations, deletions and insertions. These mutations are usually associated with male sex and smoking history (Leduc et al 2017). More than 80% of mutations on exon 18 involve the codons 719 or 709. The following variants have been reported G719X, G719A, G719C G719S and E709X. Exon 18 mutations have been reported to benefit from TKI as first line treatment as opposed to chemotherapy, particularly complex mutations involving G719A and G719X (Kobayshi et al 2013; Passaro et al 2018). However, the sensitivity of exon 18 mutations to TKI is highly varied and differs amongst the available TKI. G719X was reported by Yang et al (2015), in a post hoc analysis of uncommon mutations response to TKI in patients recruited for the Lux-Lung 2 Lux-Lung 3 and Lux-Lung 6 study to have a 75-78% response to afatinib as opposed to the 14-55% response rate to erlotinib or gefitinib reported by Frega et al (2017) and Chen et al (2017). However, the response to TKI by G719X is suggested to be short-lived. Heginer et al (2015), in a retrospective analysis of response rates of uncommon mutations to afatinib reported that for the 10 patients with G719X treated with Afatinib the median PFS was only 2.6 months. Preclinical studies, by Kench et al (2009) report that G719S is more sensitive to erlotinb than to gefitinib. Keam et al (2014), in an evaluation of rare mutations in NSCLC and its response to TKI reported a moderate response rate (33%) of G719A to geftinib or erlotinib. Costa et al (2016), reported a disease control rate of 100% and an ORR of 50% and a median time to progression as 12.2 months in one patient with the E709X mutation placed on afatinib. Other single mutations, on exon 18 that have been demonstrated to be responsive to TKI particularly second-generation versions are: V689M, S720P, S720I, P699S, N700D, G721A, V740A, L718P (Massarelli et al 2013). As regards, exon 18 insertions and deletions, little is known about tumours possessing these mutations' responsiveness to TKI due to insufficient data. A couple of relatively

old studies have suggested such malignancies are less responsive to TKI (Ackerman et al 2012).

1.10.2.2 Exon 19 deletions/mutations/insertions

Deletions in exon 19 are known to have a very good response to TKI. The superior response of exon 19 deletion appears to be associated with deletions around the LREA motif (residues 747-750). Chung et al (2012), in a retrospective analysis of response to TKI of 308 patients who were diagnosed with exon 19 deletions report that exon 19 deletions around the non LREA regions had the least overall response rates compared to those deletions from E746 or L747. The response rates reported from this study were; deletions in non LREA regions (42.9%), deletions from E746 (68.2%) and deletions from L747 (68.2%) (*P=0.6651*). PFS for non LREA regions, deletions E746, and L747 were 5.9, 9.8 and 10.5 months respectively. Exon 19 mutations account for less than 0.5% of EGFR mutations associated with NSCLC they are extremely rare kind of mutations (Russo et al 2019). Structurally, EGFR mutations are similar to EGFR deletions and have been shown to be sensitive to TKI. However, overall survival with this group is about 50% less than what is observed in patients with exon 19 deletion (Kobayshi et al 2016; Attili et al 2022). Sensitivity of exon 19 mutations to available TKI's is still not clear. The following mutations have been associated with variable sensitivity depending on the TKI treatment used L747F, P733L, K757R, and E746G. The following exon 19 deletions have shown resistance to TKI D761Y, E746V, and L747S (Klughammer et al 2016; Robichaux et al 2021).

1.10.2.3 Exon 20 mutations/insertions

After the common mutations (exon 19 deletions and point mutations L858R on exon 21) mutations and insertions on exon 20 are the third most common mutations associated with EGFR in the NSCLC pathology. This group of mutations is normally observed in non-smokers, tumours with the adenocarcinoma pathology, young patients and females. (Riess et al 2018). Exon 20 mutations and insertions are generally regarded as non-responsive to TKI. The exon 20 mutation T790M, a point mutation on codon 790 of exon 20 where methionine is substituted for threonine is the most clinically relevant of all exon 20 mutations and it is observed in about 2% of patients with stage IV advanced lung adenocarcinoma (Attili et al 2022). Several clinical studies have confirmed that this mutation confers primary resistance to EGFR TKI treatment and

about 50% of patients who have any of the common mutations and are responsive to TKI may develop a secondary T790M resistance mutation (Thatcher et al 2005; Sasaki et al 2007; Wu et al 2008; Yasuda et al 2013; Yang et al 2015). Chen et al (2016), in a meta-analysis study of three randomized controlled trials and 15 observational studies evaluated the co-existence of EGFR T790M mutation and common mutations. The group reported that T790M mutation is mostly likely to occur with L858R mutations than with exon 19 deletions and the rates of complex mutation of T790M with either exon 19 deletions or L858R mutation vary between 0.32-79%. The T790M mutation can occur as a germline mutation or induced by the tumour environment in its response to targeted therapy. The overall response rate and PFS in patients with the T790M mutation on first and second generation TKI have been reported as 10% and 2.5 months respectively. Structural, kinetic and molecular analysis of the T790M mutant EGFR receptors show that unlike the other common mutations that activate EGFR as well as having an increased affinity for TKI. The mutant T790M receptor has an increased affinity for ATP and competitively inhibits binding of EGFR TKI. This knowledge led to a design of a new drug (osimertinib) that has an irreversible binding activity with the ATP cleft (Robichiaux et al 2021). Other exon 20 mutations of clinical relevance are the C797S and S768I mutation. The S7681 mutation, has been associated with poor response to gefitinib. However, Yang et al (2015) in a post hoc analysis of response of uncommon mutations to afatinib and standard chemotherapy reported a better response to afatinib and a median PFS of 14.7 months in patients with S768I mutations. C797S mutation is associated with resistance to osimertinib (Thress et al 2015). Most exon 20 insertions are resistant to EGFR TKI especially insertions around the 762-775 residues e.g. D770_N771insNPG. Most patients with exon 18 insertions are associated with an ORR of 0-11% and a median PFS of 2-3 months when treated with TKI. However, these patients experience a higher overall response rate (58-63%) and better PFS of 6 months with platinum doublet chemotherapy. Patients with the A763_Y764insFQEA have been reported to benefit from treatment with TKI (Oxnard et al 2013; Russo et al 2019).

1.10.2.4 Rare mutations of exon 21

Rare mutations in exon 21, are usually associated with lower response /sensitivity to TKI when compared to the L858R mutation. The L861Q mutation is the second most common exon 21 mutation after L858R mutations. It accounts for about 1-2% of all EGFR mutations. Its oncogenic activity is comparable to what is observed in the L858R mutations (Banno et al 2016; Zhang et al 2017). Data from preclinical studies suggest that L861Q is less sensitive to EGFR TKI (particularly gefitinib and erlotinib) when compared to L858R mutations. An IC_{50} value of 92-103nM and 170nM was reported for cellular models of L861Q treated with erlotinib and gefitinib respectively. While an IC_{50} value of 4.5-6nM was reported for cellular models of L858R mutations. However, better sensitivity by L861Q was reported for afatinib and osmertinib an IC_{50} value of 0.5&9nM. This was similar to IC_{50} results of 0.2 & 2.5nM obtained for L858R (Kancha et al 2011). This has been validated in clinical studies. The NEJ002 prospective phase III trial comparing overall response of patients with EGFR mutations to gefitinib or platinum doublets reported a response rate of 33% for patients with the L861Q placed on gefitinib. Whilst Yang et al (2015) in a post hoc pooled analysis of response rates of uncommon mutations to afatinib reported a response rate of 56.3 %. Leduc et al (2017), in a retrospective multicentre study analysis of the clinical and molecular characteristics of 1,837 patients with EGFR mutation on TKI (gefitinib, erlotinib & afatinib) report better PFS and overall survival times for patients with the L858R mutations when compared with patients with the L861Q mutation PFS= 10.4 months vs. 4.5 months *P=0.003* (L858R vs. L861Q), overall survival=16.9 months vs. 12.2 months *P=0.04* (L858R vs. L861Q). Other mutations associated with exon 21 with low sensitivity are L861R, L862V, V851X, A859X. Mutations with uncertain sensitivity are E866K, H825L, P848L, H870Y, H870R, G863S (Kobayashi et al 2016: Russo et al 2019; Attili et al 2022).

1.10.2.5 Mixed mutations

About 4-14% of patients diagnosed with EGFR mutation in NSCLC have two or more mutations co-occurring together. The response of tumours with mixed mutations to available TKI is highly heterogeneous. Patients with exon 19deletion + L858R mixed mutation (classical mutation) appear to respond well to TKI in comparison with patients with classical mutations + resistant mutation (T790M) or classical mutations + rare mutations or combined rare mutations. Xu et al (2016) evaluated the response of

uncommon mutations to first generation TKI in 123 patients with NSCLC their results showed that patients with exon 19 deletion + L858R mutation had the best ORR 71.4% while patients with a classical mutation + T790M resistant mutation had an ORR of 22.2 % and patients with a classical mutation with an uncommon mutation had an ORR of 55.6%. Patients with rare mutations had an ORR of 46.7%. PFS reported for these groups were 9.53 months for combined classical mutations, 1.94 months for classical mutations and T790M mutation, 9.79 months for classical mutation with rare mutation and 2-8.9 months for combined rare mutations. Similar results was obtained by Zhang et al (2018), who evaluated response of 51 patients with mixed EGFR mutations to first generation TKI and reported an ORR of 75% for patients with mixed classical mutations, ORR of 60% for patients with combined classical and uncommon mutation and 71% for patients with combined uncommon mutations. PFS reported from this study was 18.2 months for combined classical mutation, 9.7 months for combined classical and uncommon mutations. 9.6 months for combined rare mutations and 1.4 months for combined classical or rare mutation+ T790M resistance mutation.

The response of mixed mutations to second generation TKI appears to be similar for combined classical mutations and mixed mutations involving the T790M resistance mutations but superior for combined rare mutations. Wu et al (2020), in a retrospective study compared the response of 195 patients with NSCLC who were diagnosed with an uncommon EGFR mutation and were stratified to either first generation TKI (gefitinib& erlotinib) or second generation TKI (afatinib). The results from this comparative study show there was no significant difference in treatment response or PFS for patients with combined classical mutations placed either on gefitinib or erlotinib or afatinib treatment response. Objective response rate reported for gefitinib, erlotinib and afatinib were 83.0% vs. 73.7 % vs. 88.2% respectively whilst, PFS was reported as 10.9 months vs. 8.5 months vs. 10.5 months respectively. However, a superior response was observed in patients with combined uncommon mutations placed on afatinib. Treatment response for patients with combined uncommon mutations on gefitinib and erlotinib was 38.9% and 20.0% respectively whilst patients on afatinib had a treatment response of 78.9%. PFS reported was 3.0 months vs. 0.9 month vs. 10.5 months for gefitinib vs. erlotinib vs. afatinib respectively.

The response of mixed mutations to third generation TKI is not clear because of insufficient data. However, available data indicates that response of uncommon mutations to third generation TKI appears to be heterogeneous and dependant on the type of mutations. Cho et al (2020) in a multicentre open label phase II trial evaluated the response of rare/uncommon mutations to osimertinib and reported that mixed mutations involving G719X and L861Q mutations had longer time to treatment failure when compared to mixed mutations with exon S768I.

1.11 Diagnosis of EGFR mutations in the clinic

1.11.1 Tumour biopsy / cytology for diagnosis of EGFR mutation in the clinic

The benefit of improved clinical outcomes that patients with EGFR mutations receive from having their treatment tailored to their genetic makeup and cost saving due to more rational use of TKI has resulted in the recommendation of molecular testing as the standard of care by the following regulatory bodies; American Society of Clinical Oncology, College of American Pathologist, International Association of the Study of Lung Cancer, Association of Molecular Pathology and the US National Comprehensive cancer network for planning treatment strategy(Kalemekrian et al 2017; Ettinger et al 2018; Lindelman et al 2018). Presently, in the clinic the gold standard for diagnosis of EGFR mutations is via tissue biopsy. This involves obtaining a fragment of the tumour through invasive biopsy and the application of molecular biology techniques such as PCR and NGS on the tumour fragment to detect the molecular alterations of EGFR. However, only about 60% of patients with NSCLC can obtain a molecular diagnosis from tumour samples because a good number of patients with NSCLC are either too sick for surgery or access to tumour sites is difficult /impossible causing a risk to health (Malapelle et al 2020). The available options, for diagnosis and or to obtain samples for biopsy and molecular characterization for advanced NSCLC involve the use of 18-22 gauge or fine needle aspiration for computerized tomography (CT) guided percutaneous biopsy, ultrasonography endoscopy guided biopsy and endobronchial ultrasound trans bronchial needle aspiration of mediastinal lymph nodes or other metastatic sites (Kangal-Shammar et al 2014; Vanderlaan & Roy-Chowduri 2020). These options are more expensive when compared with tissue biopsy, e.g., biopsy of paratracheal, peribronchial and intraparenchymal lung lesions cost as much as £1,610, while CT guided biopsy cost about £432 compared to £145 cost for tissue biopsy (National Institute for Health and Care Excellence, 2021). Furthermore, there are issues with

sample quantity and reduced tumour cellularity with these methods. Hiley et al (2016), evaluated challenges in molecular testing in NSCLC patients with advanced disease and reported that the sample quantity from the procedures discussed above is sometimes small and the cellularity is poor making it near impossible to obtain a good picture of a patient's tumour molecular pathology. This makes accurate selection of treatment for the best clinical outcome difficult or at the least delayed. Data from National Lung Cancer Audit in 2022 reported that the median time to obtain results for molecular characterization of tissue biopsy samples to diagnose EGFR mutations is 18 days. This timescale will be inadequate as some of these patients require an immediate treatment for the best clinical outcomes.

Missense mutations on exon 20 (T790M) resulting in resistance to TKI would require frequent monitoring of patients to know when to change the therapy. This would be impossible as the biopsy procedure is highly invasive. Finally, NSCLC tumours are highly heterogeneous; Hanjani et al (2017) in a prospective study to track the evolution of NSCLC analysed the whole exome from multiple regions of resected tumours from 100 patients with early-stage NSCLC prior to systemic therapy. This group reported massive intra-tumour heterogeneity in adenocarcinomas, mutations in EGFR, MET, BRAF and TP53 and about 75% of the tumours carried a subclonal driver aberration or mutation in genes such as PIK3CA, NFI, KRAS TP53 and Notch family members. Furthermore, this group also reported that without exome sequencing of at least 2 regions of the resected tumour that subclonal mutations may actually appear as clonal mutations. They suggested that multi region sequencing, repeated sampling instead of single sample analysis should be encouraged to adequately characterize molecular alterations for prioritization of drug targets and selection of therapies as drugs that target "True" clonal mutations give a more vigorous response as the mutations they target are seen across multiple sites of disease. As has been said, repeated sampling of the biopsy is not feasible because it is highly invasive, thus alternatives have been sought. Most of this, more recent, research has focused on components of tumours such as; circulatory tumour DNA (ctDNA), exosomes, circulatory tumour cells (CTC), mRNA and tumour educated platelets that may be isolated from blood (Lim et al 2018). ctDNA and/or cell free DNA (cfDNA) has been evaluated in several studies as a diagnostic tool for detecting EGFR

mutations in NSCLC have been adopted in the clinics as an alternative or complementary to tissue biopsy**.**

1.11.2 cfDNA/ctDNA as diagnostic tools for EGFR mutations in the Clinic

ctDNA, are DNA fragments shed from tumours into the blood stream through apoptotic and necrotic cellular mechanisms, active secretion of DNA from tumour cells or during the digestive mechanisms of macrophages (Karachiolou et al 2017). These DNA fragments are usually about 120-180bp in length and are present in the blood stream at low concentrations (5-10ng/ml). Several clinical studies have demonstrated the clinical utility of ctDNA harvested from plasma as diagnostic tools for EGFR mutation and therapy monitoring **Table 1.7.** All these studies involved the comparison of EGFR mutation results obtained from cfDNA to matched tumour biopsy samples to ascertain the sensitivity and specificity of cfDNA as a possible alternative to tissue biopsy for the diagnosis of EGFR mutations and therapy monitoring. Sensitivity of cfDNA for the detection of EGFR mutation from these studies ranged from 45%-100% with specificity ranging from 50-100% and concordance with result obtained from tissue biopsy was between 50-100%. Variability in sensitivity and specificity of cfDNA for the detection of EGFR mutations in these studies is attributed to the different technologies used in these studies. Technologies (**Table 1.7**) used in these studies are: mainly PCR and NGS have been used successfully in detection of EGFR mutation from tumour DNA extracted from blood particularly exon 19 deletion and L858R mutations (Cescon et al 2020; Fernades et al 2021). The success of these technologies in various clinical studies for detecting EGFR mutations from cfDNA isolated from patients with NSCLC resulted in the adoption/approval of these technologies for routine clinical use for the diagnosis of EGFR mutations from plasma by regulatory agencies. Cobas EGFR mutation test version 2 and Guardant 360 was approved by USA food and drug regulatory agency (FDA) for diagnosis of EGFR mutation from plasma following results from large scale studies that showed that these technologies were specific and sensitive for the detection of EGFR mutations from plasma (ASSESS study 2017; IGNITE study 2017; AURA study 2017; Papadimitrakopoul et al 2020). European Union Conformite Europene approved Therascreen EGFR RGQ PCR kit (Qiagen, EU) for plasma detection of EGFR mutation following results from IFUM study (Douliard et al 2014) that reported sensitivity of 65.7% and specificity of 99.7% of this technology for the detection of EGFR mutation from plasma. Amoy dx super arms EGFR mutation

plasma detection was approved by Chinese food and drug association after results from Li et al 2007; Zhou et al 2017 that showed a specificity of ≥ 90% for the detection of EGFR mutation from plasma using this technology.

Despite the success of cfDNA for the detection of EGFR mutations. Depending on the study between 20-50% of patients (**Table 1.7**) who have their blood samples analysed for EGFR mutations using cfDNA/ctDNA get a false negative result (particulary for T790M mutations). This group of patients would be denied therapies that will likely be beneficial to them. The challenge of low sensitivity associated with diagnosis of EGFR mutations using ctDNA has been linked to (1) poor precision of techniques employed for the molecular characterization of ctDNA and (2) the biology of ctDNA production- the production of DNA involves its shedding from apoptotic and/or necrotic tumour cells. Tumour cells that are resistant to therapy are usually anti-apoptotic and anti-necrotic (Kuepp et al 2022). This suggests that moderate to low sensitivity of cfDNA for detection of T790M mutations could be attributed to absence or low frequency of DNA shed from tumour cells bearing the T790M mutation. There is therefore an urgent need for the exploration or investigation for alternatives to tissue biopsy for detecting EGFR mutations that give robust information on the evolving tumour landscape.

Table: 1.7 Summary of selected clinical studies showing cfDNA as diagnostic tool for EGFR mutations

Study type	Sample size	Method of detection	Sensitivity PPA	Specificity PPA	Concordance with tissue biopsy	Reference
Prospective phase IV (IFUM study)	652	QUIAGEN therascreen EGFR RGQ PCR kit	65.7%	99.8%	94.3%	Doullia rd et al (2014)
Multi center ASSESS study	1162	QUIAGEN therascreen EGFR RGQ PCR kit Cobas EGFR mutation test kit version 2 Cycleave PNA-LNA PCR clamp	46%	97%	89%	Reck et al 2017
Multi center IGNITE study	2562	Cobas EGFR mutation test kit version 2	46.9%	95.6%	80.5%	Han et al 2017

Phase III prospective LUX-LUNG 3 &6 studies	600	Cobas EGFR mutation test kit version 2	60.5% (plasma) 28.6% (serum)	NR	NR	Wu et al 2017
AURA extension & AURA 2 phase II studies	210	Cobas EGFR mutation test kit version 2	T790M: 61% L858R: 76% Del19: 91%	T790M: 79% L858R: 98% Del19: 98%	T790M:65 % L858R: 85% Del19: 90%	Jenkins et al 2017
Retrospective AURA phase I	216	BEAMING (Sysmex)	T790M: 70% L858R: 86% Del19: 82%	T790M: 69% L858R: 97% Del19: 98%	NR	Oxnard et al 2016
Prospective multi center observational phase I TIGER X study	153	Cobas EGFR mutation test kit version 2 BEAMING (Sysmex)	Del 19/L858R-73%/82% T790M: 64%/73%	Del 19/L858R 100% T790M:98 %/50%	Del/L858R : 80% T790M:87 %/67%	Karlovich et al 2016
Prospective	180	Droplet Digital PCR (ddPCR)	Del19: 82% L858R: 74% T790M: 77%	Del19:100 % L858R: 100% T790M: 63%	Del19: 91% L858R: 80% T790M: 40%	Del19: 82% L858R: 74% T790M : 77%
Prospective	117	Droplet Digital PCR (ddPCR)	Del19:82% L858R:74% T790M: 77%	Del19:100 % L858R: 100% T790M:63 %	Del19: 91% L858R: 80% T790M: 40%	Zheng et al 2017
Retrospective Prospective	144(retrospective) 22(prospective)	NGS amplicon-based (Ion Torrent PGM®)	Del 19: 73% L858R or L861Q: 78%(retrospective) 78(prospective)	NR (retrospective) 92(prospective)	NR (retrospective) 86(prospective)	Kukita et al 2013
Retrospective TIGER X study	60	NGS amplicon-based (Ilumina Miseq platform)	T790M 93% L858R 100% Del19 87% (urine: T790M 72%; L858R 75% Del19 67%)	T790M 94% L858R 100% Del19 96% (urine: T790M 96%; L858R 100% Del19 94%)	NR	Reckamp et al 2016
Prospective	117	NGS HiSeq® 2500 (Illumina)	94%	100%	94%	Schwartzberg et al 2020

Retrospective from AURA 3 study	562	Cobas EGFR mutation test kit version 2 Droplet Digital PCR (ddPCR) Guardant 360	T790M-51%, L858R-68%, Del 19-82% T790M-58%, L858R70%Del1 973% T790M-66%, L858R-63%, Del19-79%	T790M-77%, L858R-99%, Del19-99% T790M-NR L858R-98% Del19100 % T790M-NR L858R-98% Del19-99%	T790M-61% L858R-88% Del19-88%	Papadimitrakopoulet al 2020
Prospective	15-del 19/L858R 11-T790M	Droplet digital PCR (ddPCR)	66.7%del 19/L858R 81.8%T790M	100%del19 /L858R 85.7%T790 M	70.6%del1 9/L858R 83.3%T790 M	Ishii et al 2015
Retrospective Phase I AURA open label multi-center study	103	Cobas EGFR mutation test kit version 2 QUIAGEN therascreen EGFR RGQ PCR kit Amplification refractory system (ARMS)	86%exon 19del L858R90% T790M41% 87%exon 19 del 78%L858R 29%T790M 100%exon19del 90%L858R 71%exon 19del 83%L858R 67%T790M	100%exon 19 del 100%L858 R 100%exon 19 del 100%L858 R 71%T790 M 97%exon1 9del 95%L858R 83%T790 M	89%exon 19 del 97%L858R 57%T790 M 100%exon 19del 100%L858 R 48%T790 M 83%exon1 9del 71%L858R 67%T790 M	Thress et al (2015)
Prospective	25	Cobas EGFR mutation test kit version 2	60%T790M	60%T790 M	61%T790 M	Sunderasan et al (2016)
Prospective West Japan Oncology group (WJOG8014LTR)	260	Droplet digital PCR (ddPCR)	75.8%TKI sensitizing mutations 64.5%T790M	87.5%TKI sensitizing mutations 70%T790 M	78%TKI sensitizing mutations 65.9%T790 M	Takhama et al 2016
Prospective Aura I and II extension study	534	Cobas EGFR mutation test kit version 2	61.4%T790M	78.6%T790 M	60%T790 M	Jenkins et al 2017
Prospective	50	NGS	50%T790M	87%T790 M	NR	Thompson et al 2016
Prospective	59	Droplet digital PCR (ddPCR)	42.8%T790M	97.3%T790 M	NR	Suzawa et al 2016
Prospective	21	PNA-LNA-PCR	40%T790M	100%T790 M	71%	Yoshida et al 2016

Single centre prospective study	N=105	Amoy dx Super Arms EGFR mutation detection kit	82% (TKI sensitizing mutations)	100% (TKI sensitizing mutations)	NR	Li et al 2017
Prospective study Aura 17	N=240	Amoy dx Super Arms EGFR mutation detection kit	49% (T790M)	99.8% (T790M)	NR	Zhou et al 2017

1.12. Circulatory Tumour Cells (CTC)

1.12.1 Physiology of CTC

Another biomarker from blood that has been explored as a possible alternative to tissue biopsy is circulatory tumour cells. CTC, as their name implies, are tumour cells shed into the blood stream (Pantel et al 2017). These tumour cells shed into blood stream may originate from primary or metastatic site and are usually identified by the presence of epithelial markers as most solid tumours are of epithelial origin. Epithelial markers distinct to cancer cells are; epithelial cell adhesion molecules (EpCAM), cytokeratin (CK), E-cadherin and epithelial splicing regulator 1 (ESPR1) (Barriere et al 2014; Lin et al 2021). Mesenchymal markers such as: vimentin, twist 1, fibronectin, N-cadherin, β-catenin, SNA1, AKT, $Loxl_3$ plastin3 and Zeb 1 are also distinct to cancer cells and have been used for the identification of CTC (Guan et al 2021). Additionally, markers specific to a malignancy can also be used to distinguish cancer cells from other cells in blood, e.g., HER 2, ER, AR, MRP (breast cancer), α folate receptor, telomerase activity (lung cancer) (Zhang, 2021). CTC have been proposed by scientists to be a true representation of molecular and genetic dynamics of cancer as they are descendants from multiple tumour sites. Secondly, CTC contain different varieties of cellular and subcellular components such as DNA, RNA and proteins that can be used to evaluate mutation (Wang et al 2017; Lin et al, 2021). Although the physiology of CTC looks promising as a diagnostic and monitoring tool for molecular oncology. There are issues with its isolation from blood as they are present at low concentrations in blood. It is estimated that there are around 1-20,000 CTC per 1×10^9 of blood cells. The amount of CTC present in the blood is dependent on tumour stage and malignancy type (Sawabata et al 2016). Despite the rarity of these cells in the blood, various approaches have been employed for its detection, isolation and molecular characterization of these cells from patients with NSCLC with good success (Nagrath et al 2007; Mashewaran et al 2008; Krebs et al 2011; Sudaerasan et al 2016). These approaches focus mainly on the physical properties of CTC and the principles of immuno-affinity for membrane bound markers and/or proteins expressed on its surface. The approach that focuses on the physical properties is dependent on the isolation of CTC based on the disparity in size

between CTC and other blood cells. CTC are about 8-20μm, while other blood cells are about 6-10μm and possess different deformability, dielectrophoresis and inertial focusing characteristics (Habil et al 2020). The approach that focuses on immuno-affinity is primarily based on isolation/detection of EpCAM positive CTC using anti-epithelial cell surface molecule antibody most often linked to magnetic particles or some immobile structures (Wang et al 2017).

1.12.2 Clinical validity/utility of CTC

1.12.2.1 CTC counts and NSCLC in clinics

Most clinical studies that have evaluated the validity of CTC as a biomarker in cancer have demonstrated CTC counts as prognostic and predictive markers. Presently the machine Cell Search (Menarini Sillicon Biosystems, Italy) which works with the principle of isolation of CTC using magnetic beads conjugated to EpCAM antibody and immunfluorescent staining for CK8/18&19 for its identification was approved by the US Food and Drug Agency (FDA) for the enumeration of CTC as predictive and prognostic markers for breast, colorectal and prostate cancer (Lim et al 2018). However, this technology has not been approved for use in lung cancer because of the high variable detection rates for CTC reported using this device for patients with NSCLC from numerous studies. Krebs et al (2011), analysed CTC obtained from 40 patients with stage IV NSCLC using the Cell Search technology and the isolation by size of epithelial tumor cells technology (ISET) and reported that CTC were detected in 9 out of 40 (23%) patients with counts ranging from 0-78 using the Cell Search technology and 32 out of 40 (80%) patients with counts ranging from 0-1,045 using the ISET technology. Similar detection rates were obtained from the following studies (**Table 1.8**) that used Cell Search device for isolation and enumeration of CTC to access its clinical relevance as prognostic and predictors of clinical outcomes in NSCLC.

Table 1.8: Detection rates of CTC from patients with advanced NSCLC using Cell Search

Reference	Detection rates
Isobel et al 2012	33% (8 out of 24 patients)
Hirose et al 2012	36.4% (12 out of 33 patients)
Muinelo-Romney et al 2014	41.9% (18 out of 43 patients)
Juan et al 2014	24% (9 out of 37 patients)

Crossbie et al 2016	22% (6 out of 27 patients)
Zhou et al 2017	40.08% (12 out of 30 patients)
Yang et al 2017	44% (47 out of 107 patients)
Lindsey et al 2017	40.8% (51 out of 125 patients)

Punnose et al (2012) reported a higher detection rate of 78% (28 out of 37) had a CTC detected from their blood sample. Poor detection rates with Cell Search have been attributed to (1) blood volume used by the device for CTC detection may not be sufficient for isolation of CTC as these cells are extremely rare (2) pre-processing steps before isolation of CTC may lead to destruction of these fragile cells (3) some CTC may not express the EpCAM protein perhaps due to epithelia to mesenchymal transition and thus may not be isolated (Banko et al 2019).

Although, variable detection rates have been reported using Cell Search device enumeration of CTC isolated from patients with NSCLC using this device suggest that CTC count are predictive and or prognostic of clinical outcomes. Numerous studies have associated CTC counts of ≥ 3-5/7.5ml in NSCLC as prognostic for shorter PFS and OS and predictive of poor response to therapy. Krebs et al (2011), in a single centre prospective study evaluated CTC count using Cell Search and its prognostic significance in 101 patients with advanced NSCLC before and after treatment with chemotherapy. Results from this study show that PFS and OS were significantly poorer in the CTC positive group when compared to the CTC negative group (median PFS: 6.8 months vs. 2.4 months, median OS: 8.1 months vs. 4.3 months). For the study CTC positive was recorded as ≥ 2/7.5ml of blood. Furthermore, patients who had ≤ 5 CTC/7.5ml of blood following treatment with chemotherapy had longer PFS and OS compared to patients with ≥ 5 CTC/7.5ml (median PFS: 7.6 months vs. 2.4 months, median OS (8.8 months vs. 4.3 months). CTC count as predictor of response to treatment was evaluated by Punnose et al (2012). This group evaluated CTC in association with clinical endpoints in phase II clinical trials with pertuzumab and erlotinib. In this study, CTC counts were analysed in 38 patients using Cell Search before and after treatment. The results from the study associated reduction in cell count 56 days following treatment as positive response to treatment and longer PFS. Similar results were obtained from studies outlined in (**Table 1.8**).

Another clinically validated immuno-affinity-based device that has been explored for CTC isolation and enumeration in NSCLC patients is the GILUPI CELL Collector (Nanomedizini, Germany). This device isolates CTC from blood invivo via the insertion of an anti-EpCAM functionalized wire into cubital vein. As blood passes through the anti EpCAM functionalized wire EpCAM positive cells (CTC) binds to anti EpCAM antibody present on the wire this ensures capture of CTC. Luecke et al (2015) isolated CTC from 62 patients with either NSCLC or SCLC using this device and Cell Search and reported a detection rate of 73% for GILUPI CELL Collector and 29% for Cell Search. The disparity in detection rates between the two devices has been suggested to be due to higher blood volume that the GILUPI CELL Collector analyzes; the Collector can analyze up to 1.5 litres of blood whereas the Cell Search uses 7.5 ml.

1.12.2.2 CTC and molecular characterization for EGFR mutation in NSCLC

Aside from enumeration, the possible clinical utility and validity of studying EGFR mutations in CTC as diagnostic tool has also been explored in various small-scale studies with conflicting results that appear to be affected by the techniques used in isolation and mutation analysis. The use of CTC as an efficient tool for molecular analysis is influenced greatly by purity of CTC isolated, CTC counts and technique used in detecting the EGFR mutation (Alix-Panabieres 2020; Rushton et al 2021). When CTC are impure their mutational signatures can be drowned in the large noise of wild type DNA of other blood cells (contaminants). Secondly, if CTC isolated is not representative of the activities in the tumour microenvironment it could result in under reporting of molecular alterations present. High CTC counts increases the likelihood of obtaining CTC that embody all molecular events in a malignancy (Park et al 2016; Habil et al 2020). Cell Search device (**Figure 1.7**) has been explored as a platform for processing CTC for subsequent molecular characterization. Punnose et al (2012) analysed CTC obtained from 38 patients with advanced NSCLC using Cell Search technology (Menarini, Biosystems) for EGFR mutation and reported a concordance of 12.5% in mutation results obtained when compared with matched tissue biopsy samples. Poor sensitivity associated with this study has been attributed to low purity of CTC isolated (Myung&Hong 2015; Cho et al 2018; Habil et al 2020). Marchetti et al (2014), evaluated the correlation of EGFR mutation detected from basal tumour biopsy and EGFR mutation detected from CTC in 37 patients enrolled in the TRIGGER study. This group isolated CTC using Cell Search and detected EGFR mutation using NGS.

EGFR mutation was detected in 31 of the 37 (84%) patients recruited for the study. The disparity in detection rates between the study by Punnose et al (2012) and Marchetti et al (2014) was due to (1) improved purity of CTC analyzed for mutation which involved a 6 hour long process of lysis of CTC, extraction from cartridge, washing, digestion and extraction of nucleic acid and (2) NGS technique used to evaluate for EGFR mutation is a more robust and sensitive technique for molecular characterization compared to the real time quantitative TaqMAN technique used in the study by Punnose et al 2012. CTC isolation by Cell Search, adding a post processing step to improve CTC purity and use of NGS for detection of EGFR mutation seems promising as a sensitive technology for CTC processing for molecular characterization for EGFR mutations in NSCLC. However, its routine use in the clinics is hampered by the long and laborious process required to ensure purity of isolated CTC (**Table 1.9**).

The GILUPI Cell Collector (**Figure 1.7**) as discussed previously is an in vivo immuno-affinity based technology. The Collector has also been explored as a platform for processing CTC for subsequent molecular characterization. Scheumann et al (2015), evaluated CTC count from 50 patients with NSCLC or SCLC and characterized CTC isolated using the GILUPI cell collector for EGFR and KRAS mutations using digital droplet PCR technique and reported a concordance of 100% in EGFR mutation results obtained from CTC isolated and EGFR mutation results obtained from matched tumour biopsy samples. Utility of the GILUPI Cell collector as a platform for processing CTC for subsequent molecular characterization for EGFR mutations may be impeded because: (1) it is more invasive than a single blood draw; (2) may require post enrichment techniques to ensure purity of CTC isolated; and (3) harvesting CTC from wire is a cumbersome process (**Table 1.9**) (Rushton et al 2021).

Adna test device (**Figure 1.7**) has also been explored for CTC detection and subsequent molecular characterization for mutations. This device works with the principle of immuno- magnetic separation like Cell Search. However, it has no automation in its workflow process. Its work flow process involves: pre-labelling of samples with magnetic beads conjugated to multiple antibodies (anti EpCAM, anti HER2, anti EGFR) and then washing samples on a magnetic stand with an Adna wash leucocyte reducer to ensure purity of CTC. To retrieve mRNA for subsequent molecular characterization, the CTC selected is lyzed and then RT-PCR experiments is performed

to analyse for mutations in TWIST 1, AKT-2 and P13KA genes but not for mutations in EGFR (Maly et al 2019). Although this device has been explored for CTC isolation for downstream analysis in NSCLC. Its usage in the clinics can be improved by improving its cumbersome work flow process of pre-labelling, washing and lyzing of samples (**Table 1.9**).

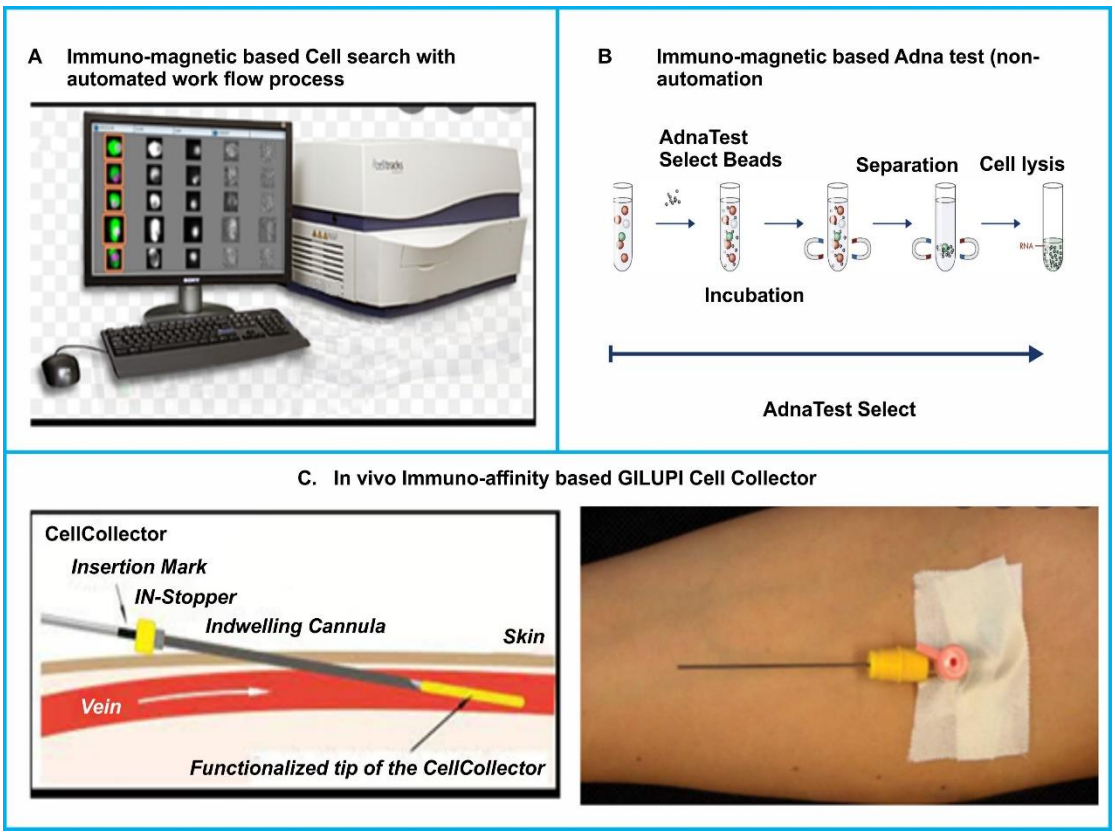

Figure 1.7 Bench top devices for CTC isolation that have explored CTC isolated for molecular characterization in NSCLC (A) CELL Search (B) Adna test work flow (C) GILUPI Cell collector

Table 1.9 Summary of key characteristics of bench top devices

Device	Brief description	Limitations
Cell Search	In-vitro lmmunomagnetic based device. Anti-EpCAM antibody is linked to a ferritin molecule to capture EpCAM positive cells	Pre-labelling may lead to loss of cells. poor purity and yield
Gilupi Cell Collector	Invivo immuno-affinity based isolation device. Anti-EpCAM antibody is linked to a gold-plated tip on a nanowire to capture EpCAM positive cells that flow through the wire when the wire inserted into the vein	Cumbersome process to harvest cells for downstream analysis and poor purity
Adna test	Invitro Immunomagnetic based device. cock-tail of antibodies is linked to a magnetic particle to capture CTC	Rigorous workflow process

1.12.2.3 Microfluidic technology for CTC isolation and detection of EGFR mutations in NSCLC

Microfluidic technologies have also been explored as platforms for CTC processing for molecular characterization to detect EGFR mutations. The theory behind clinical application of microfluidic technologies is the miniaturization of normal biological assays and the use of special design considerations that entails the fabrication of devices with intricate geometrics with precise dimensions on a microscale, surface functionalization and use of biocompatible materials. This has given rise to devices that: (1) precisely control the physics, chemistry, biology and physiology of cells and cellular events of interest in an assay (2) reduced reagent consumption as device operates at a microscale leading to cost reduction; (3) short processing time (1-4 hr) due to miniaturization and rational design; and (4) portable devices that can be used for point of care testing (Rushton et al 2021). Microfluidic technologies explored for CTC isolation and subsequent molecular characterization for EGFR mutation in NSCLC have employed mainly differences in biochemical characteristics between CTC and other blood cells for its isolation from blood. Better outcomes, in terms of capture rates of CTC and improved sensitivity and specificity in molecular characterization of EGFR mutations using microfluidic chip technology plus PCR and or NGS techniques when compared with Cell Search technology have been demonstrated (Stott et al 2010; Myung & Hong 2015; Earhart et al 2014; Sunderasan et al 2016). The success recorded by microfluidic devices for the isolation and molecular characterization of CTC in NSCLC is largely due to the ability of microfluidic device/techniques to enable high efficient processing of complex fluids such as blood with minimal damage to sensitive

cells as a result of rational design of devices with intricate structures and geometrics that control blood flow within narrow limits to allow for maximum interaction of cell of interest (CTC) with corresponding antibody functionalized on the surface of the chip or tagged to a magnet with minimum damage to cells. The antibody of choice for most of the microfluidic device that have explored CTC isolation for molecular characterization is anti-EpCAM (Cho et al 2018; Rushton et al 2021). In addition, microfluidic devices have also employed differences in size and deformability amongst cells in the blood for the isolation of CTC for subsequent analysis for EGFR mutation.

1.12.2.3.1 CTC chip

The first device to use microfluidic technology as a platform for processing CTC for subsequent molecular characterization for EGFR mutation was the CTC chip. The CTC chip designed by Nagrath et al (2007) is made up of a silicon wafer similar in size to a microscope slide. Etched onto the chip are 78,000 micropost functionalized with anti EPCAM antibody (**Figure 1.8**). When blood is pumped into the chip the antibody coated microposts break up the flow stream during blood flow thereby enhancing cell surface interactions with anti-EpCAM on the surface of the microposts. CTC positive for EpCAM adhere to the microposts etched on the chip while contaminating blood cells (red blood cells and white blood cells) are moved to the waste outlet. Captured cells are harvested from the chip by means of enzymatic digestion. The possible utility of this device as a platform for CTC isolation and subsequent molecular characterization in the clinics was demonstrated by Maheswaran et al (2008) who reported high detection rates for CTC using the CTC chip to isolate CTC from 27 patients with advanced NSCLC attending the Massachusetts General Hospital. This group captured CTC from each patient at a range of 5-771 per 10ml of blood sample. Following isolation of CTC, DNA was extracted and molecularly characterized for EGFR mutations using allelic specific polymerase chain reaction amplification: the Scorpion Amplification Refractory mutation system (SARMS technology). The result obtained was compared with EGFR mutation results obtained from matched cfDNA and tissue biopsy samples. This group reported a concordance of 95% of EGFR mutations results obtained from CTC and matched tumour biopsy samples. Mutations identified from CTC were: exon 19 deletions, exon 21 mutations and T790M mutation. Its adoption in the clinics for routine use for EGFR mutation detection and treatment monitoring in NSCLC has been marred by (1) reproducibility- the intricate micropost

design may be too difficult to reproduce to meet hospital demands (2) laborious process for removal of captured CTC from chip (3) poor throughput- samples are analysed at 1ml/hr. i.e., to analyze 5ml of sample will take a total of 5hours.

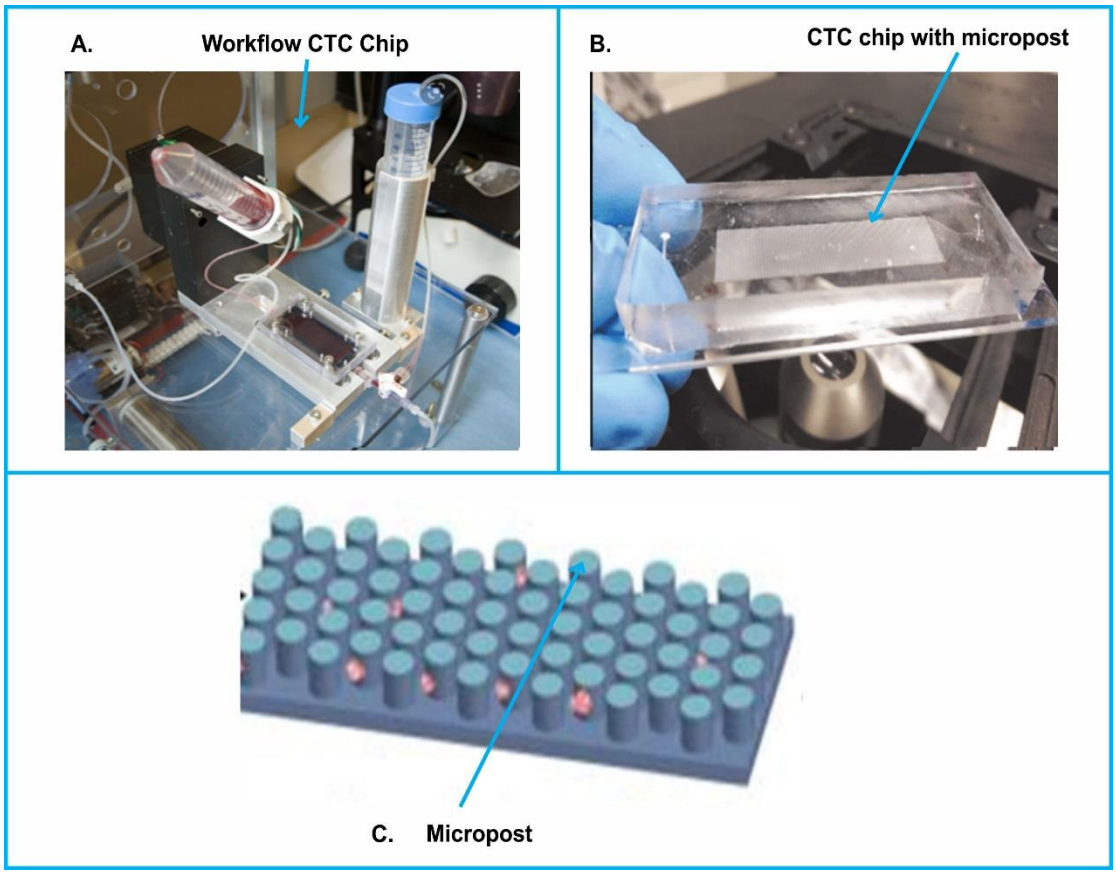

Figure 1.8 CTC Chip*:* (A) workflow of CTC chip showing blood flow inlet and waste outlet (B) microfluidic silicon chip with micropost (C) schematic representation of CTC captured on micropost**.** Nagrath et al (2007*).*

1.12.2.3.2 Herringbone Chip

Another immuno affinity based microfluidic device explored for CTC isolation and subsequent molecular characterization for EGFR mutations in patients with NSCLC is the Herringbone chip (**Figure 1.9**). Sundaresan et al (2016), in a prospective feasibility study to evaluate the potential of CTC as a therapy monitoring tool for EGFR resistance mutation used this chip for CTC isolation. The Herringbone chip is an improvement in the design of CTC chip used by Maheswaram et al (2008). The initial device had issues with limited interactions with blood and micropost because of the uniaxial and laminar flow principle by which it works, this limited CTC capture. Furthermore, the design of the micropost was complex this affected its reproducibility. Also, efficient capture with

this chip can only be achieved at a flow rate of 1ml/hr. The Herringbone chip (**Figure 1.9**) is made up of a 1 × 3 glass slide bonded to polydimethylsiloxane (PDMS). This chip comprises of eight channels with surface ridges (herringbones). The walls of the chip are coated with antibodies against EpCAM. Blood gets into the chip through a branching inlet that feeds into the eight individual channels. The geometric architecture of the chip is used to induce chaotic mixing to disrupt the stream during blood flow. This design maximized interactions between CTC and the antibody coated wells and worked best at a flow rate of 1.2ml/hr. This device was used to isolate CTC from 28 patients with advanced NSCLC. The CTC isolated were characterized for TKI resistance EGFR mutation (T790M) using PCR techniques. Mutation results obtained from tissue biopsy showed that 50% of the patients' samples had T790M mutation and there was a concordance of 74% of mutation results obtained from CTC with tissue biopsy. This study also evaluated the concordance of results for the detection of T790M mutations in CtDNA and tissue biopsy and the result was 61% using 32 matched plasma and tissue biopsy samples. The results from this study showed that Herringbone microfluidic device can be used as a platform to isolate CTC for therapy monitoring in NSCLC. One major drawback of this device that has hampered its possible routine use in the clinics is that the isolation time is long; it takes about 2-4 hours for capture and isolation. Another challenge that has limited its routine use in the clinic is post capture handling of CTC, i.e., this is a laborious process of harvesting CTC bound to stationary structures on chip.

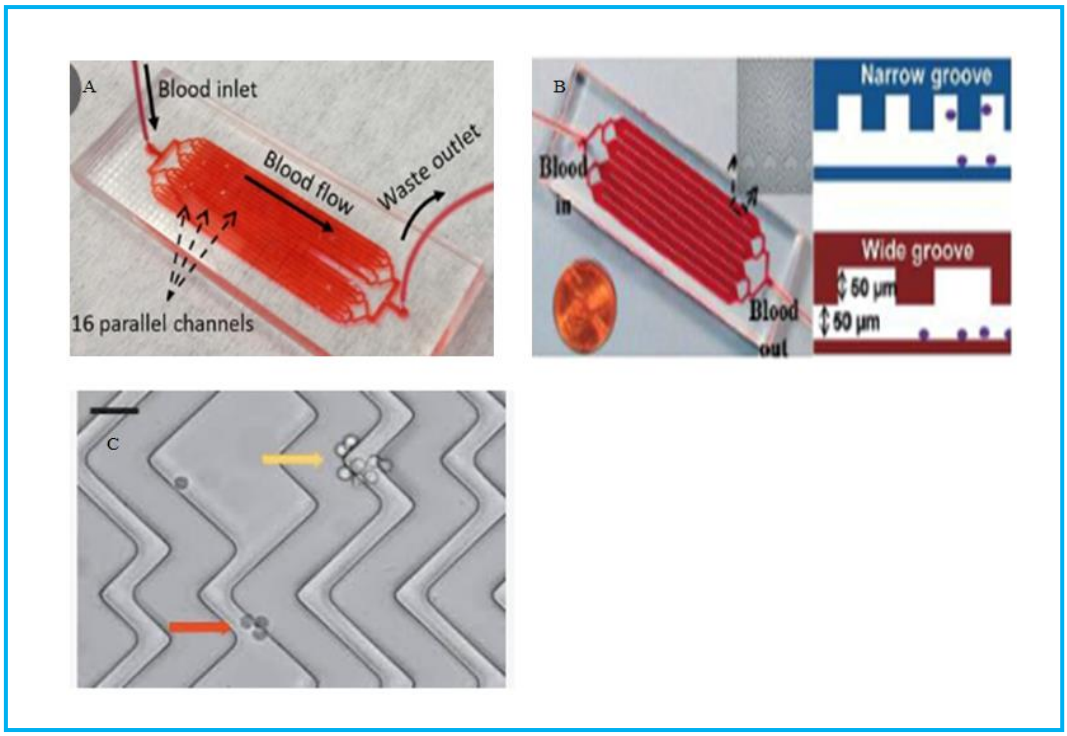

Figure 1.9 Herringbone Chip (A**)** CTC chip with Herringbone pattern on the channel roof, with a single blood inlet and waste outlet. (B) Herringbone chip showing dimensions of groove (C) electron microscopy showing CTC bound to groove during capture. Sundaresan et al (2016)

1.12.2.3.3 Nano Velcro chip

The Nano Velcro chip is another microfluidic device that has isolated CTC from blood of patients for subsequent molecular characterization for EGFR mutations. Ke et al (2015) designed a Nano-Velcro chip (**Figure 1.10**). The chip is made up PDMS with embedded silicon wires coated with anti EpCAM antibody and an overlay of a chaotic mixer to ensure adequate mixing of blood with coated silicon wires when blood is passed through the chip. CTC purity is optimized by the digital/systematic modulation of surface chemistry, flow rates and the presence of a thermos responsive polymer brush grafted into silicon wire to modulate heating and cooling cycles at temperature ranging from 4-37^{O}C. The isolated CTC are captured at 37^{O}C via a laser capture micro dissection unit ensuring high precision of single CTC for down stream analysis. The possible clinical utility of this device in the management of NSCLC was carried out in a study involving detection of EGFR mutations; L858R and T790M from CTC of 7 patients with advanced NSCLC. The results obtained were compared to EGFR mutations of matched tissue biopsy samples. This group reported a concordance of 100%. Although the results from this study seem promising, there are issues with low

throughput. Analysis of blood for CTC isolation was at 5ml/hr. The procedure is quite cumbersome for everyday use in the clinic, the CTC purification process alone happens over two rounds totalling 3 hours.

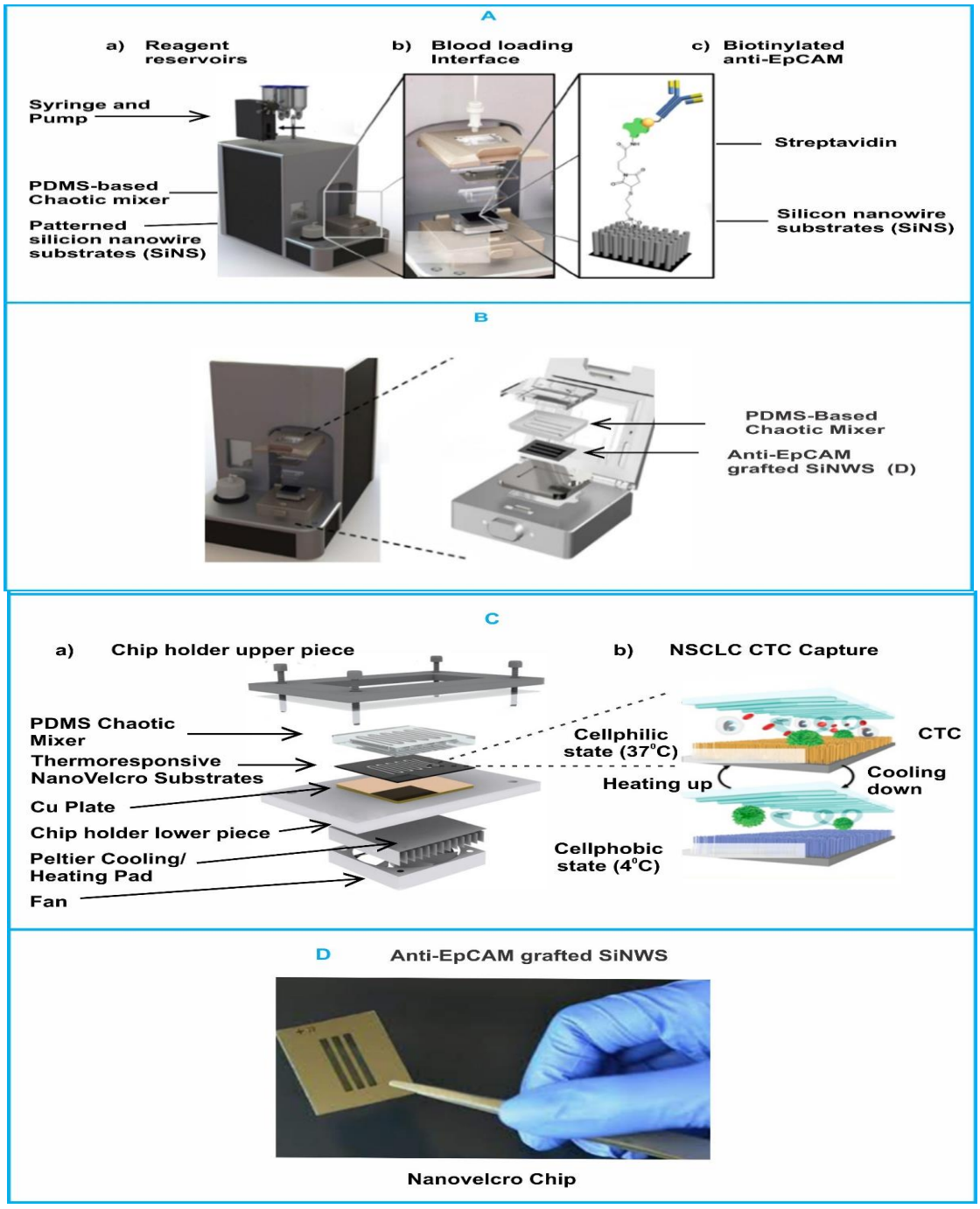

Figure 1.10*:* Nano Velcro Chip (A) work mechanism of NanoVelcro chip (B) schematic representation of chaotic mixer and silicon nanowire substrate (SINW) (C) schematic representation of mechanism of operation of the NanoVelcro chip (D) silicon nano wire substrate chip. Ke et al (2014).

1.12.2.3.4 Weir microfluidic device

Yeo et al (2015) designed a microfluidic device measuring 3.5cm×2.5cm fabricated from polydimethylsiloxane (PDMS) sheets (**Figure 1.11**). This device was designed for single cell isolation and retrieval using the principle of hydrodynamics and fluid viscous ratio. The device comprises of ten chambers lined along the outer curvature of the channel. Each chamber consists of a weir structure that allows for fluid resistance when occupied with a cell. Hydrodynamic force and the application of a sheath flow buffer will push cells entering the device into a single cell stream. The cells move into the chamber through differential pressure in the chamber and pull by a centrifugal force. Weir structures in the chamber resist fluid flow once a cell has been captured in the chamber. Collection of cells from the chamber is through positive pressure that pushes them into the main stream and then into a collection port. A single trapped CTC can be released on demand to the main channel by positive pressure. For accurate and pure selection of cells this process may have to be repeated several times. CTC isolated using this method was used to evaluate L858R mutation and T790M mutation using PCR in 7 patients with advanced NSCLC. EGFR mutation results obtained from CTC isolated using the device showed a concordance of 100% with matched tissue biopsy samples. The possible utility of this method in the clinic seems promising but it is a laborious process. Furthermore, it has poor throughput and may require highly specialized technical knowhow.

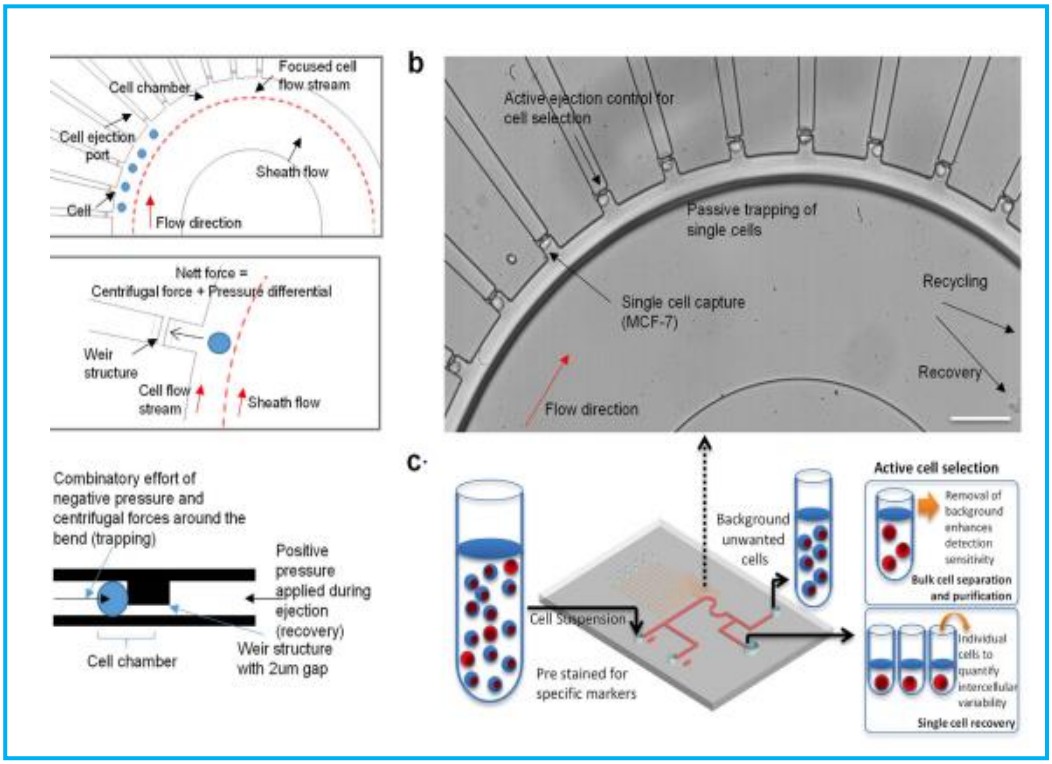

Figure 1.11: Weir Microfluidic device A&B-schematic representation of capture mechanism using hydrodynamic focusing C- work flow for capture of CTC using Weir microfluidic device. Yeo at al (2016).

1.12.2.3.5 Magnetic Sifter

The magnetic sifter designed by Earhart et al (2014), has also been explored for the isolation of CTC for subsequent molecular characterization for EGFR mutation in NSCLC. The Magnetic Sifter bio chip (**Figure 1.12**) is a magnetically active porous filter made up of silicon wafers with 40µm hexagonal shaped holes in a silver nitride membrane. The surface of the magnetic Sifter biochip is coated about 12µm thick with magnetically soft permalloy and pacified with silicon oxide to make the surface hydrophobic. Before isolation of CTC from blood, the blood sample is pre-labelled with streptavidin conjugated magnetic nanoparticles and biotintylated anti-EpCAM antibodies. The labelled sample is then pumped into a magnetic sifter, which is a dense array of magnetic pores with large equivalent magnetic forces that capture CTC coated with anti-EpCAM magnetic nanoparticles when an external magnetic field is applied. Release of captured CTC is through the removal of the magnetic force. Park et al (2016), made an improvement to this microfluidic device by creating an integrated multigene nanoplatform. This integrated nanoplatform comprises of a magnetic sifter

as described above and a nanoplatform impregnated with modular gene panels that can identify CTC and a therapy prediction and monitoring panel test. CTC captured via the magnetic shifter is seeded into a nanowell via the removal of the magnetic force. In the nanowell, fluorescence microscopy allows for the identification of captured CTC. After microscopy RT-PCR is used to detect for EGFR mutations in CTC on nanowell. The whole process takes about 6 hours. This group, using this integrated microfluidic device were able to isolate CTC from 31 patients with NSCLC and characterize CTC isolated for EGFR mutations. The device was able to detect EGFR 19 deletion, L858R and T790M mutations from seven NSCLC patients. The utility of this chip in the clinic seems promising because of the integration of different techniques on the device. However, its applicability in the clinic for routine use has been limited due to multiple experimental steps involved in the assay this makes the use of this technology tedious.

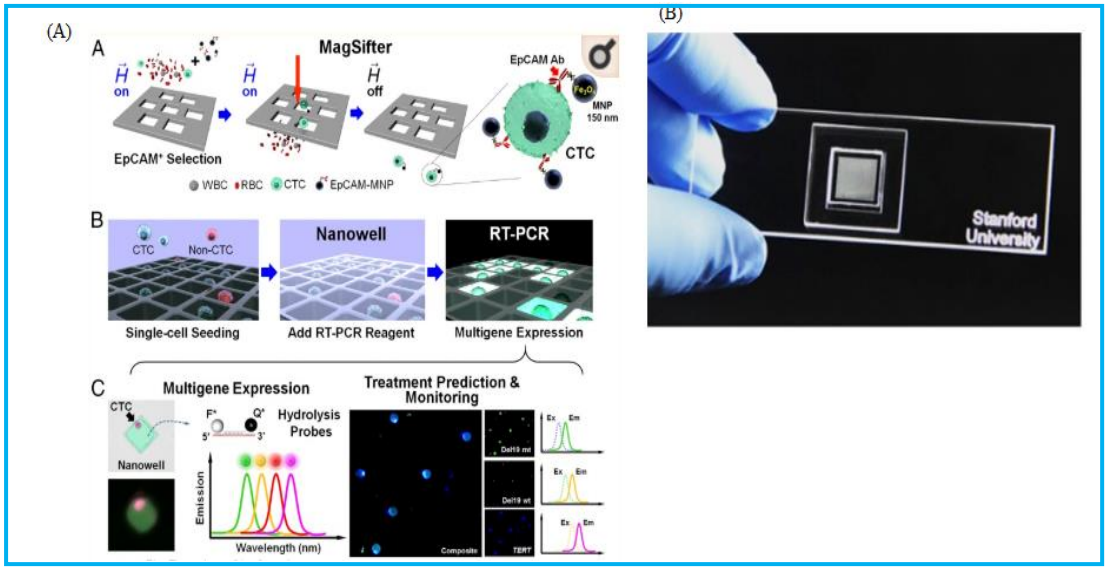

Figure 1.12 Mag Sifter*:* (A) mechanism of CTC isolation and characterization using MagSifter (B) Mag sifter chip (C) molecular characterization of CTC isolated. Park et al (2016)

1.12.2.3.6 Oncobean chip

The Oncobean chip was designed by Muridhar et al (2014) to further improve microfluidic technology as a platform for CTC processing for downstream analysis of EGFR mutations. The Oncobean microfluidic device (**Figure 1.13**) is a radial flow microfluidic device model. It differs from CTC chip and Herringbone chip linear flow based immuno-affinity microfluidic devices. This group hypothesized that the constant velocity across every cross section in linear flow based microfluidic device will be a

major limitation for efficient capture of CTC. The Oncobean chip is a PDMS chip bonded onto a glass slide. The bean shaped micropost with a radial flow design ensures a decrease in velocity with increasing cross sectional area, this result in varying shear rates at every radius and maximizes interaction of cells with anti-EpCAM antibody on bean shaped micropost. The Oncobean chip microfluidic device operates at a flow rate of 10ml/hr. Muridhar et al (2017) evaluated the clinical utility of this chip in 36 patients with NSCLC. Blood was collected from the pulmonary vein and peripheral vein of these patients. The CTC counts from the pulmonary vein were between 0-10,278/3ml and the CTC from peripheral vein varied from 0-28.5/3ml. Molecular characterization of CTC of six of the samples using RT-qPCR biomarker somatic mutation PCR array revealed the following mutations in EGFR, KRAS PIK3CA and TP53. The utility of this device in the clinic for isolation of CTC for detection of EGFR mutation and treatment monitoring in NSCLC is hampered by the laborious process it takes to harvest CTC from the device.

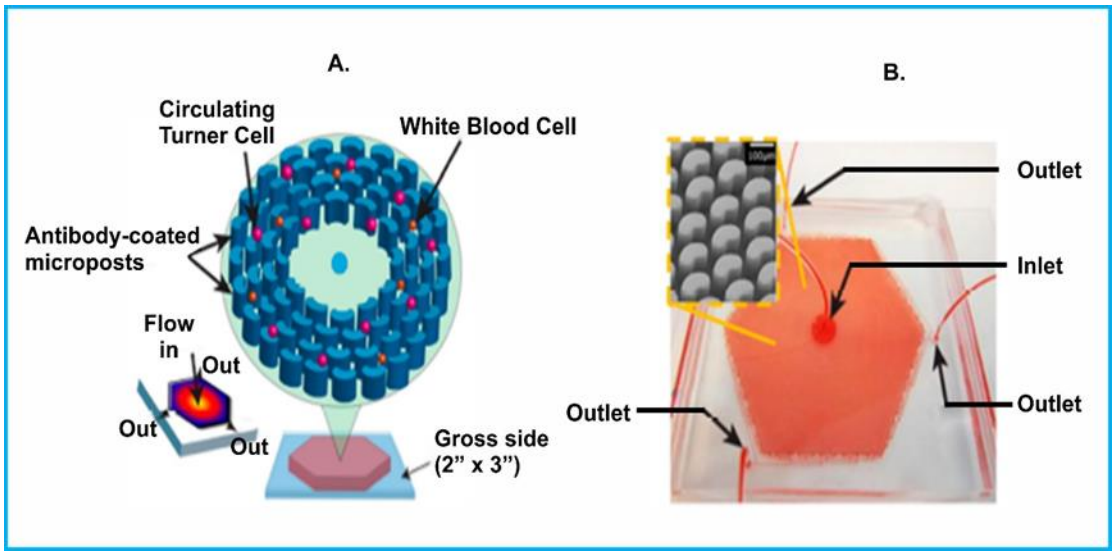

Figure 1.13 Oncobean chip: (A) schematic representation of Oncobean chip with CTC bound to antibody coated micropost with a radial design (B) Onocobean chip showing blood inlet and outlets. Murlidhar et al (2017).

1.12.2.3.7 Spiral microfluidic chip

Spiral microfluidic chip designed by Warkhani et al (2016) is a chip made from PDMS with a spiral design (**Figure 1.14**). CTC are isolated from the device when blood and sheath fluid running at 1.7ml/min are pumped into device the inertia lift and drag forces in the fluid flow cause larger cells (CTC) to stick close to the microchannel inner walls.

Whilst the smaller WBC and platelets move towards the outer wall. Purification of CTC is facilitated by 2 rounds of enrichment. Kulasinghe et al (2019), demonstrated the clinical utility of this device to isolate CTC for subsequent molecular characterization in 35 patients with advanced NSCLC. This group isolated CTC from 26 of the patients recruited and CTC counts per patient was between 3-55 cells/ml. CTC isolated was characterized for molecular alterations using immunocytological techniques. A 100% concordance was reported for EGFR mutation results (exon 19 deletion) obtained from tumour biopsy when compared to analysis for EGFR mutations from CTC stained with antibody specific for exon 19 deletion ELREA. The adoption/utility of this device in the clinic for CTC isolation and subsequent molecular characterization may be limited because of cumbersome process of pre lysing blood before commencement of test and 3-4 rounds of enrichment process before molecular characterization.

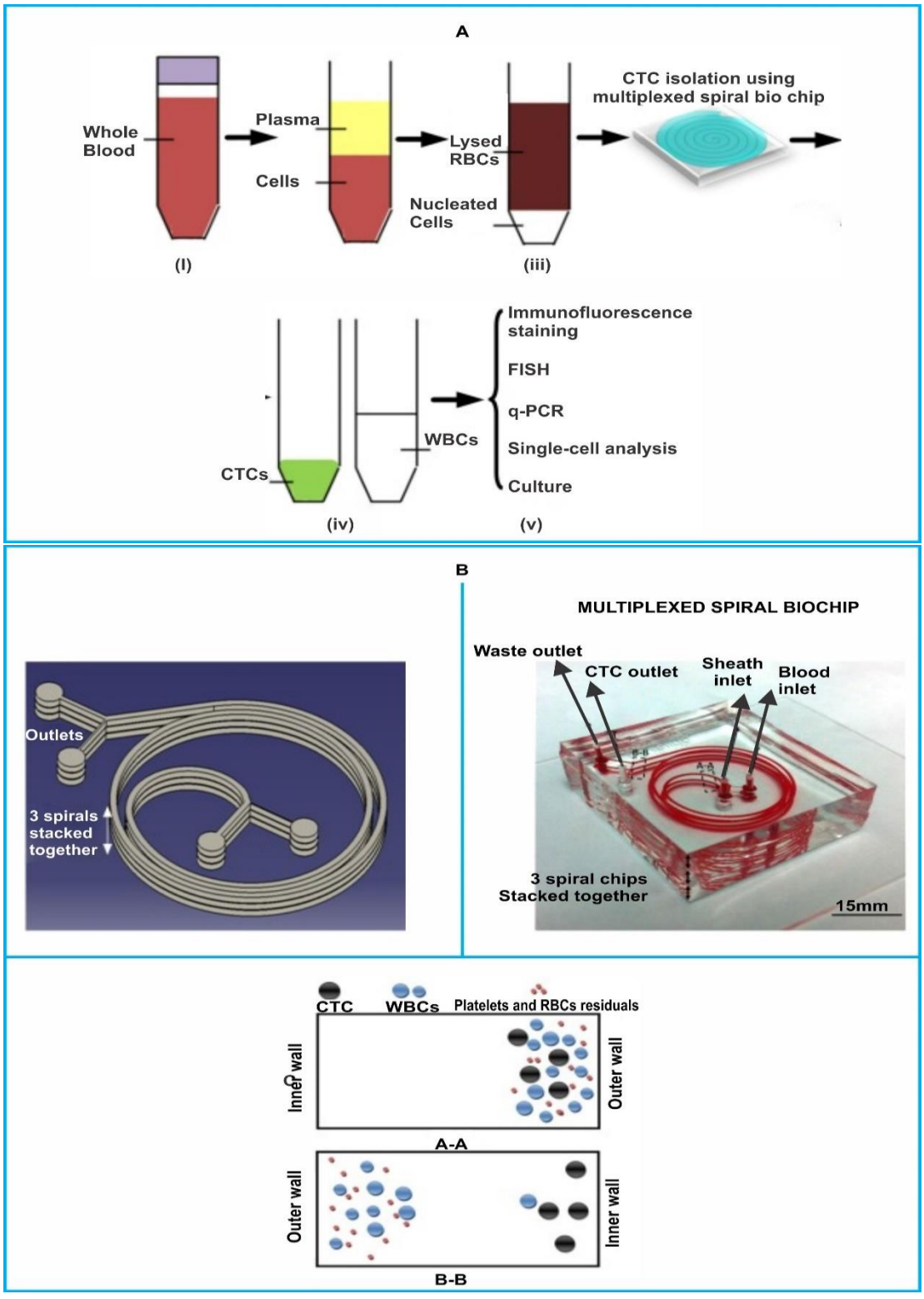

Figure 1.14 Spiral Microfluidic chip: (A)- Work flow for CTC isolation and characterization using spiral microfluidic (B)- Schematic representation/picture of spiral microfluidic chip showing inlets, outlets and how contaminants are isolated from CTC. Kulasinghe et al (2019).

1.12.2.3.8 Fluid Assisted Separation Technology disc platform (FAST)

The FAST disc microfuidic device (**Figure 1.15**), designed by Kim et al (2017), is a device that employs differences in density and size for separation of CTC. The forces applied are centrifugal and fitration to isolate CTC from blood cells. CTC is isolated when blood is put into the disc and spun in a centrifuge. The larger CTC will collect on the filterpaper at the bottom of the disc. Lim et al (2020), evaluated the utility of the FAST disc in isolating CTC and analysis of CTC isolated for EGFR mutations in 40 patients with advanced NSCLC. This group reported that CTC were isolated from all patients recruited for the study mean CTC isolated was 67 CTC per 7.5ml of blood. Exon 19 deletion, L858R and T790M mutations were also detected from CTC isolated from the device using qRT-PCR technique. The EGFR mutation results obtained from CTC were 100% concordance to what was obtained from tissue biopsy samples.

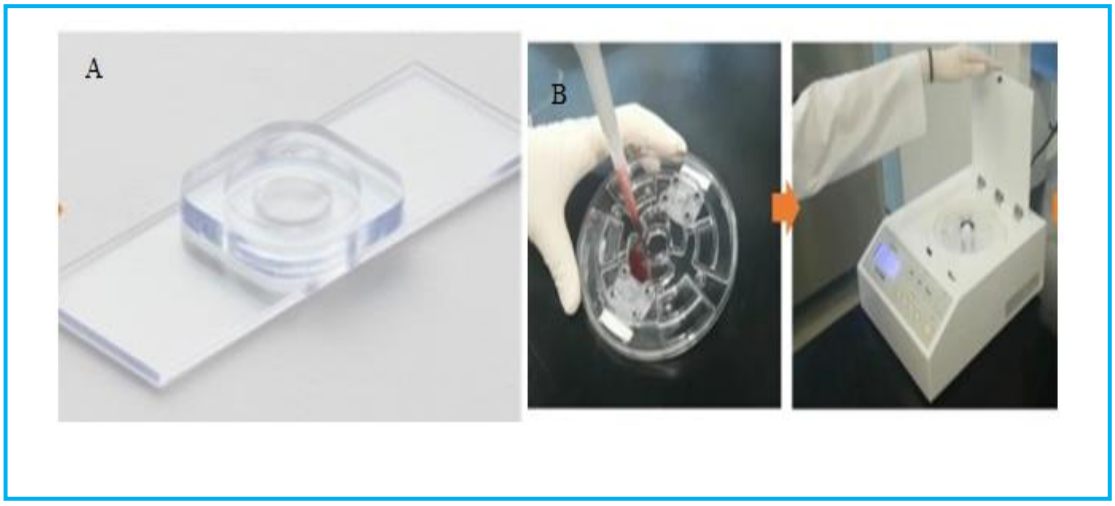

Figure 1.15: (A) FAST disc microfluidic chip (B) work flow blood is loaded onto FAST disc and then placed in centrifuge. Lim et al (2020)

1.12.2.3.9 Parsotrix microfluidic based semi-automatic bioanalyzers

Parsortrix microfluidic device (**Figure 1.16**) is a semi automatic bioanalyzer designed by (Angle, North America, King of Prussia, PA). This device isolates CTC from blood based on differences in size and deformability. It is a 2 part system comprising of a re-usable cassette clamp for microfluidic chip and a pneumatic device through which fluid is pumped with controlled pressure to the looped cassete designed chip. The looped cassete chip is the size of a standard microscope slide and comprises of loop stucture arranged in a step to step configuration with critical gaps ranging from 10µm to 4.5µm from top to bottom. When fluid is passed through the loop structure cells are trapped in

the critical gaps. After isolation, trapped cells are harvested by a unidirectional flow of a buffer. The cells isolated initially are not of high purity, the use of another looped casette for a purification round is required to improve purity of CTC. Isolation is at a rate of 5ml/hr (Miller et al 2018). CTC isolated from 48 patients with known EGFR mutations from tumour biopsy were analyzed for EGFR mutations using crystal PCR. The detection rates for EGFR mutation was 11% when compared with mutation results from tumour biopsy and a concordance of 22% was reported in mutations from CTC and matched tumour biopsy (Ntzifa et al 2021). The use of this device in the clinics as a platform to process CTC for molecular characterization may be limited by the laborious process of cell isolation and then purification done in separate steps totalling about 2 hours for 1 sample.

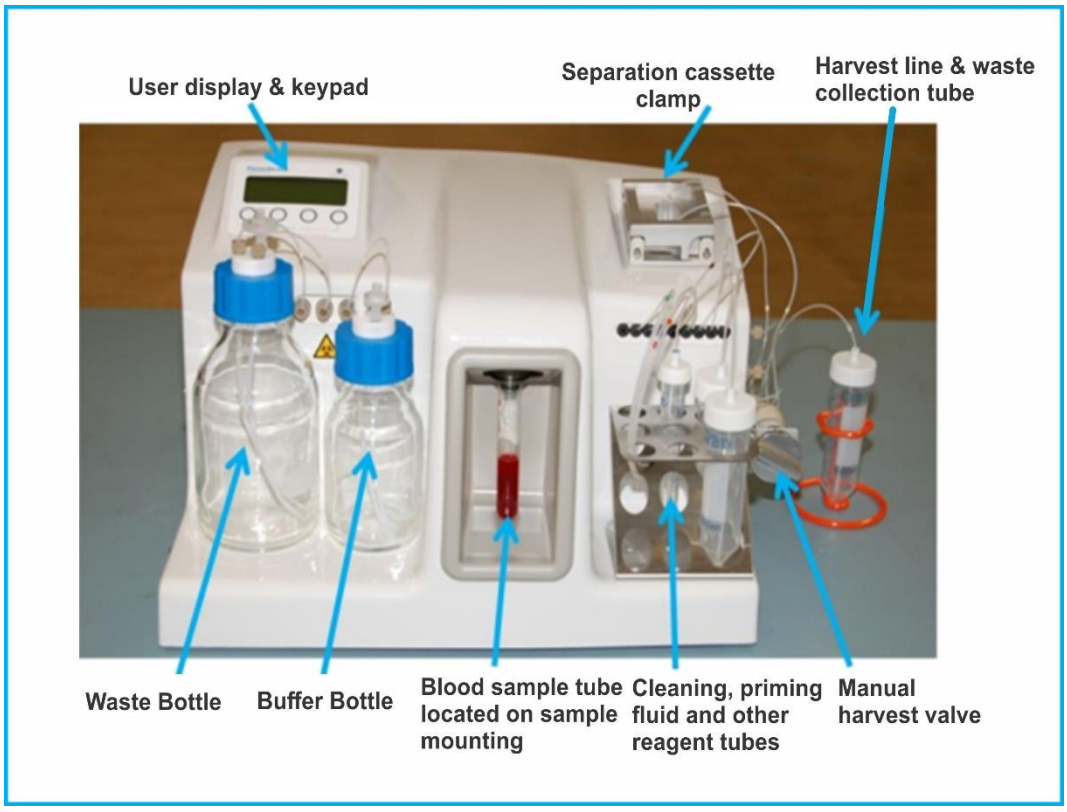

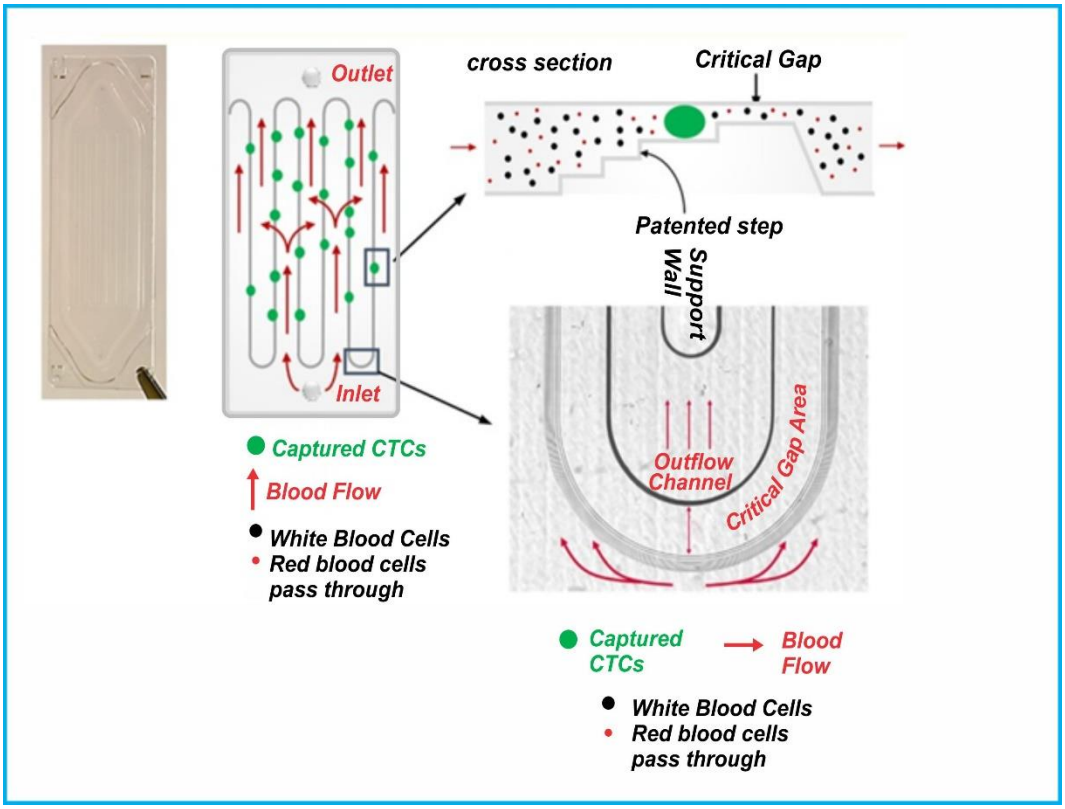

Figure 1.16 Parsotrix microfluidic based bioanalyzers showing workflow, chip and schematic representation of CTC isolation technique. Miller et al (2018)

Most of the technologies discussed above have explored the clinical utility of CTC as a diagnostic, predictive and prognostic marker through the design and production of various bench top devices and sophisticated microfluidic chips for its isolation from blood and the use of molecular biology techniques such as PCR and NGS to detect mutations with good success. However, challenges (**Table 1.10**) such as: quantity of CTC isolated, Purity of CTC, laborious work flow process and the need for specialist trained technicians for device operation has limited the usage of these devices in the clinics routinely.

Table 1.10 Summary of challenges limiting the use of microfluidic devices in the clinic

Device	Limitations
CTC chip	Laborious process for removal of captured CTC; poor throughput (1ml/hr)
Herringbone chip	Laborious process for removal of captured CTC; poor throughput (1.2ml/hr)
Nanovelcro chip	Poor throughput (5ml/hr), rigorous workflow process
Weir	Cumbersome workflow process, requires specialized technical knowhow. Isolation is at 5ml/hr
Magnetic Sifter	Multiple experimental steps. Isolation is at 5ml/hr
Oncobean chip	Laborious process it takes to harvest captured CTC. Isolation of CTC is at 10ml/hr
Spiral chip	Poor purity; Rigorous workflow.
FAST Disc	Poor purity, isolation is at 7.5ml/3min
Parsotrix	Cumbersome workflow process, poor purity. Isolation at 5ml/hr

1.13. Aims and objectives of research

Cells from primary and metastatic sites of a malignancy present in the blood stream are termed circulatory tumour cells (CTC). These cells have been proposed as excellent alternatives or complementary technology because they provide genetic information from tumor initiation to evolution (Pantel et al 2017). The use of CTC to date as a diagnostic or prognostic tool has been limited by the low concentration of these cells in the blood. Available technologies such as the clinically validated FDA approved Cell Search immuno-magnetic based device and microfluidics have explored CTC isolation for molecular characterization for EGFR mutations successfully (Nagrath et al 2007; Park et al 2014; Crossbie et al 2016; Sunderasan et al 2016; Zhou et al 2017; Lim et al 2018; Kulasinghe; et al 2019; Ntzifa et al 2021). However, implementation of these microfluidic devices for routine use in the clinics for CTC isolation for subsequent downstream analysis to detect mutations have been constrained due to challenges such as: (1) reproducibility of some of these techniques to meet clinical demands (2) cumbersome work flow process (3) costly instrumentation (4) poor throughput and purity and (5) need for skilled technicians for specimen handling and operation of the device. There is therefore an urgent need for technology that is simple in design and usage, cost efficient and isolates CTC with high capture efficiency and purity with a throughput that meets clinical demands.

The present study describes the design and conceptualization of a 2-part immunomagnetic based Lung card microfluidic device developed as part of a European Union (EU) seventh frame work programme (FP7) that is simple in design, cost efficient, with an easy work flow process that is adaptable for routine use in the clinics. The concept and workflow process of the device used in the current study differs from other immuno-magnetic and/or immuno-affinity devices explored previously for isolating CTC for subsequent downstream analysis for EGFR mutations in NSCLC in the following ways (1) magnetic field generated for CTC enrichment is via mobile permanent magnets that are moved across a field containing the blood and magnetic beads (2) elimination of pre-labelling process as functionalized magnetic beads are added directly to the blood sample making work flow less tedious (3) the chip in the present study is devoid of immobile structures but can be further functionalized to incorporate analysis units. CTC captured will be moved in a precisely controlled manner to an outlet on the chip for a one step collection of captured CTC eliminating the laborious process of harvesting cells from the chip which is common for many of the existing immuno-affinity devices discussed above.

This study hypothesizes that the principle by which the microfluidic device in the present study works to isolate EpCAM positive cells from blood with high yield and purity and the CTC isolated can be used for downstream analysis.

<u>The key processes that the project addressed are:</u>

- Description and conceptualization of the device and how its design and geometry align with the objective of a versatile, cost efficient, simple to use device that isolates EpCAM positive cells for downstream analysis.
- The ability of the microfluidic device in isolating CTC with high yield and purity will be investigated firstly in proof-of-concept studies that will involve creating models of CTC in a heterogeneous fluid by spiking cancer cell lines expressing varying levels of EpCAM into media and sheep blood at different concentrations. Quantification of the cells isolated will define capture efficiency. The ratio of EpCAM positive cells to contaminants (white blood cells) will represent purity of cells isolated. After validation for basic parameters using cell lines, capture efficiency of the device and purity of cells isolated will also be measured using CTC from the blood of patients with NSCLC.

- CTC isolated using the device will be utilized for downstream analysis by characterization of CTC for cancer specific mRNA markers and detection of mutations in exon 18-21 in EGFR.
- The clinical potential of CTC isolated will be evaluated by comparing mutations detected in CTC to mutations reported in matched tumour biopsy samples determined as part of the patient's clinical management.

Chapter 3

Materials and methods

2.0 Materials and Methods

2.1 Design, concept and capture process of Lung card version II microfluidic device

Lung card version II microfluidic device is a 2-part device comprising of a disposable microfluidic chip made up of poly methylmethacrylate (PMMA) and a microfluidic box.

2.1.1 Fabrication of glass chip

The chip (**Figure 2.2)** was designed by Dr Alex Iles, on an AutoCad DXF file, to contain a chamber into which blood and magnetic beads could be mixed and separated. Once produced this was exported to the laser cutter software. A glass sheet measuring about 1.1mm in thickness was placed on the bed of a laser cutter and cut to design specifications. The glass chip measured 98×98mm on the outside and 57×66mm on the inside. The laser cut produced 3 sheets from the glass chip; two are of similar dimensions (for the microfluidic chamber) and one sheet for the lid. After cutting, the sheets were rinsed with de-ionized water and sand papered to get rid of residues from laser cut edge and to smoothen out surface of the chip after laser cut. The two sheets with same core design and channel were bonded together. Bonding process for the fabrication of glass chip was thermal bonding. Bonding of the 2 glass sheets was initiated at room temperature and then at 115^{O}C for 1-2hr to allow for better annealing of the two glasses sheets (Ilesicu et al 2012).

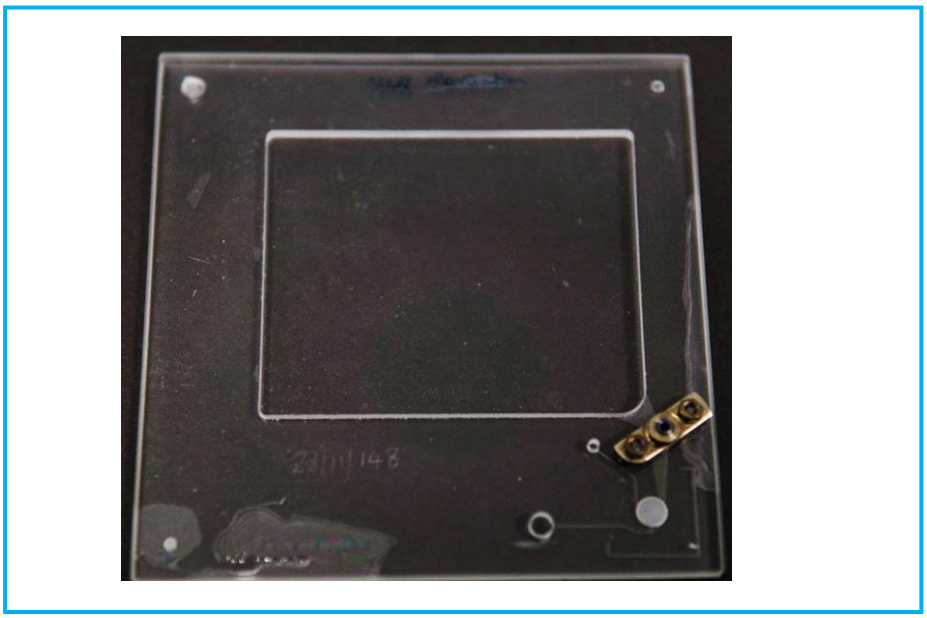

Figure 2.1- glass chip outer chamber measuring 98×98mm, inner chamber 57×66mm

2.1.2 Fabrication of PMMA chip

This chip was initially designed by Dr Alex Iles and modified with inputs from the author. The design of the chip was again drawn as an AutoCad DXF file that was exported to laser cutter software as described in Section 2.1.1. The merits of each material are discussed in Chapter 3. A PMMA sheet measuring about 1.5mm in thickness was placed on the bed of the laser cutter and was cut to design specifications. The Lung card microfluidic chip (**Figure 2.3**) comprises a chamber measuring 98×98mm on the outside and 57×66mm on the inside and a lid measuring 58×66mm. The laser cut produced 3 sheets from the PMMA; two are of similar dimensions (for the microfluidic chamber) and one sheet for the lid. After cutting, the sheets were rinsed with de-ionized water and sand papered to get rid of residues from laser cut edge and to smoothen out surface of the chip after laser cut. The two sheets with same core design and channel were bonded together (**Figure 2.3**) by dropping 1ml of 90% ethanol onto one sheet and placing the other sheet on top. The two sheets were then tightly pressed together using a clamp and put into a UV curing system for 30 seconds where the chip was irradiated at 234nm UV wavelength. After UV irradiation excess ethanol was removed with the use of a pipette. Following irradiation of ethanol treated PMMA

sheets acrylate monomers formed on each sheet diffused and merged forming a permanent bond (Tran et al 2013).

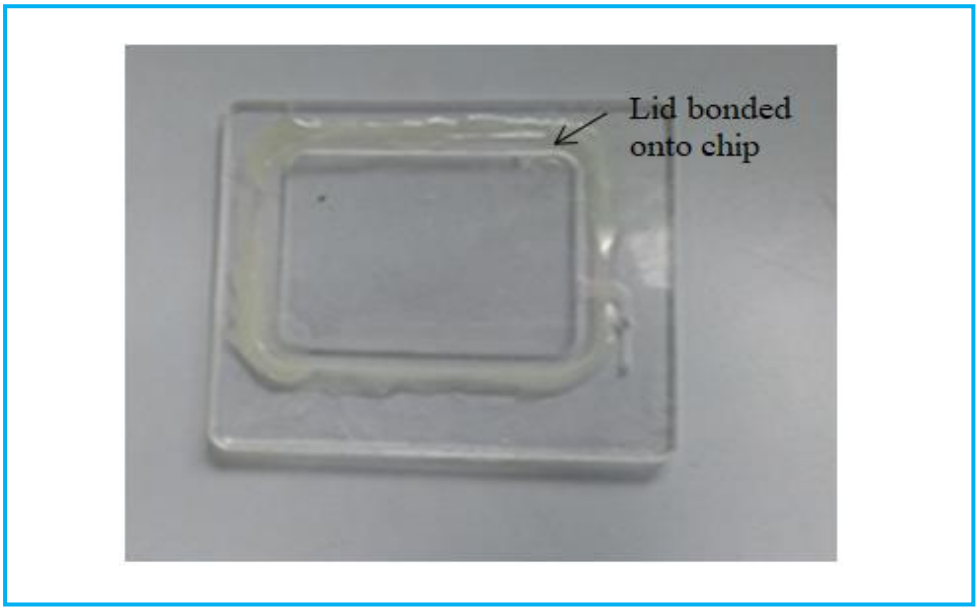

Figure 2.2- lid bonded onto microfluidic chip with outer dimensions of 98×98mm and chamber dimensions of 57×66mm

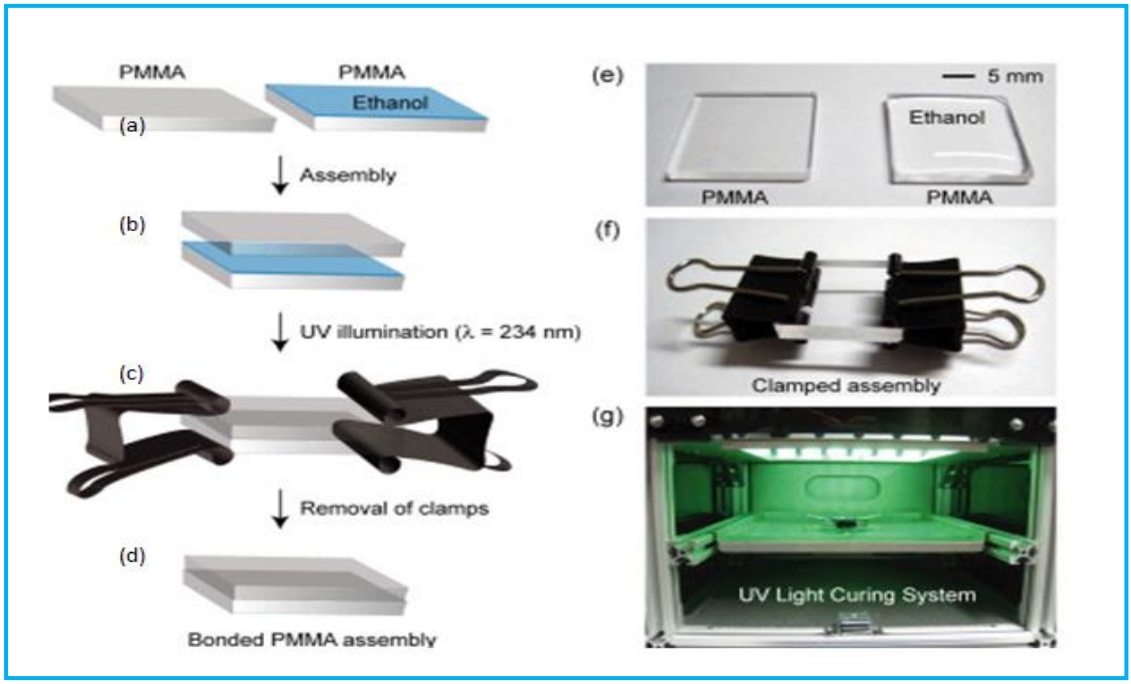

Figure 2.3- bonding process for PMMA chip. Tran et al (2013)

2.1.3 Fabrication of Lung card microfluidic box

This part of the unit (**Figure 2.4**) was built in the UK by subcontracting to a company in Leeds (Micro Lab Devices). The control systems were programmed by colleagues from Stab Vida. The unit comprises of (1) a high voltage power supply to power all mechanical action of the unit (2) An electromechanical arm with permanent Neodymium-Iron-Boron magnets (NdFeB) attached to the top and bottom part of the arm (3) a stage for the microfluidic chip (4) a segment for PCR (containing a peltier and fan) (5) A computer with the magnetic actuator program installed to control movement of the electromechanical arm (**Figure 2.4**).

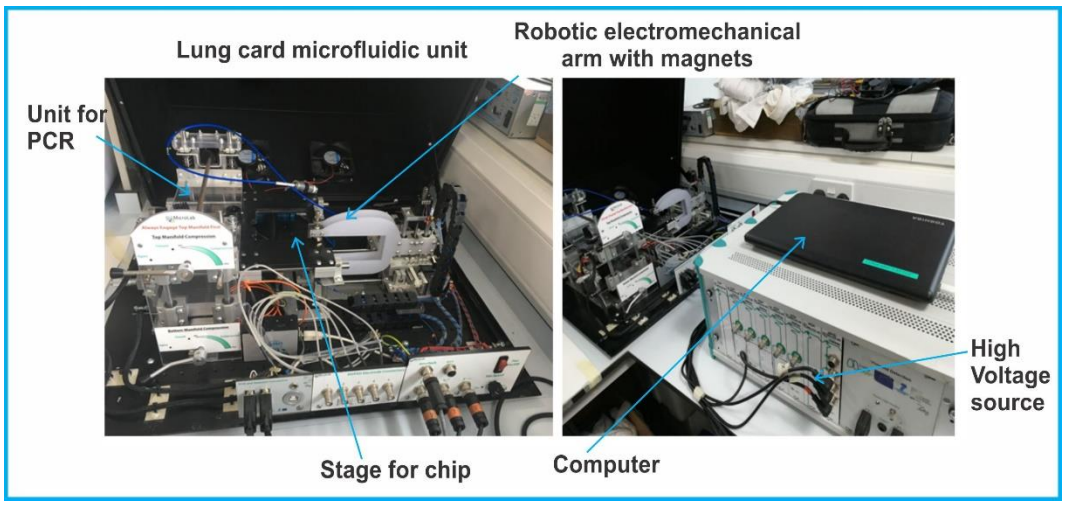

Figure 2.4- Microfluidic box consisting of (1) electromechanical arm (2) stage for the microfluidic chip (3) a peltier for PCR (4) an external high voltage power source (5) a computer

2.1.4 Preparation of glass chip for capture of EpCAM positive cells

The dry glass chip was filled with sialinising agent [consisting of 9ml of 2,2,4 methylpentane+145µl of trichloro (1H,1H,2H, 2H-perfluorooctyl) silane (PFOCTS)] and kept for 30 minutes this was done to enhance hydrophobicity of glass chip and to prevent non-specific binding of antigens and antibodies to chip. After 30 minutes the chip was washed sequentially with 10ml each of acetone, 70% ethanol and molecular grade water to remove any chemical impurity. It was air dried for 30minutes and put in the oven at 40^{O}C overnight to dry

2.1.5 Preparation of PMMA chip for capture of EpCAM positive cells

Before capture and isolation of EpCAM positive cells using the Lung card version II microfluidic device the PMMA chip was washed with 70% ethanol to remove any chemical impurity and then allowed to air dry. The chamber was then filled with 5ml of 5% w/v Bovine serum albumin (BSA) and allowed to sit for 5min to prevent non-specific binding of antigens and antibodies to the chip. After 5minutes, BSA in the chamber was discarded and then the chamber was left to dry overnight on the bench. After drying the outer lid was bonded to the chamber using Loctite 2-part Epoxy glue (Henkel, Germany) and then left to dry for 30 minutes.

2.1.6. Loading of chip unto microfluidic device for capture

The chip comprises two inlets. The first was filled with 6µl of 4×10^8 /ml Dyna magnetic anti-EpCAM beads (Invitrogen). After loading the chip with the magnetic beads (Dynal Invitrogen), a magnet was placed at the bottom of the hole and PCR tape was used to seal the hole. An aliquot of sample (13ml) was loaded using a 20 ml syringe, when filling the chamber care was taken to avoid introduction of air bubbles into the chamber. After loading of sample, the hole was sealed with a tape, the magnet was removed and the chip placed into the Lung card box for isolation of CTC (**Figure 2.5**).

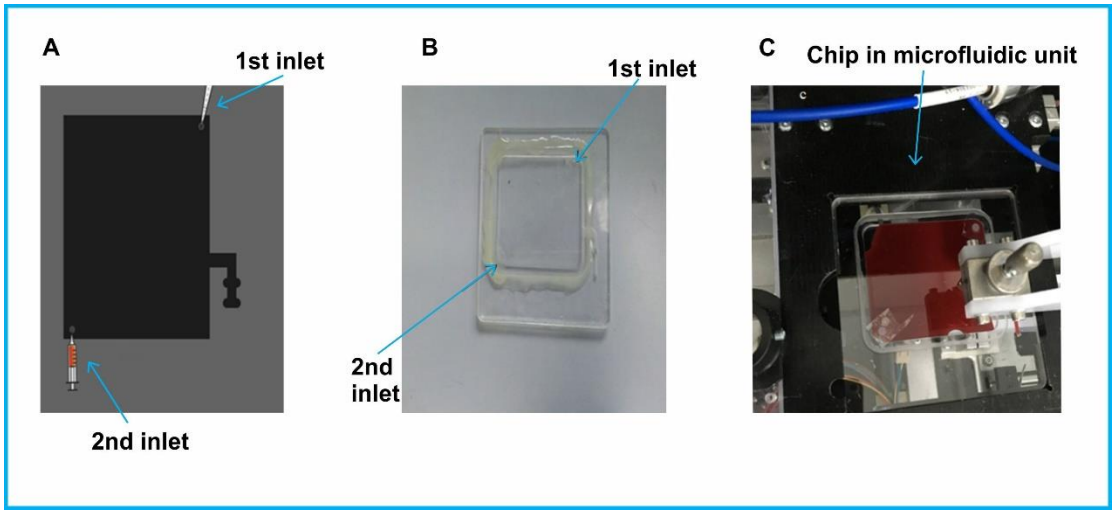

Figure 2.5 a loading of chip 1st inlet is loaded with magnetic dyna anti-EpCAM beads, 2nd inlet is loaded with heterogeneous sample containing EpCAM positive cells **b-** picture of PMMA chip showing inlets **c-** chip placed in microfluidic unit.

2.1.7 Extraction of CTC

After capture, the chip was taken out of the chamber and a NdFeB magnet measuring 20×10×4mm was attached to the collection hole. About 12ml of sample is taken away from the chip from the lower left inlet using a 20ml syringe. An NdFeB magnet was then used to swipe through the chamber from left to right (**Figure 2.6**) trying to collect and move any residual EpCAM positive cell to the outlet hole this took a total of 5 minutes. About 100 µl of PBS was infused into the collection hole to wash away excess media and/or blood from the collection hole and to see the brownish sediment more clearly. A 200µl of pipette was then used to pick the brown sediments containing magnetic bound EpCAM positive cells. Magnetic bound EpCAM positive cells were washed with PBS 3-4 times until a clear supernatant was obtained. While washing, a magnet was attached to the 500µl Eppendorf tube so that the bound EpCAM positive cells will not be eliminated during washing. After washing the brown sediments were suspended in about 15µl of PBS for further experiments.

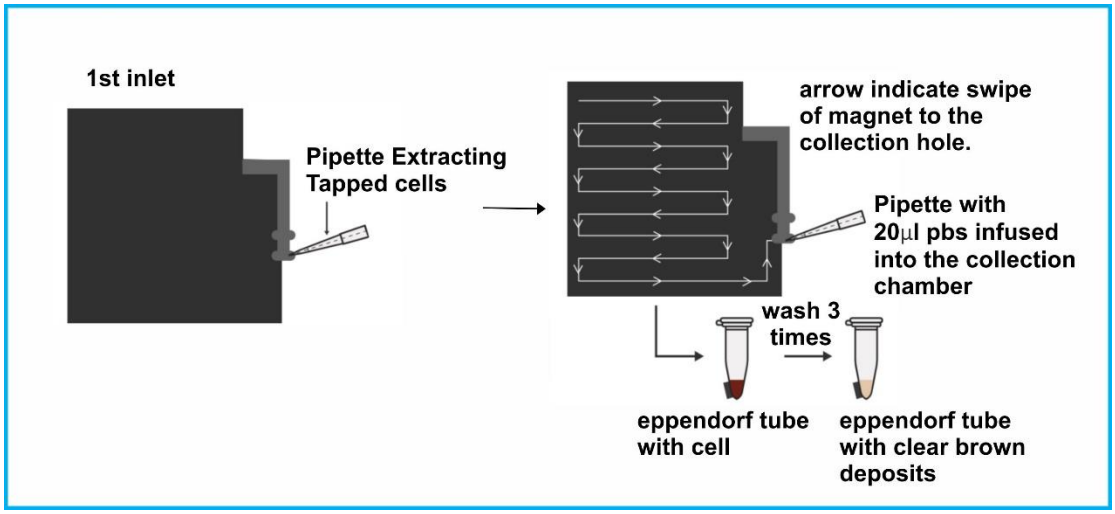

Figure 2.6-Schematic representation of extraction process. Drawn using Adobe illustrator

2.2 Cell culture experiments

The cell lines used in this study were HT 29- human colorectal adenocarcinoma cell line **(**Frogh&Trempe,1975), MCF-7- Human Caucasian breast carcinoma cell line (Abban et al, 1973), PANC-1- a pancreatic cancer cell line of ductal origin (Lieber et al 1975) and PC9 cell line- a lung adenocarcinoma cell line (Tsuji & Hyata, 1989). All cell lines were obtained from the European Collection of Authenticated Cell Cultures (ECACC, www.phe-culturecollections.org.uk). Cell lines were cultured in a T-75 adherent flask (Sarstedt, UK) and maintained in a humidified incubator at 37^{o}C with an atmosphere of 5% CO_2 (Galaxy 170 S, New Brunswick Scientific, Stevenage, UK). The cell lines were grown in RPMI-1640 media (Lonza, UK) supplemented with 10% (v/v) foetal bovine serum (Labtech.com, USA), 50µg/ml penicillin and 250µg/ml streptomycin (Lonza, UK). Cells were harvested when cells were 80 -90% confluent. Harvesting of cells was carried out in a class II biological safety cabinet (ESCO Scientific, USA) to maintain the sterility of cell lines. It involved: removal of the media used to culture the cells, then addition of 10ml of PBS (Oxoid limited, Thermofisher Scientific, Basingstoke, UK) to the flask to rinse away excess media. The PBS was then taken off and trypsin/ethylenediaminetetraacetic acid (Fisher Scientific, UK) at a concentration of 0.5mg/0.22mg/ml was put into the T75 flask and incubated at 37^{o}C for 10 minutes to allow for detachment of cells. After 10 minutes, the flask was tapped gently to ensure all cells were in suspension. Detachment of cells from the flask was confirmed by viewing under a microscope (Motic AE 2000 binocular inverted microscope, Wetzlar Germany). Once detachment of cells was confirmed, about 5ml of media was added to the flask to inhibit enzymatic action of trypsin. The contents of the flask were taken off and put in a 50ml Falcon tube using a 10 ml pipette. The cell suspension was then spun in a centrifuge (VWR megastar 3. OR) at 500g for 3 minutes. After centrifugation, the supernatant was decanted leaving a loose pellet of cells at the bottom that was re-suspended in complete RPMI medium in a 1 in 5 dilution. One ml of the re-suspended cell sediment was added to a sterile labelled flask containing 12 ml of medium for culture and to make more cell passages to be used for experiments.

2.3 Cryogenic storage of HT29, MCF-7, PC9 &Panc-1 Cell Lines

To maintain a store of the cell lines used in this study when required for future experiments and to reduce antigenic drift, cell lines used were cryogenically stored after culture. The cell lines were cultured for a maximum time of two months prior to cryogenic storage. When cells cultured in T75 (Sarstedt, UK) were 80-90 % confluent the cells were harvested as outlined in **section 2.2** above. After centrifugation, the supernatant was discarded, and the cell sediment was re-suspended in 3ml of freeze medium; 90% (v/v) FBS (Labtech.com USA) and 10% (v/v) dimethylsulphoxide (DMSO) (Sigma, Gillingham, UK). Following suspension in freeze medium the cell suspension was aliquoted into 1ml cryovials and stored in a -80^{oc} freezer for 1-2 days before transfer into liquid nitrogen storage.

2.4 Cell counting and viability check

The concentration of cells in suspension obtained after cell culture was determined using an improved Neubauer haemocytometer (Hawksley Lansing, UK). An aliquot of cell suspension (10µl) was pipetted into an Eppendorf tube an equal volume of 0.4% (w/v) Trypan blue (Sigma) was added to the cell suspension. Trypan blue enters cells with compromised membrane this results in non-viable cells acquiring blue stain in the cytoplasm. After a thorough mix of cell suspension and Trypan blue dye by gentle pipetting, 10µl of the mixture is loaded into the Neubauer haemocytometer and examined using the ×10 magnification of the microscope (Motic AE 2000 binocular inverted microscope). The number of viable cells (cells without the blue stain) were counted in quadrants 1, 2,3, 4 **see Figure 2.7 below** using a counter. The concentration of viable cells in % was determined using the equation below

Cell concentration=average cell count from 4 squares ×2 (dilution factor) ×10^4/ml×100

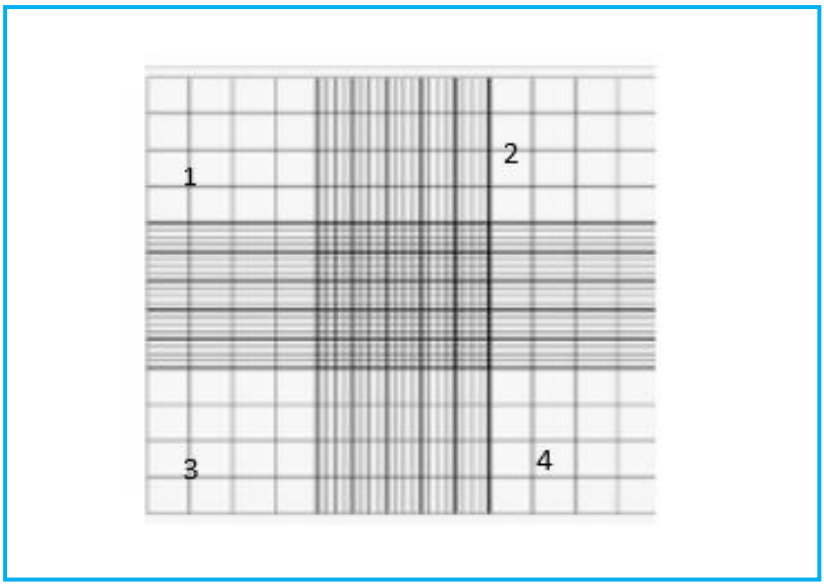

Figure 2.7- shows squares in the Neubauer counting chamber. Cells in the squares labelled 1.2.3& 4 were counted

2.5 Determination of EpCAM expression on PC9 cells, HT-29, MCF-7and PANC cells using flow cytometry

To evaluate EpCAM expression on PC9, HT-29, MCF-7and PANC-1 cell lines (ECACC, UK). These cells were cultured and counted as described in **Section 2.2 and 2.4** and a concentration of 5.0×10^{6}/ml of cells for each cell line were used for the experiments. Each test had a negative control. To each tube of the test 5ul of FITC EpCAM (Mouse anti human CD49d FITC) antibody (AbdSerotec, MCA 923F) was incubated with 50µl of each cell line in the dark for 30 minutes. To each of the negative control tubes of each cell line 5µl, of isotype negative (Mouse IgG2a) (AbdSerotec MCA929A488) antibody was added to 50µl of cell lines and incubated for 30minutes in the dark. Following incubation, the reactions were washed with PBS three times to remove unbound antibody. Washing with PBS involved putting 1 ml of PBS into the reaction and then centrifuging for 3 minutes at 300g at room temperature and then discarding the supernatant. Following centrifugation and a final wash the supernatant was extracted and the cell pellets re-suspended in 300µl of PBS and analysed with FACS Calibur (Beckton and Dickson, USA). As the cells in suspension were passed through the flow cytometer each cell was exposed to lasers. EpCAM antigens present on the cell that are bound to corresponding fluorescently labeled anti EpCAM antibody (FITC EpCAM) become excited when exposed to lasers and emit signals that are read by the flow cytometer. Data/signals emitted from each cell is integrated to obtain

information on EpCAM expression of the sample. Histogram plots were used to interpret data obtained from each cell line. The plots showed the intensity of light detected on the y axis and the number of cells emitting the intensity on the x axis.

2.6 Spiking experiments in (RPMI Media) to demonstrate validity of Lung card version II microfluidic device in isolating EpCAM positive cells

Cell spiking experiment was carried out by spiking carboxylfluorescein succinylmidyl ester (CFSE) (Invitrogen, UK) stained cell lines (HT-29. MCF-7, PC-9 &Panc-1) which had been shown to express varying levels of EpCAM into media and then isolating the EpCAM positive cells using the Lung card version II microfluidic device. The efficiency of capture was evaluated by the ability of the microfluidic device to extract CFSE stained EpCAM positive cells that was spiked into the media.

2.6.1 Staining

After culture and harvesting cell lines as outlined in **Section 2.2**, a count and viability check was done on the cell suspension as described in **Section 2.**4. All cell lines used for spiking experiments had a viability of at least 85%. A stock concentration of 1×10^6in 1.5ml of RPMI media was made up and serial dilutions of 2×10^5, 4×10^4, 8×10^3, 1.3×10^2 was made from the stock. After making up cell concentrations, the cell suspensions were stained using 5µl of CFSE (Invitrogen, UK) for 20 minutes in the dark at room temperature. After staining time had elapsed, the cell suspension was spun at 1,500rpm for 3 minutes and the supernatant removed. The cells accumulated at the bottom the tube were washed once with PBS to remove excess stain.

2.6.2 Spiking

After staining **(Section 2.6.1)**, the cells were suspended in 1 ml of complete RPMI media and spiked into 12ml of RPMI media (Lonza). Afterwards, the spiked media was loaded into Lung card version II chip for isolation /capture of EpCAM positive cells as described in **Section 2.1.6** and extraction as outlined in **Section 2.1.7**. Cells extracted from the chip were suspended in 200µl of PBS for microscopy.

2.6.3 Cell counting

Following isolation of EpCAM positive cells using Lung card version II microfluidic device and its extraction from chip. An aliquot (10µl) of EpCAM positive cells+ bead complex suspended in 200µl of PBS was loaded into a Neubauer counting chamber (Hawksley Lansing) and a count was performed as outlined in **Section 2.4** to evaluate capture efficiency of Lung card version II microfluidic device. Capture efficiency was calculated using the formulae below:

$$100 - \frac{(No\ of\ cells\ spiked\ into\ the\ media - No\ of\ cells\ isolated)}{No\ of\ cells\ spiked\ in\ media} X\ 100\%$$

2.6.4 Fluorescence microscopy

The stained cell lines were observed before isolation under a Zeiss fluorescence microscope (Zeiss, Germany) with the ×40 objective lens using brightfield and Alexa fluor 488 imaging and Zeiss imaging app. The EpCAM positive cells captured and the media left over after capture were also examined under a Zeiss Fluorescence microscope (Zeiss, Germany) using the above-mentioned imaging and objective.

2.7 Spiking experiments in blood to demonstrate the validity of Lung card version II microfluidic device in isolating EpCAM positive cells

Cell spiking experiment was carried out by spiking CFSE stained cell lines (HT-29. MCF-7, PC-9 & Panc-1) expressing varying levels of EpCAM at varying concentrations into sheep Blood (Rockland Immunochemicals) and then isolating EpCAM positive cells spiked in sheep blood using Lung card version II microfluidic device. The efficiency of capture was evaluated by the ability of the microfluidic device to extract as many EpCAM positive cells that was spiked into sheep blood.

2.7.1 Staining

Concentration and staining of cell lines used in spiking experiments in blood is as outlined in **Section 2.6.1.**

2.7.2 Spiking

After staining, the cells were suspended in 1 ml of complete RPMI Media and spiked into 12ml of Sheep blood. Afterwards, the spiked blood was loaded into Lung card Version II chip for isolation /capture of EpCAM positive cells as described in **Section**

2.1.6 and extraction as outlined in S**ection 2.1.7**. Cells extracted from the chip were suspended in 200µl of PBS for microscopy.

2.7.3 Cell counting

Following isolation of EpCAM positive cells using Lung card version II microfluidic device and its extraction from chip. About 10µl of EpCAM positive cells+ bead complex suspended in 200µl of PBS was loaded into a Neubauer counting chamber (Hawksley Lansing) and a count was performed as outlined in S**ection 2.4** to evaluate capture efficiency of Lung card version II microfluidic device. Capture efficiency was calculated using the formulae below:

$$100 - \frac{(No\ of\ cells\ spiked\ into\ the\ blood - No\ of\ cells\ isolated)}{No\ of\ cells\ spiked\ in\ blood} X\ 100\%$$

2.7.4 Fluorescence microscopy

The EPCAM positive cells captured were observed using the brightfield and green field imaging of the Olympus BX53 fluorescence microscope and the cell entry image app with × 40 objective lens.

2.8 Spiking experiments to show purity of EpCAM positive cells isolated using Lung card version II microfluidic device

Purity of EpCAM positive cells isolated using the microfluidic device was evaluated by spiking CFSE (Invitrogen) stained HT-29, or MCF-7, or PC9 or Panc-1 cancer cell lines at varying concentrations as **outlined in Section 2.6.1** into 12ml of complete RPMI media containing 3×10^6 concentration of cell tracker far red stained leucocytes. After spiking, EpCAM positive cells were isolated from the spiked media using Lung card version II microfluidic device as described in **Section 2.1.6&2.1.7** and the purity evaluated via imaging with a fluorescence microscope. Percentage purity was evaluated using the formulae below:

$$\frac{\text{CTC Isolated}}{CTC + WBC\ isolated} X\ 100\%$$

2.8.1 Isolation of peripheral blood mononuclear cells from blood (PBMC)

About 50 ml of blood sample was obtained by venipuncture into heparin coated syringes (2 ml: 5000 iu/ml) from healthy controls (Cone blood from National Blood Transfusion Service). PBMC was isolated from whole blood under sterile conditions in a class II biological safety cabinet using the density gradient centrifugation method. Blood was first diluted (1:1v/v) with PBS (Oxoid). After dilution 20ml of diluted blood was added into an equal volume of lymphocyte separation medium (LSM1077 PAA) before centrifugation at 400xg for 30 minutes. After centrifugation, three layers were generated an upper clear layer a middle cloudy layer (buffy coat) containing PBMC and a bottom layer packed with red blood cells (**Figure 2.8)**. The clear layer and the buffy coat layer were removed using a pipette and transferred to a Falcon tube. An equal volume of PBS (Oxoid) was then added to the Falcon tube containing the clear layer and buffy coat to wash the PBMC. Washing of PBMC was by centrifuging the PBS plus clear layer and buffy coat at 400xg for 10 minutes. After centrifugation, the supernatant was discarded, and pellets of cells were left at the bottom of the tube. The pellets of cells at the bottom of the tube were re-suspended in PBS for another wash. After washing, the cells were re-suspended in freeze medium (Foetal bovine serum containing 10%v/v DMSO). The PBMC suspension was put into 1ml cryovials and placed in cryogenic storage as outlined in **Section 2.3**

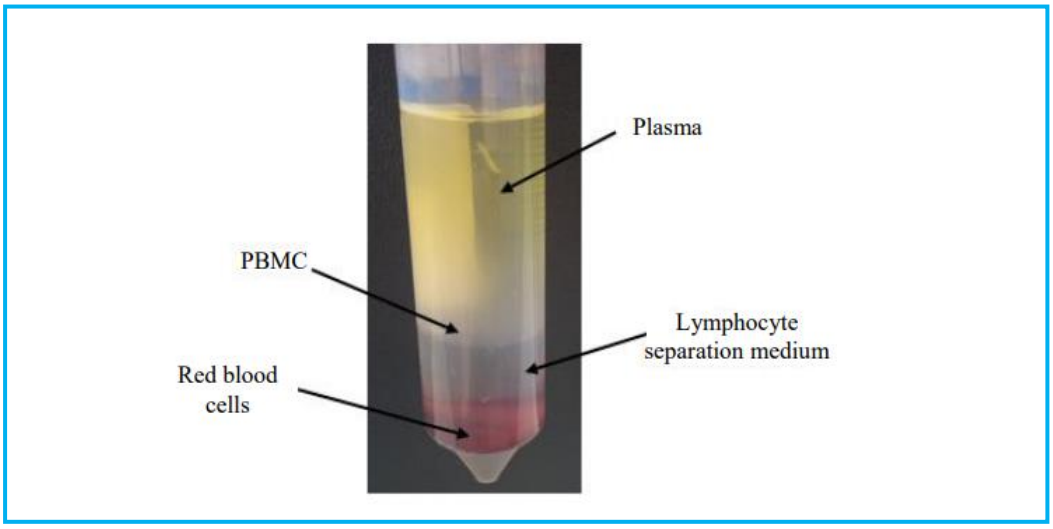

Figure 2.8 Layers formed after differential centrifugation of whole blood on lymphocyte separation medium to isolate PBMC Blood samples were diluted (1:1 v/v) with PBS and layered on top of an equal volume of lymphocyte separation medium before centrifugation at 400 x g for 30 minutes without brake to generate the different layers, the PBMC are within the cloudy "buffy coat" layer.

2.8.2 Isolation of PBMC spiked in media to demonstrate specificity of Lung Card version II microfluidic device to capture and isolate only EpCAM positive cells

PBMC obtained from cryovials was spun at 1,500RPM (VWR megastar 3. OR) for 3 minutes. After centrifugation the pellet of cells at the bottom of the tube was re-suspended in PBS and washed as described in **Section 2.8.1**. After washing the cells were counted and a viability check was done as outlined in **Section 2.4.** A viability of at least 85% was obtained for all the PBMC used in this study. About 1ml of 1×10^6/ml of PBMC cell suspension was stained with 5µl CFSE (Invitrogen,) for 20 minutes at room temperature. After 20 minutes, the cell suspension was spun at 1,500RPM for 3 minutes and the supernatant removed, the cell pellets accumulated at the bottom the tube were washed once with PBS to remove excess stain. After washing, the cells were suspended in 1 ml of complete RPMI Media. Afterwards, the spiked media was loaded into the Lung card Version II chip and isolation /capture of EpCAM negative PBMC was performed as outlined in **Sections 2.1.6 and 2.1.7**. Following capture, imaging of captured cells was performed using bright field and Alexa 488 imaging of the Olympus BX53 fluorescence microscope and the cell entry image app.

2.9 Isolation of CTC from blood of patients with cancer to demonstrate clinical utility of microfluidic device

2.9.1 Patient sample collection

This study was funded by Yorkshire Cancer Research and approved by North East-Newcastle& North Tyneside research ethics committee and institution review board prior to recruitment of participants (REC13/NE/0242). Fifty-nine patients aged between 47and 81 years attending the oncology clinic at the Queens center Castle Hill hospital Hull, diagnosed for lung cancer using tumor biopsy were recruited for the study. These patients had an evaluation for EGFR mutation using the PCR technique (Cobas EGFR mutation test) on tissue biopsy and 38 of the 59 patients recruited for the study had their blood samples collected to isolate CTC. Fourteen ml of peripheral blood was collected in a 3.2% trisodium citrate anticoagulant bottle (BD, USA) for each patient. All samples were anonymized and encoded before the analysis.

2.9.2 Patient sample analysis for CTC

Whole blood sample to be analyzed was collected in a 3.2% tri sodium citrate vacutainer sample bottle (BD, USA) in the recruitment centers mentioned above and transported within 15 minutes of collection in a blood bag with an ice pack to the laboratory. On arrival in the laboratory, a visual check was done on the blood to ensure that the blood collected was free from clots. The analysis process started within 10 minutes of arrival in the laboratory. The analysis process involved the transfer of blood from the trisodium citrate anticoagulant bottle into a 50 ml Falcon tube in a class II biological safety cabinet (ESCO Scientific). After transfer of blood to the Falcon tube, 3ml of PBS was added to the tube to reduce the viscosity of blood, but avoiding the introduction of air bubbles. The PBS and blood mixture was mixed thoroughly by inverting the Falcon tube 5 times. After mixing the blood was loaded into the microfluidic chip as outlined in **Section 2.1.6.** After capture, the Isolated EpCAM positive CTC was extracted from chip as outlined in **Section 2.1.7**

2.9.3 Microscopy analysis of captured EpCAM positive CTC from blood of patients with NSCLC

EpCAM positive CTC extracted from chip after capture process were centrifuged and concentrated onto a microscope slide using a cytospin. Thereafter, the cells were fixed, stained and examined under a microscope.

2.9.3.1 Preparation of slide to be used for cytospin

Frosted glass slides (Knittel glasser, Germany) were labelled with a grease free pencil and slotted into a slide clip holder ensuring that the frosted upper part of the slide was placed upwards. A filter card (Fisher scientific) was then placed in such a way that the absorbent part was touching the slide. The cytofunnel (Fisher Scientific) was then placed next to the filter paper ensuring that all holes above were evenly matched **(Figure 2.10)**, the holder was then fastened. Following fastening, the holder was placed in its corresponding centrifuge bucket. About 50µl, of bead + EpCAM positive CTC isolated from the blood of patients was pipetted into the cryo funnel and spun at 100xg for 5 minutes with the cytospin **(Figure 2.11).**

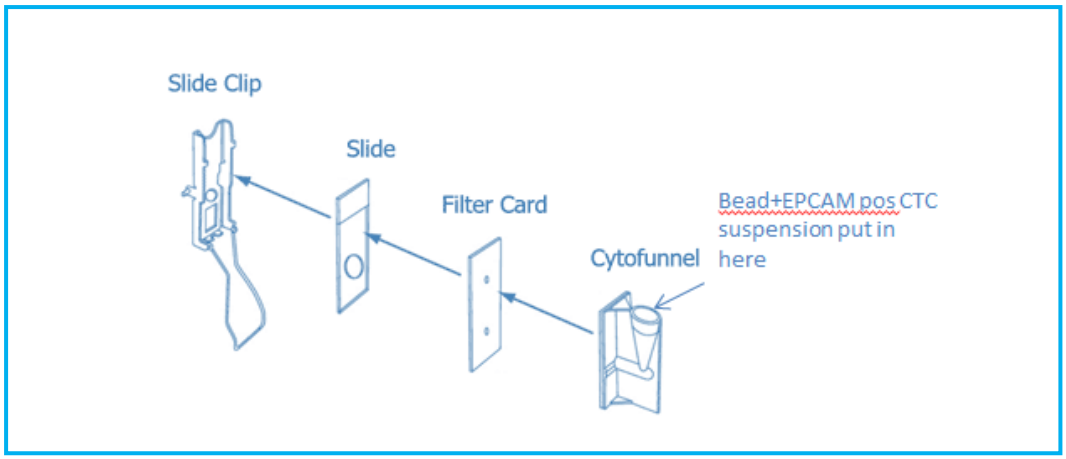

Figure 2.9- Preparation of slide in a cyto spin holder from https://www.thermofisher.com/es/es/home/brands/thermofisher-scientific.html

Figure 2.10- Cyto spin holders in a cyto spin centrifuge from https://www.thermofisher.com/es/es/home/brands/thermofisher-scientific.html

2.9.3.2 Fixing of cells after cytospin

After spinning the slides, the filter cards and cyto funnels were removed from the centrifuge, care was taken when removing the filter paper from the slides so as not to damage or smudge the cells. The slides were then placed on a tray and allowed to dry for 2 hours. Following drying, the slides were fixed for 10 minutes in 100% methanol and allowed to dry overnight on the bench.

2.9.4 Fluorescence microscopy

After fixing the bead+ EpCAM positive CTC complex, the slides were viewed under brightfield imaging using the ×40 objective of the Olympus BX53 Fluorescence microscope and the cell entry image app.

2.10 Immunocytostaining/RT-PCR to determine if EpCAM positive cells isolated from blood of patients emanate from cancer cells

To evaluate this the study used the following image analysis algorithm comprising staining with 4,6-diamidino-2-phenylindole (DAPI) (Vectashield, USA) for DNA content and using fluorescein conjugated pancytokeratin monoclonal antibody (SIG 3464 (914202) Biolegend, USA) specific for epithelial cells and rhodamine conjugated Mouse anti-Human CD 45 antibodies (BD Biosciences, USA) specific for haematological cells. Cells staining for cytokeratin were scored as CTC positive whilst cells staining positive for CD45 cells were scored as normal haematological cells. Furthermore, this study also investigated for the presence of mRNA markers unique to cancer cells from EpCAM positive cells isolated from blood. The mRNA markers investigated were cytokeratin 7 (CK-7) and Survivin.

2.10.1 Staining

After fixing the cells with methanol and then drying **Section 2.9.3.1 & 2.9.3.2 above.** The slides were rinsed in tap water and placed on a sequenza rack. TBS (1×TBS) was then put on the slides for 10 minutes. After 10minutes the slides were rinsed in tap water then horse serum (Thermo Fisher Scientific, UK) was put on the slides for 10minutes. After 10 minutes had elapsed, 100µl of fluorescein conjugated pancytokeratin antibody (Biolegend) was added onto the slides and allowed to sit for 30 minutes. After 30 minutes the slides were rinsed with 1×TBS thrice and 100µl of Rhodamine conjugated Mouse anti-Human CD45 stain (BD Biosciences, USA) was added onto the slides and left for 30 minutes. After staining the slides were rinsed thrice with 1×TBS and 100 µl of secondary antibody Alexa Fluor488 Donkey anti-Mouse IgG (Thermo Fisher, UK) was added onto the slides and allowed to sit in the dark for 30 minutes. After 30 minutes, the slides were washed three times in 1×TBS and rinsed in running tap water and mounted with DAPI (Vectashield, USA).

2.10.2 Fluorescence microscopy

Bright field and Alexa488 imaging of the slides was viewed using Zeiss microscope and Carl Zeiss software to identify CTC and to check for WBC contamination.

2.10.3 RNA extraction

PBS was taken off EpCAM positive cells+bead suspension obtained from blood of patients after isolation by spinning the suspension at 12,000g for 2 minutes. The upper PBS layer was pipetted from the suspension after centrifugation. Triazol reagent (125µl) (Sigma Aldrich, UK) was added to the cell pellets at the bottom of the Eppendorf tube in a fume hood and the mixture placed in a rocker (Thermo Fisher Scientific, UK) for 5 minutes for Trizol and cells to mix properly. After mixing, the Trizol and cell mixture was incubated on ice for 5 minutes to allow for complete dissociation of the nucleoprotein complex. Following incubation on ice 25µl of chloroform (Sigma Aldrich, UK) was added to the Trizol+cell mixture and mixed by inverting the tube ten times to get a milky solution. This step was essential for precipitation of RNA. The mixture was then incubated on ice for 3 minutes and then centrifuged for 15minutes at 1200g at 4^{o}C. After centrifugation, the mixture separated into a lower red phenol choloroform, an interphase and a colourless upper aqueous phase. The colourless aqueous phase was transferred to a new Eppendorf tube by placing the Eppendorf tube containing the mixture at a 45^{o}C angle and slowly pipetting the colourless aqueous solution out to a new tube. To the tube containing the colourless aqueous liquid, 62.5µl of isopropanol (Sigma Aldrich, UK) was added to the tube and inverted 5 times for adequate mixing and thereafter centrifuged for 10 minutes at 1,200g at 4^{o}C. After centrifugation, the supernatant was discarded and RNA (pellets) left at the bottom of the tube was washed twice. The wash process involved: the addition of 125µl of 75% ethanol to the pellet, mixing by vortexing and centrifugation at 750g at 4^{o}C. After the wash process, the supernatant obtained after centrifugation was discarded using a pipette. The RNA pellet left at the bottom of the tube was air dried with the lid open on a heat block in a fume hood (ESCO Scientific) for 5 minutes at 37^{o}C. After 5 minutes had elapsed the RNA pellets were re-suspended in 10µl of RNASE free water and put on a heating block for 10 minutes at 55^{o}C. After incubation the concentration of RNA extracted from CTC was evaluated spectrophotometrically using the Nanodrop (Thermo Fisher Scientific, UK). The RNA extracted was stored at -80^{O}C for a maximum of two weeks for further experiments.

2.10.4 Synthesis of cDNA (reverse transcription)

An aliquot (10µl) of (80ng) RNA extracted as described in (**Section 2.10.3**) above was re-suspended in 11.7µl of nuclease free water. To RNA re-suspended in nuclease free water the following reagents were added: 4µl of reverse transcriptase buffer (Bioline, UK), 2µl of 4MM dNTP's (Bioline, UK), 1µl of oligo dT (Bioline, UK) and 0.3µl of reverse transcriptase (Bioline, UK). After addition of the reagents outlined above the sample was incubated at 37^{O}C for 1 hour on a heating block. After incubation the samples were centrifuged at 800g for 30 seconds and re-incubated at 100^{O}C on a heating block for 5 minutes. Following incubation, the samples were centrifuged for 30 seconds at 800g and re-suspended in 180µl of PCR grade water. The diluted sample was stored in the freezer at -20^{O}C to be used for further experiments.

2.10.5 End point PCR to check for cancer specific mRNA markers

To determine if the above mRNA markers unique to cancer cells are present in EpCAM positive CTC isolated from blood of patients. Primers spanning the exon and intron boundaries were designed for survivin and CK7 **(Table 2.2)**. To normalize expression levels of survivin and CK7 the house keeping gene GADPH was used as internal control. Amplification of cDNA obtained to check for mRNA markers outlined above involved the addition of a reaction mix containing: 4µl of high fusion polymerase buffer (Thermo Fisher Scientific, UK), 1µl of 10mm DNTPS (Thermo Fisher Scientific, UK), 0.75µl each of forward and reverse primers, 0.25µl of Phusion DNA polymerase (F150) (Thermo Fisher Scientific, UK), 0.75µl of $MgCl_2$ (Thermo Fisher Scientific, UK) and 10.5µl of nuclease free water to 3µl of cDNA in a 20µl PCR tube and then putting into a Thermocycler (BioRad, USA) in amplification conditions shown in **Table 2.3**. For each PCR run positive and negative controls was performed. To ensure reproducibility of results all genes tested were investigated in triplicates. After amplification, PCR products were analysed by gel electrophoresis on 2% agarose gel. To make up 2% agarose gel. 1.5 g of agarose powder (Thermo Fisher Scientific, UK) was added into 75ml of 1×TAE buffer (Thermo Fisher Scientific, UK) and 2ul of Sybr safe DNA stain (Sigma, UK). The mixture was put in the microwave for 2 minutes until the agarose is completely dissolved. When the agarose was warm to touch the agarose was poured into a gel tray with the well comb in place and left to solidify completely. About 2.5µl, of loading buffer (Bioline, UK) was added to 10µl of PCR products and loaded into a well on the solidified gel. The agarose gel, was then placed in an electrophoretic tank

filled with 1×10 TAE buffer, ensuring that the gel is adequately covered. The gel was run at 110 volts for 60 minutes. Amplification of mRNA markers of interest in cDNA was confirmed by appearance of band of specific size **(Table 2.2)** using the gel doc system.

Table 2.1 List of Primers used for PCR

Primers	Forward Sequence (5'-3')	Reverse Sequence (3'-5')	size of product (bp)
Survivin	AAGAACTGGCCCTTCTTGGA	CAACCGGACGAATGCTTTT	**253**
CK-7	GACATCGAGATCGCCACCTAC	ATTGCTGCCCATGGTTCCC	**162**
GADPH	GAAGGTGAAGGTCGGAGTC	GAAGATGGTGATGGGATTTC	**225**

Table 2.2 Thermocycling conditions for amplification

mRNA markers	Pre-Denaturation	Denaturation	Annealing	Extension	Cycles
Survivin	**95^{oc}**(2min)	**95^{oc}**(5sec)	**60**^{oc}(20sec)	72^{oc}(30sec)	40
CK7	**95^{oc}**(2min)	**95^{oc}**(15sec)	**65**^{oc}(30sec)	72^{oc}(30sec)	**40**

2.11 PCR experiments for detection of EGFR exon 18-21 mutation from EpCAM positive cells

To examine the utility of EpCAM positive cells isolated using the device for its detection of EGFR mutations in exon 18-21. This present study firstly, assessed the performance of the PCR system in amplifying mutated exon 18-21 EGFR gene by using gDNA from a cell line (PC9) representative of NSCLC. Secondly, the current study investigated the detection of mutations in exon18-21 of the EGFR gene from EPCAM positive PC9 cells isolated from media and blood in spiking experiments. Furthermore, detection of exon 18-21 mutation on the EGFR gene from EPCAM positive CTC isolated from blood of patients with NSCLC was also investigated. Two sets of primers were used for this study (**Table 2.4**). One set of primer designed by Dr Pedro Alvarez of the University of Hull was for the detection of exon 19 deletion and L858R mutations on the EGFR gene while the other primers designed by the Stab Vida group (Portugal) targeted amplification of exon 18, 19 20 and 21 regions of the EGFR gene for sequencing to screen for mutations.

2.11.1 Preparation of gDNA from PC9 cells as positive control for experiments

Genomic DNA (gDNA) was extracted from PC9 cell line. The gDNA was extracted from PC9 cell lines because it is known to carry exon 19 deletions and T790M resistance mutations. gDNA, was used in our PCR experiments as a quality check to see if PCR reagents, primers, thermocycling temperatures are adequate for all our PCR experiments. PC9 cells at a concentration of 5.5×10^6 cells per ml were used for gDNA extraction. gDNA extraction was achieved by following the instructions of the QIAMP DNA and RNA extraction kit (Qiagen Germany). After extraction, the concentration of gDNA released was measured spectrophotometric ally using Nanodrop (Thermo Fisher Scientific, UK). The concentration obtained was 72ng/µl. The purity of gDNA extracted was evaluated by taking a measurement of the absorbance at 260nm and 280nm. The ratio obtained for this experiment was 1.9 (acceptable purity ratio 1.8-2.2).

2.11.2 PCR experiments and gel electrophoresis to ascertain the utility of EpCAM positive cells and EpCAM positive CTC isolated to detect exon 18-21 mutations.

EpCAM positive cells extracted using microfluidic device from media, citrated Sheep blood and blood samples from patients with NSCLC were subjected to amplification of EGFR gene fragments with two sets of primers **(Table 2.4)**. Prior to amplification, 3µl of cells isolated were treated with a 25µl of PCR mix (first set of primers). The PCR mix used for each reaction was made up of: 0.5µl of DNTP's (Thermo Fisher Scientific, UK), 3µl of high fusion polymerase buffer (Thermo Fisher Scientific, UK), 0.4µl of 1.5mm $MgCl_2$ (Thermo Fisher Scientific, UK), 0.2µl of Taq polymerase (Thermo Fisher Scientific, UK), 6.9µl of nuclease free water (Thermo Fisher Scientific, UK) and 3µl of primers at a concentration of 10pmol/µl (forward and reverse). Each experiment had a positive and a negative control. Amplification of EGFR was performed with the following thermocycling cycles using the first set of primers. A denaturing step at 100^{o}C for 5 minutes and 10 amplification rounds performed at 100^{o}C for 100 seconds, 61^{o}C for 100 seconds, 72^{o}C at for 100 seconds. An extension round of 30 cycles comprising of 95^{o}C for 30 seconds 61^{o}C for 30 seconds and 72^{o}C for 30 seconds.

Table 2.3-Primers used to amplify exon 18-21 segments of the EGFR gene

Exon	Forward sequence (5'-3')	Reverse Sequence (3'-5')	Size (bp)	Primer
19	CTGCCAGTTAACGT	AAAAGGTGGGCCTGAGGTT	172	UOH
21	TCAAGATCACAGATTTTGGGC	GAGCATCCTCCCCTGCATGTGTTA	388	UOH
18	GCTGAGGTGACCCTTGTCTC	TGGAGTTTCCCAAACACTCAG	300	SV
19	GCTGGTAACATCCACCCAGA	TTATCTCCCCTCCCCGTATC	261	SV
20	CACACTGACGTGCCTCTCC	TTATCTCCCCTCCCCGTATC	251	SV
21	AGCCATAAGTCCTCGACGTG	CCTGGTGTCAGGAAAATGCT	320	SV

UOH-university of Hull primers SV-Stab Vida primers

The second set of primers used for PCR experiments was designed by our partners at Stab Vida (Portugal) (**Table 2.4)**. Prior to amplification, cells isolated via magnetic extraction of EpCAM positive cells were treated with a 50µl of PCR mix. The PCR mix for each reaction was made up of: hot Taq DNA polymerase, DNTP, 1.5mm $MgCl_2$, PCR buffer, 37µl of nuclease free water and primers. Each experiment had a positive and a negative control. Amplification of EGFR fragments was performed via the following thermo cycling temperatures. A denaturing step of 98ºC for 15 minutes, 40 amplification rounds of 94ºC for 30 seconds, 58ºC for 1 minute and 75 ºC for 1 minute and an elongation step of 70 ºC for 5 minutes.

PCR products were analysed by gel electrophoresis on 2% (w/v) agarose gel. To make up 2% agarose gel. 1.5 g of agarose (Fisher Scientific, UK) was added into 75ml of 1×TAE buffer (Thermo Fisher Scientific, UK) and 2µl of Sybr safe DNA (Sigma). The mixture was put in the microwave for 2 minutes until the agarose was completely dissolved. When the agarose was warm to touch the agarose was poured into a gel tray with the well comb in place and left to solidify completely. After solidification 2.5µl of loading buffer was added to 10µl of PCR products and loaded into a well on the solidified gel. The agarose gel was then placed in an electrophoretic tank filled with 1×10TAE buffer (Thermo Fisher Scientific, UK), ensuring that the gel is adequately covered. The gel was run at 110 volts for 60 minutes. Amplification of EGFR gene fragment was confirmed by appearance of bands of specific size using the gel doc system. For the first set of primers: a fragment/band size, of 194bp was confirmed to

be exon 19 (wildtype), a fragment/band size of 172bp suggests an exon 19 deletion, a fragment/band size of 388BP suggest an L858R exon 21 mutation. For the second set of primers: a fragment/band size of 300bp, 261bp, 251bp and 320bp suggest amplification of exon 18, 19, 20 and 21 regions of the EGFR gene.

2.12 Next generation sequencing to detect sequence variants in exon 18-21 mutations detected from EpCAM positive CTC isolated from blood of patents with NSCLC.

CTC enriched samples obtained from patients with NSCLC were screened for mutations in exon 18-21 using next generation sequencing. Results obtained were compared to EGFR mutation results from matched tumor biopsy samples.

2.12.1 Purification of PCR products

After the first PCR run **(Section 2.11.2),** PCR products were purified using the following protocol.18µl of Surf Mag beads (Stab Vida) was added to 10 µl of PCR products in a 2ml Eppendorf tube and mixed thoroughly by pipetting up and down 10 times. After mixing the surf mag beads + PCR products was allowed to incubate for 2 minutes to allow for maximum interaction between amplified DNA with the surf mag beads. Following incubation, the tube was placed on a magnetic stand until the supernatant was clear. The supernatant was discarded using a 30 µl pipette. Care was taken when removing the supernatant so that the beads at the bottom of the tube were not disturbed. With the tube on the magnetic stand 150 µl of freshly prepared 70% ethanol was added to the magnetic beads at the bottom of the tube and allowed to incubate for 1 minute. After 1 minute, the 70% ethanol added was removed carefully so as not to disturb the beads at the bottom of the tube. This step was done twice. After removal of ethanol the tube was left open under a class II biosafety hood and the pellets of bead at the bottom of the tube was left to dry for 10minutes. Following drying, the bead pellets were re-suspended in 20 µl of molecular grade water and left to incubate at room temperature for 5minutes. After incubation, the tube was placed on a magnetic stand until the sample was clear. About 25 µl of clear sample was transferred from the 2ml Eppendorf tube to a PCR tube. After purification, DNA quantification was carried out using the Nanodrop spectrophotometric technique.

2.12.2 Second PCR run

After DNA quantification a 2nd PCR round was performed using a minimum of 40ng of PCR products from Ist PCR. In addition, sequence primers were used for this PCR run. This primer had fluorescent probes attached to them to identify DNA sequence. The protocol and thermocycling conditions for second PCR is shown in **Table 2.4 and Table 2.5**

Table 2.4 Protocol second PCR run

1st PCR	Negative control	Samples/positive control
My Taq mix(µl)	12.5	12.5
Forward EGFR Exon 18, 19 20 and 21 ILU Primers 10µm (µl)	0.3 each	0.3 each
Reverse primers EGFR exon 18 19 20 and 21 ILU primers10µm (µl)	0.3 each	0.3 each
Molecular grade water	11.1	10.1
DNA 40 ng (µg)	-	1
Total volume (µl)	25	25

Table 2.5 Thermocycling conditions second PCR run

Temperature(ºC)	Time(minutes)	No of cycles
98	15	1
94	30 seconds	
65	1	40
70	1	
70	5	1
4	Pause	Infinity

After 2nd PCR run the PCR products were purified using the protocol described in **section 2.12.1** above and the DNA quantified spectrophotometrically using Nanodrop (ThermoFisher Scientific).

2.12.3 Sequencing

Amplicon generation and library preparation was done according to protocol of Nextera XT (15031942) (Illumina, USA) and the amplicon generated sequenced using Illumina sequencer. Genomic data was processed with Trim galore (version 0.4.3.1) and Prinseq (version 0.20.4). Genomic data generated was aligned to the reference with BWA (MEM) version 0.7.17.1 and the variants detected with VAR direct version from 07.03.2018. Sequencing analysis was done by our partners at Stab Vida.

Chapter 3

Device description, conceptualization and workflow

3.1 Background

The role of personalized therapy in improving the poor mortality and morbidity statistics for patients with non-small cell lung cancer (NSCLC) is evidenced by data from over 80 prospective and retrospective clinical studies involving more than 50,000 patients globally that report longer PFS and OS in patients with EGFR mutations who are placed on TKI compared with patients who had EGFR mutations and were treated with chemotherapy. Furthermore, these studies also reported longer PFS and OS in patients **without the EGFR mutation** placed on chemotherapy when compared with patients who did not have the EGFR mutation but were placed on TKI (IDEAL, 2005; IPASS 2009; Lux lung 2012; Ensure 2015).

The fulcrum of personalized therapy in oncology is precision diagnosis of mutations that drive the cancer as this should help to guide clinicians in the selection of a therapy that fits the patient's molecular mutation needs (Siegel 2017; WHO 2021). Currently in the clinic the sample matrix of tumor biopsy and/or cfDNA used for diagnosing EGFR mutations in patients with NSCLC is inefficient. This is evidenced by about 50% of patients with NSCLC not having access to therapies tailored to their mutational needs for the following reasons; (1) patients being too ill to have surgery so biopsy sample to evaluate mutation status cannot be taken; and (2) DNA obtained from the blood may not be from tumors but from debris or cellular events causing sensitivity issues (Durendez-Saez et al 2017). This is discussed fully in **Sections 1.11.1 and 1.11.2**. The challenges listed above shows that there is an urgent need for alternatives to tissue biopsy / cfDNAor a companion diagnostic tool for precision diagnosis of EGFR mutations as well other potential key genes. Malignant cells in the circulation (CTC) have been explored as a diagnostic tool for detecting EGFR mutation in real time with good success. However routine use in the clinic has been limited due to their relative low abundance, i.e., 1ml of blood contains approximately 10 million leucocytes, 500 million erythrocytes but only 1-10,000 CTC depending largely on the tumour stage (Krebs et al 2010; Lin et al 2021). Isolation of these cells from millions of other cells has been very difficult. Technologies that have isolated CTC successfully from blood of patients with NSCLC for subsequent molecular characterization to detect EGFR mutations are not utilized routinely in the clinics.

3.1.2. Technologies for CTC isolation that have been applied for molecular characterization of EGFR mutations

Technologies such as: the FDA approved and commercially available Cell Search (**see Chapter 1, Figure 1.7 A**) initially used for CTC isolation and enumeration has been explored for isolation and subsequent characterization of EGFR mutations. This device uses the specificity of a high affinity anti EpCAM antibody linked to a magnetic microparticle for capture of EpCAM positive CTC (Quian et al 2021). Molecular characterization of EGFR mutations from CTC isolated using Cell Search device when compared with analysis of EGFR mutations using tumour biopsies showed a poor sensitivity (Krebs et al 2011; Punnose et al 2012). This has been attributed to poor purity, a relatively low volume of blood being utilized by the device (7.5ml), processing conditions before and during analysis that result in some cell loss which combined negatively affecting the device's capture efficiency. Another factor that has limited its use is cost. The cost of the equipment is $220,000 and each sample cost $1,000 to analyse (Yagi et al 2017). The in-vivo Gilupi cell collector (**Chapter 1, Figure 1.7C**) is another immuno-affinity device validated in the clinics that have been explored for CTC isolation and subsequent diagnosis for mutations in EGFR. This device is a stainless-steel medical wire designed to capture CTC from up to 1.5 L of blood when inserted into the cubital vein. Capture of CTC is achieved when EpCAM positive CTC adhere to the anti EpCAM antibody attached to the hydrogel tip of the wire (Dizdar et al 2019). This device has been shown to be effective in capturing CTC for subsequent molecular characterization for EGFR mutations with results in >80% concordance to matched tissue biopsy samples (Fleichacker et al 2015; Scheumann et al 2015). However, it's wide spread use in the clinic is limited- because of the long (8 hours) and laborious process for CTC isolation prior to molecular characterization involving: fixation, staining, microscopic evaluation and fragmentation of the medical wire. Additionally, this device requires the use of highly skilled technicians to operate the device.

Microfluidic bio analyzers have also been utilized for CTC isolation for subsequent molecular characterization for precise molecular diagnosis in cancer. These devices have the advantage of creating a structured environment through intricate design and application of active manipulation forces to influence/control the behaviour of cells in blood (Zou & Cui 2018; Descamps et al 2022). Most biophysical microfluidic devices

that have isolated CTC to detect EGFR mutations in NSCLC have applied the principle of hydrodynamics. Devices such as; the spiral microfluidic device designed by Warkhani et al (2016), Weir microfluidic channel device for single cell isolation designed by Yeo et al (2015) and the FAST disc microfluidic device designed by Kim et al (2017) have all employed the use of sophisticated designed micro-channels and/or microstructures that manipulate the velocity of blood flowing into the device such that, coupled with lift forces causes cells in the blood to be separated based on differences in size and deformability (Habili et al 2020). EGFR mutations detected from CTC isolated using these devices were reported to be in high concordance (≥80%) with molecular alteration results obtained from tumor biopsy samples (Yeo et al 2015; Warkhani et al 2016; Kim et al 2017). However, the routine use of these devices in the clinics may not be realized primarily due to cumbersome pre-processing prior to isolation and difficulty in batch processing for large scale chip production because of the intricate design of these chips and or devices (**Chapter 1, Section 1.12.2.3**). Some biochemical based microfluidic bio analyzers have used the immuno-affinity approach for isolation of CTC. The immuno-affinity approach for biochemical microfluidic based devices usually employs the specificity of an anti-EpCAM antibody linked to a stationary surface or a magnetic nanoparticle for EpCAM positive cells. Devices- such as: the CTC chip, Herringbone chip, Oncobean chip and Nano Velcro chip have all explored the isolation of CTC with subsequent mutational analysis for EGFR mutations. The ability to vary flow rates through rational design of devices with geometries that allow for maximum interaction between EpCAM positive CTC present in blood and anti EpCAM antibody attached to stationary surface on the devices are the key technology. Alternatively, the "Magnetic Sifter" can isolate CTC via the affinity of EpCAM positive CTC for an anti EpCAM antibody linked to a magnetic nanoparticle. Although CTC isolated using the above-mentioned devices have been used to detect mutations in NSCLC. Release of CTC captured on the stationary surface of these devices for molecular analysis is a cumbersome process involving lysis and washing of cells this affects integrity of CTC used for molecular characterization (Nagrath et al 2007; Masherewan et al 2008; Earhart et al 2014; Murdhilar et al 2014; Ke et al 2015; Park et al 2016; Sundaresan et al 2016). This challenge has limited its adoption in the clinics for routine use. Furthermore, poor throughput for CTC isolation, laborious workflow and reproducibility of chips has also contributed to the hesitancy of the adoption of these devices in the clinic.

3.1.3. Aim of study

This chapter describes the conceptualization and design of a 2-part microfluidic device for isolation of CTC from blood that is: versatile, low cost, simple in design, excludes blood pre-processing and labelling processes and ensures ease of release of CTC after capture for easy off chip CTC recovery. The present study also evaluates the proof of concept/principle by which the device works for CTC capture for downstream analysis by spiking an EpCAM positive cell lines (PC9) representative of NSCLC into media. Finally, the molecular alterations in exons 18-21 of the EGFR gene were determined by PCR analysis of the cells isolated in spiking experiments.

3.2 Materials and methods

3.2.1 Incorporation of immuno-magnetic approach to the design concept of Lung card version II microfluidic device

Lung card version II microfluidic device is based on an immuno-magnetic approach for isolation of CTC from blood. The approach used in this study involves positive selection of CTC from a population of mixed blood cells through the specificity of an antibody linked to a magnetic particle binding with the corresponding antigen expressed on CTC. The CTC + antibody+ magnetic particle can be isolated from blood on application of a magnetic field **Figure 3.1**.

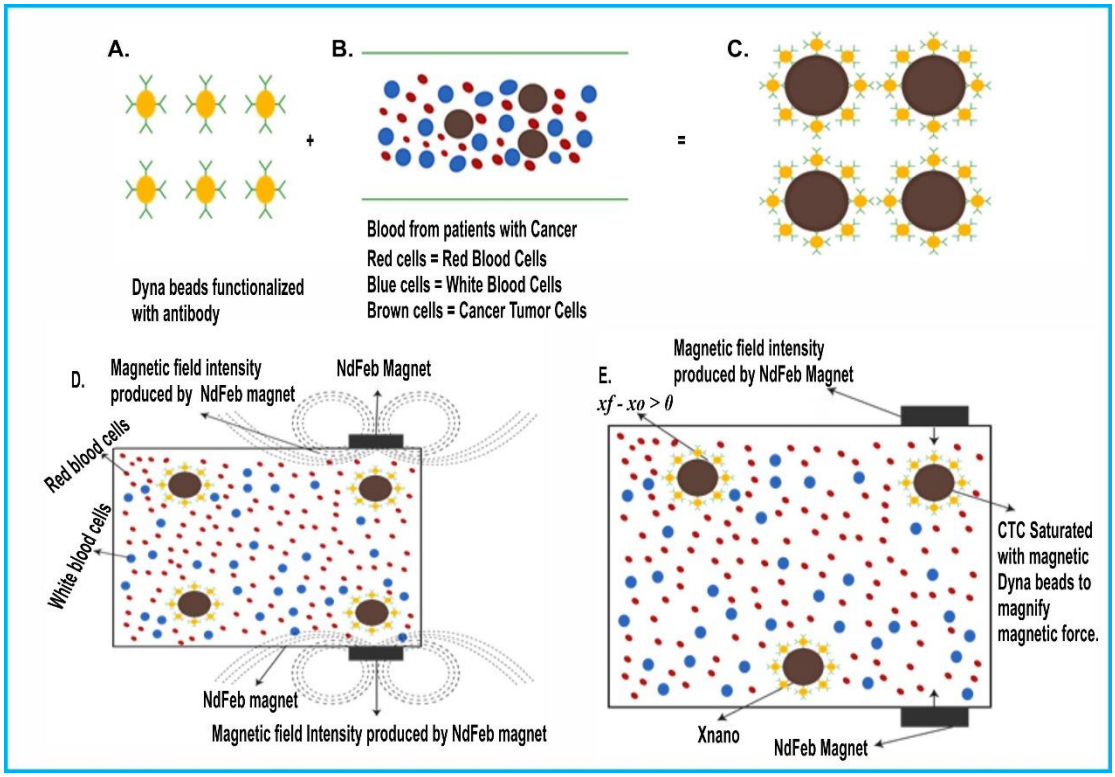

Figure 3.1: **A-** super paramagnetic Dyna beads (yellow) functionalized with BerEP4 (anti EpCAM) in green **B-** diagrammatic representation of cells in the blood of patients with cancer; **red** = red blood cells, **blue** = white blood cells (WBC) and **brown** = tumor cells **C-** shows super paramagnetic Dyna beads functionalized with BerEP4 antibody **D-** shows affinity/specificity of functionalized Dyna bead for EpCAM bearing tumour cells in blood on chip. Magnets in close proximity to the chip generate a magnetic field gradient that magnetizes the CTC+ super paramagnetic bead complex and moves/traps this complex at a precise location leaving unbound cells e.g., WBC (blue) in solution **E-**sum of all forces acting on CTC+super paramagnetic bead complex to ensure isolation of CTC at the desired location.

The antigen unique to CTC in use in this study is EpCAM. The magnetic nanoparticles used for positive selection of CTC from other blood cells are the Dyna beads (Invitrogen, UK). These nanoparticles are super-paramagnetic polystyrene beads measuring about 4.5µm in diameter coated with monoclonal antibody specific for 34&

39 kDa glycoprotein membrane antigens. It is well established that cells from cancerous lung tissues express the two splice variants of EpCAM (Barriere et al 2014; Lin et al 2021). We hypothesize that when a specified volume of these magnetic Dyna beads is put into the microfluidic chamber containing blood the mouse IgG 1 monoclonal antibody clone (BerEP4) tagged to the magnetic Dyna beads will bind to any CTC in the blood forming a complex that can be isolated as explained above.

3.2.2 Design/Capture

The chip was initially designed by Dr Alex Iles from glass and then fabricated in PMMA to facilitate further modifications by the author in response to testing (these iterations by the author are explained in **Section 3.3.2.1**).

3.2.2.1 Fabrication of glass chip

The design of the glass chip takes into consideration the objective of a simple device devoid of microstructures. The chip was first drawn on an Auto Cad DXF file and Laser cut from glass sheets (**Section 2.1.1**).

3.2.2.2 Fabrication of PMMA chip

The design of the PMMA chip also takes into consideration the objective of a chip devoid of microstructures. The same fabrication process for glass chip was applied for the PMMA chip but produced a safer more user-friendly unit (**Section 2.1.2**).

3.2.2.3 Fabrication of Lung Card Microfluidic Box

This part of the unit was built in the UK (**Section 2.1.3**) by subcontracting to a company in Leeds (MicroLab devices). The control systems were programmed by colleagues from Stab Vida (www.stabvida.com).

3.2.2.4 Preparation of PMMA chip for capture of EpCAM positive cells

Before the capture and isolation process chip were washed and air dried in a class II cabinet using 70% ethanol and molecular grade water (**Section 2.1.4**) has the full details.

3.2.2.5 Preparation of glass chip for capture of EpCAM positive cells

The dry glass chip was filled with sialinising agent (consisting of 9ml of 2,2,4 methylpentane+145µl of trichloro (1H,1H,2H, 2H-perfluorooctyl) silane (PFOCTS) and incubated for 30 minutes. The chip was washed and dried in a series of wash steps involving acetone and molecular grade water in a class II cabinet (**section 2.1.5**).

3.2.3 Proof of principle that the technique proposed for CTC capture works

The first aim was to demonstrate that the present study's technique of immuno-magnetic isolation of EpCAM positive cells from a heterogeneous cell population works. PC9 cells representative of lung cancer adenocarcinoma were spiked into media and isolated using the microfluidic device.

3.2.3.1 Cell Culture

The cell line used in this study PC9 cell line a lung adenocarcinoma cell line (Tsuji & Hyata, 1989) obtained from European Collection of Authenticated Cell Cultures (ECACC, www.phe-culturecollections.org.uk was cultured at 37^{O}C in 5% CO_2 in RPMI-1640 media (Lonza, UK) in a T75 flask (Sarstedt, UK) as described in (**section 2.2**). Harvesting of cells for experiments was done when cells were > 85% confluent (**Section 2.2)**.

.

3.2.3.2 Evaluation of EpCAM expression on PC9 cell lines using flow cytometry

EpCAM expression on the PC9 cell line was evaluated before its use in spiking experiments using flow cytometry. PC9 cell lines at a concentration of 6.3×10^{6}/ml cells were used for the experiment. Details of the flow cytometry methodology are described in **section 2.5**.

3.2.3.3 Spiking of PC9 cell lines in RPMI media

The PC9 cell lines at the following concentrations 1×10^6, 2×10^5, 4×10^4 per ml were spiked into 12ml of complete RPMI media and loaded into PMMA chip for isolation with the EpCAM positive beads as described in **section 2.1.6 &2.1.7**.

3.2.3.4 Microscopy

The EpCAM positive cell lines isolated from media were visually evaluated using a microscope to investigate capture of cells using the ×40 objective lens of a Zeiss microscope.

3.2.4 Utility of EpCAM positive cells isolated using Lung card Version II microfluidic device for downstream analysis

PC9 cell lines are known to have an exon 19 deletions and T790M mutation. The isolated cells were evaluated for mutations in exon 18-21 of the EGFR gene using two sets of primers. Sequence of primers, protocols for PCR and thermocycling conditions are given in **Table 2.4 & Section 2.11.2.** PCR products were analysed by gel electrophoresis on 2% (w/v) agarose gel (**Section 2.11.2**) Amplification of EGFR gene fragment was confirmed by appearance of bands of expected size. For the first set of primers a fragment size of 194bp was confirmed to be exon 19 (wildtype), a fragment size of 172bp represented an exon 19 deletion, a fragment size of 388bp reflected an exon 21 mutation. For the second set of primers fragment sizes of: 300bp indicate amplification of exon 18, 261bp indicated an exon 19 amplification, 251bp indicated an exon 20 amplification and a size of 320bp indicated an exon 21 amplification.

3.3 Results

3.3.2 Device Geometries

This section describes the geometrical layout of the 2-part lung Card Version II microfluidic bio analyzer (**Figure 3.2**) for CTC isolation and subsequent molecular characterization of EGFR mutational status in patients with NSCLC and discusses how it aligns with the design objectives of the current study.

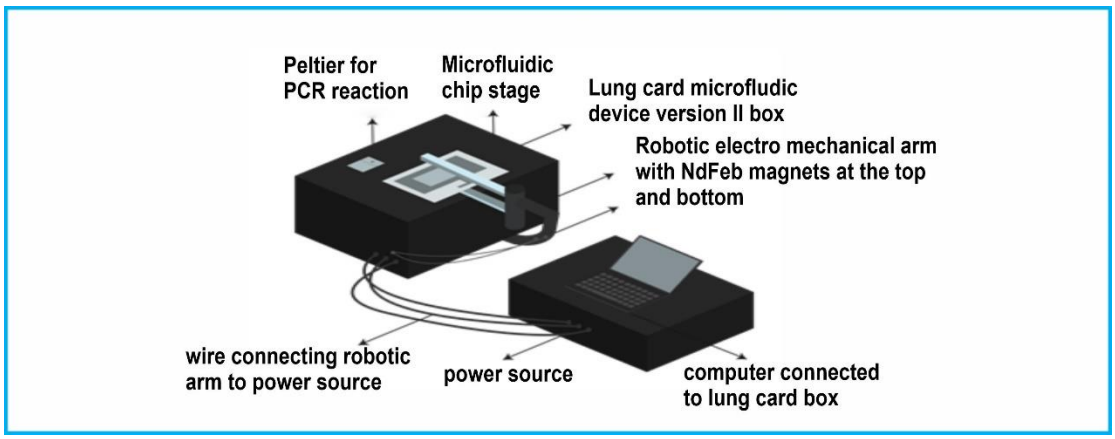

Figure 3.2: Lung Card version II microfluidic device: **A**- diagrammatic representation of Lung Card version II microfluidic device comprising a power source, magnetic robotic electromechanical arm, a computer to implement magnetic actuator programme that controls movement and direction of robotic arm and a chamber/stage for disposable microfluidic chip.

3.3.2.1 Chip geometry aligns with design objective

The design of the device aligns with the design objective of a microfluidic unit that is technically simple to operate and re-usable. **Figure 3.3 A-D and Figure 3.4 A & B.**

At the beginning of this study the 1st chip (Ist generation chip) designed was made of glass with chamber dimensions measuring 58×68mm - the idea was to design a chip that following isolation and trapping of the bead+CTC complex in one part, the complex could be moved via magnetic attraction to another part of the chamber where PCR reagents will be added for on chip DNA amplification to detect EGFR mutations **(Figure 3.3 A)**. This chip was expensive to manufacture and required a cumbersome and time-consuming process of oven drying and sialylination of chips before use. In addition, poor elastomeric properties of the glass chip made fluidic control difficult. The study then explored the design and manufacture of a 2nd generation chip made from poly methymetacrylate (PMMA). This material was more suited to the design objective of the study because of: (i) safety- glass chips are associated with breakage whilst PMMA are durable thermoplastics; (ii) flexibility- PMMA chip can easily be fabricated

or modified to include microreactors wire printing, nanoparticles or chemicals used in molecular biology techniques for DNA analysis; (iii) better elastomeric properties for fluid control than glass; (iv) preparation/modification of chip before CTC isolation is less laborious as it simply involves coating the chip with 5% (w/v) BSA and does not require an elaborate instrumentation; and (v) cost of production using PMMA is relatively low. It was estimated that it would cost less than 20p to produce 1 chip at a commercial scale (this is after the inclusion of person time and machine cost) (Matellan & del Rio Hernandez et al 2018).

The first PMMA microfluidic chip (**Figure 3.3B**) used in this study had similar dimensions to the glass device of 56×68mm with a depth of 3mm. These dimensions were sufficient to contain about 13ml of blood. However, during validation experiments it became evident that there were issues with purity as cells leftover in the chamber after isolation of EpCAM positive cells had a tendency to move easily into the collection outlet. This resulted in the modification of the first PMMA chip by Dr Iles, the author of this thesis and collaborators from Stab Vida. The second iteration of the PMMA chip (**Figure 3.3C**) was of similar dimension as the first PMMA chip but had a longer channel length such that cells isolated were trapped at the collection outlet at a farther distance from the main chamber limiting mixing of cells. The 2nd PMMA chip chamber is also capable of containing 13ml of blood **(Figure 3.3 C-F)**. A microfluidic chip with dimensions capable of containing 13 ml of blood will improve sensitivity for the detection of rare CTC. One of the challenges associated with poor sensitivity for the detection of CTC using Cell Search bioanalyzer in NSCLC was the blood volume (7.5ml) used in analysis (Dizdar et al 2019). Furthermore, the microfluidic chamber used in this study is simple in design, i.e., no micropost or microstructures in the blood chamber **(Figure 3.3 C &D)**. The present study also hypothesizes that a lack of microstructures embedded in the device and maintenance of the blood in a static phase will result in minimal destruction of the relatively rare CTC thereby, boosting capture efficiency (Myung & Houng, 2015). Also, a chip devoid of intricate geometricies allows for a device that is capable of being remodeled to incorporate additional analysis units. The simple design of the chip is associated with the objective of creating a low cost, scalable device for routine clinical use. The design of the chip also ensured that harvesting CTC isolated using the microfluidic device was easy as the captured CTC

were trapped at an outlet in the chamber by magnetization and harvesting was performed using a pipette to extract the CTC+bead complex **(Figure 3.3 C&D).**

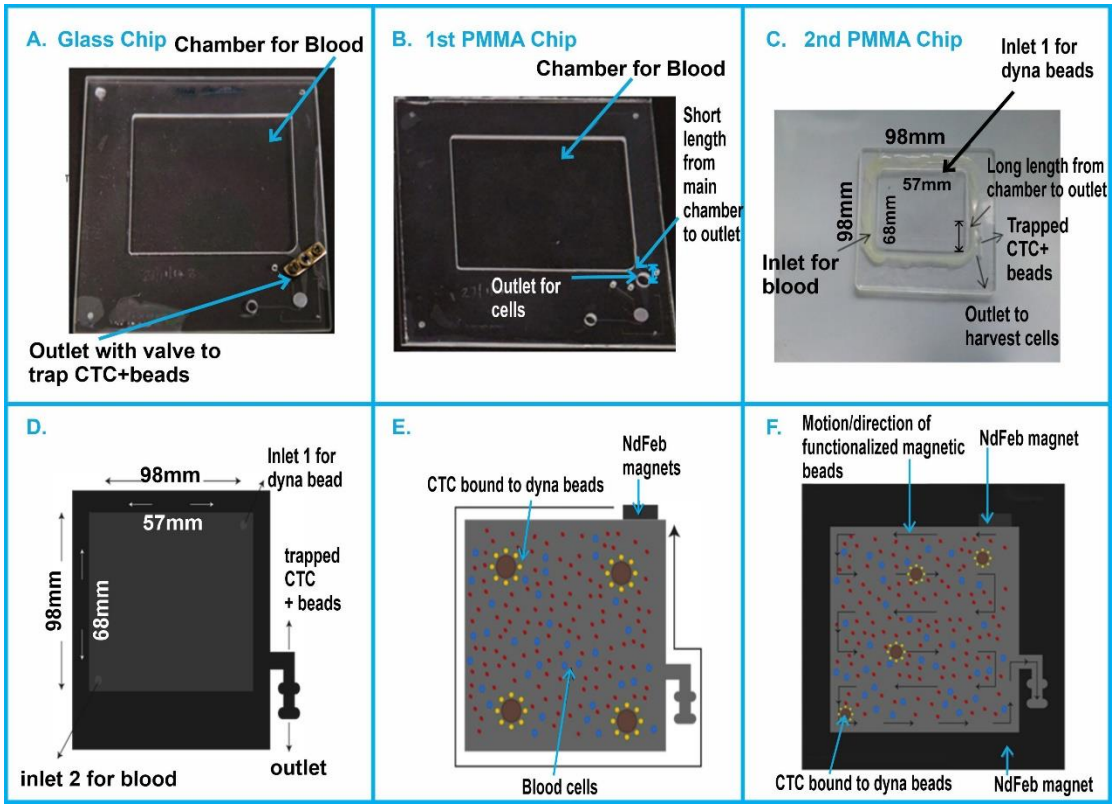

Figure 3.3: Chip geometry: **A-** 1st generation glass chip **B-** 1st generation PMMA chip with short channel length (3mm) from main chamber to collection outlet **C-** 2nd generation PMMA chip with long channel length from main chamber to collection outlet (7mm) **D-** schematic representation of 2nd PMMA chip showing long channel length from main chamber to outlet where cells are harvested. The chamber for blood measures 57mm×68mm with a depth of 3mm (dimensions sufficient to contain 13ml of blood) it has two inlets for dyna beads and blood respectively. E- depicts CTC bound to beads in chip F- shows the movement of beads in the chip following the path of the magnetic arm.

3.3.2.2 Lung card version II microfluidic unit aligns with design objective

The microfluidic unit consists of a robotic electromechanical magnetic arm that generates a magnetic force that controls the movement of epithelial enriched magnetic beads across the microfluidic chip (**Figure 3.4)**.

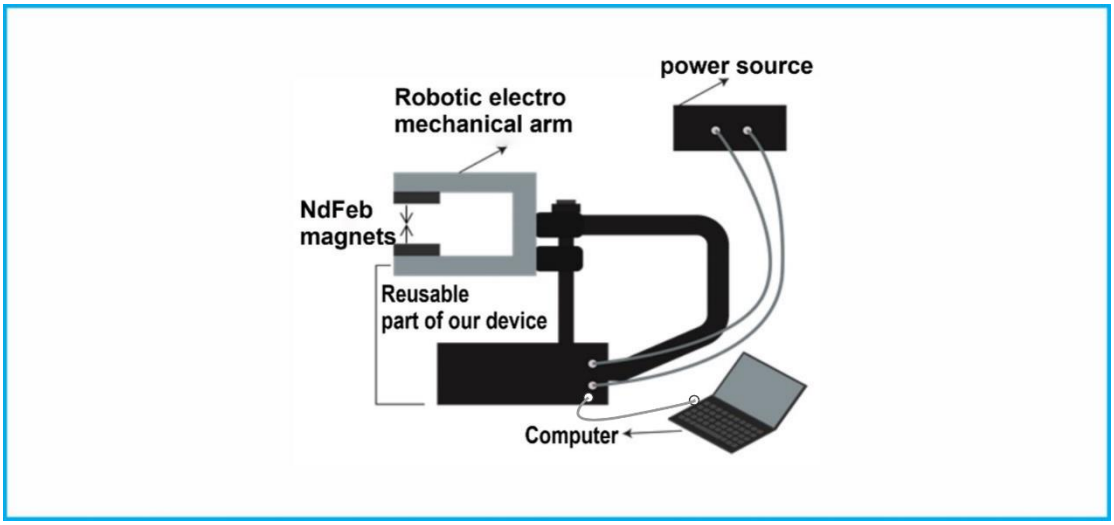

Figure 3.4: Diagrammatic representation of the reusable part of the device comprising of a robotic electro mechanical arm to which NdFeb magnets are attached to the top and bottom. This arm is powered by an electrical source and controlled by a magnetic actuator programme implemented by the computer. Figure drawn using Adobe illustrator.

The robotic electromechanical magnetic arm is designed to have no direct contact with the chip containing blood. It is separate and re-usable; it contains two NdFeB magnets measuring 20×5×4mm that are positioned at the top and bottom of the arm at a distance of 3mm from the top and bottom of the chip. The lung card microfluidic device also comprises a peltier for PCR **(Figure 3.2).** The x y and z motion of the robotic magnetic arm that is responsible for generating and distributing magnetic force acting across the chip is controlled by a magnetic actuator App installed on the laptop **(Figure 3.4)**. The program used by the magnetic actuator App was designed specifically for chip dimensions. Motion of the robotic arm begins from the first inlet where the Dyna beads are placed and there is delay of 10 seconds before motion of the magnet carrying robotic arm moves across the chip generating a magnetic field gradient that ensures motion of the functionalized magnetic beads seeking EpCAM positive cells **(Figure 3.3E & F)**. The speed and distance at which the magnets will move across the x, y and z axis is predetermined. The movement of the robotic arm across the microfluidic chip is not continuous there are step delays of 6 seconds in between movements this allows for sufficient time during motion for essentially all magnetized cells to be dragged through the fluid trapped together until they arrive at the outlet for harvesting. The speed times and interval were determined empirically (7-15mm/10seconds). The mechanisms of the microfluidic unit in this study aligns with the device objectives in the following ways: (1) the use of mobile magnets whose motion is precisely controlled and chip specific

systematically moves the functionalized magnetic beads through the blood maximizing the opportunity for EpCAM positive cells to be bound by sufficient anti-EpCAM coated magnetic beads for collection. This will result in capturing CTC with high yield. (2) the specificity of the antibody for EpCAM positive cells and the difference in magnetic field intensity between captured mobile EpCAM positive cells bound to functionalized magnetic beads and surrounding static blood cells ensures that only cells that express EpCAM are isolated and (3) precise movement of magnetic arm within a specified time will facilitate analysis of 13ml of blood in 50 minutes.

3.3.3 Lung Card Version II microfluidic device isolates EpCAM positive PC9 cell lines spiked in media

PC9 cell lines were evaluated for EpCAM expression using flow cytometry (**Figure 3.5)**. The shift of the green histogram plot towards a relatively high fluorescence indicates EpCAM expression by PC9 cells when compared with purple histogram plots representing negative isotype control.

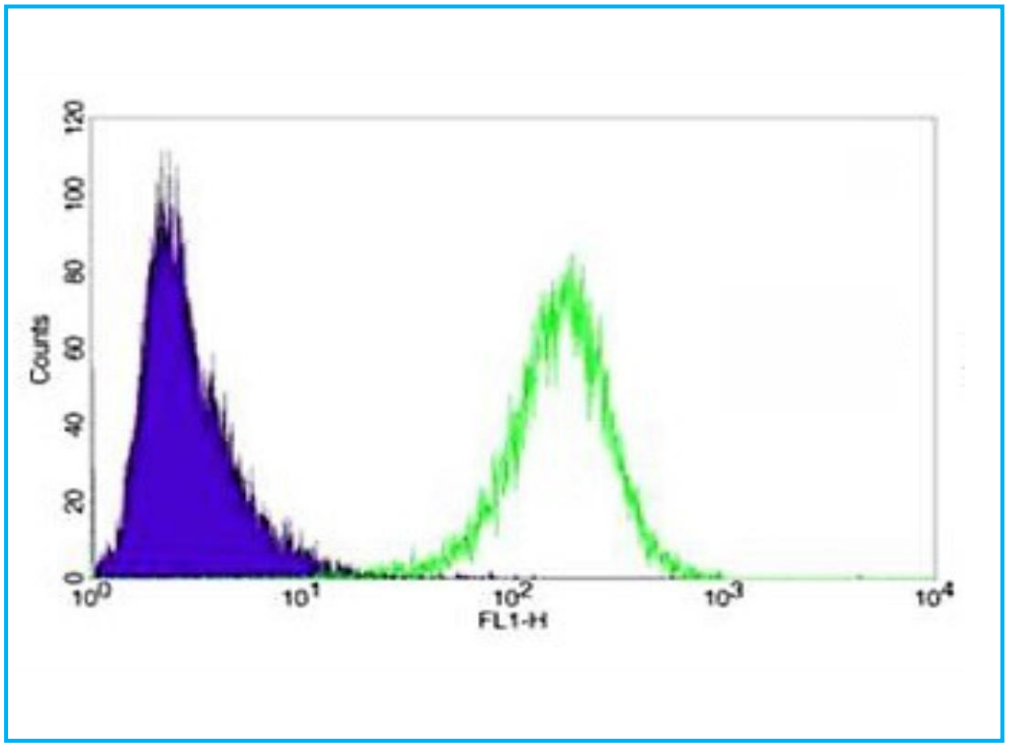

Figure 3.5 Histogram plot showing-EpCAM expression of PC9 cancer cell lines after flow cytometric analysis. PC9 cell lines were labelled with a FITC labelled anti-EpCAM antibody and analyzed using a FACS Calibur (Becton-Dickson). Analysis of PC9 cell lines to evaluate EpCAM expression was done in 3 separate experiments. Results from the repeat experiments

are in the appendix. The purple peak represents the isotype negative control. The right shift of the green plot is indicative of an increase in fluorescence intensity and thus expression of EpCAM compared with the negative control.

Following demonstration that PC9 cell lines express consistently high levels of EpCAM, 1 ml of 1×10^5 PC9 cell lines was spiked into 12ml of RPMI complete media and loaded into PMMA microfluidic chip. The PC9 cell lines were then isolated using the Lung card version II device as described in **Section 2.1.6 & Section 2.1.7**. The isolated cells were observed under a Zeiss Microscope using the × 40 objective to view capture of EpCAM positive cells by the device (**Figure 3.6**). Microscopy results show capture of EpCAM positive cells by functionalized magnetic beads.

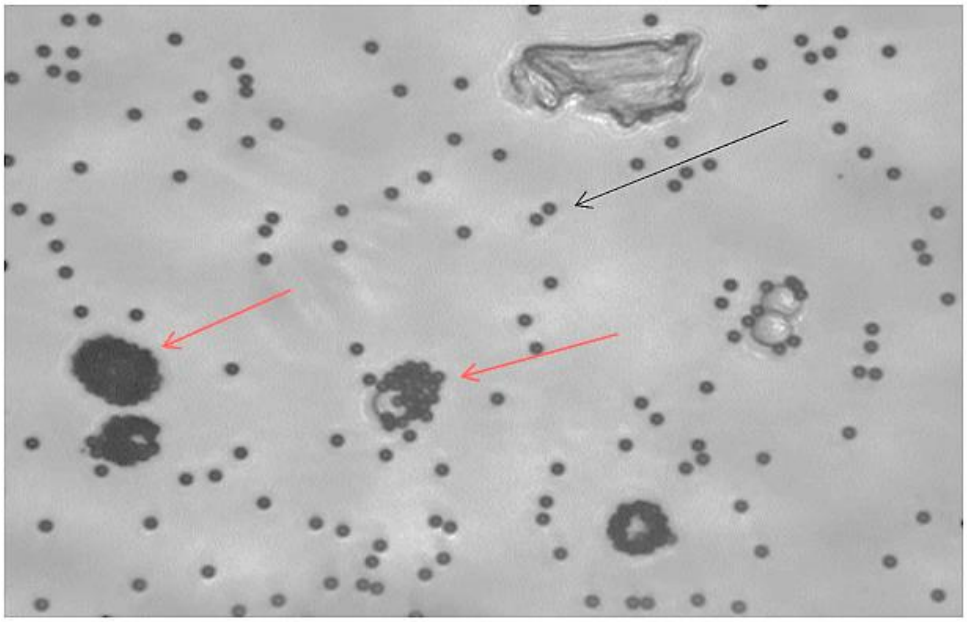

Figure 3.6: Shows capture of EpCAM positive PC9 cells spiked in media using the Lung card version II microfluidic device. Red arrows depict cells captured by magnetic beads functionalized with anti-EpCAM antibody whilst, the black arrows show unbound magnetic beads. Spiking experiments of PC9 cells in media and isolation of cells using the microfluidic device was done on three separate occasions results from other experiments can be found in the appendix.

3.3.4 EpCAM positive cells isolated/captured using the Lung Card Version II microfluidic device can be used for subsequent downstream PCR analysis

PC9 cells isolated using the microfluidic device were then used for downstream analysis to detect EGFR mutations. PCR experiments were performed on PC9 cells using two sets of primers (**Table 2.3**). The SV primers (**Figure 3.7A)** were for the

amplification of the entire exon 18-21 regions whilst, the UOH primers were for the detection of exon 19 deletion and exon 18 L858R mutation (**Figure 3.7B)**. The result from this experiment showed that PCR detection of mutations in exon 18-21 from cells isolated using the device in this current study was possible. **Figure 3.7A** shows amplification of exon 18 (300bp) in (lane 3), exon 19 (261bp) in (lane 5), exon 20 (251bp) in (lane 7) and exon 21 (320bp) in (lane 8) of the EGFR gene from isolated PC9 cells spiked in media. **Figure 3.7B** shows multiplex PCR displaying; exon 19 deletion-172bp, exon 19 WT-194bp, L858R mutation-388bp (lane 3). The limit of detection was studied by spiking EpCAM positive cells into media at the following concentrations (1×10^6/ml, 2×10^5/ml, 4×10^4/ml and 8×10^3/ml) and the feasibility of isolating sufficient cells to be utilized for downstream analysis for EGFR mutation was then tested. Results, from multiplex end point PCR experiments (**Figure 3.7C)** showed amplification of exon 18-21 regions of the EGFR gene using SV primers in lanes 3, 4, 5 and 6 irrespective of initial concentration of spiked cells.

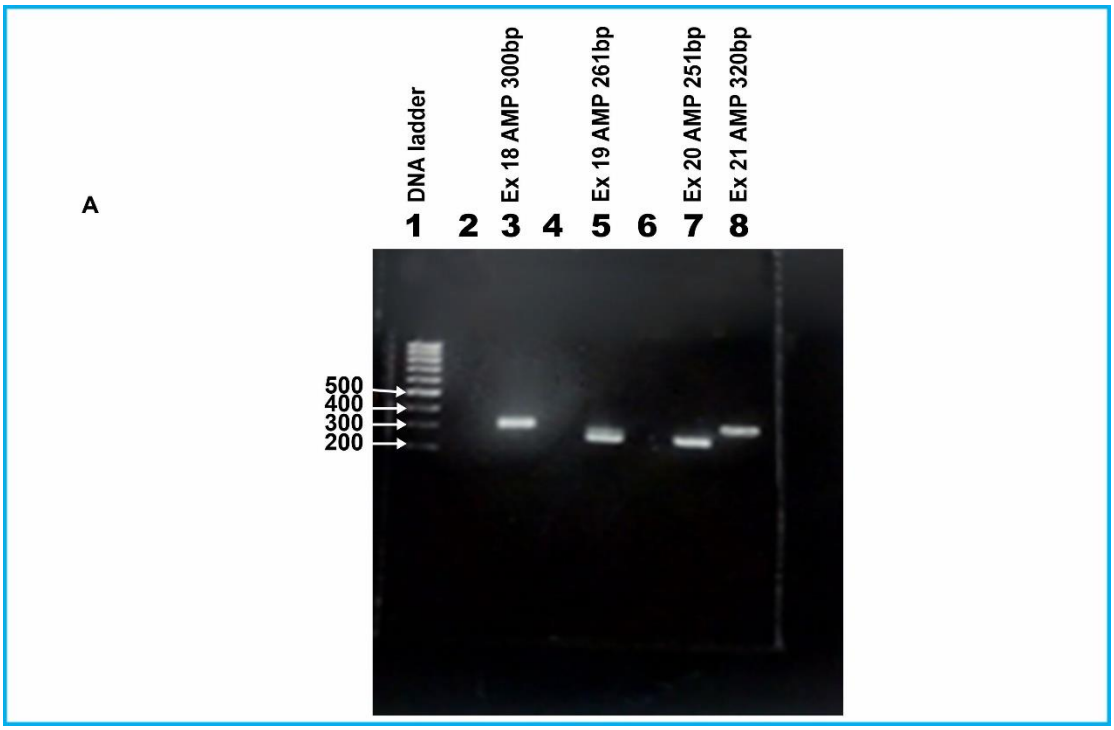

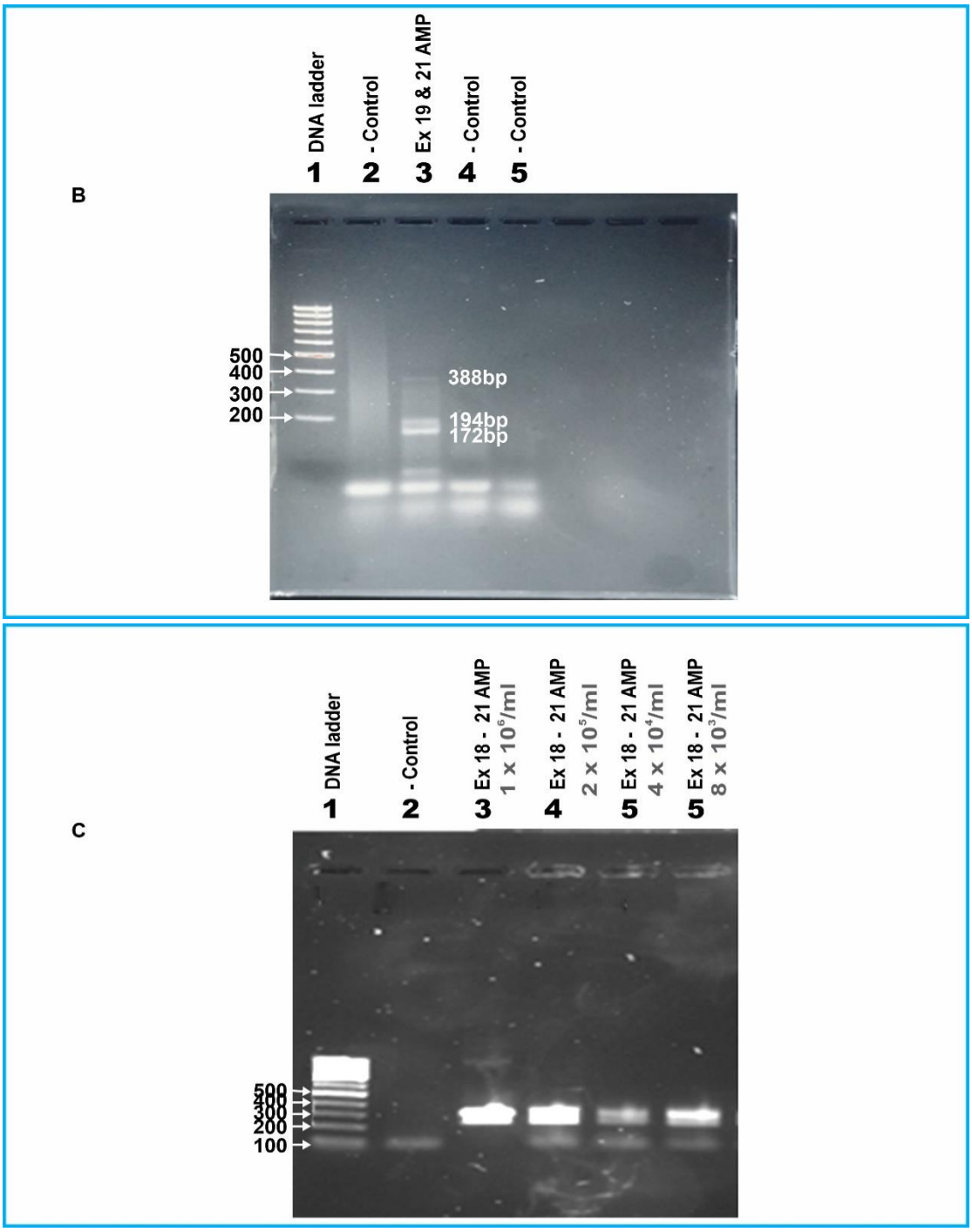

Figure 3.7 Gel electrophoresis showing amplification of exon 18-21 of the EGFR gene of EpCAM positive PC9 cell lines. PCR was done in 2 separate experiments, results from the second experiment is shown in the appendix. **A-** Shows amplification of exons 18 (300bp) exon 19 (261bp) exon 20 (251bp) and exon 21 (320bp)- regions in (**lanes 3,5,7&8 respectively**) using primers from Stab Vida (SV) included on the gel are DNA ladders and negative control on **lane1&2** respectively **B-** shows detection of exon 21 L858R mutation 388bp, exon 19 WT-194bp and exon 19 deletion 172 bp all in (**lane 3**) using primers from university of Hull. **C-lanes 3, 4, 5& 6** show amplification (multiplex PCR) of exon 18 (300bp), exon 19 (261bp), exon 20 (251bp) and exon 21 (321bp) regions of EGFR gene in PC9 cell lines spiked in RPMI media at the following concentrations 1×10^6, 2×10^5, 4×10^4 and 8×10^3/ml respectively. **Lanes 1& 2** are DNA ladder and negative control respectively.

3.4 Discussion

The present study describes the conceptualization and design of the Lung card version II microfluidic device and how it aligns with the objective of a versatile, cost efficient, easy to use device for isolating CTC efficiently from blood for downstream analysis for EGFR mutations.

The concept of a 2-part device comprising of a disposable microfluidic chip and a re-usable microfluidic unit (**Figure 3.2**) differs from other microfluidic devices that have isolated CTC for subsequent molecular characterization. Previously described microfluidic bioanalyzers (**Section 1.11.2**) have their microfluidic unit merged to the chip (Sequist et al 2009; Park et al 2014; Murdihlar et al 2017; Miller et al 2018). The device in this current study has the following advantages over the microfluidic bioanalyzers outlined above: (1) it addresses biohazard issues as the only part of the device in contact with blood is disposable chip; (2) has reduced cost as, the main microfluidic unit is re-usable; and (3) offers flexibility, as novel-technologies and/or structures can be incorporated independently into each unit depending on the specific analysis required.

The microfluidic chip (**Figure 3.3**) is fabricated from PMMA. The choice of PMMA as material for chip fabrication was because of its elastomeric properties, compatibility with body fluids, surface stability, cost, flexibility and ease of manufacturing i.e., laser micro machining used is a rapid, accurate and a cost-efficient process (Chen et al 2008; Matellan& del Rio Hernandez et al 2018). The PMMA disposable chip used for this study compares favourably with other microfluidic chips as its surface stability allows for the integration/machining of technologies into the chip to permit a wide breadth of application e.g., incorporation of microreactors, wire-imprinting, and surface modification with nanoparticles for genomic analysis (Chen et al 2000; Xu et al 2002; Hashimoto et al 2006; Chen et al 2008; Scott &Ali, 2021). Machining and incorporation of technologies into chips made up of silicon, glass and PDMS is a challenge because of brittleness associated with silicon and glass chips, difficulty in deposition technologies such as electrodes has been reported with PDMS chips (Tsao, 2016). In terms of cost PMMA is relatively cheap in comparison with silicon, glass and PDMS. Silicon and glass cost about 10-20 cents per cm^2 whilst PDMS and PMMA cost around 0.2-2 cents per cm^2 (Scott & Ali 2021). Although PDMS material is similarly cheap the laborious process of heating, curing and plasma bonding increase device manufacturing costs (Annabestani et al 2020). In total it cost less than £1 to manufacture the PMMA

chip used in this study. The PMMA chip in this study is devoid of intricate microstructure or architecture this also facilitates production, reproducibility and future scale up (**Figure 3.3**). This is unlike all the microfluidic devices that have isolated CTC for downstream analysis highlighted in the introductory chapter. Furthermore, the ability of the chamber to hold 13ml of blood for isolation of CTC improves the probability of isolating CTC especially if present at low concentrations. Larger blood volumes have been associated with increased capture yield of CTC from patients with cancer. Scheumann et al (2015) reported higher detection rates for CTC using the GILUPI cell collector when compared with Cell Search in 50 patients with lung cancer (58% vs 28% respectively). The Gilupi Cell collector analysed 18ml of blood whilst, the Cell Search bioanaltzer only held 7.5ml. The maximum volume of blood used by any of the microfluidic bioanalyzers reported in the literature for CTC isolation is 10ml. This current study reports that the microfluidic unit's (**Figure 3.4**) technique of moving functionalized magnetic beads systematically across static blood on a chip ensures that EpCAM positive cells are captured efficiently. This study also reports that the design of mobile external permanent magnets and absence of fluid flow gives Lung card version II microfluidic device an advantage over other immuno affinity based devices that have explored CTC isolation for downstream analysis for EGFR mutation in NSCLC in the following ways: (1) the permanent mobile NdFeB magnets used in the device are capable of generating a large magnetic field sufficient for capture with no joule heating which is in contrast with the immuno-magnetic based approach used in Cell Search that has stationary electromagnets incorporated into the device, merging of electromagnets into a device's mechanism can cause joule heating and destruction of fragile CTC (Pamme 2007); (2) the absence of fluid flow will help in the preservation of CTC (Myung & Hong 2015; Zuo & Cui, 2018). Furthermore, this study also suggest that the Lung Card microfluidic device has benefit over other devices highlighted in the introductory section of this chapter (**Section 3.1.3**) in-terms of ease of harvesting cells from chip for off chip downstream analysis for molecular alterations. The cells+ bead complex isolated are collected at an outlet for a one step harvesting using a pipette this is unlike other devices discussed previously that isolate CTC based on its capture on a stationary surface. Harvesting of CTC from a stationary structure requires a rigorous process involving mechanical and chemical manipulations (Zuo & Cui, 2018).

Work in this chapter has also shown that captured EpCAM positive cells can be used to assess molecular alterations in exon18-21 of the EGFR gene by PCR. Spiking cells

at various concentrations has shown that as few as 8×10^3/ml cells can be efficiently isolated and analyzed for mutations associated with exon 18-regions of EGFR gene from PC9 cell lines (**Figure 3.6 & 3.7**).

3.5 Conclusion

The present study describes a microfluidic device that is versatile, low cost, easy to use and reproducible. This study shows that the platform successfully isolates EPCAM positive PC9 cells which can then be analyzed for EGFR mutations by PCR.

Chapter 4

Validation of Lung card version II microfluidic device to assess capture efficiency, purity and throughput

4.0 Background

Utilizing CTC for downstream molecular analysis is highly dependent on techniques/devices used for the isolation. The technique must isolate CTC with high capture efficiency, purity and if it is to be taken up in the clinic have relatively high throughput (Habili et al 2020). It is important that any device isolating CTC captures these efficiently so that results from molecular analysis report genomic events in the tumour landscape in its entirety (Alix-Panabieres, 2021). Capture efficiency of a device is usually evaluated by quantifying its ability to isolate tumour cells of known concentration spiked either in PBS, media or blood (Cho et al 2018).

Purity of CTC refers to the capacity of a device to capture CTC specifically from a heterogeneous group of interfering cells. Purity of CTC isolated is essential so that all molecular signals from cells isolated is not obscured by wildtype signals from interfering cells. The purity of isolated CTC is normally assessed as a ratio of the number of CTC isolated to the total number of nucleated cells recovered (Banko et al 2019). Throughput represents the volume or number of samples a device can analyse per unit time and it is a key factor for widespread adoption in the clinic (Myung & Hong, 2015; Deschamps et al 2022).

4.1 Performance indices of basic parameters of devices that have explored CTC isolation for molecular characterization of EGFR mutations

Validation studies to assess capture efficiency of **Nagarath's CTC chip** involved spiking fluorescently labeled cancer cell lines (high and low EpCAM expressing) at concentrations ranging from 50-50,000 cells/ml in PBS and blood of healthy individuals. Efficiency rates from their study were reported to be ≥65% for spiking experiments with PBS using various cell concentrations and across all cell lines, and ≥60% for spiking experiments involving blood (Nagrath et al, 2007). Good capture efficiency was also demonstrated for this chip by its ability to isolate CTC from 116 patients diagnosed with either breast, pancreatic, prostate, colorectal and NSCLC cancers. The numbers of CTC isolated from patients with these cancers were 5-1,284 cells/ml. Purity of CTC isolated from these patients was evaluated using immunofluorescence. Purity values reported from the study were 52% (NSCLC), 49% (prostate cancer), 53% (pancreatic cancer) 60% (breast cancer) and 67% (colon cancer).

All samples were analysed at flow rates of 1ml/hr. (Nagrath et al 2007; Habil et al 2020).

The capture efficiency rate for the **Herringbone chip** from validation experiments involving spiking fluorescently labelled PC3 cells (Prostate cancer) in 1ml of media at a concentration of 1,000 cells/ml was reported to be 75%±4.5%. Capture efficiency of the Herringbone chip in isolating CTC from clinical samples has been demonstrated by its ability to isolate CTC from 28 out of 42 patients with NSCLC. Purity of EpCAM positive PC3 cells isolated using the device was also evaluated by spiking cells in PBS with a background of contaminating white blood cells. Purity from this experiment was reported to be only 14.0%±0.1%. Samples analysed in these validation and clinical studies were run at a rate of 1.2ml/hr (Stott et al 2010; Suderasan et al 2016,).

Experiments to assess the capture efficiency of the **Oncobean chip** involved the spiking of fluorescently labeled EpCAM expressing cancer cell lines at a concentration of 1,000cells/ml into whole blood from healthy donors. Capture efficiency was reported to be ≥85% for the cell lines (Murdilhar et al, 2014). Efficiency of capture using the Oncobean chip has also been reported in clinical studies. Murdihlar et al (2017) isolated CTC from the pulmonary vein and artery of 36 patients with NSCLC during surgery and reported CTC counts of 0- 10,234 from the pulmonary vein of patients and CTC counts of 0-28.5 from the pulmonary artery. Samples were analysed at 10ml/hr. for validation experiments and 3ml/hr. for the clinical studies. No purity values have been reported using the Oncobean chip either from validation studies with cell lines or clinical studies (Banko et al 2019).

Capture efficiency of the **Nano Velcro chip** was evaluated by spiking 200 cells/ml of EpCAM positive cancer cell lines stained with Diogreen fluorescent dye into 1ml of RPMI media containing 5×10^6 WBC/ml. Capture yield obtained from this experiment was ≥70%. A CTC count of 0-98 was reported from 100 patients with metastatic castration resistant prostate cancer, and purity was ≤ 35%. Samples were analysed at a flow rate of 2ml/hr for validation studies and 7.5ml/hr for clinical studies (Ke et al 2015; Chen et al 2016).

Device performance of **Magnetic Sifter** in terms of capture efficiency and purity was evaluated by spiking fluorescent labeled high and low EpCAM expressing cancer cell lines at concentrations ranging from 50-100 cells/ml in blood from healthy donors. Capture efficiency was reported to be ≥ 95.7% for cell lines expressing relatively high levels of EpCAM and ≤ 48% for cell lines expressing relatively low levels of EpCAM. A total of 31-96 CTC was isolated from 6 patients with NSCLC. Each sample was analysed at a rate of 10ml/hr. The purity of CTC isolated was reported to be 17.7±9.3%. Each sample was analysed at a rate of 10ml/hr (Park et al 2016).

Validation studies for **biophysical based devices** (Spiral microfluidic chip, FAST Disc, Weir-structured microfluidic chip and Parsotrix) report that these devices have a capture efficiency of ≥ 70% from spiking experiments. These experiments involved spiking cancer cell lines at concentrations ranging from 100-1,000 per ml into whole blood or media. These devices have also been employed for CTC capture in patients with cancer. CTC counts reported from these studies ranged from 2-500. Samples used for these studies were analysed at 7.5ml/min for spiral microfluidics, 10ml/hr for weir-structured microfluidic chip, 5ml/hr for parostrix and 3ml/min for FAST disc (Yeo et al 2015; Warkiani et al 2016; Lim et al 2020). Purity of CTC isolated was not reported in these studies. Biophysical based microfluidic devices are usually not associated with high purity (≤50%) additional post processing steps are normally included in the workflow to enhance this parameter (Ferreira et al 2016; Miller et al 2018; Zhang et al 2020).

Taken together, validation studies discussed above suggest that these microfluidic devices do not meet all the required criteria for devices processing/isolating CTC for downstream analysis for detection of mutations mainly because of issues with low throughput and purity. The rarity of CTC in blood has led to the proposition that blood volumes ≥ 7.5ml should be used as a standard for efficient isolation of CTC (Myung & Hong 2015; Banko et al 2019). Applying this standard to devices such as CTC chip, Nano Velcro chip and Herringbone chip that analyse samples at rates between 1-5ml/hr. could mean isolating CTC from a sample using these devices would take between 3.5-8 hr this is unrealistic for routine clinical use. In addition, there is no set standard for purity. However, the general belief is that higher purity equates to better molecular characterization (Rushton et al 2021).

4.1.2 Aim of study

Results from the previous chapter (**Chapter 3**) suggest that the concept and design of Lung Card microfluidic device isolates EpCAM positive cells and cells isolated using the device can be used for downstream analysis to detect EGFR mutations. This chapter determines the capture efficiency and purity of the device to isolate CTC and investigated the feasibility of the device to act as a platform for CTC processing for molecular analysis.

To demonstrate the validity of the device described in this present study to capture EpCAM positive cells. Models of CTC were created in a heterogeneous fluid by spiking CFSE labelled cancer cell lines expressing varying levels of EpCAM into RPMI media and sheep blood at clinically relevant concentrations. The utility of the device in isolating CTC from patients with NSCLC was also evaluated.

To evaluate purity of CTC isolated using the device each CFSE labelled cancer cell line used in the study were spiked at clinically relevant concentrations into RPMI media containing PBMC of known concentration stained with cell trace far red dye (ThermoFisher). Purity was determined by quantifying the ratio of CTC isolated to WBC isolated.

The utility of the device to serve as a platform for CTC processing for downstream analysis to detect molecular alterations was assessed using RNA and DNA extracted from isolated CTC from blood of NSCLC patients recruited for the study and evaluated for cancer specific markers and mutations in exon 18-21 of the EGFR gene.

4.2 Materials and methods

4.2.1 Cell culture experiments

The cell lines used in this study HT 29- a human colorectal adenocarcinoma cell **(**Frogh & Trempe,1975), MCF-7- human Caucasian breast (Abban et al, 1973), PANC-1- human pancreatic cell lines of ductal origin (Lieber et al 1975), PC9- human lung adenocarcinoma (Tsuji & Hyata, 1989) were cultured as described in **Section 2.2 & 2.4**.

4.2.2 Determination of EpCAM expression on PC9 cells, HT-29, MCF-7 and PANC-1 cells using flow cytometry

Flow cytometry was used to evaluate EpCAM expression on PC9, HT29, MCF-7 and PANC-1 cell lines so that the Lung card Version II microfluidic device could be assessed in terms of isolating cells with varying levels of EpCAM. The flow cytometry set up was as described in **section 2.5**.

4.2.3 Spiking experiments in media to evaluate capture efficiency of cells with varying levels of EpCAM expression

4.2.3.1 Spiking

After culture and harvesting cell lines as outlined in **section 2.2**, a count and viability check was done on the cell suspension as described in **section 2.4**. All cell lines used for spiking experiments were at a concentration of 5.0×10^6/ml and had a viability of at least 90%. A stock concentration of 1×10^6/ml in 1.5ml of RPMI media was made up and serial dilutions of 2×10^5, 4×10^4, 8×10^3, and 1.3×10^2 were made and cells were stained using 5µl of CFSE for 20 minutes in the dark at room temperature. After staining, 1ml of cells was added to 12ml of complete RPMI media (Lonza) supplemented with 10% (v/v) foetal bovine serum (Labtech) and 50µ/ml penicillin and 250µg/ml streptomycin (Lonza). The spiked media was loaded into the Lung card version II chip for isolation /capture of EpCAM positive cells as described in **section 2.1.6** and extraction as outlined in **section 2.1.7**. Cells extracted from the chip were suspended in 200µl of PBS for microscopy.

4.2.3.2 Cell Counting

Ten micro litres of EpCAM positive cells+bead complex suspended in 200µl of PBS was loaded into a Neubauer counting chamber (Hawksley Lansing, UK) and a count was performed as outlined in **section 2.4** to evaluate capture efficiency. **Section 2.6.3** describes the formula used for calculating the efficiency.

4.2.3.3 Fluorescence Microscopy

The stained cells were observed before isolation under a fluorescence microscope (Zeiss) with the ×40 objective lens using both brightfield and Alexa 488 imaging. Captured EpCAM positive cells as well as the media left over after capture were also both examined microscopically as outlined above.

4.2.4 Spiking experiments in sheep blood to evaluate capture efficiency of the Lung card version II microfluidic device

4.2.4.1 Spiking

Cell spiking experiments were carried out by adding CFSE stained cell lines HT-29 (high level of EpCAM expression). MCF-7 (high level of EpCAM expression), PC-9 (high level of EpCAM expression) & Panc-1 (low level of EpCAM expression) at clinically relevant concentrations as outlined in **Section 2.2, 2.4, 4.2.3.1** into sheep blood (Rockland Immunochemicals) and then isolating EpCAM positive cells using the microfluidic device as outlined in **section 2.4**. The efficiency of capture was evaluated using the formula described in **section 2.6.3.**

4.2.4.2 Fluorescence Microscopy

The EpCAM positive cells captured were observed using the brightfield and green field imaging of the Olympus BX53 fluorescence microscope with ×40 objective lens.

4.2.5 Determination of purity of EpCAM positive cells isolated

4.2.5.1 Spiking experiments to evaluate purity

The purity of EpCAM positive cells isolated using the microfluidic device was evaluated by spiking 1ml of 3×10^6 peripheral blood mononuclear cells (PBMC) stained with Cell Tracker far red dye (Invitrogen) into 12ml of RPMI Media (Lonza) containing HT-29, or MCF-7, or PC9 or Panc-1 cancer cells stained with CFSE (Invitrogen) at

varying concentrations. Concentrations, dilution and spiking protocol are outlined in **Section 2.6.1**& **2.8.3** After spiking, EpCAM positive cells were isolated from the media using Lung card version II microfluidic device and purity was evaluated via imaging with a Confocal microscope as outlined in **Section 2.8**

4.2.6 Isolation of PBMC from media using Lung Card version II microfluidic device to demonstrate its specificity.

PBMC obtained from cryovials were spun at 405*g* for 3 minutes. After centrifugation the pellet of cells were re-suspended in PBS and washed as described in **Section 2.8.1.** After washing, the cells were counted, and a viability check was done as outlined in **Section 2.4.** A viability of at least 90% was obtained for all the PBMC used in this study. PBMC cell suspension (1ml of 1×10^6 cells/ml) was stained with 5µl CFSE (Invitrogen) as described in **Section 2.6.1**. After washing the cells were suspended in 1 ml of complete RPMI Media and spiked into 12ml of RPMI media for isolation /capture of EpCAM negative PBMC using Lung Card version II microfluidic device as outlined in **Section 2.1.6 and 2.1.7.** After capture, imaging of captured cells was performed using bright field and Alexa 488 (Olympus BX53 fluorescence microscope).

4.2.7 Utility of Lung Card version II microfluidic device to isolate CTC from blood of patients with cancer

4.2.7.1 Patient sample collection

Patients (n=59) with ages ranging from 47-81years diagnosed with NSCLC from tissue biopsy attending the Oncology clinic at the Queens Centre (Castle Hill Hospital) were recruited for this study (**see Section 2.9.1)**. Clinico-pathological characteristics of these patients are summarized in **Table 5.1**. Thirty-eight of the 59 patients recruited for the study had their blood samples analyzed for CTC. Fourteen ml of peripheral blood was collected in a 3.2% trisodium citrate anticoagulant bottle (BD, USA). All samples were anonymized and encoded before the analysis.

4.2.7.2 Patient sample analysis for CTC

The whole blood sample to be analyzed was collected and transported within 15 minutes of collection in a blood bag with an ice pack to the laboratory. On arrival in the laboratory, a visual check was done to ensure that the blood collected was free from

clots. The analysis process of blood collected is as described in **Sections 2.1.6, 2.1.7 &2.8**

4.2.7.3 CTC Enumeration

After isolation of EpCAM positive CTC using Lung card version II microfluidic device and its extraction from chip. An aliquot of 10µl of EpCAM positive CTC+ bead complex suspended in 200µl of PBS was loaded onto a slide and counted using a fluorescence microscope as outlined in **Section 2.4**

4.2.7.4 Cytospin preparations to evaluate capture of EPCAM positive CTC from blood of patients

Cytospin experiments are as described in **Section 2.9.3.1 & 2.9.3.** After cytospin experiments the slides were viewed under the Olympus BX53 fluorescence microscope using the ×40 objective.

4.2.8 Determination of purity of EpCAM positive CTC isolated from blood of patients with NSCLC using the microfluidic device

4.2.8.1 Staining

An image analysis algorithm comprising of: staining with 4,6-diamidino-2-phenylindole (DAPI) (Vectashield, USA) for DNA content using fluorescein conjugated pancytokeratin monoclonal antibody (SIG 3464 (914202) Biolegend, USA) for epithelial cells and rhodamine conjugated mouse anti human CD45 antibody (BD Biosciences, USA) for haematological cells was used to evaluate purity. Cells isolated using the Lung Card Version II microfluidic device staining for cytokeratin were scored as CTC positive whilst cells staining positive for CD45 cells were scored as normal haematological cells see **Section 2.10.** After staining the cells were observed under a fluorescence microscope (Zeiss, Germany) using bright field and Alexa 488 imaging to identify CTC and WBC contamination

4.2.9 Utility of Lung Card version II microfluidic device to isolate CTC for down stream analysis

The presence of mRNA markers (surviving and CK7) unique to cancer cells was investigated in the EpCAM positive cells isolated from blood of patients with NSCLC to assess the applicability of CTC isolated using the device for downstream analy**4.2.9.1**

4.2.10 End point PCR to check for the presence of the following mRNA markers; Survivin and Cytokeratin 7 (CK7)

Firstly, RNA was extracted from EpCAM positive CTC+ bead cell suspension using TRIZOL method full details of protocol for RNA extraction is outlined in **Section 2.10.3.** cDNA was then synthesized from RNA extracted as described in **Section 2.10.4**. Survivin and CK7 segments of cDNA synthesized were amplified using primers spanning the exon and intron boundaries. To normalize expression levels of Survivin and CK7 the housekeeping gene GADPH was used as internal control details of primers are outlined in **(Table 2.2)**. Protocol for PCR and gel electrophoresis for analysis of PCR products are outlined in **Section 2.10.5**.

4.2.10.1 Utility of EpCAM positive cells isolated using Lung card Version II microfluidic device to determine EGFR mutation

The utility of EpCAM positive cells isolated using the device to detect EGFR mutations was investigated by amplifying exon 18-21 regions of the EGFR gene in EpCAM positive cell lines isolated from media/ blood, and EpCAM positive CTC using two sets of primers. Details of primers are described in **Table 2.4 & Section 2.11.2.**

4.2.10.2 PCR analysis to ascertain the utility of detecting EGFR mutated gene fragments in isolated positive cells

EpCAM positive cells extracted using the microfluidic device were subjected to amplification of mutated EGFR gene fragments with two sets of primers **(Table 2.4)** Protocols used for PCR reaction, thermo cycling temperatures and gel electrophoresis are outlined in **Section 2.11.2.**

4.3 Results

4.3.1 EpCAM expression varies in different cancer cell lines

Epithelial derived tumours in the circulation that have not undergone an epithelial to mesenchymal transition express EpCAM (Pantel et al 2017; Habili, 2020). A panel of cell lines representative of epithelial tumours were evaluated for EpCAM expression using flow cytometry. These cell lines were then used to investigate the ability of the new microfluidic device to isolate cells expressing varying levels of EpCAM.

Flow cytometry results (**Figure 4.1 a-d**) showed that all the cells expressed EpCAM as there was a right shift of the test (green) histogram plots when compared to the negative (purple) isotype control. A representative experiment showed that MCF-7 (**Figure 4.1a)** had a high level of EpCAM expression with a mean fluorescence of 158.05. The negative control had a mean fluorescent of 2.88. The ratio of fluorescence intensity of MCF-7 cell line to its negative isotype control was 54.9. HT-29 (**Figure 4.1b)** also had a high level of EpCAM expression with a slightly more varied level of fluorescence and a mean fluorescence of 153.54. The negative isotype control had a mean fluorescence of 4.61 and the ratio of fluorescence intensity of HT-29 cell line to its negative isotype control was 33.1. PC9 (**Figure 4.1c)** had the highest level of EpCAM expression with a mean fluorescence of 183.33 as compared with its negative isotype control with a value of 4.03. The ratio of fluorescence intensity of PC9 cell line to its negative isotype control was 46. Panc-1 (**Figure 4.1d)** was a low EpCAM expressing cell line There was a little shift to the right of the green histogram plot when compared to the purple histogram. The mean fluorescence of the green histogram plot was 10.02 as compared with its isotype control with a mean fluorescence of 8.1. The ratio of fluorescence intensity of Panc-1 cell line in comparison to its negative isotype control was 1.2. Taken together, the high EpCAM expressing cancer cell lines in this present study were MCF-7, PC-9, and HT-29 whereas, Panc-1 only expressed a low level. A similar order of EpCAM expression was seen in an independent, repeat, experiment.

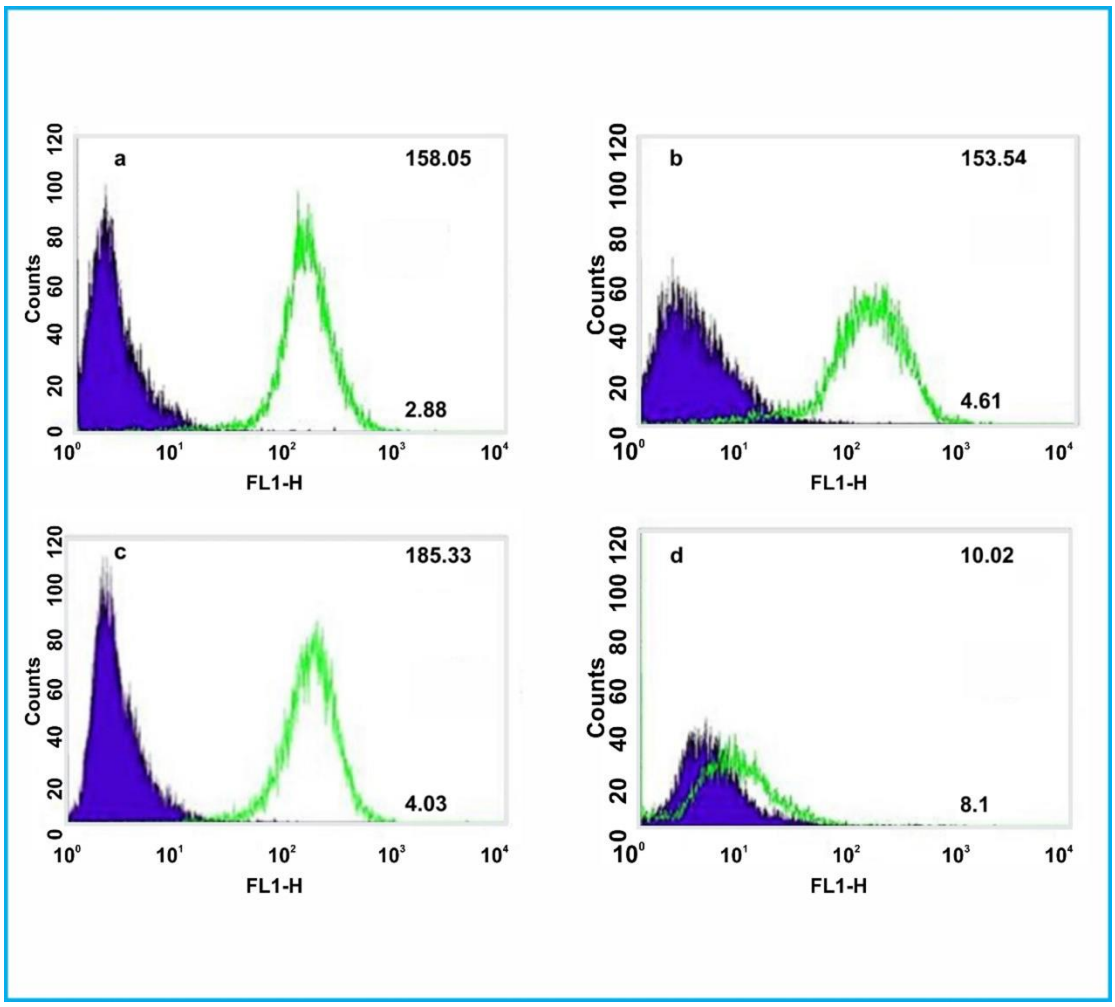

Figure 4.1: Histogram plots from flowcytometry experiments showing EpCAM expression of cell lines used in this study. Purple plots represent negative isotype controls whilst green histogram plots represent test (**a**) EpCAM expression in MCF-7 cell lines (**b**) EpCAM expression in HT-29 cell lines (**c**) EpCAM expression in PC9 cell lines (**d**) EpCAM expression in Panc-1 cell line. Representative data from experiments performed in duplicates.

4.3.2 Lung card version II microfluidic device isolates cancer cell lines with varying levels of EpCAM expression spiked in media with good efficiency

To validate the ability of the new microfluidic device to isolate CTC. Established tumour cell lines were spiked into media as a model. The four cell lines- PC9, MCF-7, HT-29 and Panc-1 were all studied as they express varying levels of EpCAM **(Figure 4.1)**. The results (mean ± S.D) from three experiments show that a capture efficiency of ≥80% (**Table 4.1**) was achieved by the Lung card version II device of MCF-7, PC9, and HT-29, irrespective of the concentration of cells spiked in 13ml of media (**Figure 4.2)**. The highest capture efficiencies were observed for all three cell lines at a concentration of 1×10^6cells/ml with the three cell lines having capture efficiencies of ≥90%; MCF-7- 92%, PC9 and HT-29 both had efficiencies of 90%. At cell

concentrations of 2×10^5cells/ml the capture efficiencies were MCF 7- 85%; PC9- 85% and HT 29-83%. For cell concentration of 4×10^4/ml capture efficiencies were: MCF7-81%, PC9-83% and HT-29-80%. Finally at cell concentrations of 8×10^3/ml capture efficiencies were MCF-7-81%, PC9- 82% and HT-29- 80%. Capture efficiency was not possible at a concentration of 1.3×10^2 cells/ml as no cells could be identified on the haemocytometer. However, brightfield and Alexa 488 imaging from fluorescence microscopy **Figure 4.3 e, l and t** shows that cells were captured at the lowest concentration investigated. The results obtained from capture efficiency at all concentrations correlated well with visual assessments from brightfield and Alexa 488 imaging. **Figure 4.3 a-t** shows excellent capture of cells by magnetic anti-EpCAM beads at varying concentrations of cells spiked in media. In some pictures the cells are overwhelmed by the beads. Waste depicted in **Figure 4.3w-y** had a minimum number of cells when compared to the pictures of cells isolated/captured using the microfluidic device.

The results from the low EpCAM expressing cell lines (Panc-1) (**Table 4.1 & Figure 4.2d)** showed lower capture efficiency rates when compared to cell lines with high EpCAM expression (HT-29, MCF-7 and PC9). At the highest concentration of cells (1×10^6cells/ml) spiked in media the efficiency of capture by the device was only 45% at a cell concentration of 2×10^5cells/ml efficiency was decreased to 40% and at cell concentration of 4×10^4cells/ml efficiency of recovery was only 37%. Fluorescence microscopy confirmed the isolation of few cells with an abundance of functionalized beads (**Figure 4.3f**). Microscopy also showed there were more cells left in the waste compared with experiments using higher expressing EpCAM cells **(Figure 4.3 u & v)**. Capture efficiency was only evaluated at the higher concentration of cells as the poorer capture was evident. In summary, EpCAM levels influence capture efficiency, and for CTC to be effectively isolated cells would need to have reasonable expression levels of the targeted marker.

Table 4.1: Summary capture efficiency of Lung card version II from spiking experiments in media

Concentration of cells spiked in 13ml of media	**Mean± S.D of** PC9 **cells isolated**	**Mean± S.D of efficiency % of cells isolated**	**Mean± S.D of** HT-29 **cells isolated**	**Mean± S.D of efficiency % of cells isolated**	**Mean± S.D of** MCF-7 **cells isolated**	**Mean± S.D of efficiency % of cells isolated**	**Mean± S.D of** Panc-1 **cells isolated**	**Mean± S.D of purity of cells isolated**
1×10^6/ml	9×10^5/ml ± 1.73×10^4	90±2.08	9.2×10^5/ml ± 2.0×10^4	90±2.0	9.28×10^5/ml ± 7.21×10^3	92±0.91	4.5×10^5/ml ± 5.0×10^4	45±5
2×10^5/ml	1.75×10^5/ml ± 8.02×10^3	85±4.01	1.6×10^5/ml ± 4.04×10^3	83±2.02	1.69×10^5/ml ± 3.61×10^3	85±2.75	3.35×10^5/ml ± 4.0×10^5	40±4.2
4×10^4/ml	3.23×10^4/ml±7×10^2	83±1.91	3.22×10^4/ml± 2.89×10^2	80±0.58	3.22×10^4/ml±5×10^3	81±2.31	1.43×10^4/ml±2.08×10^3	37±5.3
8×10^3/ml	6.6×10^3/ml ± 2.0×10^2	82±2.5	6.43×10^3/ml ± 7.64×10^1	80±0.58	6.53×10^3/ml ± 5.77×10^1	81±0.58		

Data was obtained from 3 lndependent experiments S.D-standard deviation

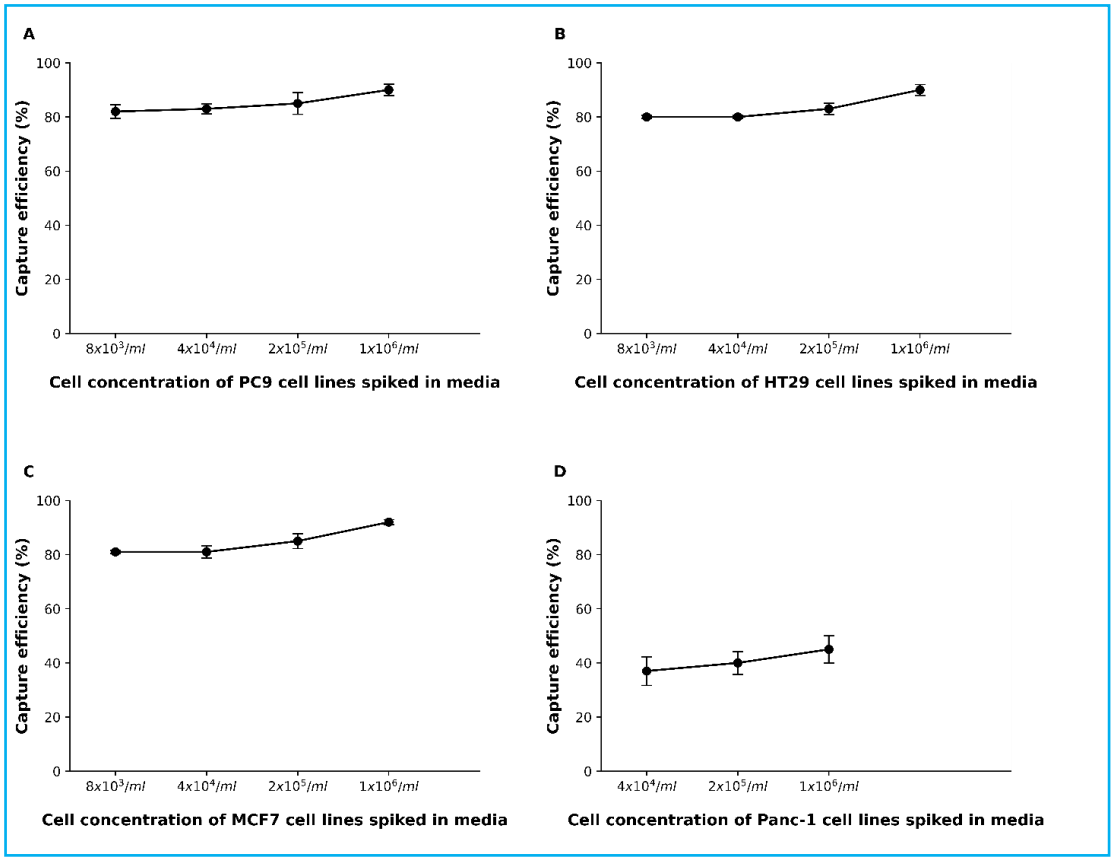

Figure 4.2: Graphical representation capture efficiency of Lung card microfluidic device to isolate **(a)** PC9 **(b)** HT-29 **(c)** MCF-7 and **(d)** P anc-1 cell lines spiked in 13ml of RPMI media at a range of concentrations. Note that the x axis increases in 5-fold increments, efficiencies were evaluated in 3 separate experiments and data shown as mean±S.D

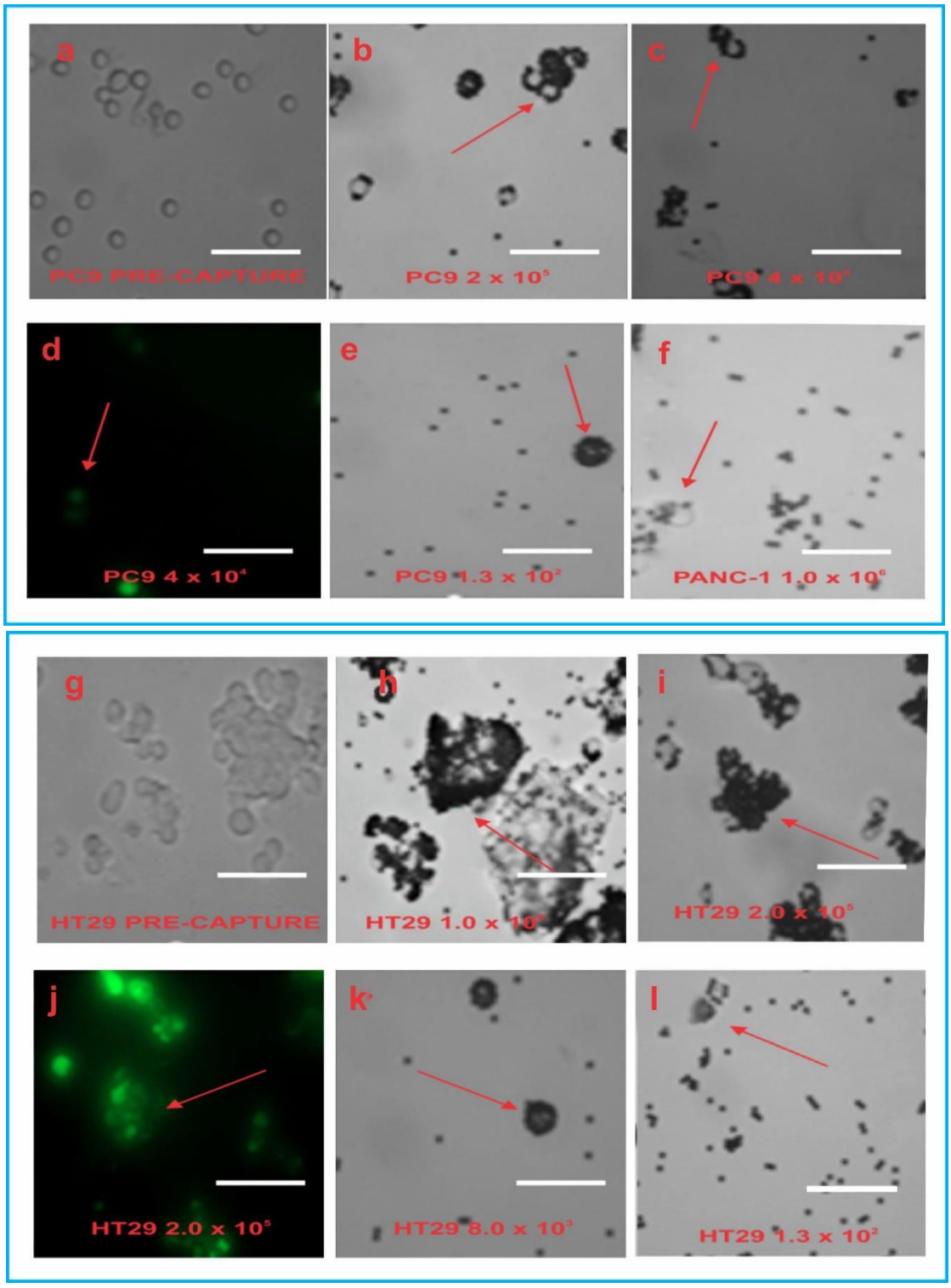
a
PC9 PRE-CAPTURE
b
PC9 2 x 10⁵
c
PC9 4 x 10⁴
d
PC9 4 x 10⁴
e
PC9 1.3 x 10²
f
PANC-1 1.0 x 10⁶
g
HT29 PRE-CAPTURE
h
HT29 1.0 x 10⁴
i
HT29 2.0 x 10⁵
j
HT29 2.0 x 10⁵
k
HT29 8.0 x 10³
l
HT29 1.3 x 10²

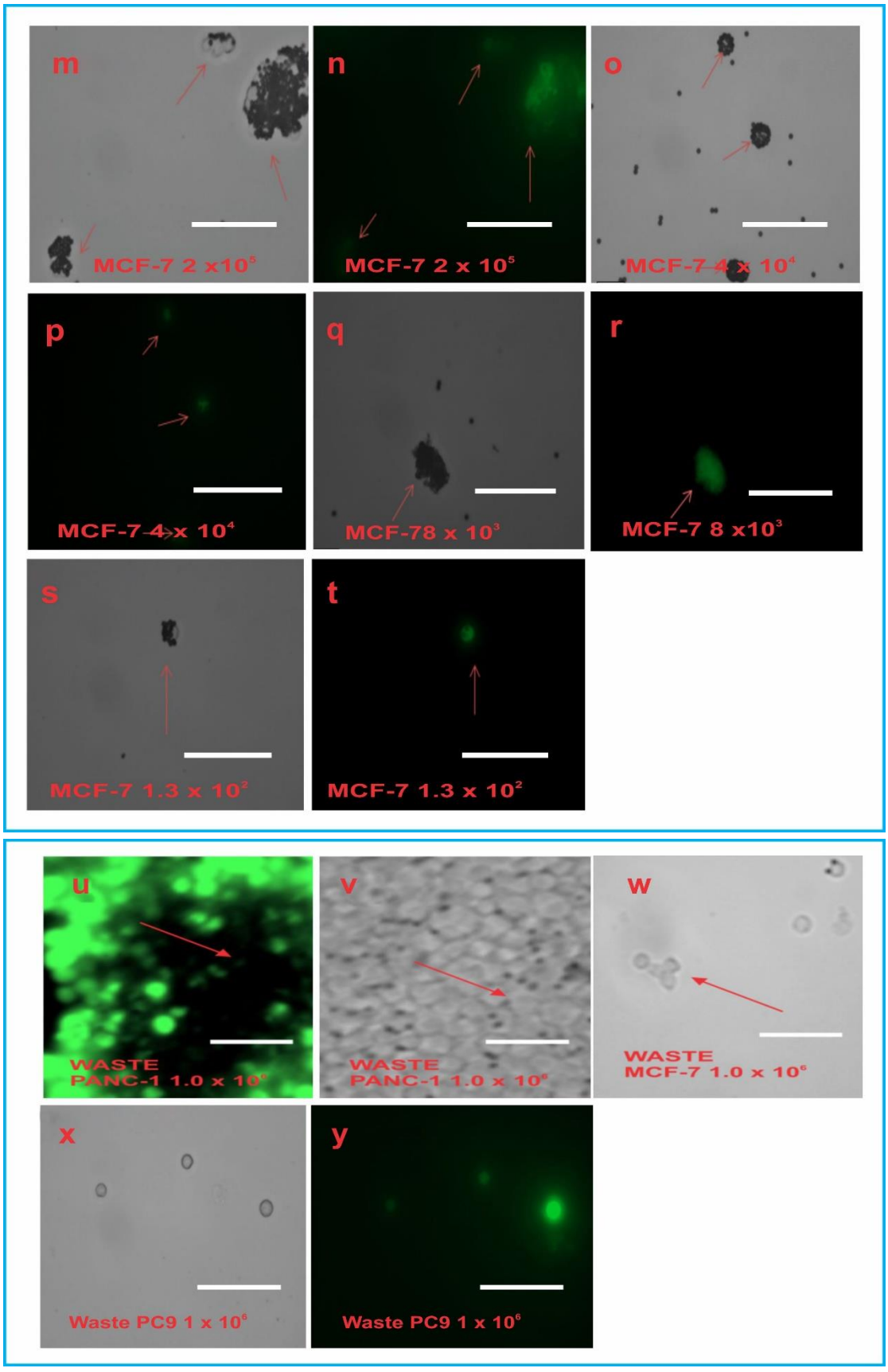

Figure 4.3 Shows capture Bright field and Alexa 488 imaging (green imaging) of CFSE stained cell lines (scale bar at 10µm) used for validation experiments in this current study, the slides were viewed with × 40 magnification **a-e** depicts capture of PC9 cell lines spiked in media at

varying concentrations, capture is depicted by red arrows showing anti-EpCAM beads binding/surrounding EpCAM positive cells. **f**-depicts capture of low EpCAM expressing Panc-1cell lines **g-l** -shows capture of HT-29 cell lines depicted by red arrows **m-t**-shows capture of MCF-7cell lines **u and v** shows the waste of PANC-1 with relatively large number of cells. **w-y** –shows the waste from cell lines expressing moderate to high level of EpCAM few cells are present. The data shown is a summary from 2 independent experiments.

4.3.3 Lung card version II microfluidic device isolates cancer cell lines with varying levels of EpCAM expression from blood with good efficiency

Following effective capture from spiking experiments with EpCAM expressing cancer cell lines in media, the next step was to investigate the capture efficiency results under more physiological conditions by spiking the CFSE stained EpCAM expressing cancer cell lines into sheep blood using the same concentrations outlined in **Section 4.3.2**. Efficiency of capture was again evaluated as described in **Section 2.6.3**. The results (mean ± S.D) from three experiments show that capture efficiencies of ≥65% were achieved with the EpCAM expressing cell lines (MCF-7, PC9, HT-29) at all cell concentrations (**Table 4.2**, **Figure 4.4)**. The highest capture efficiency was observed for these lines at a concentration of 1×10^6cells/ml. At this concentration all three cell lines had a capture efficiency of ≥75%. The efficiency rates were: 80% for MCF-7 and PC-9 cell lines and 78% for HT-29 cell line. At cell concentration of 2×10^5cells/ml efficiencies were: MCF-7-77%, PC9-76%, and HT-29-73%. At cell concentrations of 8×10^3cells/ml efficiency dropped to ≥65% the same decrease in capture efficiency was observed in spiking experiments in media where there was a drop to 80% when using this concentration of cells. At a cell concentration of 1.3×10^2cells/ml again capture efficiency could not be calculated as no cells could be identified on the haemocytometer. However, fluorescence microscopy **Figure 4.5** shows that capture was still possible at that concentration. The results obtained from capture efficiency corroborated well with brightfield and Alexa 488 microscopic imaging. **Figure 4.5** shows capture of cells by magnetic anti- EpCAM beads at varying concentrations of cells spiked in blood. In some pictures the cells are clumped and are overwhelmed by magnetic beads. Capture of cells clumped together suggests that the device is capable of isolating CTC cells that exist in clusters.

The results from low EpCAM expressing cell lines (Panc-1) **Figure 4.4d** showed lower capture efficiency rates when compared to high EpCAM expressing cancer cell lines. At the highest concentration of cells 1×10^6cells/ml spiked in blood only gave an

efficiency of capture of 40%. This dropped to 35% when a spiked concentration of 4×10^4cells/ml was used. Fluorescence microscopy results (**Figure 4.5)** corroborate well with efficiency rates as pictures show isolation of few cells. Evaluation of capture efficiency was restricted to the higher concentrations.

Table 4.2: Summary capture efficiency of Lung card version II from spiking experiments in blood

Cell Concentration spiked in 13ml of Sheep blood	**Mean± S.D of** PC9 **cells isolated**	**Mean± S.D of efficiency (%) of cells isolated**	**Mean± S.D of** HT-29 **cells isolated**	**Mean± S.D of efficiency of cells isolated**	**Mean± S.D of** MCF-7 **cells isolated**	**Mean± S.D of efficiency of cells isolated**	**Mean± S.D of** Panc-1 **cells isolated**	**Mean± S.D of purity of cells isolated**
1×10^6/ml	7.78×10^5/ml ± 4.3×10^4	80±2.0	7.77×10^5/ml ± 2.52×10^4	78±3.61	7.95×10^5/ml ± 4.77×10^4	80±4.25	4.03×10^5/ml ± 2.0×10^4	40±5
2×10^5/ml	1.51×10^5/ml ± 3.51×10^3	76±1.76	1.46×10^5/ml ± 9.71×10^3	73±5.13	1.55×10^5/ml ± 1.42×10^4	77±3.28	7.57×10^4/ml ± 6.03×10^3	38±2
4×10^4/ml	2.85×10^4/ml±1.32×10^3	71±1.31	2.87×10^4/ml± 1.15×10^3	72±2.89	3.0×10^4/ml±2.15×10^3	75±2.8	1.38×10^4/ml ±1.32×10^3	35±4.5
8×10^3/ml	5.23×10^3/ml ± 2.31×10^2	65±2.89	4.93×10^3/ml ± 1.15×10^2	65±1.73	5.50×10^3/ml ± 5.0×10^2	70±3.0		

Data was obtained from 3 independent experiments

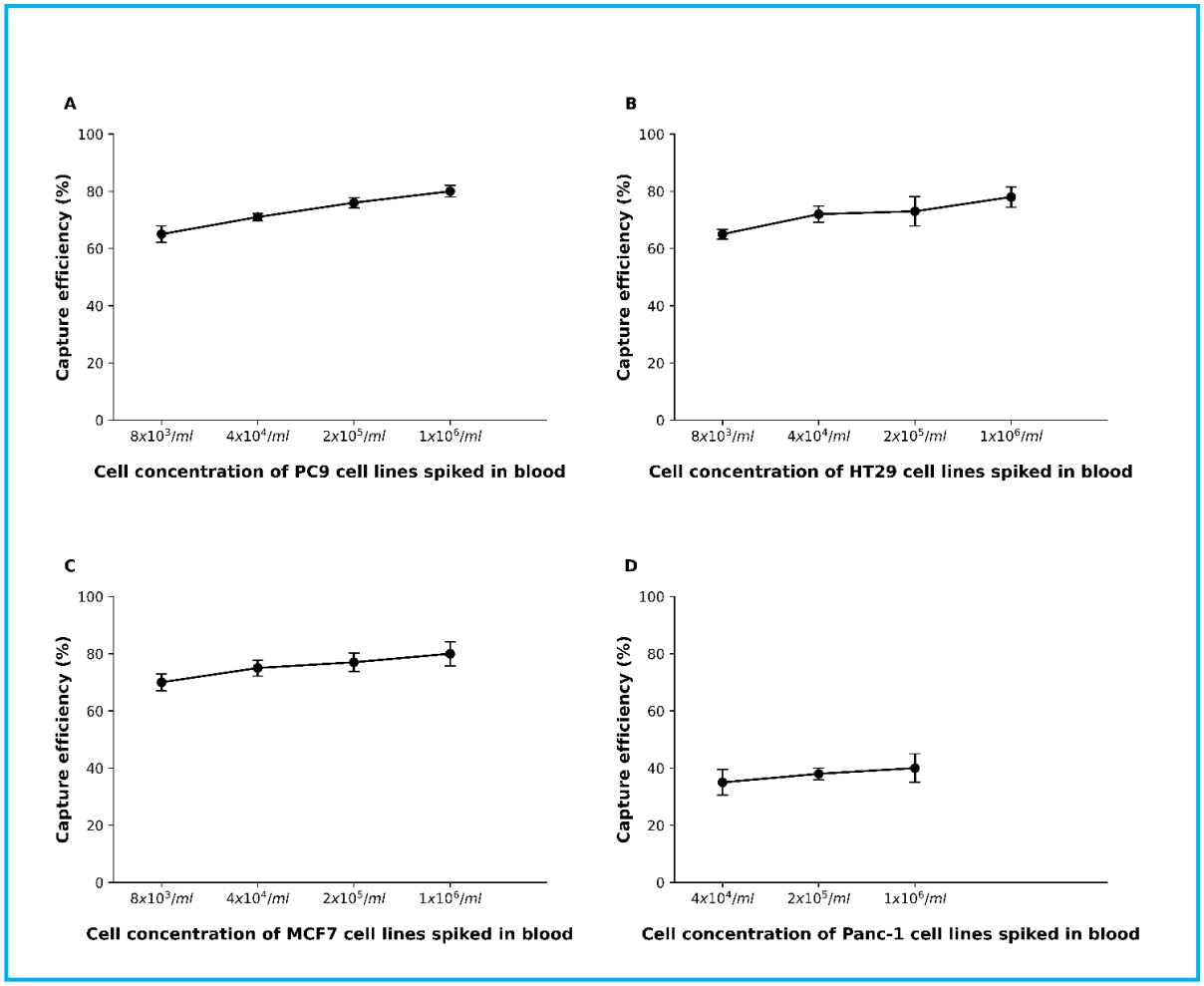

Figure 4.4: Graphical representation capture efficiency (%) of Lung Card microfluidic device to isolate PC9, HT29, MCF7 & Panc-1 cell lines spiked in 13ml of blood at different concentrations. Note that the x axis increases n 5-fold increments, efficiencies were evaluated in 3 separate experiments. Data shown is mean± S.D

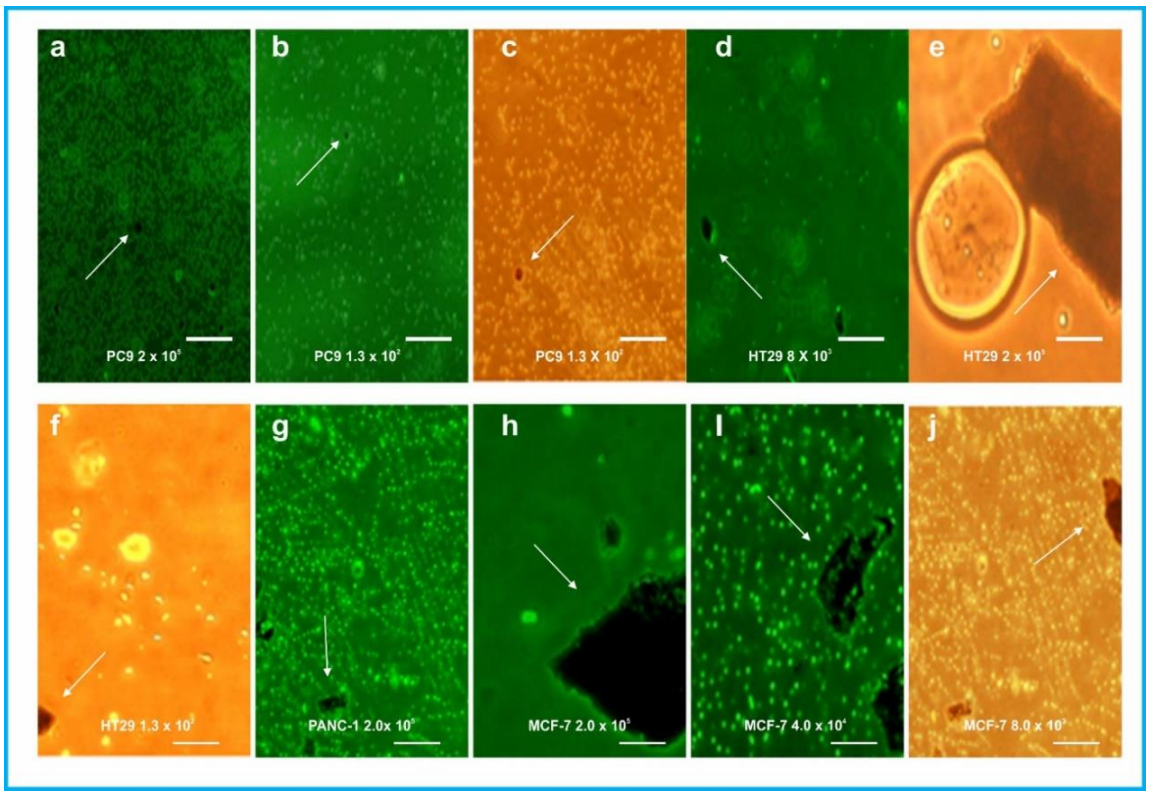

Figure 4.5: Bright field and Alexa 488 imaging (scale bar at 10µm) depicting capture of CFSE stained cell line (PC9, HT-29, MCF-7 and Panc-1) spiked in 13ml of sheep blood at a range of concentration. White arrows show capture of cells by magnetic beads, the green background seen in Alexa 488 imaging is due to autofluorescence. Magnification to view image was done at ×40 magnification.

4.3.4 EpCAM positive cancer cell lines isolated using the Lung card version II microfluidic device are of high purity.

The purity of CTC isolated is a key requirement for precise diagnosis of molecular alterations that drive cancer. To investigate the device capability for isolating CTC with high specificity and purity; a blood model was created to evaluate the specificity of the device in isolating strictly EpCAM positive cells in the presence of haematological cells that are of similar physical characteristic with CTC. This was done by spiking CFSE stained PBMC obtained from healthy donors at a cell concentration of 3×10^6cells/ml into 13 ml of complete RPMI media and then attempting to isolate cells. Fluorescence microscopy was used to evaluate capture of PBMC. Furthermore, purity was also investigated by isolating CFSE stained cancer cell lines at varying concentrations spiked into complete media containing of 3×10^6 cells/ml of PBMC stained with Cell Trace far red dye. Purity was evaluated via imaging with a confocal microscope. Percentage purity was determined as outlined in **Section 2.8.**

The results obtained in **Figure 4.7** following spiking of 3×10^6 CFSE stained PBMC from healthy donors into RPMI media suggest that the device and concept is specific for the isolation of EpCAM positive cells. The device did not isolate any cell**.** Brightfield and Alexa 488 imaging in **Figure 4.7a&b** show only beads coming through and no PBMC whilst **Figure 4.7c** shows relatively large number of PBMC in the waste. The study **Figure 4.6, Table 4.3- 4.6** reported a purity of ≥ 96% of EpCAM positive cancer cell lines isolated using the device. This level of purity rate was observed for all cell lines irrespective of level of EpCAM expression and cell concentration tested. Confocal imaging (**Figure 4.7 e-l**) shows the ratio of EpCAM positive cells isolated (CFSE stained cells are green) to PBMC cells (Cell Trace far red stained cells are red). EpCAM positive cells were predominantly isolated with very small numbers of contaminating PBMC isolated. In summary the results from specificity and purity experiments showed that the device isolated EpCAM positive cells with high specificity and purity.

Table 4.3: Summary of purity results obtained from spiking experiments with **PC9**

Cell Concentration	Mean ± S.D of EpCAM +ve cells isolated	Mean ± S.D of WBC isolated	Ratio of cells: WBC	Mean ± S.D of purity
1×10^6	2,000±157	43±30	1,998.7:40.3	98±1.06
2×10^5	1,070±251	27±15	1,066.7:26.7	98±0.91
4×10^4	426±109	15±13	426.3:15.0	97±1.12
8×10^3	60±5	1.67±0.58	60.0:1.7	97±0.92
1.3×10^2	5±2	0.33±0.57	5:0.3	96±6.64

Data from 3 independent experiments

Table 4.4: Summary of purity results obtained from spiking experiments with **HT-29**

Cell Concentration	Mean ± S.D of EpCAM +ve cells isolated	Mean ± S.D WBC isolated	Ratio of cells: WBC	Mean ± S.D of purity
1×10^6	1,940±246.69	34±34.79	1,943.3:33.7	98±1.24
2×10^5	948±62.5	14±1.53	948.3:13.7	99±0.12
4×10^4	413±110.26	7±5.7	413.0:6.7	99±1.0
8×10^3	67±9.3	2±1.0	60.7:2.0	99±0.76
1.3×10^2	6±3.1	0.33±0.58	5.7:0.3	97±6.6

Data from 3 independent experiments

Table 4.5: Summary of purity results obtained from spiking experiments with **MCF-7**

Cell Concentration	Mean ± S.D of EpCAM +ve cells isolated	Mean ± S.D WBC isolated	Ratio of cells: WBC	Mean ± S.D of purity
1×10^6	2,440±303.92	53±27.02	2,440.0:50.3	97±0.7
2×10^5	1,150±186.69	28±15.90	1,140:28.7	98±1.18
4×10^4	491±63.52	9±8.08	491.3:9.3	98±1.35
8×10^3	66±7.7	1±1.15	65.7:1.3	99±1.5
1.3×10^2	6±3.1	0.33±0.58	6.3:0.3	97±5.7

Data from 3 independent experiments

Table 4.6: Summary of purity results obtained from spiking experiments with **Panc-1**

Cell Concentration	Mean ± S.D of EpCAM +ve isolated	Mean ± S.D WBC isolated	Ratio of cells: WBC	Mean ± S.D of purity
1×10^6	230±68.84	6±4.04	230.0:5.67	98±1.05
2×10^5	542±3.76	1±1.53	53.7:1.3	98±1.82
4×10^4	7.33± 2.55	0.33±0.58	7.3:0.3	98±1.82

Data from 3 independent experiments

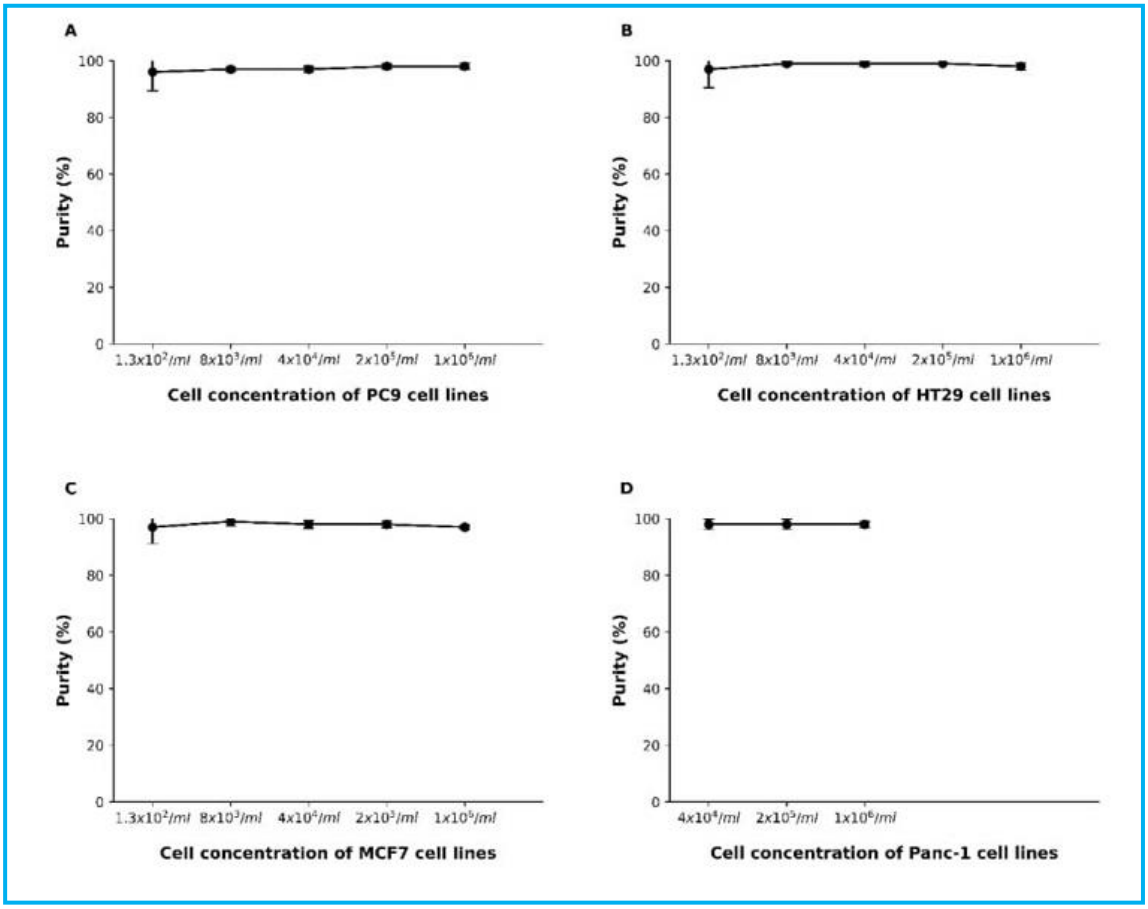

Figure 4.6 Graphical representation purity (%) of EpCAM positive PC9, HT29, MCF7 & Panc-1 cell lines spiked in media with a background of contaminating cells (PBMC) and isolated using the device. Note that the x axis increases in 5-fold increments, purity was evaluated in 3 separate experiments. Data is shown in mean±S.D.

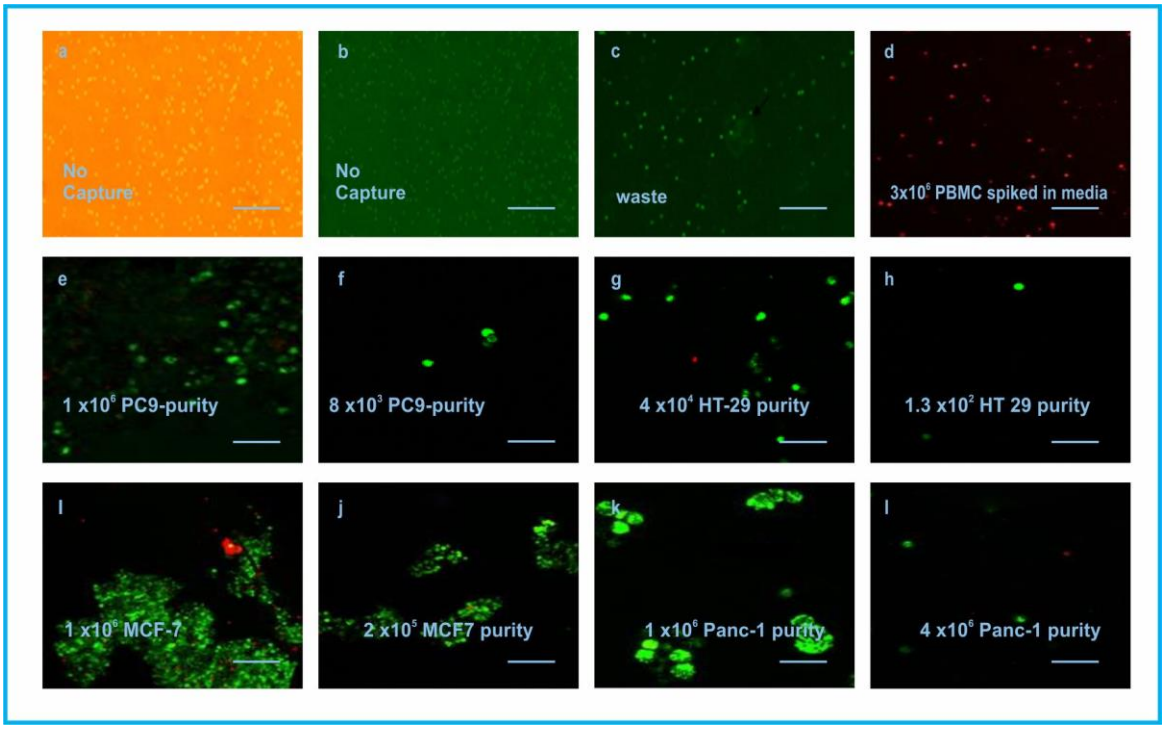

Figure 4.7: a, b&c confocal imaging (scale bar at 20µm) of PBMC spiked in media and then isolated with the device. Image was viewed at ×10 magnification **d**. PBMC spiked in media **e-l** purity of CFSE stained EpCAM positive cells isolated after spiking at different concentrations into 13ml of media containing cell tracker far red stained PBMC at a concentration of 3×10^6 /ml. Purity was expressed as a ratio (%) of green staining EpCAM positive cells to red staining PBMC. Data is a summary from three independent experiments.

4.3.5 Lung Card version II microfluidic device shows utility in isolating EpCAM positive CTC from blood of patients with NSCLC

Having successfully completed validation experiments with prototypes of CTC created from spiking cancer cell lines in media and/or blood that showed the device was capable of isolating EpCAM positive cells with good capture efficiency and purity; the device was then tested for its ability to isolate CTC from patient blood for subsequent molecular characterization of EGFR mutation. Thirty-eight patients' samples were analyzed in this study. The device isolated CTC from all 38 patients with the number of CTC isolated ranging from 3-550 cells in 13ml of blood (**Figure 4.8 a-h**); patients with higher CTC counts had stage IV disease (**see Tables 5.2 & 5.6** in **Chapter 5**) Purity of capture from the immuno-staining experiments, defined by ratio of pancytokeratin positive cells (CTC) to CD45 positive cells (leucocytes) was ≥95% (**Figure 4.8 i-m**) this was expected as very few CD45 positive cells were non specifically isolated by the magnetic beads coated with the anti EpCAM antibody. In

summary, the results that the device is capable of isolating EpCAM positive cells with good specificity and sensitivity from blood of patients with NSCLC.

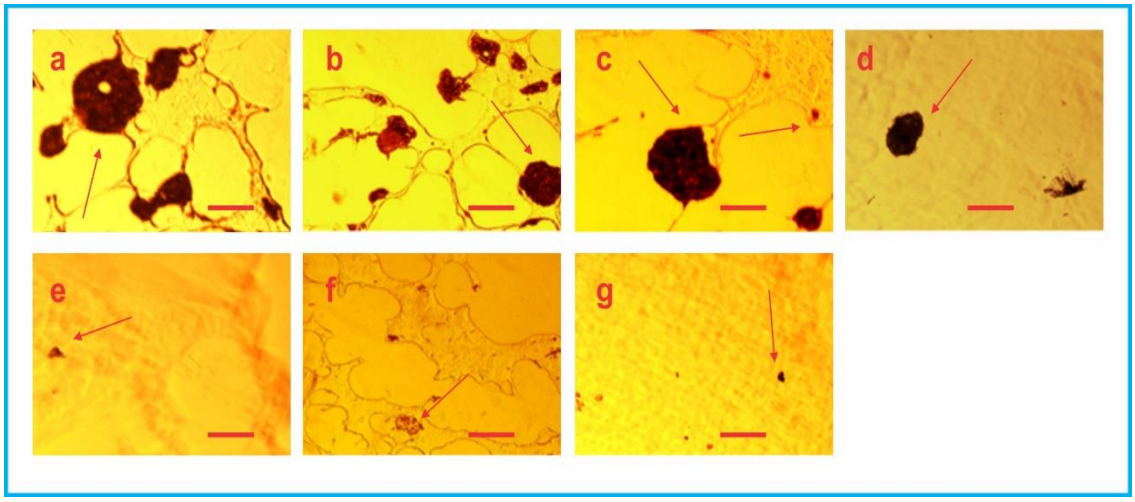

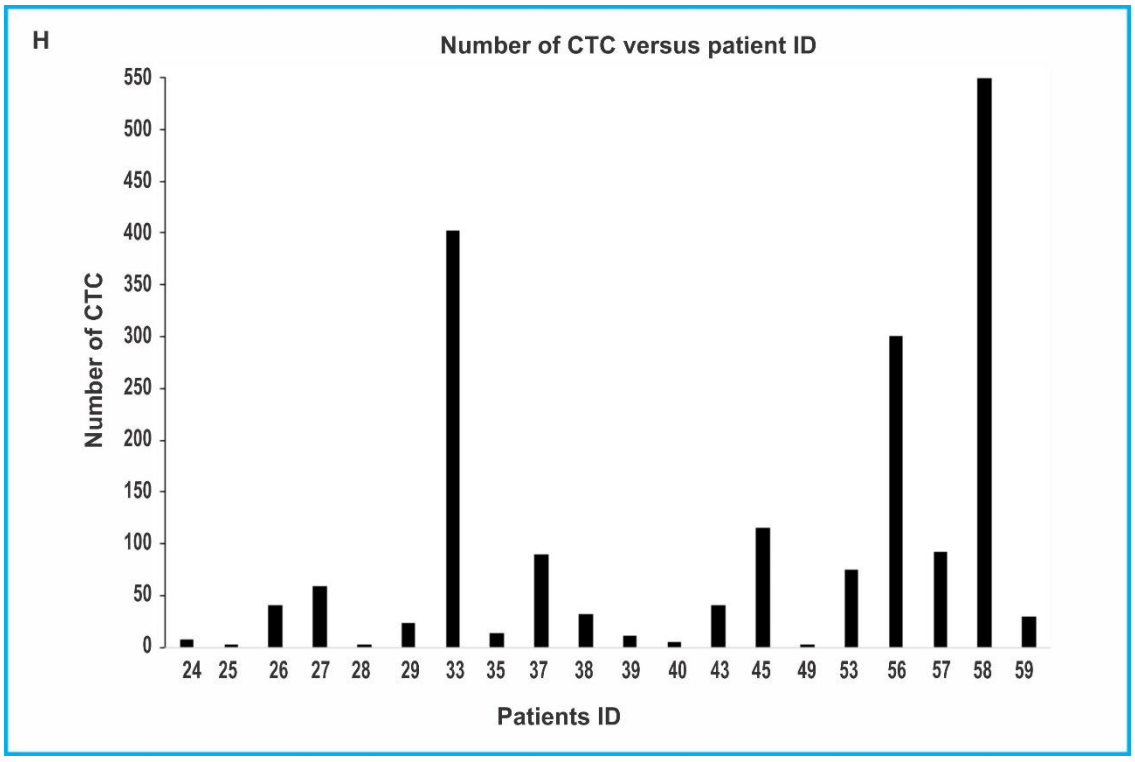

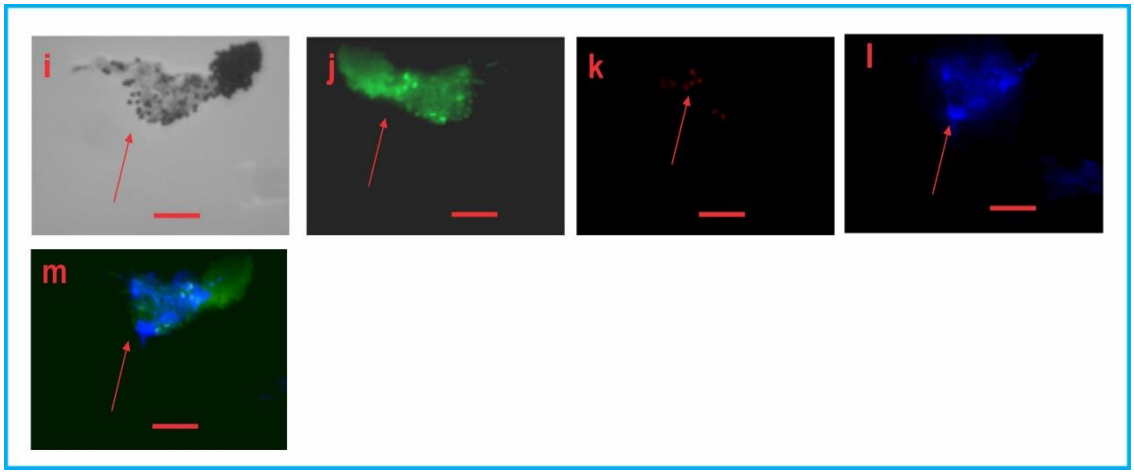

Figure 4.8 showing lung card version II microfluidic device ability to isolate EpCAM positive cells from the blood of patients with cancer (NSCLC) **a-g** – bright field imaging (scale bar 40µm) of CTC captured from patient's sample evidenced by beads surrounding cells (depicted by red arrow), size of these cells ranged from 15-25µm. **h**- bar chart representation of number of CTC isolated from 13ml of blood of patient **i-m** -immunostaining (scale bar 40µm) of isolated CTC for identification of EpCAM positive CTC and to ascertain purity of CTC isolated **i**- represents brightfield imaging of isolated EpCAM positive CTC **j**- EpCAM positive cells staining positive for fluorescence conjugated pan cytokeratin **k**- represents cells staining positive for rhodamine conjugated Mouse anti-human CD45 **l**- nuclei of cells staining with DAPI **m**-composite image of the three fluorescence channels(green, blue and red channels). All slides were viewed at × 40 magnification

4.3.6 CTC isolated from blood of patients are positive for tumor specific markers

To determine if isolated/captured EpCAM positive cells from blood of patients with NSCLC using the device can be characterized at the molecular level. Two tumour specific mRNA markers CK-7 and Survivin were analyzed by PCR. RNA was extracted from EpCAM positive isolated cells and cDNA synthesized from patients where sufficient cells were available. End point-PCR analysis was performed on the isolated tumour cells and cDNA synthesized from PBMC obtained from healthy donors, the latter being used as a negative control.

The results from the amplification of the CK7 and Survivin regions from CTC isolated from patients with NSCLC show that EpCAM positive cells isolated from blood of patients with NSCLC all expressed CK7 and 6/11 also expressed detectable Survivin (**Figure 4.9 A and B**). No amplification for CK7 or Survivin was observed in the cDNA from PBMC obtained from healthy donors. In summary these results suggest that the device is a suitable tool for isolating and analyzing CTC from blood for downstream molecular PCR analysis.

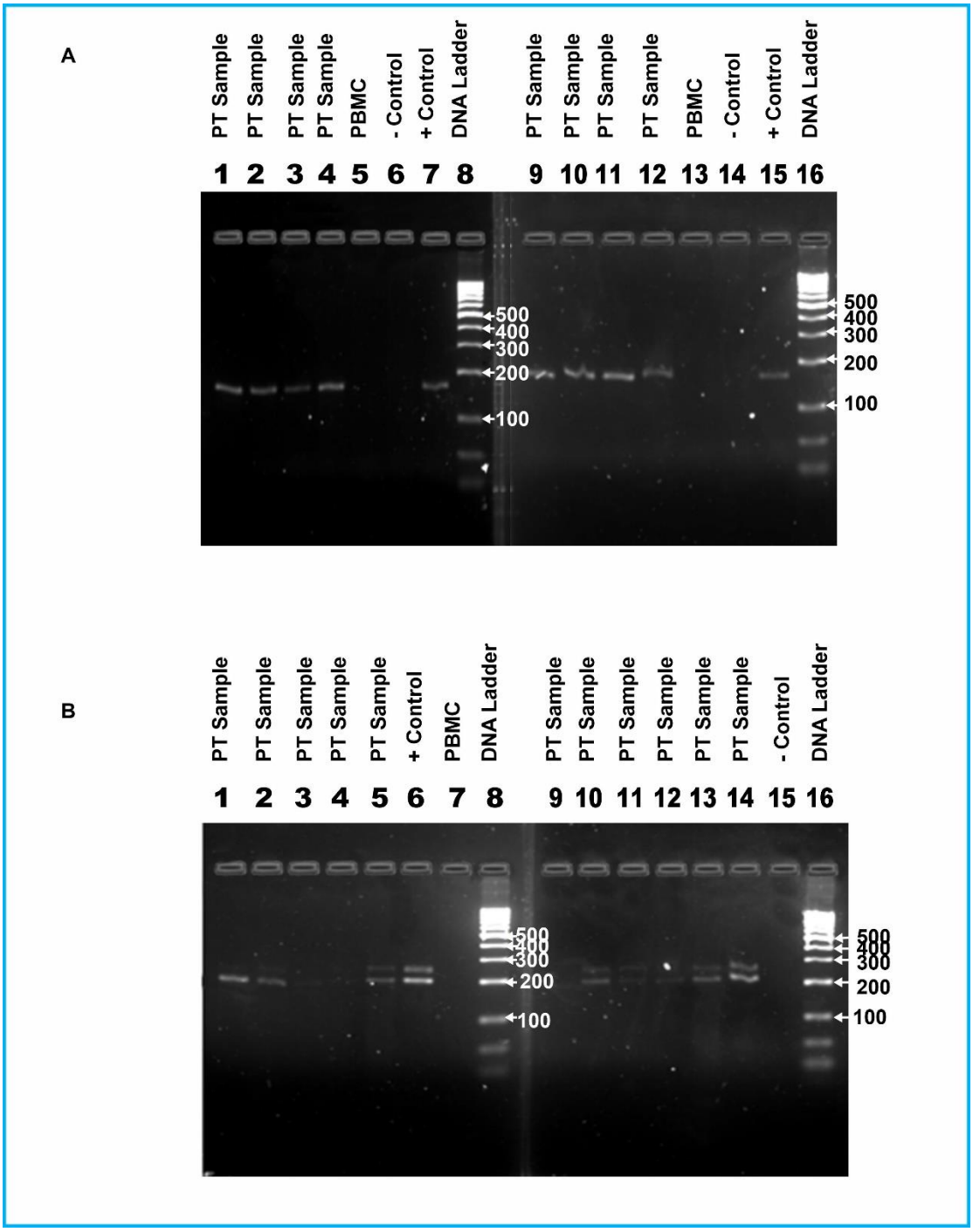

Figure 4.9 Gel electrophoresis results showing amplified CK7 and Survivin genes in isolated patients CTC**. Gel A- lanes 1-4 and 9-12** shows amplified CK7 region (band size-162bp) from cDNA obtained from patient CTC enriched samples. **Lanes 6 &14** represent negative controls (no cDNA), **lanes 5 &13** represent amplification of cDNA of PBMC from healthy donors no CK7 gene expression was identified, and **lanes 7 &15** are positive control (cDNA from PC9 cell lines). **Gel B- lanes 1-5 and 9-14** shows amplified Survivin gene (253bp), & GADPH (225bp) of cDNA obtained from patient CTC enriched samples. **Lanes 5, 10-14** show prominent bands for Survivin **Lanes 6 and 15** are positive and negative controls respectively whilst **lane 7** represent cDNA from PBMC showing no amplification.

4.3.7 EpCAM positive CTC isolated from blood of patients are analyzed for EGFR mutations.

Results from immunofluorescence microscopy experiments that showed EpCAM positive cells isolated from the blood of patients using this device are of good purity. In addition, end point PCR experiments demonstrated that EpCAM positive CTC isolated express tumour specific mRNA markers. The next step was to test the feasibility of determining EGFR mutations in the isolated EpCAM positive CTC. cDNA from these cells was amplified using 2 sets of primers for exon 18-21 regions of the EGFR gene. The first set of primers detected deletions and mutation using end point PCR, these mutations were chosen as they are the most common and are most responsive to TKI treatment. PCR Results were available within 4 hours of sample collection. The project then progressed to a more thorough investigation of exon 18-21 by NGS hence the need for alternative primers and PCR protocol.

Results showed that CTC isolated using the device can be used as a tool for diagnosis of EGFR mutation (**Figure 4.10**). Approximately 75% of patients were diagnosed with one or more mutations in exons 18-21. The clinical significance and potential future value of EGFR mutations detected from CTC enriched samples using NGS is discussed in depth in chapter 5.

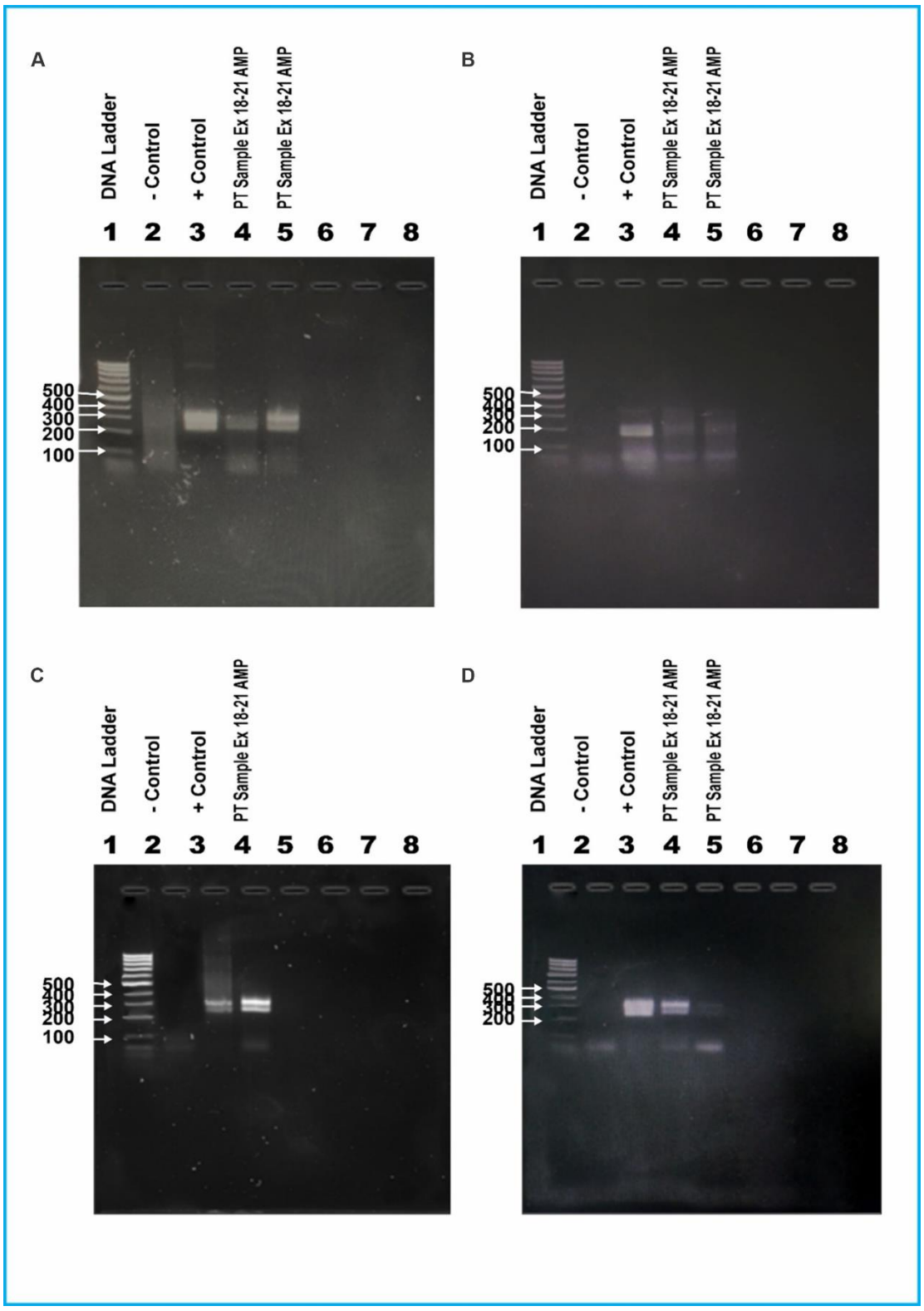

Amp-amplification

Figure 4.10-Gel electrophoresis results showing amplification of exon 18- 21 regions of EGFR gene from EpCAM positive CTC isolated from blood of patients with NSCLC using the Lung card version II microfluidic device. **Lanes 4 and 5** in **a,b,c & d** show exon18-21 amplification of EGFR regions in patient's CTC enriched samples**. Lanes 1, 2 and 3** show DNA ladder negative and positive controls respectively.

4.4 Discussion

This current study shows the ability of the Lung card version II microfluidic device to isolate EpCAM positive cells with good capture efficiency, purity and throughput and the feasibility of the device to be used as a tool for CTC processing for detection of molecular alterations in exons 18-21 of the EGFR gene. Results from spiking experiments in media at a throughput of 13ml/50minutes showed that the device was able to isolate CTC with a capture efficiency of ≥80% **(Table 4.1, Figure 4.2&4.3**) at the lowest cell concentration (1.3×10^2cells/ml) in cancer cell lines expressing high levels of EpCAM (MCF-7, PC9 &HT-29). Capture efficiency for low EpCAM expressing Panc-1 cell line was ≤ 45% at a cell concentration of 1×10^6cells/ml. Results from spiking experiments in blood **(Table 4.2, Figure 4.4 & 4.5)** showed that the good capture efficiency demonstrated in spiking experiments in media was also reproducible in blood; a more physiological relevant fluid as capture efficiency of ≥ 65% was demonstrated at a cell concentrations of 1.3×10^2cells/ml in cancer cell lines expressing high levels of EpCAM **(Table 4.2, Figure 4.4 & 4.5)**. Capture efficiency for low EpCAM expressing Panc-1 cell line from spiking experiments in blood was ≤ 40% for cell concentration of 1×10^6cells/ml **(Table 4.2, Figure 4.4 & 4.5)**.

Results of capture efficiency from spiking experiments in media and blood from this study compare well with capture efficiencies from validation studies of other immuno-affinity based microfluidic devices that have explored CTC isolation for subsequent molecular analysis in NSCLC. Nagrath et al (2007), reported capture efficiency of ≥ 65% and ≥60% in spiking experiments with different cancer cell lines (H1650-NSCLC, SKBR-3-breast, PC3-Prostate, T-24-bladder) expressing varying levels of EpCAM spiked in media or blood respectively at concentrations of 50-50,000 cells/ml in validation studies for CTC chip. Throughput for the CTC chip was 1ml/hr. Murdlihar et al (2014), characterizing the Oncobean chip reported capture efficiency of ≥ 80% for H1650 (NSCLC) and MCF7(breast cancer) cell lines spiked at a concentration of 1,000 cells/ml in blood of healthy donors; the throughput for this device was 10ml/hr.

Taken together, capture efficiency results obtained from the Lung card device is comparable with previously described biochemical based microfluidic devices. However, the new device in this study has a better throughput **13ml/50min**. In comparison to biophysical based microfluidic devices such as FAST disc, Spiral

microfluidic the current device is less good as the previously reported devices can isolate CTC from 3ml of blood in one minute and 7.5ml in 5 minutes (Khoo et al 2014; Lim et al 2020). Finally, the results **(Figures: 4.2, 4.3, 4.4 & 4.5)** also show that cellular EpCAM expression affects capture behaviour in the Lung card device as low EpCAM expressing cancer cell line had a lower capture efficiency as has been reported previously (Earhart et al 2014; Rushton et al 2021). A way to circumvent this potential limitation is to use a cocktail of antibodies, although the level of nonspecific isolation would also need to be checked as this could rise. The use of multiple antibodies will be explored in future studies using the device. Microscopic visualization of capture (**Figure 4.3 & 4.5**) showed that the device was able to capture /isolate EpCAM positive cells singly and in clusters this suggest that the design, concept and isolation process of the device collects EpCAM positive cell with little or no destruction or disruption to their morphology.

Results from purity experiments **(Figure 4.6, 4.7 and Tables 4.3-4.6)** showed that the device was able to isolate CTC with high specificity and purity i.e., ≥96% for all cell lines. Results from this present study compared very favourably with purity studies reported from previously published studies. The purity of the Herringbone chip after isolation of PC3 cell lines spiked in blood from healthy donors was reported to be 14.0%±0.1%. The oncobean chip purity was reported to be ≤35% following isolation of H1650 and MCF7 cell lines spiked at a concentration of 1,000 cells/ml in 5ml of blood from healthy donors. Purity results from the NanoVelcro chip involving isolation of 200 cells/ml of H1650, HC827 and A549 cells spiked into 2ml of media containing 5×10^6/ml of WBC were ≤ 30% after 30 minutes of isolation and purification. However, after an additional purification step lasting 1.5 hours purity was improved to between 88-98%. The purity from the Magnetic Sifter after isolating 50-100cells/ml cancer cell lines spiked into 10ml of blood was reported to be 17.7%±9.3% (Stott, 2010; Muridhlar, 2014; Ke et al 2015; Park et al 2016). Considering all the key parameters for a robust unit, the Lung card device isolates EpCAM positive cells with the highest purity of any previously described literature. High purity of CTC is facilitated by: (1) the absence of a pre labeling step; (2) high specificity of magnetic dyna beads for EpCAM positive cells; (3) elimination of non-specific capture by functionalizing the chip with 5% (w/v) BSA before capture/isolation to reduce non-specific binding of rare CTC to the chip; and (4) the magnetic field intensity generated by the 2 NdFeB permanent magnets

creating a sufficiently strong magnetic field to drag magnetic anti-EpCAM beads effectively through static blood

.

Clinical utility of the device was demonstrated by its ability to isolate CTC from blood of patients with NSCLC recruited for the study (**Figure 4.8**). Sensitivity of the device in isolating EpCAM positive CTC was also demonstrated by the ability of the device to isolate CTC even at lower concentrations in blood, although at a lower efficiency (**Figure 4.8**). The results from the clinical samples demonstrates the potential of the device for future studies as the recovery again compares favourably with other microfluidic devices (discussed in **Chapter 1, Section 1.12**) that have explored CTC isolation from blood of patients with cancer for subsequent molecular analysis (Nagrath et al 2007; Mashewaran et al 2009; Ke et al 2015; Lim et al 2020). These devices have been reported to isolate CTC from ≥ 90% of patients recruited for thier studies and with numbers ranging from 5-1,300 cells. The capability of the new device to isolate cells singly and in clusters is also similar to the Oncobean chip that has been reported to isolate CTC from blood in clusters (Murdihlar et al 2017). It must be noted however that efficiency of capture was seen to be reduced at $8x10^3$ cells/ml, which is higher than the upper levels commonly observed in the blood of cancer patients suggesting that improvements in isolation would be needed for clincal use.

The suitability of EpCAM positive CTC captured using the device for subsequent molecular analysis was demonstrated by the detection of cancer specific genes: CK7 and Survivin alongside mutations on exons 18-21 of the EGFR gene (**Figure 4.9 & 4.10**). Together these results demonstrate the potential of the Lung card device to be used as a platform for CTC based molecular analysis.

4.5 Conclusion

This present study reports that the device isolates EpCAM positive cells from a heterogeneous mixture of cells with good capture efficiency, high purity and throughput. Results from this study suggest that the device presents a robust platform for use in combination with other techniques for post capture characterization for molecular alterations. The clinical potential of CTC isolated from the peripheral blood of patients with NSCLC using the device was demonstrated by the detection of cancer specific mRNA markers (CK7 and Survivin) and the detection of EGFR mutated

segments from CTC using end point PCR techniques. In summary the Lung Card version II microfluidic device could be used for cancer research in combination with other technologies in the future.

Chapter 5

Clinical potential of isolated CTC

5.0 Background

Management of patients with NSCLC in the last decade has evolved from the dogma of one drug/ therapy fits all, to the selection of therapies that are tailored to a patient's genetic or mutational needs. Land-mark events that influenced this change were the improved progression free survival times of patients whose tumours possessed mutations in their epithelial growth factor receptor (EGFR) when treated with TKI compared with patients who receive the same TKI but had no mutation in their EGFR gene; these patients had a worse outcome than those treated with standard chemotherapy. (IDEAL I&II, 2005; INTACT I&II 2005; EUROTAC 2012; ENSURE 2015; Lux-Lung 2015).

5.1.1 EGFR

EGFR is a protein belonging to the ErbB family of cell surface tyrosine kinase (**Section 1.5**). It is about 170kDa in size and comprises: **(1)** an extracellular ligand binding and dimerization domain **(2)** transmembrane domain and **(3)** an intracellular domain; this final domain is made up of a juxta membrane segment and a tyrosine kinase domain (Cymer & Schneider, 2010; Rosokoski, 2014; Wee & Wang, 2017). The physiological role of EGFR in regulation of cell survival, proliferation and differentiation is initiated through molecular mechanisms that involve ligand stimulation of the extracellular domain. Ligands that stimulate the extra cellular domain of EGFR are: endothelial growth factor (EGF), transforming growth factor α (TGF-α), heparin binding EGF (Hb-EGF), amphiregulin, epiregulin betacellulin and neuroregulin. Stimulation of the extracellular domain of the receptor leads to receptor dimerization then catalytic activation of the tyrosine kinase domain and consequent transfer of phosphate groups from ATP, by the tyrosine kinase domain to target proteins. These target proteins play key roles in the activation of several pathways that are important for cell growth and senescence (Olayioye 2000; Enders et al 2014).

5.1.2 Epidemiology of EGFR mutation

Globally between 10-30% of patients with NSCLC have an EGFR mutation. The occurrence of these mutations varies with race, histology type and epidemiology. About 50% of patients of Asian origin with NSCLC have an EGFR mutation; while only 15-20% patients of Caucasian origin with NSCLC possess an EGFR mutation (Graham et al 2018). EGFR mutation is predominantly diagnosed in non-smoking patients with the

adenocarcinoma histopathology (Sun et al 2007; Rossel et al 2009). Between 80 -90% of patients with an EGFR mutation have an in-frame deletions in exon 19 most commonly; a 15-nucleotide deletion from nucleotide 2481-2495 or 2482-2496 eliminating codon 746-750, or a point mutation of codon 858 in exon 21 where leucine is exchanged for arginine (L858R). **Table 1.3** in the introduction summarises the range of mutations commonly observed (Lynch et al 2004; Maemondo et al 2010; Chodhury et al 2022). The success of first generation TKI (gefitinib, erlotinib) in improving clinical outcomes in patients with NSCLC with EGFR mutation has been suggested to be due to their specificity for binding to the ATP cleft. Mutations around the cleft allow the TKI to bind inhibiting auto phosphorylation and blocking of heightened catalytic activation following ligand binding. Consequently, reducing/eliminating uncontrolled cellular signaling that promotes rapid cell growth and resistance to apoptosis (Pao et al 2004; Pao et al 2011).

5.1.3 EGFR mutations and TKI response

Response of EGFR mutations to TKI has been proposed by clinicians to be mutation specific. Results from some clinical studies show that patients with the exon 19 deletion (E746_A750delELREA) and L858R mutations have the best response to first generation TKI in terms of longer PFS (Jackman et al 2006; Janne et al 2012; Wu et al 2015). Furthermore, patients with exon 19 deletion (E746_A750delELREA) appear to have better response to first line TKI when compared to patients with the L858R mutation. Lee et al (2015), in a meta-analysis of data from 7 trials comparing treatment response of NSCLC with EGFR mutations on TKI (gefitinib, erlotinib& afatinib) to standard chemotherapy reported that 872 of the 1649 patients evaluated had the exon 19 deletion and 686 had the L858R mutations. Subgroup analyses of treatment response in this study show that patients with the exon 19 deletions had a 50% greater PFS benefit when treated with TKI (gefitinib, erlotinib) with a pooled HR for PFS of 0.24 (95% CI, 0.20-0.29:P<0.001) than did patients with exon 21 L858R point mutation who had a pooled HR for PFS of 0.48(95% CI, 0.39-0.58 P =0.001). The response of other EGFR mutations to first generation TKI have been reported to be highly varied and short lived-in effect (Russo et al 2019).

Mutations such as G719X and E709X in exon 18 have been reported to be responsive to TKI, particularly second-generation agents. Yang et al (2015) reported a 75-78%

response rate to afatinib in patients expressing these mutations, this was an improvement on the 14-55% response rate of patient possessing these mutations to gefitinib and erlotinib reported from earlier studies (Frega et al 2007; Chen et al 2007). Other exon 18 mutations reported to be responsive to TKI's are V689M, S720P, S720I, P699S, N700D, G721A, V740A and L718P (Massarelli et al 2013; Costa et al 2016). Tumours with deletions or insertions in exon 18 were reported to be non-responsive to TKI.

Deletions in exon 19 not originating from the LREA regions (amino acid residues 747-750) are less responsive to TKI when compared to deletions originating in this motif. Chung et al (2012), in a retrospective analysis of response to TKI in 308 patients with exon 19 deletions reported a PFS of 5.9 months in patients with non LREA deletions compared with 9.8- 10.5 months in deletions originating in the LREA motif (residues 747-750). Furthermore, mutations in exon 19 (L747F, P733L, K757R, E746G, V742X D761Y, E746V and L747S) have been associated with varied response and resistance to TKI (Klughammer et al 2016).

Mutations in exon 20 of clinical relevance are T790M, C797S and S768I. Around 50% of patients with exon 19 deletion (E746_A750delELREA) or L858R mutation on exon 21 initially responsive to first and second generation TKI subsequently develop a point mutation on codon 790 of exon 20 where methionine is substituted for threonine (T790M) (Gazdar 2009; Chen et al 2016). Overall response rate and PFS in patients with the T790M mutation on first or second generation TKI have been reported as only 10% and 2.5months respectively. However, patients with T790M mutations have been reported to have a better response to third generation drugs such as osimertinib. Mok et al (2017), in a phase III open label prospective trial, evaluated the response rates of 419 patients with the T790M mutations placed on osimertinib (80mg/d) or platinium +pemetrex. This study reported an overall response rate of 71% vs. 31% between the group on osimertinib and the group on platinum +pemetrex and median OS of 8.5 months vs. 4.2 months between the two groups. Patients with exon 20 insertions around the 762-775 residues are associated with resistance to first, second and third generation TKI. However, clinical studies by Zhou et al (2021) report that patients with exon 20 insertions are responsive to the FDA approved TKI Mobocertinib. An OS time of 24 months was reported for 114 patients with this mutation in the study.

Mutations in exon 21 other than L858R mutations are associated with lower response and sensitivity to TKI. Leduc et al (2017), in a retrospective multicenter study analysis of the clinical and molecular characteristics of 1,837 patients with EGFR mutation on TKI (gefitinib, erlotinib & afatinib) report better PFS and OS times for patients with the L858R mutations when compared with patients with the L861Q mutation PFS= 10.4 months vs. 4.5 months *P*=0.003 OS=16.9months vs. 12.2 months *P*=0.04. Other mutations associated with exon 21 with low sensitivity are L861R, L862V, V851X and A859X. Mutations with uncertain sensitivity are E866K, H825L, P848L, H870Y, H870R and G863S (Kobayashi et al 2016; Attili et al 2022).

5.1.4 Diagnosis of EGFR mutations in the clinic

The varied responses of EGFR mutations to TKI depict the immense value of precision diagnosis in stratification of NSCLC patients to therapies that suit their genetic/molecular needs. In the clinic, analysis of tissue biopsy is the gold standard for diagnosis of the EGFR mutational status of patients with NSCLC. However, between 15-40% of patients with NSCLC are not eligible for tissue biopsy either, because their cancer is diagnosed at an advanced stage or because the patient is too weak for surgery (Durandez-saez et al 2017; Sung et al 2021). For this cohort of patients, cytological samples obtained from lungs and mediastinal lymph nodes using computer tomography (CT) and endobronchial ultrasound guided fine needle aspiration are used for recovery of tissue for diagnosis of EGFR mutations. Furthermore, specimens from serous effusions, bronchial washing and brushing are sometimes used for diagnosis of EGFR mutations in these patients (Makarem et al 2020; Russano et al 2020). None of the above-mentioned sampling methods meets the demands of a robust sampling matrix that is sensitive and easily accessible for all patients because of the following challenges, (1) sampling a single lesion or segment of a tissue biopsy may not provide sufficient information on the true genomic landscape of the tumour as malignancies are highly heterogeneous and (2) resampling to check for mutated clones is difficult (Linderman et al 2018; Chen et al 2020).

The challenges highlighted explain the need for alternative approaches to be explored. Liquid biopsy is an approach adopted in the clinics as an alternative and/or complementary method to tissue/cytological specimens for the diagnosis of EGFR mutations. The International Association for the Study of Lung Cancer (www.iasc.org)

recommends that liquid biopsy be used as the first approach for testing for EGFR T790M mutations for patients who have developed resistance to first or second generation TKI, and secondly to be used in specific clinical situations where the patient is not fit for invasive tissues sampling or when the tissue sample is not adequate for analysis for EGFR mutations. cfDNA is the liquid biopsy sample matrix widely used in the clinics for diagnosis of EGFR mutations. Although, this sample matrix has been used successfully in the diagnosis of EGFR mutations, quite a few studies reported sensitivities of approximately 60% for detecting T790M mutation when compared with results obtained from matched tissue biopsy samples. For example, Jenkins et al (2017) in a prospective multi-center study analysed cfDNA samples and matched tissue biopsy samples for T790M mutation in 324 and 373 patients recruited for the AURA extension and AURA II clinical trial who had an EGFR mutation but had progressed after first line therapy. Results from this study showed that the detection rates using cfDNA were 64% and 63% for AURA extension and AURAII studies respectively when compared with T790M mutation results obtained from matched tissue biopsy samples. Similar results have been obtained from other clinical studies (Karlovich et al 2016; Oxnard et al 2016). These studies show that about 40 % of patients with EGFR mutations may not have access to therapies that would best suite their tumours molecular profile. The issue with sensitivity for the detection of T790M discussed above has led to the exploration of other liquid biopsy alternatives such as circulatory tumour cells (CTC). CTC may represent a better sample matrix for liquid biopsy because the hypothesis is that the tumor cells in the circulation are representatives of both primary malignancy and metastatic sites and are purported to give an accurate picture of the genomic land scape of a malignancy (Alix-Panabieres, 2021).

5.1.5 Aim of the study

This present study aimed to demonstrate the clinical potential of CTC isolated from patients with NSCLC using the Lung card version II microfluidic device for analysis of EGFR mutations in exon 18, 19, 20 and 21. Next generation sequencing (NGS) was used in this study to evaluate for EGFR mutations because this approach: screens the entire nucleotide sequence of the target region (exon 18-21 of EGFR), quantitatively evaluates mutant allele and identifies all somatic mutations. Furthermore, the present study evaluated if CTC testing for EGFR mutation using NGS is complementary to matched tissue biopsies. Molecular testing for EGFR mutation used in the biopsy samples in this study involved the use of a commercial PCR based Cobas EGFR mutation test (Roche, Molecular Systems) which detects the presence of 42 mutations in exons 18, 19, 20 and 21. This method was used for tissue biopsy EGFR mutation analysis because in 2019, at the start of this study this was the method of choice in the Castle Hill Hospital (Hull). This study also investigated the clinical outcome of patients who had their mutations identified using CTC+NGS but had been stratified to therapies based on EGFR mutation results obtained from biopsy+Cobas analysis. Finally, this study also explored the effect of single and mixed mutations diagnosed using CTC+NGS in treatment response and reported a series of novel mutations detected using the CTC+NGS matrix.

5.2 Materials and Methods

5.2.1 Patient cohort and Ethics- Fifty-nine patients aged between 47 and 81 years attending the Oncology clinic at the Queens Centre Castle Hill Hospital (Hull) diagnosed for lung cancer using tumour biopsy were recruited for the study (**section 2.9.1**). These patients had an evaluation for EGFR mutation using the PCR technique (Cobas EGFR mutation test) on the tissue biopsy and 38 of the 59 patients had their blood samples taken from which CTC were isolated and examined.

5.2.2 Whole blood collection for CTC isolation

A whole blood sample (14ml), was collected in a 3.2% tri sodium citrate vacutainer bottle (BD, USA) in the recruitment centre. The analysis process started immediately on arrival in the laboratory **see Section 2.9.2** for details of the pre analytical process before CTC isolation.

5.2.3 CTC isolation/extraction from chip

Protocol for CTC isolation and extraction from chip is as described in **Sections 2.1.6 and 2.1.7** of the materials and methods section

5.2.4 PCR amplification of exon 18-21 regions of EGFR gene

Following isolation of CTC from blood of patients using Lung card version II microfluidic device. The DNA extracted was amplified using primers (Stab Vida, Portugal) spanning the intron and exon regions of exon 18, 19, 20 and 21 of the EGFR gene. Details of primers and protocol for PCR reaction are in **Table 2.4 and Section 2.11.2**

5.2.5 Next generation sequencing and analysis of sequencing data to detect mutation variants

PCR products were processed in a series of steps involving purification of the first PCR reaction, a second round of PCR amplification and second purification of the PCR products prior to NGS analysis. The Protocols are in **Table 2.5, & 2.6, Sections 2.12.2 and 2.12.3** of the materials and methods chapter. Sequencing and analysis of data was done at the laboratory of Stab Vida (Lisbon, Portugal) and involved: amplicon generation and library preparation according to protocol of Nextera XT (15031942)

(Illumina, USA) using an Illumina sequencer. Genomic data was processed with Trim galore (version 0.4.3.1) and Prinseq (version 0.20.4). Genomic data generated was aligned to the reference genome with BWA (MEM) version 0.7.17.1 and the variants detected with VAR direct version from 07.03.2018. NGS was undertaken for 38 CTC enriched samples.

5.2.6 Data collection

Demographic/clinicopathological characteristics of patients were obtained from their medical records by Professor Michael Lind and were provided in a pseudo-anonymised form. Patients who were diagnosed for an EGFR mutation using tissue biopsy samples were given a TKI for first line treatment while EGFR mutation negative patients were treated with chemotherapy, immunotherapy or basic supportive care. PFS for this study was defined as the period from when molecular assessment for EGFR mutation was done to the date disease progressed.

5.2.7 Statistical analysis

The likelihood of CTC or tumour biopsy to detect EGFR mutation was compared using Fisher exact test. The relationship between mutational status and patient characteristics was compared using Chi square. All data was analyzed with Prism v 9.0 (Graph pad software, San Diego California USA).

5.3 Results

5.3.1 Patient Characteristics

A total of fifty-nine patients aged between 47and 81 years attending the Oncology clinic at the Queens Centre Castle Hill Hospital Hull, diagnosed for NSCLC using tumour biopsy were recruited for the present study (**Table 5.1**). The mean age at diagnosis was 66.7 years. Twenty-nine (49.1%) of these patients were female and thirty (50.9%) were male. Thirteen (22%) of these patients were smokers and fifty-four (91.5%) had the adenocarcinoma NSCLC subtype. In the current study forty-six (67.9%) patients were diagnosed at stage IIIb or IV and forty-nine (83.1%) patients had PDL1 expression. Thirty-eight patients of the fifty-nine patients recruited had their CTC enriched samples analyzed for an EGFR mutation **Figure 5.1**

Table 5.1- Clinicopathological characteristics of patients recruited for this study

	N (%)
Age	
Median age	66.7 years
Range	47-81years
Sex	Male 30(50.9) Female 29 (41.9)
Smoking Status	Unknown 32 (54.2) Yes 13 (22) No 4 (6.8)
Type of NSCLC	
Adenocarcinoma	54 (91.5)
Large cell	1 (1.7)
Squamous cell	1 (1.7)
Other	2 (5.12)
Stage of Cancer	
IIb	6 (10.1)
IIIA	7 (11.9)
IIIb	11(18.6)
IV	35(59.3)
Metastatic regions	Lung 14(23.7) Lymphnodes 4(6.8) Bone 13(22) Liver 4 (6.8) Kidney 1(1.7) Pleura 7 (11.7) Brain 5 (8.5) Neck 2 (3.4) Mediastinal 12 (20.4)
PDL1 expression≥ 1%	49 (83.1)
Other mutations	ROS1 1 (1.7)

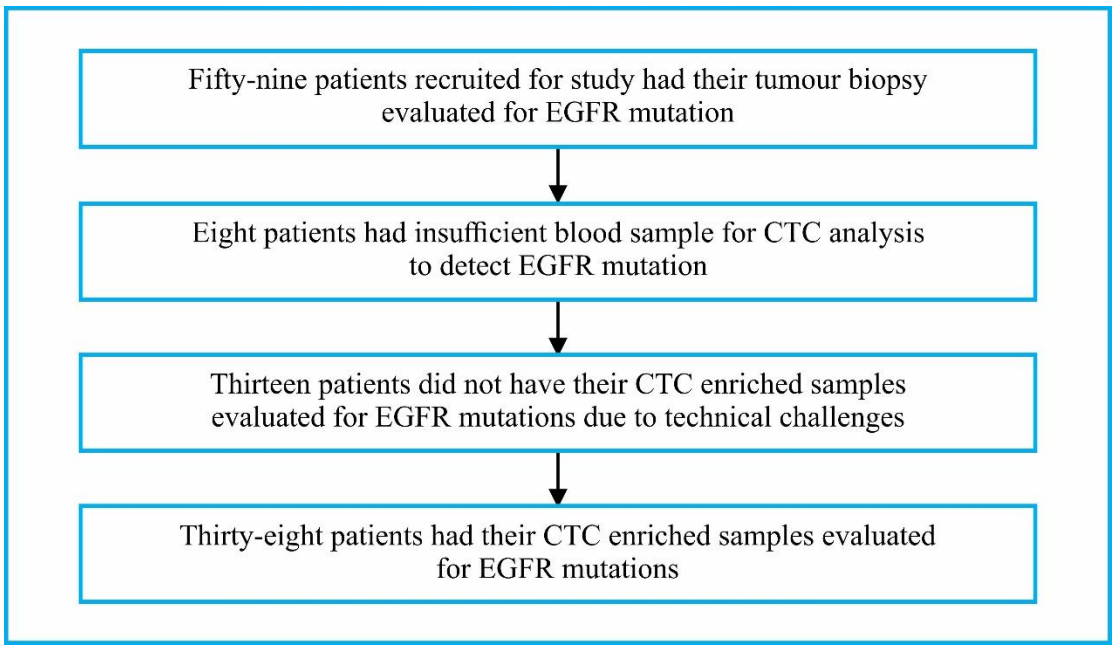

Figure 5.1: Flow chart of patient recruitment

5.3.2. EGFR mutations are detected from CTC isolated from blood of patients with NSCLC using NGS

CTC isolated from the blood of patients with NSCLC using Lung card version II microfluidic device were analyzed for EGFR mutations using NGS. Of the 38 CTC enriched samples analyzed for EGFR mutation 30 (78.95%) had an EGFR mutation on exons 18-21 with 8 (21.05%) having no EGFR mutation. The percentage of EGFR mutated events in this study's CTC enriched samples ranged from 0.55- 55.39% (**Table 5.2**). Exon 19 was the exon with the highest number of genetic variants at 26 (86.7%) with the commonest deletion being E746_A750 delELREA. Whilst exon 21 had the highest frequency of point mutations 7 (23.3%) and exon 20 the highest frequency of single nucleotide variants/single nucleotide polymorphisms 4 (13.33%) (**Figure 5.2 & 5.3**). L858R and P848L point mutations on exon 21 were the point mutations with the highest frequency (3 occurrences 7.9%). (**Figure 5.3**). Mixed EGFR mutations were detected in 9 (31%) of CTC enriched samples positive for an EGFR mutation (**Table 5.3**). All of the patients with a mixed mutation had an exon 19 deletion (**Table 5.3**). Uncommon EGFR mutations were also identified from CTC enriched samples: patient 20 and 56 had an R766H mutation on exon 20, patient 32 had an L703P mutation on exon 18 and a P848L mutation on exon 21, patient 39 had an N700D mutation on exon 18, patient 40 had an L841P mutation on exon 20 patient 43 had a V843L mutation on exon 21. This study also reported the detection of extremely uncommon EGFR single

nucleotide variants/single nucleotide polymorphisms on exon 18, 19, 20 and 21 of varied clinical significance (**Table 5.4**).

Table 5.2: EGFR mutation detected from CTC

Patient ID	Exon	EGFR mutation in CTC	Percentage of mutation NGS	No of CTC counted
1		**WT**		
3		**WT**		
8		**WT**		
9	**21**	**L858R**	**ND**	**NR**
10		**WT**		
11		**WT**		
13	**19**	**Deletion (**E746_A750delELREA)	**ND**	**NR**
14		**WT**		
15	**19**	**Deletion (**E746_A750delELREA)	**ND**	**NR**
16	**19**	**Deletion (**E746_A750delELREA)	**ND**	**NR**
17	**19**	**Deletion (**E746_A750delELREA)	**ND**	**NR**
	21	**L858R**	**ND**	**NR**
19	**19**	**Deletion (**E746_A750delELREA)	**ND**	**NR**
20	**21**	**L858R**	**ND**	**NR**
21		**WT**		
22		**WT**		
24	**19**	**Deletion(**E746_A750delELREA)	**2.01**	**7**
	20	C.2389T>A	**1.3**	
25	**20**	**c.2375T>C**	**0.6**	**4**
26	**19**	**Deletion (**E746_A750delELREA)	**55.39**	**39**
27	**19**	**Deletion (**E746_A750delELREA)	**6.18**	**63**
28	**19**	**Deletion (**E746_A750delELREA)	**3.4**	**3**
	19	**P733L**	**1.74**	
29	**21**	**c.2573T>G**	**0.76**	**23**
30	**19**	**Deletion (**E746_A750delELREA)	**3.19**	**35**
	19	**P733L**	**1.13**	
	20	**c.2318A≥G**	**0.58**	
31	**19**	**Deletion (**E746_A750delELREA)	**1.4**	**81**
	20	**R766H**	**1.2**	
	20	**c.2327G>A, c.2375T>C**	**0.75,0.55**	
32	**19**	**Deletion (**E746_A750delELREA)	**2.4**	
	19	**P735S G696E**	**1.2**	
	18	**L703P**	**1.01**	
	21	**P848L**	**0.86**	
34	**19**	**Deletion (**E746_A750delELREA)	**0.65**	
	21,19	**c.2573T>c, c.2281G>A**	**0.55,1.21**	
36	**19**	**Deletion (**E746_A750delELREA)	**2.65**	
	19	**c.2281G≥A**	**1.17**	
37	**19**	**Deletion (**E746_A750delELREA)	**2.65**	**75**
	18	c.2123A>G	**0.83**	
38	**19**	**Deletion (**E746_A750delELREA)	**6.11**	**32**

39	**19**	**Deletion (**E746_A750delELREA)	**5.83**	**21**
	20	**T790M**	**0.83**	
	18	**N700D**	**0.69**	
40	**19**	**Deletion (**E746_A750delELREA)	**19.67**	**5**
		L841P	**1.4**	
43	**19**	**Deletion (**E746_A750delELREA)	**2.43**	**47**
	21	**V843L**	**0.53**	
53	**19**	**Deletion (**E746_A750delELREA)	**8.47**	
54	**19**	**Deletion (**E746_A750delELREA)	**1.11**	
55	**19**	**Deletion (**E746_A750delELREA)	**14.34**	
56	**19**	**Deletion (**E746_A750delELREA)	**3.26**	**300**
	20	**R776H**	**1.34**	
57	**19**	**Deletion (**E746_A750delELREA)	**32.64**	**81**
58	**19**	**Deletion (**E746_A750delELREA)	**22.85**	**505**
59	**19**	**Deletion (**E746_A750delELREA)	**1.66**	**42**

WT= Wild type- (Negative for an EGFR mutation), ND-Not done, NR-No result

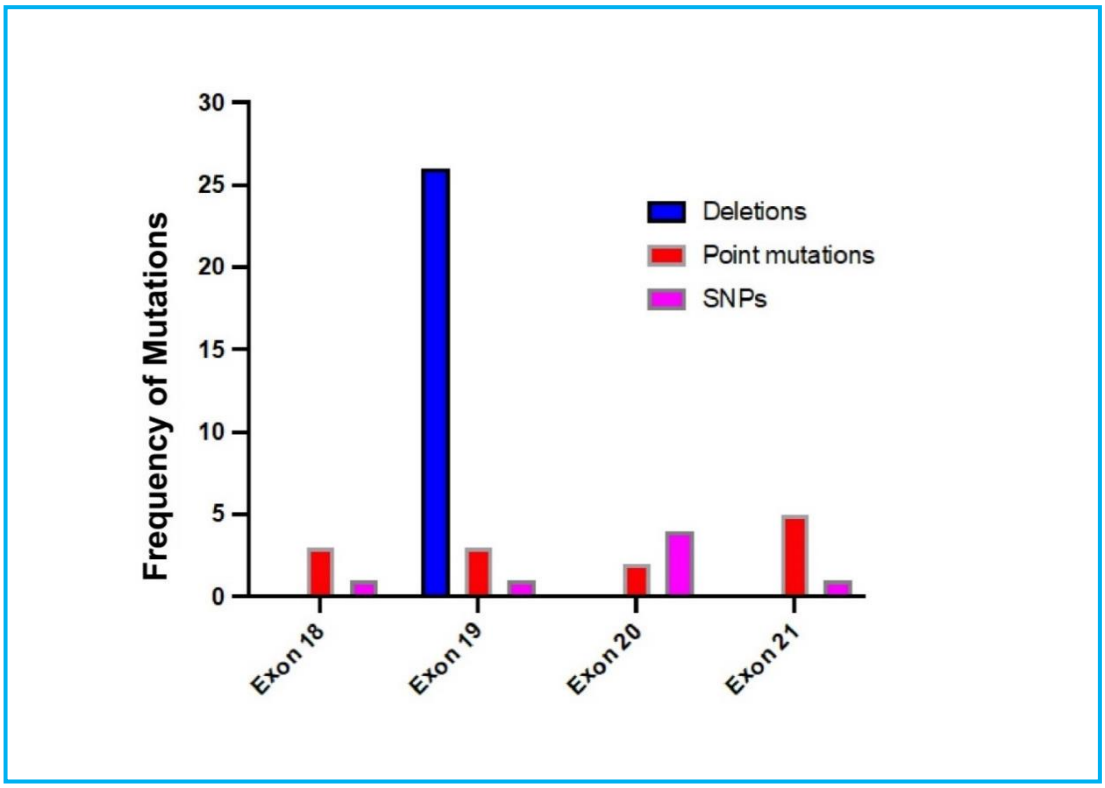

Figure 5.2 Frequency of mutations/deletions in exon 18, 19, 20 and 21 from CTC enriched samples obtained from patients with NSCLC. Exon 19 has the highest number of mutations, which were mostly deletions (c.2235_2249del) whilst exon 21 has the highest frequency of point mutations and exon 20-the highest number of single nucleotide polymorphism (SNP).

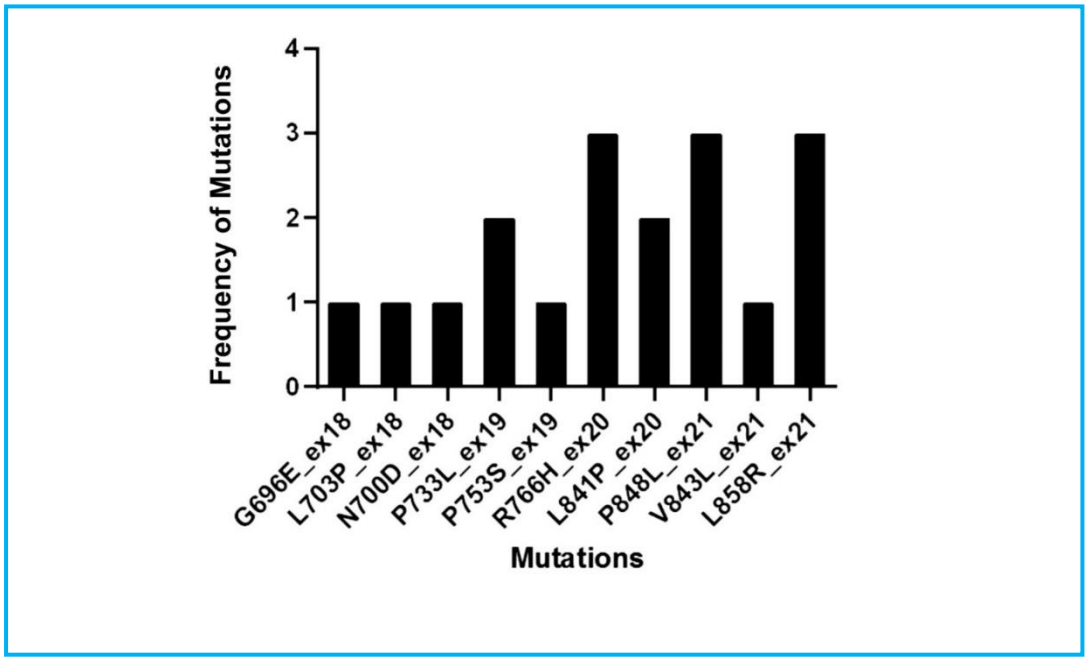

Figure 5.3 Distribution of point mutations in exons 18-21. Exon 21 has the highest frequency of point mutations.

Table 5.3 Patients with mixed EGFR mutations

Patient No	Exon	Mutations
28	19	**Deletion (E746_A750delELREA) P733L**
30	19	**Deletion (E746_A750delELREA) P733L L841P**
31	19 20	**Deletion (E746_A750delELREA)** **R776H**
32	19 21 18	**Deletion (E746_A750delELREA), P753S** **P848L** **G696E, L703P**
39	19 20 18	**Deletion (E746_A750delELREA)** **T790M** **N700D**
43	19 21	**Deletion (E746_A750delELREA)** **V843I**
17	19 21	**Deletion (E746_A750delELREA)** **L858R**
40	19 20	**Deletion (E746_A750delELREA)** **L841P, P848L**
56	20	**R766H**

Table 5.4 Rare EGFR single nucleotide variants identified from patients CTC enriched samples using NGS

Patient ID	Nomenclature (SNV)	Exon	RS no	Amino acid	Comments
31,34	**c.2375T>C**	20	132563568	**L792P**	Pathogenic mutation of somatic origin
24	**c.2389T>A**	20	1057519861	**C797S**	Pathogenic mutation of somatic origin, associated with drug resistance
31	**c.2327G>A**	20	483352806	**R509H**	Germline origin of uncertain significance
30	**c.2318A>G**	20	121913432	**H506R**	Somatic likely pathogenic
37	**c.2123A>G**	18	144932466	**K708R**	Somatic likely pathogenic
34	**c.2281G>A**	19	121913418	**D761N**	Somatic likely pathogenic
29	**c.2573T>G**	21	121434568	**L591R**	Somatic, associated with a drug response

5.3.3 CTC detects more mutations than tumour biopsy

EGFR mutation results obtained from CTC enriched samples using NGS were compared with EGFR mutation results obtained from matched tissue biopsy samples using the Cobas EGFR mutation test to investigate the similarities and differences (**Table 5.5**). The results, show that significantly more mutations were detected in the CTC enriched sample than were found in the tissue biopsy (Fisher's exact test, P value=0.0173). Thirty CTC enriched samples had an EGFR mutation diagnosis, but only 4 patients; 17, 27, 40 and 59 (**Table 5.5**) with matched tissue biopsy samples were diagnosed with an EGFR mutation. The data also shows that CTC+ NGS have a higher likelihood ratio of detecting EGFR mutation (Fisher's exact test, likelihood ratio 1.855, P value=0.0173) than the tumour biopsy sampling + Cobas test (**Figure 5.4**). Furthermore, only 1 of the 4-tissue biopsy sample diagnosed with an EGFR mutation had the same mutation detected in its matched CTC sample (patient 27 had an exon 19 deletion diagnosed in tissue biopsy and CTC). The other 3 tissue biopsy samples showed distinct mutations from their matched CTC enriched samples, i.e. patient 17 was diagnosed with an exon 20 insertion from its tissue biopsy sample wheras its matched CTC enriched sample had an exon 19 deletion and an L858R point mutation,

patient 40 and 59 both had an exon 21 L858R mutation detected from their tissue biopsy samples but had exon 19 deletion, L841P and P848L mutations (patient 40) and an exon 19 deletion (patient 59) diagnosed from their CTC enriched samples (**Table 5.5**). The 8 CTC enriched samples carrying no apparent EGFR mutations also had no EGFR mutation detected in their matched tumour biopsy sample (**Figure 5.4**). Also, no mixed mutations were detected in any tumour biopsy samples.

Table 5.5: Comparison of EGFR mutation detected from CTC+NGS and Tumour biopsy+Cobas EGFR mutation test

Patient ID	Exon EGFR CTC	EGFR mutation in CTC	Percentage of mutation NGS	Exon EGFR biopsy	EGFR mutation tumor biopsy	Matched Yes or No
1		**WT**			**WT**	Yes
3		**WT**			**WT**	Yes
8		**WT**			**WT**	Yes
9	**21**	**L858R**			**WT**	No
10		**WT**			**WT**	Yes
11		**WT**			**WT**	Yes
13	**19**	**Deletion** (E746_A750delELREA)			**WT**	No
14		**WT**			**WT**	Yes
15	**19**	**Deletion** (E746_A750delELREA)			**WT**	No
16	**19**	**Deletion** (E746_A750delELREA)			**WT**	No
17	**19**	**Deletion** (E746_A750delELREA)		20	**Exon20 insertion**	No
	21	**L858R**				
19	**19**	**Deletion** (E746_A750delELREA)			**WT**	No
20	**21**	**L858R**			**WT**	No
21		**WT**			**WT**	Yes
22		**WT**			**WT**	Yes
24	**19**	**Deletion** (E746_A750delELREA),	**2.01**		**WT**	No
	20	c.2389T>A	**1.3**			
25	**20**	**c.2375T>C**	**0.6**		**WT**	No
26	**19**	**Deletion** (E746_A750delELREA)	**55.39**		**WT**	No
27	**19**	**Deletion** (E746_A750delELREA)	**6.18**	19	**Exon 19 del**	Yes
28	**19**	**Deletion** (E746_A750delELREA)	**3.4**		**WT**	No
	19	**P733L**	**1.74**			
29	**21**	**c.2573T>c**	**0.76**		**WT**	No
30	**19**	**Deletion** (E746_A750delELREA)	**3.19**		**WT**	No
	19	**P733L**	**1.13**			
	20	**c2318A≥G**	**0.58**			
31	**19**	**Deletion** (E746_A750delELREA)	**1.4**		**WT**	No

	20	c.2375T>c, c.2327>G	**0.55, 0.75**			
	20	**R766H**	**1.2**			
	20	**c2441T≥A**	**0.75**			
32	**19**	**Deletion (**E746_A750delELREA)	**2.4**		**WT**	No
	19	**P735S**	**1.2**			
	18	**L703P**	**1.01**			
	21	**P848L**	**0.86**			
34	**19**	**Deletion (**E746_A750delELREA)	**0.65**		**WT**	No
	19	c.2281G>A	**0.58**			
	21	**c2573T≥c**	**0.55**			
36	**19**	**Deletion (**E746_A750delELREA)	**2.65**		**WT**	No
	19	**c2281G≥A**	**1.17**			
37	**19**	**Deletion (**E746_A750delELREA)	**2.65**		**WT**	No
	18	c.2123A>G	**0.83**			
38	**19**	**Deletion (**E746_A750delELREA)	**6.11**		**WT**	No
39	**19**	**Deletion (**E746_A750delELREA)	**5.83**		**WT**	No
	20	**T790M**	**0.83**			
	18	**N700D**	**0.69**			
40	**19**	**Deletion (**E746_A750delELREA)	**19.67**	21	**L858R**	No
	20	**L841P**	**1.4**			
43	**19**	**Deletion** (E746_A750delELREA)	**2.43**		**WT**	No
	21	**V843L**	**0.53**			
53	**19**	**Deletion (**E746_A750delELREA)	**8.47**		**WT**	No
54	**19**	**Deletion** (E746_A750delELREA)	**1.11**		**WT**	No
55	**19**	**Deletion (**E746_A750delELREA)	**14.34**		**WT**	No
56	**19**	**Deletion** (E746_A750delELREA)	**3.26**		**WT**	No
	20	**R766H**	**0.92**			
57	**19**	**Deletion (**E746_A750delELREA)	**32.64**		**WT**	No
58	**19**	**Deletion (**E746_A750delELREA)	**22.85**		**WT**	No
59	**19**	**Deletion** (E746_A750delELREA)	**1.66**	21	**L858R**	No

WT= Wild type- (Negative for an EGFR mutation)

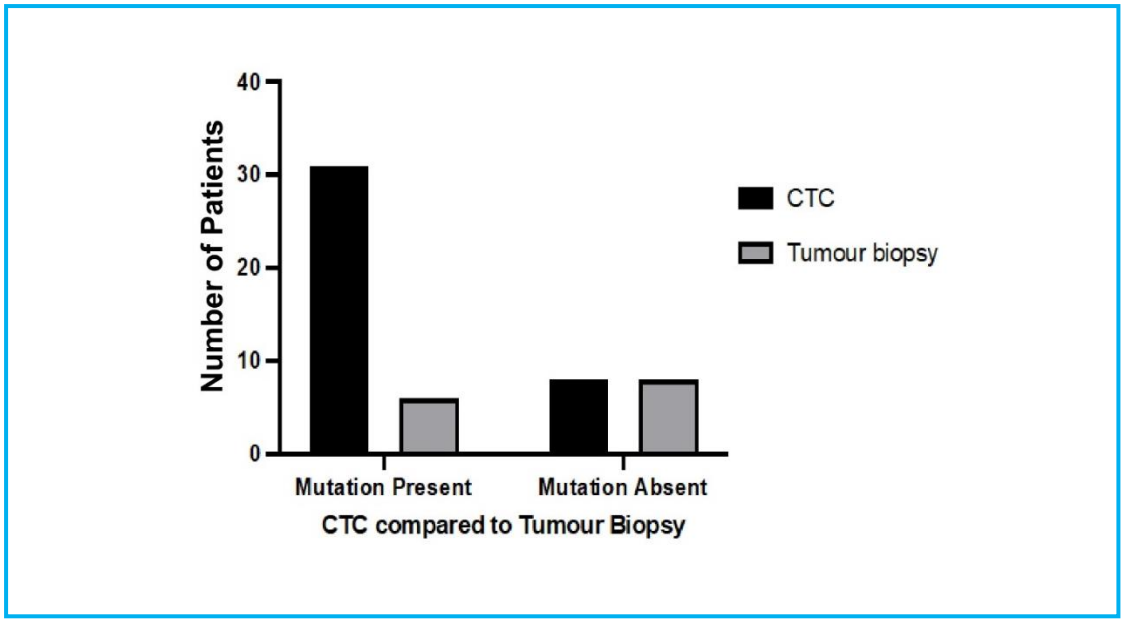

Figure 5.4: showing presence and absence of EGFR mutations in matched CTC and tumor biopsy samples. Statistical analysis using Fisher's exact test shows that CTC significantly (P=0.0173) detects more EGFR mutation when compared to tissue biopsy and the likelihood of detecting EGFR from CTC samples is 1.855 (Fisher's exact test).

5.3.4 Clinical outcome of patients with CTC containing EGFR mutations who were stratified to therapies based on EGFR mutation results obtained from tissue biopsy

The present study sought to further evaluate the clinical potential of EGFR mutation results obtained from CTC by investigating the clinical outcome/ response to therapy of patients who had an EGFR mutation diagnosed from their CTC but were stratified to therapies based on EGFR results obtained from their tumor biopsy samples. Patients diagnosed for an EGFR mutation from tissue biopsy were treated with a TKI as indicated by standard clinical care guidelines. Analysis showed that the overall responses of patients who had an EGFR mutation obtained from CTC but were stratified to therapies based on EGFR mutation results obtained from tumor biopsy was significantly different from patients whose CTC enriched samples had no EGFR mutation (P value<0.05) **(Figure 5.5)**. Clinical response was defined according to the response evaluation criteria in solid tumours (RECIST). Of the 30 CTC enriched samples positive for EGFR mutation 20 (66.67%) had a progressive disease: only 1 (5%) of the patients with a progressive disease was placed on targeted therapy, 7 (35%) patients were placed on immunotherapy, 3 (15%) patients were placed on immunotherapy/chemotherapy, 6 (30%) patients had chemotherapy alone and 3(15%)

patients were receiving basic supportive care **(Table 5.6**). Of the 6 patients (20%) with CTC enriched sample positive for EGFR mutation that had a partial response: 3 were receiving immunotherapy, 1 had immunotherapy/chemotherapy, 1 had chemotherapy alone and 1 received TKI. Of the 5 patients (16.67%) with CTC enriched sample positive for an EGFR mutation with stable disease 3 patients were placed on immunotherapy 1 patient was on chemotherapy and 1 was on basic supportive care (**Table 5.6**). Out of a total of 8 CTC enriched samples negative for EGFR mutation 3 (37.5%) patients had a progressive disease, 2 were placed on immunotherapy and 1 on immunotherapy/chemotherapy. Three patients had a partial response 2 of the patients showing partial response were on chemotherapy and 1 was on immunotherapy. Two patients with stable disease were on immunotherapy (**Table 5.6**).

This study also evaluated clinical outcome (overall response) of patients whose CTC enriched samples were either positive or negative for EGFR mutations but stratified to chemotherapy or immunotherapy based on EGFR mutation results obtained from the tumour. Analysis showed that there was no statistically significant difference ($P>0.05$) in overall response between patients whose CTCs had a detectable EGFR mutation as compared with patients with no EGFR mutation and were placed on chemotherapy or immunotherapy (**Figure 5.6**). Of the 8 patients whose CTC possessed an EGFR mutation and were placed on chemotherapy 6 (75%) of them had a progressive disease and 1 patient had a stable disease and 1 had a partial response. There was no progressive disease observed in patients with no EGFR mutation detected from their CTC placed on chemotherapy. In contrast, 2 patients without the EGFR mutation who received chemotherapy had either a stable disease or a partial response **(Figure 5.6A**). Of the 10 patients whose CTC possessed an EGFR mutation placed on immunotherapy 4 of them had a progressive disease 3 patient had a stable disease and 3 showed a partial response. Seven patients whose CTC sample had no EGFR mutation were placed on immunotherapy 3 of these patients had a progressive disease, 2 of these patients had a partial response and 2 had a stable disease (**Figure 5.6B**).

5.3.5 Clinical outcome of patients whose CTC detected a single mutation compared with patients with a mixed mutation (these patients were stratified to therapy based on biopsy analysis)

Conflicting evidence exist as regards the effect of mixed mutations on clinical outcome. This study evaluated the relationship between mutational status and overall response. Analysis indicated that there was no statistically significant difference (P>0.05) in overall response between patients with a mixed mutation and patients with a single mutation (**Figure 5.7**) Of the 9 patients with a mixed mutation 6 (66.67%) had progressive disease, 2 had a partial response and 1 had a stable disease. Of the 21 patients with single mutations 13 (61.9%) had progressive disease, 5 had stable disease and 3 had a partial response (**Figure 5.7**).

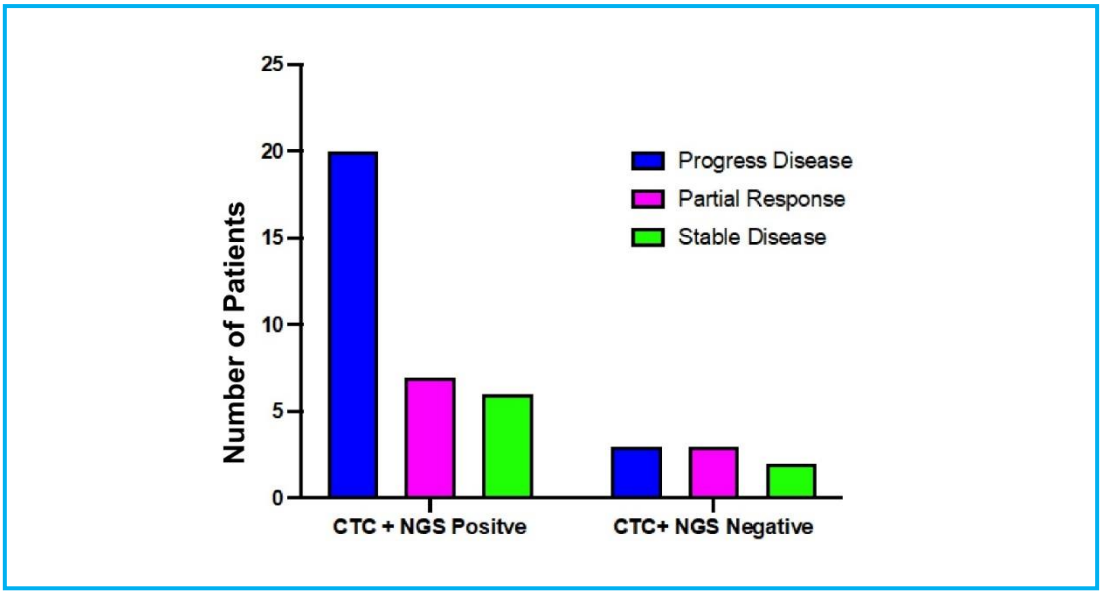

Figure 5.5-Clinical outcome (overall response) of CTC+ NGS, patient's commenced treatment based on results from tumour biopsy+cobas EGFR mutation test before CTC sampling for NGS. There was a statistically significant difference P<0.05 in treatment response between CTC+NGS EGFR positive samples and CTC+NGS EGFR negative samples. Of the 20 patients who had a progressive disease only one of them was placed on TKI.

Table 5.6- Patients EGFR mutation status, therapy, response to therapy, progression free survival and dead or alive status

ID	CTC	biopsy	PFS	Histology	Stage	Therapy	ORe	Status 01/09/21
1	**WT**	**WT**	**23**	Adenocarcinoma	IV	Chemotherapy	**PR**	Alive
3	**WT**	**WT**	**4**	Adenocarcinoma	IV	Immunotherapy	**PR**	Dead
8	**WT**	**WT**	**6**	Adenocarcinoma	IIIA	Chemotherapy	**PD**	Alive
9	**L858R**	**WT**	**2**	Adenocarcinoma	IIIB	Immunotherapy	**PR**	Alive
10	**WT**	**WT**	**23**	Adenocarcinoma	IV	Immunotherapy	**SD**	Dead
11	**WT**	**WT**	**6**	Adenocarcinoma	IV	Immunotherapy	**PR**	Alive
13	**Deletion**	**WT**	**24**	Adenocarcinoma	IIIA	Immunotherapy	**SD**	Alive
14	**WT**	**WT**	**26**	Adenocarcinoma	IV	Immunotherapy	**SD**	Alive
15	**Deletion**	**WT**	**1**	Adenocarcinoma	IIIB	Chemotherapy	**PD**	Dead
16	**Deletion**	**WT**	**26**	Adenocarcinoma	IV	Immunotherapy	**SD**	Dead
17	**Deletion**	**Exon20 insertion**	**1**	Adenocarcinoma	IV	Basic Supportive Care	**PD**	Dead
	L858R							
19	**Deletion**	**WT**	**9**	Adenocarcinoma	IIIB	Immunotherapy	**SD**	Alive
20	**L858R**	**WT**	**6**	Adenocarcinoma	IIIB	Immunotherapy	**PD**	Alive
21	**WT**	**WT**	**8**	Adenocarcinoma	IV	Immunotherapy	**PD**	Dead
22	**WT**	**WT**	**1**	Adenocarcinoma	IIIB	Immunotherapy	**PD**	Dead
24	**Deletion** c.2375T>C	**WT**	**1**	Adenocarcinoma	IV	Basic Supportive care	**SD**	Dead
25	c.2375T>C	**WT**	**8**	Adenocarcinoma	IIIB	Chemotherapy	**PD**	Dead
26	**Deletion**	**WT**	**26**	Adenocarcinoma	IV	Immunotherapy	**PD**	Alive
27	**Deletion**	**Deletion**	**28**	Adenocarcinoma	IV	Targeted therapy	**PD**	Dead
28	**Deletion**	**WT**	**2**	Adenocarcinoma	IV	Chemotherapy	**SD**	Dead
	P733L							
29	**c2573T>G**	**WT**	**4**	Adenocarcinoma	IIB	Basic Supportive Care	**PD**	Dead

30	**Deletion** c2318A>G	**WT**	**5**	Adenocarcinoma	IV	Chemotherapy	**PD**	Dead
	P733L							
	c2318A≥G							
31	**Deletion** c2327G>A c2375T>C	**WT**	**10**	Adenocarcinoma	IV	Immunotherapy/ Chemotherapy	**PR**	Alive
	R766H							
	L841P							
32	**Deletion**	**WT**	**6**	Adenocarcinoma	IV	Immunotherapy/ Chemotherapy	**PD**	Alive
	P735S							
	L703P							
	P848L							
34	**Deletion**	**WT**	**9**	Adenocarcinoma	IIIB	Basic Supportive Care	**PD**	Dead
	c2281G>A							
36	**Deletion**	**WT**	**2**	Adenocarcinoma	IV	Chemotherapy	**PD**	Dead
37	**Deletion** c2123>G	**WT**	**7**	Adenocarcinoma	IIIB	Immunotherapy/ Chemotherapy	**PD**	Dead
38	**Deletion**	**WT**	**3**	Adenocarcinoma	IV	Immunotherapy	**PR**	Dead
39	**Deletion**	**WT**	**2**	Adenocarcinoma	IIB	Chemotherapy	**PD**	Dead
	T790M							
	N700D							
40	**Deletion** R766H	**L858R**	**36**	Adenocarcinoma	IIIA	Targeted therapy	**PR**	Dead
43	**Deletion**	**WT**	**4**	Adenocarcinoma	IIIB	Chemotherapy	**PR**	Dead
	V843L							
53	**Deletion**	**WT**	**2**	Adenocarcinoma	IV	Chemotherapy	**PD**	Alive
54	**Deletion**	**WT**	**5**	Adenocarcinoma	IIIB	Immunotherapy	**PD**	Dead
55	**Deletion**	**WT**	**8**	Adenocarcinoma	IV	Immunotherapy	**PR**	Alive
56	**Deletion**	**WT**	**1**	Adenocarcinoma	IV	Immunotherapy/ Chemotherapy	**PD**	Alive
57	**Deletion**	**WT**	**2**	Adenocarcinoma	IV	Immunotherapy	**PD**	Dead
58	**Deletion**	**WT**	**4**	Adenocarcinoma	IV	Immunotherapy	**PD**	Alive
59	**Deletion**	**L858R**	**5**	Adenocarcinoma	IV	Basic Supportive care	PD	Dead

WT= Wild type-, all deletions were **(**E746_A750delELREA) on exon 19 PFS (months)-progression free survival OR-overall response

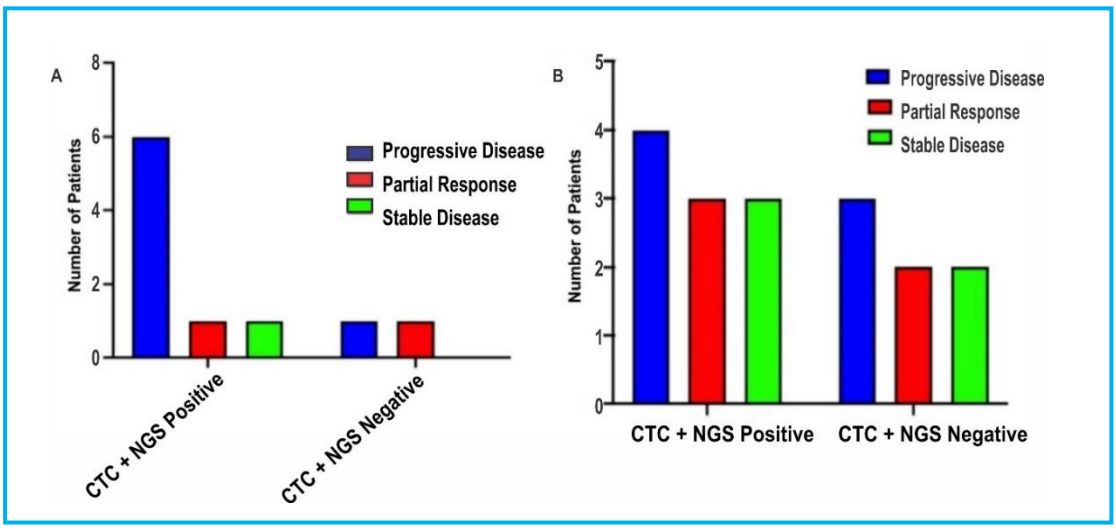

Figure 5.6 Clinical outcome (overall response) of CTC enriched sample positive for EGFR mutation and CTC enriched sample negative for EGFR mutation receiving immunotherapy (**A**) or chemotherapy (**B)** There was no statistically significant difference in overall response (*P<0.05)* between the two groups PD-progressive disease, SD-stable disease PR- partial response

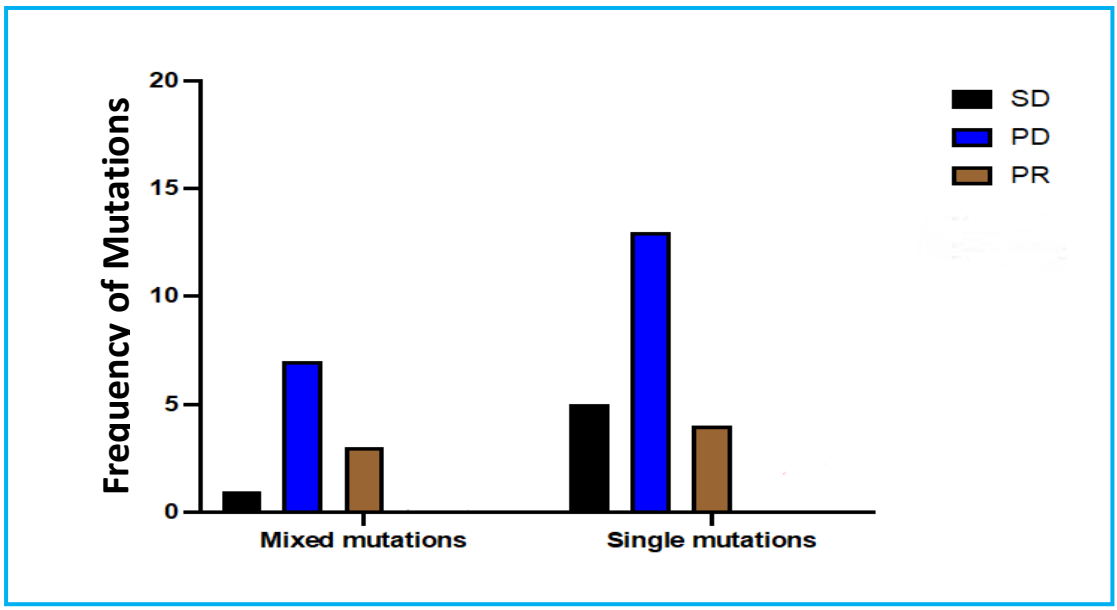

Figure 5.7: relationship between mutation status and overall response. There was no statistically significant difference in overall response between single and mixed mutation (*P<0.05*) PD-progressive disease, SD-stable disease PR- partial response

5.3.6 Comparison Progression Free Survival (PFS) based on mutational status and therapy of CTC enriched samples

This study also explored the clinical potential of CTC as a tool for precision diagnosis for EGFR mutation by examining the survival benefit or lack thereof in NSCLC patients whose CTC enriched sample and matched tissue biopsy sample were diagnosed with an EGFR mutation but stratified to therapies based on EGFR mutation results obtained from tissue biopsy. This study compared (1) PFS between CTC enriched samples negative for an EGFR mutation and CTC enriched sample positive for an EGFR mutation (2) PFS between CTC enriched samples negative for an EGFR mutation and CTC enriched samples positive for an EGFR mutation stratified to chemotherapy (3) PFS between CTC enriched samples negative for an EGFR mutation and CTC enriched samples positive for an EGFR mutation stratified to immunotherapy and finally (4) PFS between CTC enriched samples with a mixed mutation and CTC enriched samples with single mutation. The results from our analysis using log rank Mantel-Cox statistical test (**Figure 5.8**) showed that there was no statistically significant difference in any of the groups compared (**Table 5.7**)

Table 5.7: Comparing PFS amongst CTC groups

CTC Groups	Statistics
EGFR mut negative VS EGFR mut positive	Median PFS 26 vs. 10months P value=**0.3420**, Hazard ratio 0.76 95% CI=0.2498-2.319
EGFR mut negative VS EGFR mut positive stratified to chemotherapy	Median PFS 14.50 vs. 10months P value=**0.5002**, Hazard ratio 0.4892 95% CI=0.1273-3.200
EGFR mut negative VS EGFR mut positive stratified to immunotherapy	Median PFS 26 vs. 9months P value=**0.2584**, Hazard ratio 2.889 95% CI=0.6330-13.9
Single mutation vs mixed mutation	Median PFS 23 vs. 10 months P value=**0.5**, Hazard ratio 0.9514 95% CI=0.212-4.348

Mut-mutation, VS-versus

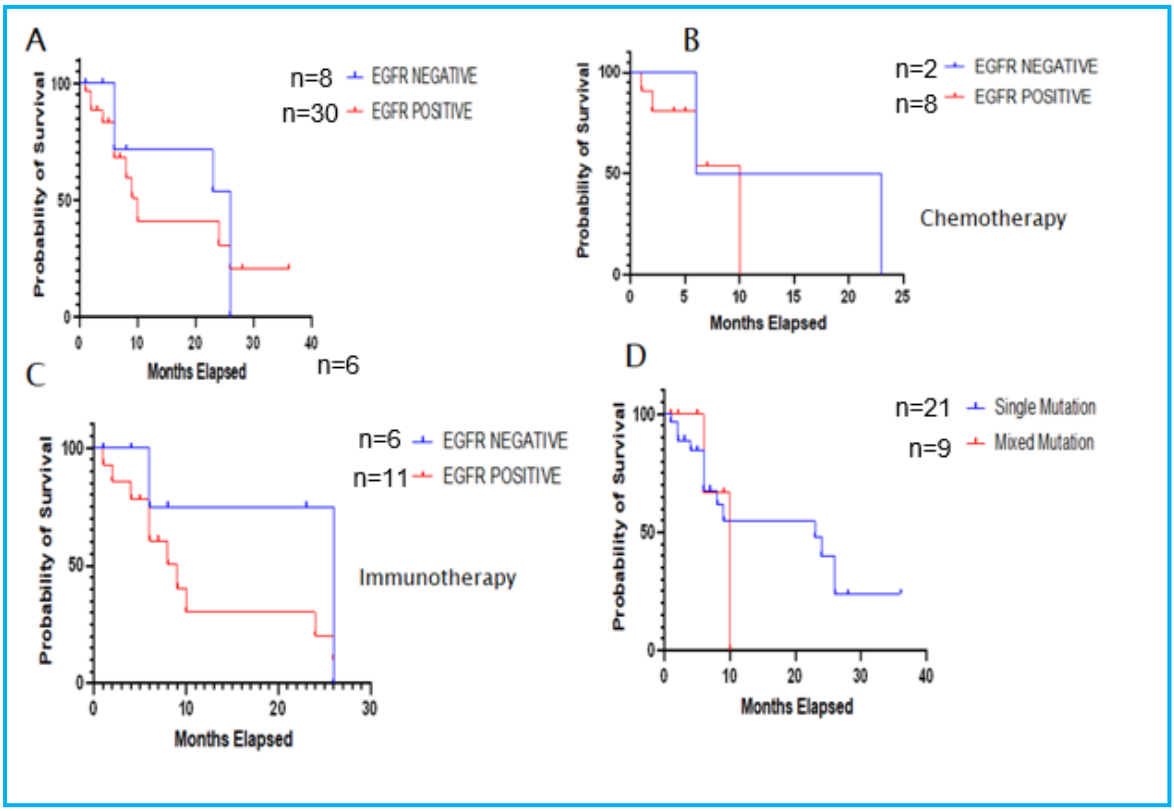

Figure 5.8- Kaplan Meir survival curves for progression free survival (PFS) **(A)** PFS EGFR mutation negative CTC enriched samples vs. EGFR mutation positive CTC enriched samples **(B)** PFS EGFR mutation negative CTC enriched samples vs. EGFR mutation positive CTC enriched samples on chemotherapy **(C)** PFS EGFR mutation negative CTC enriched samples vs. EGFR mutation positive CTC enriched samples on immunotherapy **(D)** PFS CTC enriched samples with mixed mutation vs. CTC enriched samples with single mutation.

5.4 Discussion

The present study was devised to evaluate the clinical potential of CTC to detect EGFR mutation and to investigate the concordance between EGFR mutation status in basal tumour biopsies diagnosed using PCR based Cobas EGFR mutation test and EGFR mutation status diagnosed using NGS from matched CTC enriched samples obtained from NSCLC patients. Blood samples were collected from 38 patients enrolled for the study and subjected to CTC processing/isolation using Lung card version II microfluidic device.

Results (**Table 5.2**) show that 30 out of 38 (78.95%) CTC enriched samples possessed one or more EGFR mutations in exon 18- 21 of the EGFR. The relatively high rate of patients with an EGFR mutation detected from their CTC enriched samples is in contrast to a number of previous epidemiological studies that reported the incidence of EGFR mutation in NSCLC amongst Caucasian population to be around 10-40% (Midha et al 2015; Zheng et al 2016; Graham et al 2018). What may account for the difference in incidence of EGFR mutation results are firstly, most of the earlier studies analyzed tumour biopsy samples to detect EGFR mutations whereas this current study detected EGFR mutation using CTC enriched samples. The majority of reviews, experimental and clinical, have proposed that CTC may be superior and/ or complementary to tissue biopsy for the diagnosis of EGFR because these cells are purported to give a truer picture of tumour heterogeneity (Calabuig-Farinas et al 2016; Sun et al 2018; Keup et al 2022). CTC in blood are cells emanating from both primary and metastatic sites unlike the tissue biopsy where tumour cells are only from the primary site. Secondly, issues with sample collection and pre-processing tissue for DNA analysis to detect EGFR mutation may affect the quality of results (Weber et al 2014; Chedid et al 2022). Thirdly, the majority of studies in the literature used PCR based techniques (digital PCR, amplification refractory mutation system, restriction fragment polymorphism mutant alleles, locked PCR clamping) for detection of EGFR mutations. These techniques detect only specific mutations whilst NGS screens the whole genome for mutations (Thompson et al 2016; Chodhury et al 2022). Finally, NGS is sometimes associated with high false discovery rates particularly with DNA extracted from formalin fixed and paraffin embedded tissues. Exaggeration of mutations by NGS has been attributed to sequence artifacts due to use of low-quality DNA, clonal amplification of DNA strands, excessive PCR cycles and chemical modifications

during NGS processing/workflow (Singh et al 2020). The high incidence in mutations from CTC reported from our study may be due to sequence artefacts. However, this present study analyzed CTC for mutations at a read depth of × 10,000 this limits the probability of obtaining errors. Moreover, some studies have argued that since CTCs are relatively rare any CTC detected is of good quality and therefore any mutation detected in CTC with sufficient coverage should be taken as a variant (Heitzer et al 2013). Whilst some have proposed that for a mutation to be identified from CTC samples, single CTC analysis is essential to avoid the averaging of bulk analysis and a mutation should only be accepted if it is detected in two or more CTC libraries. This ensures that mutations detected in CTC are actual representatives of genomic events of the malignancy and not from amplification or sequencing errors (Wang et al 2019). The results on incidence of EGFR mutation using CTC+NGS sample matrix will be confirmed in future studies using single CTC mutation analysis.

Common and uncommon mutations were detected from CTC+NGS matrix (**Figures 5.2& 5.3, Table 5.2**). Exon 19 deletion was the most prevalent form of mutation detected, 26 out of 30 (86.67%) and all the deletions were around the LREA regions 746-750 (**Figure 5.2**). The present study also detected the following rare mutations in CTC were also discovered: L792P, C797S, H506R and L591R **(Table 5.4)**. These mutations have been previously reported in patients with NSCLC (Lynch et al 2004; Tsao et al 2005; Gonzalez-Manzano et al 2008; Thress et al 2015). L591R has been associated with drug response to gefitinib whilst the C797S mutation is associated with drug resistance to osimertinib (Lynch et al 2004; Thress et al 2015). The D761N mutation has also been reported in NSCLC as well as cancers of the prostate and colon (Tsao et al 2005; Fu et al 2014; Kim et al 2019). The K708R mutation has previously been identified in ovarian cancers (Tanaka et al 2011) and linked to aberrant phosphorylation of AKT and ERK but not in NSCLC. This study reports the first case of the K708R mutation in NSCLC. CTC analysis for EGFR mutation in this study also identified 9 (31%) out of 30 patients (**Table 5.3**) who possessed an EGFR mutation had a mixed mutation.

Results from CTC mutational profile are somewhat consistent with results of mutational profiles from other studies. Exon 19 deletion **(**E746_A750delELREA) and exon 21 mutations (L858R) (common mutations) account for 80-90% of EGFR

mutations associated with NSCLC (Janne et al 2012; Wu et al 2015; Graham et al 2018). The CTC+NGS sample matrix detected exon 19 deletion in 86.67% of patients who had their CTC enriched samples diagnosed for an EGFR mutation.

Also, the frequency of mixed mutations (30%) detected from this study is markedly higher than frequency rates for mixed EGFR mutations reported from other studies. Three large studies on frequency of EGFR mutations in Caucasian population, report a frequency rate for mixed mutations to be between 5-7% (Evans et al 2019; Martin et al 2019; Sousa et al 2020). The disparity in frequency rates in the CTC enriched samples when compared to rates reported from other studies could be attributed to relatively small sample size- this may have increased the probability of detecting more mutations and/or difference in sampling methods and techniques used to detect EGFR mutation as discussed above. Most studies, that have reported frequency rates for mixed mutations have focused on mutation profiles detected from tumour biopsy. Tumour cells obtained for EGFR diagnosis from a biopsy are obtained from only one site. Whereas, the CTC may have come from multiple sites: primary and metastatic, the latter may well have acquired more mutations as they develop away from the tumour mass (Kawachi et al 2019; Fares et al 2020). Furthermore, most of the literatures have used PCR based techniques and or Sanger sequencing for the detection of mutations for both tissue biopsy and CTC enriched samples. PCR based techniques which employ a targeted approach will detect a limited number of mutations (Presseur et al 2015; Zhang et al 2019; Sousa et al 2020; Ntzifa et al 2021). The only study, to the best of the authors knowledge that has utilized NGS of CTC for detection of EGFR mutations in NSCLC patients reported a frequency of 13% for mixed mutations of the 31 CTC enriched samples positive for mutations in exon 18-21 in the EGFR gene (Marchetti et al 2014), this rate was lowere than what was observed in the current study. Finally, sequencing artefacts as mentioned in previous paragraphs may have contributed to the high incidence of mixed mutations reported in this study. Future work on single CTC mutational analysis for EGFR mutation will give a clearer picture on the incidence of mixed mutation.

Results, from evaluation of the concordance between data from tissue biopsies analyzed by the Cobas EGFR test and matched CTC samples using NGS, showed that there were more EGFR mutations detected from the latter samples. Thirty out of 38 (78.95%)

matched CTC and tumour biopsy samples had an EGFR mutation detected from CTC while only 4 (13.3%) matched tissue biopsy samples had an EGFR mutation. CTC detected significantly more mutations than in the tissue biopsy P value=0.0173 and CTC had a higher likelihood ratio (P value 0.0173, likelihood ratio 1.83) of detecting EGFR mutations than in the tissue biopsy (**Figure 5.4** & **Table 5.5**). The frequency rate for EGFR mutation diagnosed from tissue biopsy is consistent with EGFR mutation rates (10-20%) in Caucasian population reported in previous studies (Midha et al 2015; Zheng et al 2016; Graham et et al 2018) while the frequency rates of EGFR mutations from CTC is higher than published data on incidence of EGFR mutations in Caucasian population. Similarity in frequency rates between EGFR mutation results obtained from tissue biopsies and frequency rates in several published data on the incidence of EGFR mutation in Caucasian population can be linked to similarities in sampling and techniques used in detecting EGFR mutations. More than 90% of publications reporting incidence of EGFR mutations in Caucasian population used either a tissue biopsy or cfDNA sampling and a targeted PCR based technique for the detection of EGFR mutations (IPASS 2009; NEJ 2010; EUROTAC 2012; Krebs et al, 2016).

Detection rates for EGFR mutation obtained from CTC (78.95%) in comparison to tumour biopsy (13.3%) differ from other studies. Most studies that have explored CTC for the detection of EGFR mutations have reported similar detection rates in CTC and matched tissue biopsy samples (Mahesawaram et al 2008; Ke et al 2015; Marchetti et al 2014; Sunderasan et al 2016). Whilst some studies have reported lower detection rates for EGFR mutation with CTC when compared with matched tissue biopsy samples (Punnose et al 2012; Zhang et al 2019; Ntzifa et al 2021). Most of the studies that have compared EGFR detection rates in CTC and tumour biopsy only analyzed CTC for EGFR mutations in patients whose biopsy samples were positive for a mutation. The current study had a wider scope for comparison because CTC samples were analyzed for mutations from both patients whose biopsy samples possessed a mutation and patients whose biopsy samples possessed no mutation, i.e., the samples were analyzed "blind". Furthermore, high detection rates of CTC enriched samples used in this study for EGFR mutation can be attributed to the platform used for CTC processing from blood. The platform used in this study- the Lung card version II microfluidic device isolated CTC from blood samples with a capture efficiency of ≥ 65% and purity of ≥ 95% this provided sufficient CTC with high purity such that EGFR mutations were not

obscured by wild type signals from contaminating white blood cells i.e., this study assumes that all EGFR mutation signals came through without any disruption and obstruction because of the high purity of CTC isolated. Lower detection rates in CTC for EGFR mutations in comparison with detection rates from tumour biopsy has been linked to low sensitivity and specificity of techniques used for CTC isolation and detection of mutations (Punnose et al 2012; Banko et al 2019; Ntzifa, 2021). Also, as previously highlighted tumour heterogeneity may be a factor responsible for the disparity. EGFR mutation obtained from CTC may be representative of molecular events of an evolving malignancy and its interaction with its environment. Whilst EGFR mutation result obtained from tumour biopsy are representative of molecular events at the primary malignancy hence the relatively low number of EGFR mutations detected in the tissue biopsy (Alix-Panabieres 2020; Chodhury et al 2022).

The discordance in EGFR mutations detected from tumour biopsy and CTC for patients 17, 27, 40 and 59 (**Table 5.5**) has been reported in others studies. Zhang et al (2019), reported a discordance in mutation results obtained from 1 of 4 matched CTC and tissue biopsy samples positive for an EGFR mutation, Ntzifa et al (2021) reported a discordance in mutations detected in 2 of 7 matched CTC and tissue biopsy samples positive for an EGFR mutation. These studies attributed the differences to tumour heterogeneity as discussed above. CTC counts have also been proposed to have some influence on the detection of mutation signals from CTC (Shaw et al 2017). Shaw et al 2017 and Keup et al 2020 in a comparative study on P1K3CA and ESR1 mutations detected from cfDNA and CTC in patients with breast cancer reported that the discordance observed in number of mutations and type between the two sample matrices may be linked to cell counts as patients with fewer mutations detected in their CTC samples when compared with their matched cfDNA had smaller CTC counts whilst patients with more mutations in CTC had higher CTC counts. Perhaps the discordance in mutations observed may be linked to quantity of CTC isolated. **Chapter 4** of this current study highlighted that one of the limitations of this study is the use of magnetic beads covalently linked to only one anti-body (anti-EpCAM) to capture CTC and that capture efficiency can be improved if a cocktail of anti-tumour antibodies is used to capture CTC. There is therefore a possibility that the CTC isolated may not be a fair representation of the entire spectrum of mutational events ongoing in the malignancy as low EpCAM expressing cells or cells not expressing EpCAM may not

have been isolated for mutational analysis hence the discordance. In addition, as discussed earlier bulk mutation analysis from pooled CTC may not reflect the true heterogeneity of CTC, there is a need to evaluate if mutations detected arise from single or multiple cell clones (Park et al 2014; Wang et al 2019).

Uncommon mutations and extremely rare mutations (**Figure 5.3, Table 5.3 & 5.4**) detected in CTC but not in the tumour biopsy can be attributed to differences in sampling and technique used in detecting EGFR mutations. Mao et al (2021) evaluated the spectrum of EGFR mutations in 21,324 patients attending different oncology clinics in China and reported that of the 642 uncommon mutations identified 71% were identified through NGS, 45% by Sanger sequencing and 35% by qPCR. The use of NGS for the detection of mutations in CTC in this study may have increased the probability of detecting more mutations as it is a scanning technique whilst Cobas EGFR mutation test kits detect only a total of 42 mutations. Furthermore, NGS is a very sensitive method for detecting EGFR mutations; this technique is capable of detecting mutations in tumor biopsy specimens with only 5% cellularity. Clinicians and biomedical scientists have advocated for its routine use in the clinics because of its high sensitivity for detecting EGFR mutations (Chen & Zhao, 2019; Chodhury et al 2022).

The benefits of precision diagnosis and/or the consequences of inefficient diagnosis for EGFR mutations on clinical outcomes were also evaluated in this current study. The benefits assessed in this study were response rates and PFS in patients whose EGFR mutational profiles were diagnosed from their CTC enriched sample and matched tissue biopsy samples, but therapies were based on EGFR mutation results obtained from tissue biopsy as this was the current clinical practice at the beginning of the study. The result from the comparative analysis showed that the OR of patients who had an EGFR mutation obtained from their CTC but were stratified to therapies based on EGFR mutation results obtained from tumour biopsy was significantly different from patients whose CTC enriched samples had no EGFR mutation **(Figure 5.5)**. Of the 30 CTC enriched samples positive for EGFR mutation, 20 (66.67%) had PD, but only 1 of these was placed on targeted therapy **(Figure 5.5, Table 5.6**). The high proportion of patients who had an EGFR mutation in their CTCwith PD suggests that patients may have been stratified to therapies not suitable for their mutational needs. Data from several clinical trials have reported that patients with an EGFR mutation receive moderate/no benefit

from standard chemotherapy or immunotherapy (Takano, 2019; Hardstock 2020). This result suggests inefficient precision diagnosis of EGFR mutations.

This study also evaluated overall response rate of patients stratified to chemotherapy and immunotherapy. The results (**Figure 5.6**) showed that there was no significant difference ($P \leq 0.05$) in response rates between patients who had an EGFR mutation placed on chemotherapy or immunotherapy and patients who did not have an EGFR mutation placed on chemotherapy or immunotherapy. Although there was no significant difference between EGFR mutation positive patients on chemotherapy and EGFR mutation negative patient on chemotherapy. Data from this study showed that 75% of EGFR mutation positive patients stratified to chemotherapy had a PD whilst no PD was observed for EGFR negative patients stratified to chemotherapy. This result is consistent with results from other studies that report patients with an EGFR mutation placed on chemotherapy have a moderate response to therapy, whilst patients without the EGFR mutation, placed on chemotherapy, had a better response, whereas patients expressing programmed death ligand 1 (PDL-1) had a better response to immunotherapy. Most of these previous studies involved more than 600 patients (Mok et al 2009; First signal 2012; OPTIMAL, 2015; Rittmeyer et al 2017; Hardstock et al 2020), thus the fact that no statistically significance difference is observed in this study is perhaps due to the relatively small sample size.

There was no statistically significant difference observed in OR between patients with single mutations and patients with a mixed mutation (**Figure 5.7**). These results are inconsistent with reports from other studies that observed better overall response to therapy for patients with a single mutation when compared to mixed mutations (Kobayashi et al 2013; Atilli et al 2022). In these other studies there was rational stratification of patients to therapies to suit their molecular needs. In this current study most patients with a single mutation had an exon 19 deletion. Only 1 out of these patients was stratified to TKI. Patients not stratified to appropriate therapy could be linked to similarity in response rates between patients with a mixed mutation and patients with a single mutation.

This current study also reported that no survival benefit was attained for patients due to "rational stratification" of patients to therapies tailored to their mutational needs.

Stratification of patients to therapy based on EGFR mutation results obtained from their tumour biopsy samples did not result in a PFS benefit (**Figure 5.8 & Table 5.7**). There was no statistically significant difference in PFS between patients whose CTC enriched samples were negative for EGFR mutation and patients whose CTC enriched samples were positive for an EGFR mutation. However, patients negative for an EGFR mutation appeared to have a longer PFS (26 months) when compared to the 10 months observed for EGFR mutation positive patients. Shorter PFS observed for EGFR mutation positive patients could be linked to possibly wrong stratification of patients to therapy not suited for their mutational needs or the existence of concomitant mutations. As explained in the introduction chapter patients with EGFR mutations do not respond well to non TKI therapies and have been reported in several large-scale clinical trials to have shorter PFS with chemotherapy and immunotherapy (ENSURE, 2012; Rittmeyer et al 2017). In addition, the co-existence of other mutations such as KRAS with EGFR mutations has been reported to influence PFS negatively (Chen et al 2020). However, its possible influence on survial outcome in this study cannot be efficiently evaluated as the study did not analyze for other mutations from CTC.

No statistical significance difference in PFS was also observed between patients with no EGFR mutation and patients with an EGFR mutation stratified to chemotherapy or immunotherapy. Even though, there was no statistically significant difference in PFS. Patients who had no EGFR mutation placed on chemotherapy had a longer PFS (14.5 months) vs. 10 months for patients with a mutation. Patients who were negative for an EGFR mutation placed on immunotherapy had a longer PFS of 26 months whilst patients positive for an EGFR mutation had a PFS of 9 months. As stated, earlier patients with EGFR mutations receive little benefit from chemotherapy or immunotherapy whereas patients without an EGFR mutation receive some benefit from standard chemotherapy (Lux-Lung 6 2014; Takano et al 2019). Most clinical trials that have reported a significant difference in PFS when comparing patients with an EGFR mutation placed on TKI and patients placed on chemotherapy and or immunotherapy have involved a larger population (ENSURE, 2012; Lux-Lung 6 2014; Rittmeyer et al 2017; Takano et al 2019; Hardstock et al 2020).

5.5 Conclusion

The results from this study suggest the clinical potential of CTC processed using the Lung card version II microfluidic device for the detection of EGFR mutation and management of patients with NSCLC. However, the present study is limited by sample size and further studies with a larger cohort of patients would be required to explore more thoroughly the clinical potential of CTC+ NGS matrix for detecting EGFR mutations. Future studies would also be required to study the benefits of implementation of this technology for developing precision treatment regimens if utilized routinely in the clinics. Its clinical implications need evaluation requiring single cell analysis.

Chapter 6
Final Discussion

6.0 Discussion

Evidence from numerous clinical studies in NSCLC have shown that EGFR mutations in exon 18-21 are predictors of response to TKI, and this has led to the integration of precision oncology into mainstream clinical practice for the management of these patients (Ideal, 2005; Lux lung 2012; Ensure, 2015). Precision oncology involves molecular profiling of tumours to identify targetable mutations. The success of this approach is highly dependent on the genomic markers used for genomic testing. Any marker used must capture thoroughly the genomic landscape of a malignancy. In addition, it should be relatively accessible so as to allow monitoring of tumour evolution due to tumour progression and/or response to drug use (Schwarzerberg et al 2017; Chedid et al 2022). Another consideration for the success of precision oncology is the sensitivity of the molecular techniques used for testing (Alix-Panabieres, 2021). In the clinics, the diagnostic markers used routinely have not truly met these requirements primarily due to issues with safety associated with re-biopsying to problems with monitoring tumour evolution and only moderate sensitivity in detection of resistance mutation (Oxnard et al 2016; Jenkins et al 2017; Malpelle et al 2020; Chedid et al 2022).

CTC in the blood or other aqueous fluid have been explored in several studies as potential alternatives or additional factors for detecting clinically important mutations. These studies have used disparity in size between the malignant cells and other haematological cells or tumour antigens e.g, EpCAM unique to them for isolation. The results from these studies have shown that CTC are good markers for genomic testing as these cells are accessible (harvested from a simple blood draw) and there is a likelihood of obtaining detailed information on tumour heterogeneity as they originate from both primary and metastatic sites (Nagrath et al 2007; Mahesawaran et al 2008; Park et al 2014; Sunderasan et al 2016; Rushton et al 2021). Despite these positive attributes' utilization of CTC in the clinics for routine use as diagnostic markers for EGFR mutations has been limited by the rarity of these cells. Also, technologies that have successfully isolated CTC from blood cannot be utilized efficiently in the clinics due to cost, laborious/cumbersome workflow for CTC isolation, low throughput, difficulty in reproducibility/scalability of devices for widespread use and poor purity of the CTC isolated. The current study describes the design, optimization and

characterization of an immuno-magnetic based microfluidic device (Lung card version II) that isolates EpCAM positive CTC from blood for downstream analysis for EGFR mutation that can be utilized routinely in the clinic: the current study investigated NSCLC.

The microfluidic device is a 2-part system made up of a disposable PMMA chip and a re-usable microfluidic unit. The disposable chip is simple in design devoid of any intricate architecture or geometry. Its simplicity ensures low cost, scalability and reproducibility of the chip for widespread clinical use. The isolation concept of the device in this current study maximizes capture efficiency by its removal of fluid flow and the use of mobile, external, permanent magnets not merged to the chip or in direct contact with blood to move magnetized anti-EpCAM antibody coated beads systematically across the chip. These mechanisms limit damage to these fragile cells as varying flow rates and joule heating when magnets come in direct contact with blood leads to cell damage. The ease in removal of captured CTC from the device for off chip molecular characterization is another advantage the current unit has over other existing devices. Other devices employ the use of cumbersome chemical and mechanical processes to remove captured CTC from the surface of immobile complex structures. The device/workflow process in this study (**Figure 6.1**) requires a one step process for the removal of captured CTC from chip thus making it user friendly for widespread use in the clinics.

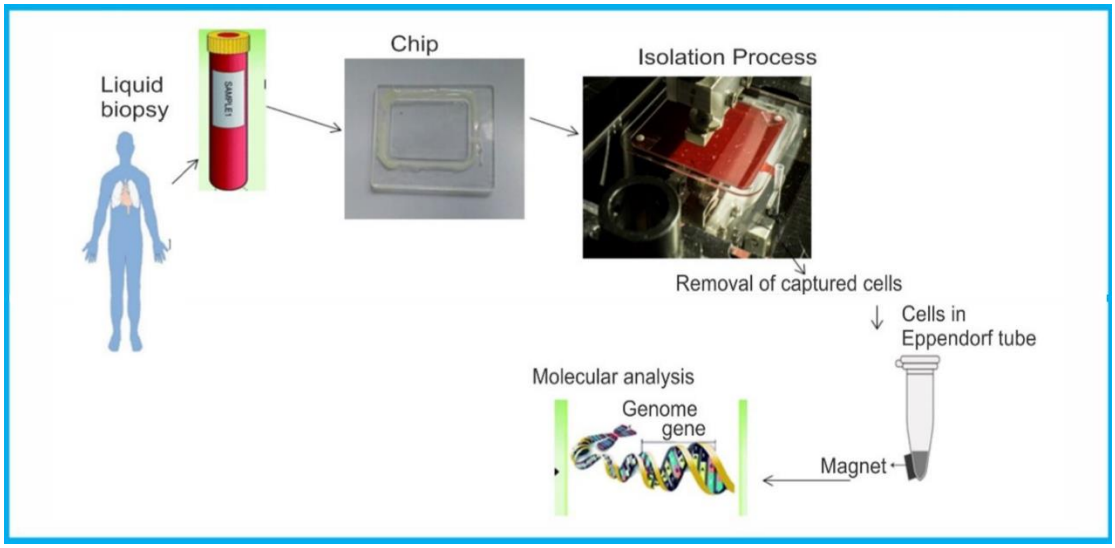

Figure 6.1 Work flow process for CTC as liquid biopsy for molecular characterization for EGFR mutation using Lung card version II device for CTC isolation

The device was evaluated to ascertain its capture efficiency and purity of cells isolated. Results from validation experiments show that capture efficiency of the device was ≥ 80% and ≥ 65% for relatively high EpCAM expressing cell lines spiked in media and sheep blood respectively but was ≤45% for low EpCAM expressing cell lines. Results from validation experiments compared favourably with other immuno-magnetic based microfluidic devices because the device has the capability to isolate EpCAM positive cells in 13 ml of blood in 50 minutes. Other immuno-magnetic based microfluidic devices isolated EpCAM positive cell lines from heterogeneous fluid at rates ranging from 1ml/hr. to 10ml/hr (Sequeist et al 2009; Park et al 2016; Sunderasan et al 2016). In addition, the results also suggest that the use of magnetic beads functionalized with only anti EpCAM antibodies may not be adequate for every type of malignancy especially low EpCAM expressing tumours. For the device to have a wider scope in the clinic for precision oncology, functionalizing magnetic beads with a cocktail of antibodies concurrently with anti-EpCAM antibody will allow for isolation of CTC that are both low and high EpCAM expressing.

The device was also demonstrated to isolate EpCAM positive cell lines singly and in clusters from heterogeneous fluid using fluorescence imaging techniques. Also, purity results of ≥ 97% obtained from validation experiments in this study was better than purity results obtained from all studies of other microfluidic technologies that have employed CTC isolation for downstream analysis. These studies had purity values of 10-70% (Nagrath et al 2007; Muridhalar et al 2014 et al 2016; Sunderasan et al 2016). The ability of the device to preserve the morphology of EpCAM positive cells and the high purity of cells isolated suggests that CTC isolated from body fluids using the device can be used as a tool for research on molecular cancer biology for more insight into tumour heterogeneity and the genomics of metastasis associated with cancer cell clusters.

The utility of the device for use in the clinic as a platform for CTC processing for downstream applications was demonstrated firstly by the capability of the device to isolate EpCAM positive CTC ranging from 3- 500 cells from all CTC enriched patient samples with high purity (≥95%). CTC counts have been reported to be prognostic and predictive markers in breast, prostate and colorectal cancers using cell search device (Descamps et al 2022). Results from this study suggest that CTC isolated using this

device can be enumerated and could be extrapolated and used as predictors of response to therapy. Incorporation of an image analysis algorithm to the device technology/ work flow process would result in the inclusion of enumeration of CTC to its isolation mechanisms. Secondly, the ability to characterize CTC at the genomic and transcriptomic levels further enhances the usefulness, as mutations in exon 18-21 of the EGFR gene was detected. The cancer specific CK7 and Survivin genes were used as two well-established markers known to be commonly upregulated in NSCLC (Yu et al, 2013) to demonstrate the ability fo post-isolation analysis.

The clinical potential of genetic information from CTC to be used as a tool for decision making was evaluated by comparing exon 18-21 mutation obtained from tumour biopsy using Cobas EGFR v2 detection kit with results obtained from matched CTC enriched samples using NGS and assessing clinical outcomes of patients who were stratified to therapies based on mutation results obtained from tumour biopsy. Results from this current study showed that CTC detected significantly more mutations than tumour biopsy. Of the 4 patients positive for an EGFR mutation from tumour biopsy only 1 had a mutation that was in concordance to what was obtained from matched CTC enriched sample. Twenty of the 30 patients whose CTC enriched samples possessed an EGFR mutation had a progressive disease but Only 1of these was stratified to TKI. There was no significant difference in PFS for patients whose CTC enriched samples had no EGFR mutation compared with patients whose CTC had a mutation (Median PFS 26 vs. 10 months *P value=0.3420*, Hazard ratio 0.76 95% CI=0.2498-2.319).

Taken together, data from these results suggest CTC+NGS appear to detect more mutations when compared with tumour biopsy+Cobas EGFR test. The detection of more mutations in CTC could have positive clinical implications such as a simple blood draw can give a more informative mutational profile of the malignancy. Genetic information obtained from CTC could also be useful for real time monitoring to detect disease re-occurrence and development of drug resistance, as it is less invasive. However, before implementation of CTC+ NGS sample+ technique matrix in the clinics for mutation profiling the following issues will have to be addressed (1) false discovery rates due to sequence artifacts (2) do the techniques used for isolation capture CTC such that cells captured are a fair representation of the molecular events ongoing in a malignancy. To address these issues the use of a cock-tail of antibodies for CTC

isolation may be necessary to ensure that cells captured embody genomic/molecular events in a neoplasm. Furthermore, the value of pooled and single CTC analysis would have to be explored for its reliability in detecting true mutations.

Poor clinical outcomes observed for patients who were positive for an EGFR mutation from their CTC enriched samples but, were stratified to therapies based on mutational profile from tissue biopsy and the discordance in mutations reported from CTC enriched samples and biopsy suggest: that mutational profile from one sample matrix may not be sufficient for precision diagnosis to make informed decisions on what therapy to adopt for a patient and that accurate molecular profiling of tumour for precision oncology may involve the integration of genomic data obtained from more than one sample matrix. Currently, as part of an extension of this project a preliminary study on the incidence of exon 18-21 mutations in female breast cancer patients in Nigeria is being undertaken comparing CTC enriched samples and cfDNA sample matrices as diagnostic tools and NGS has been used to screen for mutations. Results so far show that there is discordance in mutation results obtained from CTC and cfDNA. Of the 7 patients evaluated for mutations only 1 patient had a concordance of mutations in CTC and matched cfDNA. This data suggest that genomic information obtained from more than one sample matrix may be essential for accurate molecular profiling of tumours. Furthermore, techniques or bioanalyzers involved in processing these sample matrices for molecular profiling of a cancer must be comprehensive so that any sample matrix used represents accurately the genomic landscape of a malignancy.

6.1 Future Work

The current study demonstrates the clinical utility of an immuno-magnetic based microfluidic device as a platform for processing CTC for subsequent characterization for molecular alterations. The device in the present study shows potential for commercialization for widespread clinical use. However, incorporation of a technology for single CTC isolation and a PCR unit for molecular analysis will further enhance its reliability and cost effectiveness. Integration of single cell analysis to the unit will involve visualization of the cells using a microscope and suctioning single cells using a micropipette and placing them into chambers shown in **Figure 6.2.** At present the cost of isolating CTC from blood of one patient using the device is around £2. However, on inclusion of off chip PCR techniques and/or NGS for molecular characterization to

detect mutations the cost increases to £400- £800 for one patient. Cost effectiveness, and throughput in the clinics can be improved further by incorporating PCR and/or NGS to the device. Integration of PCR techniques to the device will have the following advantages: (1) isolation of CTC and molecular characterization to detect mutations will be less labour intensive as both processes occur on chip in a sequential order; (2) reduced reagent consumption as a result of miniaturization will lead to reduction in cost to about (£20-£100) per patient; (3) reduced time for DNA amplification due to rapid heat transfer and decreased thermal mass, will increase throughput. Amplification of DNA using off chip PCR takes between 1-3 hr., small thermal mass and increased heat transfer rates associated with miniaturization in microfluidic devices will reduce this time by half; and (4) improved portability of the device/work flow as a result of integration of the 2 mechanisms on chip. Future focus will be the design of a microfluidic chip (**Figure 6.2**) with cell trapping chambers of specific dimensions to accommodate precise reagent and sample volumes. Also, micro valves could be incorporated into the chip to control fluid flow and keep manual operation to the barest minimum allowing integration of single cell separation, washing and trapping of cells onto chip for subsequent molecular characterization on chip instead of off chip. Molecular characterization on chip will involve the integration of PCR and or NGS technology into the reusable microfluidic unit such that following isolation of CTC the chip can be transferred via an electromechanical arm to the compartment for PCR or NGS in the microfluidic unit for molecular characterization of CTC isolated. To achieve this the chip will have to be thermo responsive to withstand cyclic changes in temperature characteristic of PCR. **Figure 6.2** shows chip with thermo-responsive tape beneath the chamber for PCR this will help thermal conductivity of PMMA chip to ensure heat transfer into chip.

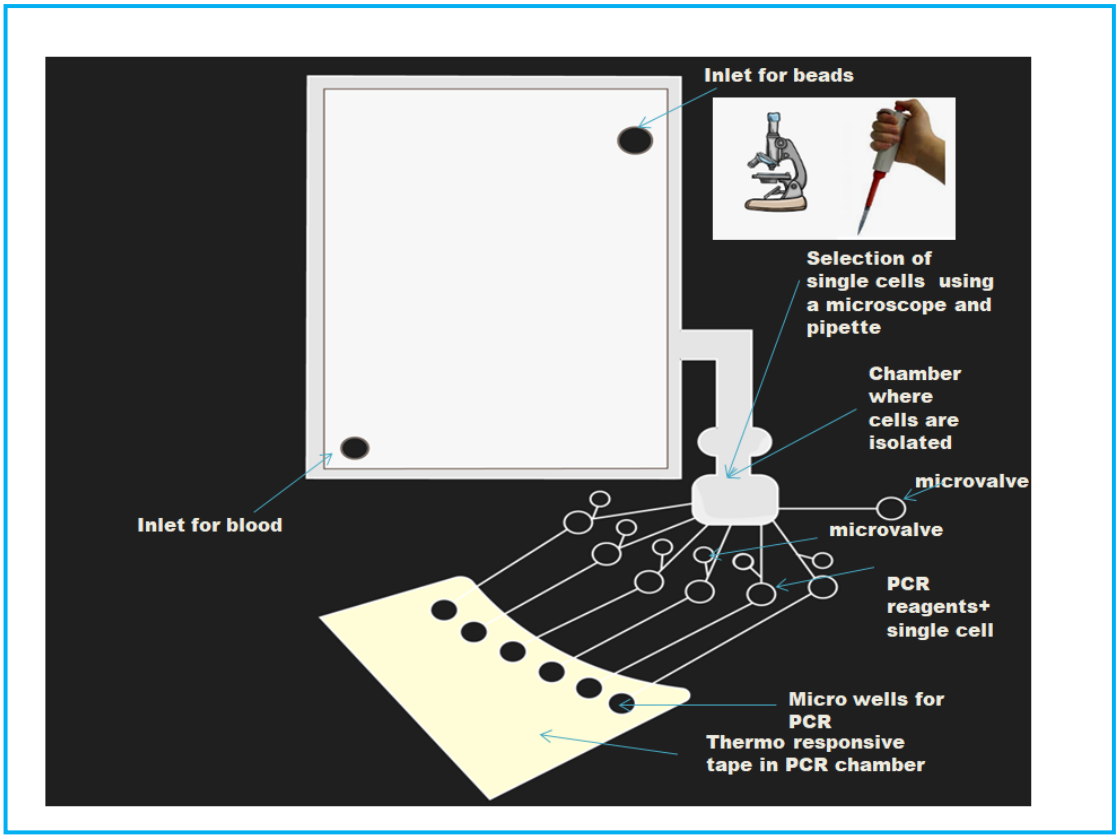

Figure 6.2: schematic representation of proposed integrated chip with microscope and micropipette for visualization and suctioning of single cells and a PCR chamber. Yellow section of chip in diagram shows thermos-responsive tape beneath the microwells for PCR.

Results from validation studies suggest that the device isolates EpCAM positive CTC/cells efficiently. However, low EpCAM expressing cells are isolated less efficiently. Functionalized magnetic beads comprising of anti-EpCAM antibody and other antibodies corresponding to tumour specific antigen will be explored in further studies to ensure that EpCAM expressing cells, Low EpCAM expressing cells and non EpCAM expressing cells can be isolated more efficiently using the device. One potential antibody that could be functionalized with magnetic beads alongside anti-EpCAM is the anti-folate α receptor antibody. Folate receptor alpha antigen binds folic acid and it is highly expressed in solid tumours and minimally expressed in normal cells and hence may be good cellular marker for differentiating cancer cells from normal haematological cells (Zhou et al 2021).

To further confirm the reproducibility of the device in processing CTC for molecular characterization and to explore further the clinical potential of CTC+NGS as a diagnostic tool in precision oncology. Studies involving a larger patient cohort with

lung cancer will need to be undertaken to detect targetable mutations in genes and downstream signaling proteins (e.g., exon 18-21 mutations, mutations in KRAS and BRAF, ALK and ROS-1 re-arrangements) from CTC processed using the Lung card device. Mutation results obtained will be compared with results obtained from tumour biopsy and/or cfDNA. Any discordance in mutations between liquid and tumour biopsies will be investigated by resampling at various time points during the course of the disease to verify if the discrepancies are caused by subclones and/or heterogeneity in bulk tumour tissues.

6.2 Conclusion

This present study describes the design, conceptualization and optimization of an immunomagnetic based microfluidic device that is cost efficient, flexible, easy to use and capable of processing CTC for detection of EGFR mutations with high efficiency and purity with a throughput that, once produced as a commercial unit, would meet the demands of the clinic. This study also demonstrates the utility of CTC processed to be characterized for molecular alterations at the genome and transcriptomic levels. However, integrating a molecular analysis unit into the device would significantly improve its usefulness in the clinic, especially if not requiring skilled technical input. Furthermore, discordance in mutation results obtained from CTC and tumour biopsy suggest that one genetic marker does not give the entire information on molecular events of a malignancy from inception to metastasis and response to treatment. Precise mutation profiling of a malignancy will most probably require information obtained from multiple genetic markers, which can then be correlated with disease response to various treaments.

References

Abaan OD, Polley EC, Davis C, et al. (2013). The exomes of the NCI-60 panel: a genomic resource for cancer biology and systems pharmacology. *Cancer Res*. 73(14):4372-82.

Abedi-Ardekemi B, Ahmad Dar N, Muzaffar Mir M, et al. (2012). Epidermal growth factor receptor (EGFR) mutations and expression in squamous cell carcinoma of the esophagus in central Asia. *BMC Cancer* 12:602 doi; 10.1186//471-2407-12-62.

Aberle M, Adams A, Berg C, et al. (2011). Reduced Lung cancer mortality with low dose computed tomography screening *N. Eng. J Med* Aug (4), 365(5):395-409.

Ackerman A, Goldstein M, Kobayashi S, et al. (2012). EGFR delE709_T710insD: A Rare but Potentially EGFR Inhibitor Responsive Mutation in Non–Small-Cell Lung Cancer. *J. Thoracic Oncol*., 7, e19–e20.

Adams D, Zhu P, Makarova E, et al. (2014). The systemic study of circulating tumor cells isolation using lithographic microfilters. *Resc adv;*9 :4334-42.

Adeniji A, Dawoodu O, Habeeb M, et al. (2020). Distribution of breast cancer subtypes among Nigerian women and correlation to the risk factors and clinicopathological characteristics. *World J Oncol* Aug: 11 (4):165-172.

Adzie J, tweech J, Khakwam A et al (2021). Biomarker testing for people with advanced lung cancer in England. *J. Clin. Resp*. June;2 (6): 100176

Alberg AJ, Ford JG, Samet JM, et al. (2007). Epidemiology of lung cancer: ACCP evidence-based clinical practice guidelines (2nd edition). *Chest* 132 (3 Suppl): 29S-55S.

Allemani C, Weir H, Carreira H, et al (2015). Global Surveillance of cancer survival 1995-20009: analysis of individual data for 25,676,887 patients from 279 population-based registries in 67 countries (CONCORD-21). *Lancet* Mar 14:385(9972):1010 doi: 10.1016/s0140-6736 (14 62038-9 Epub 2014 Nov 28.

Alix-Panabieres C (2021). The future of liquid biopsy. *Nature* Vol.579 No.7800

Annabestani M, Esmaeili-Dokha P, Fardmanesh M (2020). A novel, low cost and accessible method for rapid fabrication of the modifiable microfluidic devices. *Scientific reports 10;16513*

Argyri E, Tsimplaki E, Marketos C, et al (2017). Investigating the role of human papilloma virus in lung cancer. *Papilomavirus Res*; 3:7-10.

Arrieta O, Cardona A, Martin C, et al (2015). Updated frequency of EGFR and KRAS mutations in non small cell lung cancer in Latin America. The Latin America consortium for the investigation of lung cancer (CLIcap). *J of thoracic Oncol.* Vol. 10 Iss 5 pg 838-843.

Ashworth, T.R., (1869). A case of cancer in which cells similar to those in the tumors were seen in the blood after death. *Aust. Med. J.* 14, 146–149.

Attili I, Passaro A, Pisapia P et al (2022). Uncommon EGFR compound mutations in Non small cell lung cancer (NSCLC) a systemic review of available evidence. *Curr.Oncol;* 29:255-266. https://doi.org/10.339011.

Azubike S, Murihead C, Hayes L et al (2018). Rising global burden of breast cancer: the case of Sub-Saharan Africa (with emphasis on Nigeria) and implications for regional development. a review. *World J Surg Oncol*. Mar 22;16 (1):63 doi:10.1186/s12957-018-1345-2.

Baek J, Sun J, Min Y, et al (2015). Efficacy of EGFR tyrosine kinase inhibitors in patients with EGFR mutations non small cell lung cancer except both exon 19 deletion and exon 21 L858R. A retrospective analysis in Korea. *Lung cancer* Feb.:87(2);148-54.

Bakker J., Spitts M., Neefejes J et al (2017). The EGFR odyssey from activation to destruction in space and time. *J cell Sci* 130 (24):4087-4096.

Banko P, Lee S, Nagygyorgy V, et al (2019). Technologies for circulatory tumour cell separation from whole blood. *Journal of haematology and oncology* 12:48 https://:doi.org110.1186/s13045-019-0735-4.

Banno E, Togashi Y, Nakamura Y, et al (2016). Sensitivities to various epidermal growth factor receptor-tyrosine kinase inhibitors of uncommon epidermal growth factor receptormutations L861Q and S768I: What is the optimal epidermal growth factor receptor-tyrosine kinase inhibitor? *Cancer Sci.*, 107, 1134–1140.

Barnfield PC, Ellis PM (2016). Second-Line Treatment of Non- Small Cell Lung Cancer: New Developments for Tumours Not Harbouring Targetable Oncogenic Driver Mutations. *Drugs; 76:1321*-36.

Barriere G, Pietro F, Gallerani G et al (2014). Circulating tumour cells and epithelial mesenchymal and stemness markers: characterization of cell population. *Ann transl Med* Nov;1(11):109

Barta J, Powell C, Wisnivesky J (2019). Global epidemiology of Lung cancer. *Annals of global health* 85(1) pg 8 :http://doi.org.10.5334/aogh.2419.

Behdarvand A, Zamani M, Sadeghi F (2017). Evaluation of Merkel cell polyomovirus in non-small cell lung cancer and adjacent normal cells. *Micropatholog;* 108:21-26 doi: 10.1016/j.micpath.2017.04.033.

Bergethon K, Shaw AT, Ignatius OU, et al (2012). ROS1 rearrangements define a unique molecular class of lung cancers. *J Clin Oncol* 30: 863–870.

Bell DW, Lynch TJ, Haserlat SM, et al (2005). Epidermal growth factor receptor mutations and gene amplification in non-small-cell lung cancer: molecular analysis of the IDEAL/INTACT gefitinib trials. *J Clin Oncol* ; 23: 8081–92.

Bianchi F, Nicassio F, Marzi M, et al (2011). A serum circulating miRNA diagnostic test to identify asymptomatic high-risk individuals with early-stage lung cancer. *EMBO Mol Med.;* 3:495–503. https://doi. org/10.1002/emmm.201100154.

Bissel M, Hines W (2011). Why dont we get more cancer. A proposed role of the microenvironment in restraining cancer progression. *Nat Med:* 17:320-9.

Bitting R, Boomanthan R, Rao C (2013). Development of a method to isolate circulatory tumor cells using mesenchymal based capture *methods:* 64; 129-36.

Blair A, Freeman LB (2006) Lung cancer among nonsmokers. *Epidemiology*. *;* 17(6):601–13.

Bleeker FE, Felicioni L, Buttitta F, et al (2008). *AKT1*^{E17K} in human solid tumours. *Oncogene* 27: 5648–5650.

Blows F, Driver K, Schimdt M, et al (2010). Subtyping of breast cancer by immunohistochemistry to investigate a relationship between sub type and short- and long-term survival: a collaborative analysis of data of 10,159 cases from 12 studies. *Plos Med*. May 25. 7(5): e1000279.

Brenner D, Boffetta P, Duel E, et al (2012). Previous lung disease and lung cancer risk. A pooled analysis from the international lung cancer consortium. America *Journal of Epidem* volume 176 issue 7 pg 573-585 https://doi.org 10.1093/aje kws151.

Budhiarko D, Putra T, Harson A et al (2018). L858R EGFR mutant expression in triple negative luminal and HER 2 breast cancer. *Stem cell oncol* pg 271-277.

Calabuig-Farinas S, Janutus-Lewintre E, Herreros-Pomares A, et al (2016). Circulating tumor cells versus circulating tumor DNA in lung cancer-which one will win? *Trans Lung Cancer Res* ;(5):466-482.

Camidge D, Pao W, & Sequist L (2014). Acquired resistance to TKIs in solid tumours: learning from lung cancer. *Nat Rev Clin Oncol* 11**,** 473–481.

Cancer Genome Atlas Research Network (2012). Comprehensive genomic characterization of squamous cell lung cancers. *Nature; 489*: 519–25.

Cannon-Albright L, Carr SR, Akerleym W (2019). Population-based relative risks for lung cancer based on complete family history of lung cancer. *J Thorac Oncol.* ; 14(7):1184–1191. Doi: 10.1016/j.jtho.2019.04.019

Capuani F, Conte A, Argenzio E, et al (2015). Quantitative analysis reveals how EGFR activation and downregulation are coupled in normal but not in cancer cells. *Nat Commun* 6, 7999.

Cappuzzo F, Hirsch FR, Rossi E, *et al*. (2005). Epidermal growth factor receptor gene and protein and gefitinib sensitivity in non-small cell lung cancer. *J Natl Cancer Inst* 97: 643–655.

Castellonos E, Field F, Horn L (2017). Driven by mutation: The predictive value of mutation subtype in EGFR mutations non small cell lung cancer. *J thorac Oncol* Apr: 12(4):612-623.

Cescon DW, Bratman SV, Chan SM, et al (2020). Circulating tumor DNA and liquid biopsy in oncology *Nat Cancer*, 1 (3), pp. 276-290.

Chan B, Hughes G (2015). Targeted therapy for non-small cell lung cancer: current standards and the promise of the future, *Transl. Lung Cancer Res.* 4 36e54.

Chang Y, Cheng M, Huang K et al (2014). Clinicopathological and prognostic significance of EGFR, KRAS and BRAF mutations in bilary tract carcinomas in Taiwan. *Journal of gastroenterology and hepatology* Vol 29 issue 5 pg 119-25.

Chedid J, Allam S, Chamseddine N et al (2022). Role of circulating tumor DNA and circulating tumor cells in breast cancer: History and updates. *SAGE Open Medicine*. January 2022. doi:10.1177/20503121221077838.

Chen Z, Liu H-B, Yu C-H, et al (2014). Diagnostic value of mutation-specific antibodies for immunohistochemical detection of epidermal growth factor receptor mutations in nonsmallcell lung cancer: a meta-analysis. *PLoS One;* Sep 9; 9: e105940. http://dx.doi.org/10.1371/journal.pone.0105940. E-Collection.

Chen Y. H., Chen S. H., (2000) *Electrophoresis*, 21, 165–170

Chen Y, Zheng L Chen G (2008). Fabrication, modification and application of poly methyl methacrylate microfluidic chip. *Electrophoresis*, 29;1801-1814

Chen K, Yu X, Wang H, et al (2017). Uncommon mutation types of epidermal growth factor receptor and response to EGFR tyrosine kinase inhibitors in Chinese non-small cell lung cancer patients. *Cancer Chemother. Pharm.*, 80, 1179–1187.

Chen M, Zhao H (2019). Next generation sequencing in liquid biopsy: cancer screening and early detection. *Human Genomics* 12 No.4.

Chen H, Liu M, Dai Z et al (2020). Concomitant genetic alterations are associated with response to EGFR targeted therapy in patients with lung adenocarcinoma. *Trans. Lung Res.* Aug: 9 (4) 1225-1234

Cheng Yu, Chiou, H Shen G, et al (2001). The association of human papiloma virus 16/18 infection with lung cancer among non smoking Taiwanese women. *Cancer Res; 61:2799*-803.

Chevallier M, Borgeaud M, Addeo A et al (2021). Oncogenic driver mutations in non small cell lung cancer past present and future. *World J clin oncol* April 24:12(4); 217-237.

Chiu C-H, Yang C-T, Shih J-Y, et al (2015). Epidermal Growth Factor Receptor Tyrosine Kinase Inhibitor Treatment Response in Advanced Lung Adenocarcinomas with G719X/L861Q/S768I Mutations. *J. Thoracic Oncol.* , *10*, 793–799.

Cho H, Kim J, Song H et al (2018). Microfluidic technologies for circulating tumour cells isolation. *Analyst* June 25:143 (13); 2936-2970

Cho JH, Lim SH, An HJ et al (2020). Osimertinib for Patients with Non-Small-Cell Lung Cancer Harboring Uncommon EGFR Mutations: A Multicenter, Open-Label, Phase II Trial (KCSG-LU15-09). *J. Clin. Oncol,* 38, 488–495.

Chodhury Y, Tan M, Shi J et al (2022). Complementing tissue testing with plasma mutation profiling improves therapeutic decision making for patients with lung cancer. *Front med (Lausanne)* 9:758464 doi 10.3389/fmed2022.758464.

Chou T, Chiu L, Li L et al (2005). Mutations in the tyrosine kinase domain of epidermal growth factor receptor is a predictive and prognostic factor for gefitinib treatment in patients with Non small cell lung cancer. *Clin Cancer Res* 11(10) pg 3750-3257.

Chudasama D, Barr J, Besson J et al (2017). Detection of circulatory tumour cells and survival of patients with non small cell lung cancer. *Anti Cancer Res*.37:169-174.

Chung KY, Shia J, Kemeny NE, et al (2005). Cetuximab shows activity in colorectal cancer patients with tumors that do not express the epidermal growth factor receptor by immunohistochemistry. *J Clin Oncol.;* 23:1803–1810.

Chun K-P, Wu S-G, Wu J-Y. et al (2012). Clinical Outcomes in Non-Small Cell Lung Cancers Harboring Different Exon 19 Deletions in EGFR. *Clin. Cancer Res.*, 18, 3470–3477.

Cobas EGFR Mutation Test v2. 2016. Available Online: http://www.fda.gov/Drugs/InformationOnDrugs/ApprovedDrugs/ucm504540.htm.

Cohen S, Punt C, Iannoti N et al (2008). Relationship of circulating tumour cells to tumour response progression free survival and overall survival in patients with metastatic colorectal cancer. *J clin Oncol*. Jul: 26(19):3213-21.

Conte A., Sigsmund, S (2016) Control of EGFR Endocytosis and Signaling. Programme. *Mol. Biol. Transl. Sci.* 141,225-276.

Cooper W, David C, Lam L, O'Toole S, Minna J (2013). Molecular biology of Lung Cancer. *J Thorac Dis*; 5(S5): S479-490.

Cortez-Funes H, Gomez C, Rosell R, et al. (2005). Epidermal growth factor receptor activating mutations in Spanish gefitinib-treated non-small-cell lung cancer patients. Ann Oncol 16: 1081–1086.

Costa D.B (2016). Kinase inhibitor-responsive genotypes in EGFR mutated lung adenocarcinomas: Moving past common point mutations or indels into uncommon kinase domain duplications and rearrangements. *Transl. Lung Cancer Res. 5*, 331–337.

Cote M, Liu M, Bonasi S, et al (2012). Increased risk of lung cancer in individuals with a family history of the disease. A pooled analysis from the international lung consortium *Eur J cancer* Sep: 48 (13):1957-1968.

Couraud S, Vaca-Paniagua F, Villar S, et al (2014). Noninvasive diagnosis of actionable mutations by deep sequencing of circulating free DNA in lung cancer from never-smokers: a proof-of-concept study from BioCAST/IFCT-1002. *Clin Cancer Res; 20*: 4613-24.

Cowley G, Smith J, Guterson B (1986). Increased EGF receptors in human squamous carcinoma cell lines. *Br.J. Cancer* 53, 223-229.

Cristofanilli M, Budd GT, Ellis MJ, et al (2004). Circulating tumor cells, disease progression, and survival in metastatic breast cancer. *N Engl J Med* 351, 781– 791.

Crossbie P.A, Shah R, Krysiak P, *et al* (2016). Circulating tumor cells detected in the tumor-draining pulmonary vein are associated with disease recurrence after surgical resection of NSCLC**.** *J. Thorac. Oncol.* 11 pp. 1793-1797.

Cymer F, Schneider D (2010). Transmembrane helix-helix interactions involved in ErbB receptor signaling. *Cell Adhes. Migr.* 2010, 4, 299–312.

de Bono JS, Scher HI, Montgomery RB et al (2008). Circulating tumour cells predict survival benefit from treatment in metastatic castration resistance prostate cancer. *Clin cancer Res*. Oct: 14(19):6302-9 doi: 10.1159/1078-0432.CCR-08-0872

de Olivera T, Do Amaral C, De Franca et al (2018). Prescence and activity of HPV in primary lung cancer. *J Cancer Res Clin oncol*; 44(12):2367-2376.

Dejima H, Linuma H, Kanaoka R, et al (2017). Exosomal microRNA in plasma as a non-invasive biomarker for the recurrence of non small cell lung cancer. *Oncol Let 113* pg 1256-1263.

Descamps L, Le roy D, Deman A. (2022) Microfluidic based technologies for CTC isolation:A review of 10 years of intense efforts towards liquid biopsy. *Int.J. Mol Sci* 23;1981://doi.org110.3390ijms23041981.

Di Fiore P.P, Pierce J.H, Fleming T.P, et al (1987). Overexpression of the human EGF receptor confers an EGF-dependent transformed phenotype to NIH 3T3 cells. *Cell* vol 51 issue 6 pg1063-1070.

Ding X, Chen Y, Yang J, et al (2018). Characteristics of familial lung cancer in Yunnan-Guizhou plateau of China. *Front Oncol*; 8 (637):1–10. doi: 10.3389/fonc.2018.00637.

Dizdar L, Fluegen G, Dalum G et al (2019). Detection of circulating tumour cells in colorectal cancer patients using the GILUPI CellCollector. Results from a prospective single centre study. *Molecular Oncol* 13; 1548-1558.

Dominion I, Imprector A, Rovere F, et al (2000). Stage 1 non small cell lung carcinoma. Analysis of survival and implications for screening *Cancer:* 89:2334-44.

Douillard JY, Ostoros G, Cobo M, et al (2014). Gefitinib treatment in EGFR mutated Caucasian NSCLC: circulating-free tumor DNA as a surrogate for determination of EGFR status. *J Thorac Oncol; 9:1345*-53.

Doward D, Walsh K, Oniscu A, et al (2017). Molecular pathology of non small cell lung cancer. *Diagnostic Histopathology* (23):10 pg 450-456.

Du Z, Brown B, Kim S et al (2021). Function analysis of oncogenic EGFR kinase domain duplication reveals insights into activation and a potential approach for therapeutic targeting. *Nature communications* (12):1382 https://doi.org/10.1038/s41467-021-21613-6.

Dublin S & Griffin D (2020). Cancer in non-smokers. *MO med* Jul-Aug 117 (4): 375-379.

Dutt A, Ramos AH, Hammerman PS, et al (2011). Inhibitor-sensitive *FGFR1* amplification in human non-small cell lung cancer. *PloS One* 6: e20351 doi: 10.1371/journal.pone.0020351.

Drilon A, Rekhtman N, Arcila M, et al (2016). Cabozantinib in patients with advanced RET-rearranged non-small-cell lung cancer: an open-label, single-centre, phase 2, single-arm trial. *Lancet Oncol* ;17:1653-60.

Durendez-Saez E, Azkarate A, Meri M, et al (2017). New insights in non small cell lung cancer: circulating tumor cells and cell free DNA. *J Thorac Dis; 9 (*suppl13): S1332-S1345.

Dutt A, Ramos AH, Hammerman PS, et al (2011). Inhibitor-sensitive FGFR1 amplification in human non-small cell lung cancer. PLoS One; 6: e20351.

Earhart CM, Hughes CE, Gaster RS, et al (2014). Isolation and mutational analysis of circulating tumor cells from lung cancer patients with magnetic sifters and biochips. *Lab Chip*. 14: 78–88. https://doi.org/10.1039/c3lc50580d.

Eberhard DA, Johnson BE, Amler LC, *et al*. (2005). Mutations in the epidermal growth factor receptor and in KRAS are predictive and prognostic indicators in patients with non-small-cell lung cancer treated with chemotherapy alone and in combination with erlotinib. *J Clin Oncol* 23: 5900–5909.

Endres, N.F.; Barros, T.; Cantor, A.J, et al (2014) Emerging concepts in the regulation of the EGF receptor andother receptor tyrosine kinases. *Trends Biochem. Sci.* 39, 437–446.

Ettinger DS, Aisner DL, Wood DE, et al (2018). NCCN guidelines insights: non-small cell lung cancer. *J Natl Compr Canc Netw.* 16:807–21. doi:10.6004/jnccn.2018.0062.

Evans M, O'Sullivan B, Smith M, et al (2020). Large-Scale EGFR Mutation Testing in Clinical Practice: Analysis of a Series of 18,920 Non-Small Cell Lung Cancer Cases. *Pathol Oncol Res,* 25, 1401–1409.

Fares, J, Fares, M, Khachfe H, et al (2020). Molecular principles of metastasis: a hallmark of cancer resistance. *Signal transduction and targeted therapy* 5 article number 28

Fernades M, Sousa C, Jacob M, et al (2021). Resistance profile of osimertinib in pre treated patients with EGFR T790M mutated non small cell lung cancer. *Front.Oncol.* May 6; 11:602924 doi: 10.3389.

Ferreira M, Ramani V, Jeffery S et al (2016). Circulating tumour cells technologies. *Mol Oncol*: 10 (3); 374-394

Ferreira J, Castro F, Rocha F, et al (2018). Protein crystallization in a droplet based microfluidic device. Hydrodynamic analysis and study of the phase behaviours. *Chemical Engineering Sciences* vol 19 pg 232-244.

Field W, Withers F (2012). Occupational and Environmental causes of cancer. *Clin Chest Med.* December; 33(4): doi: 10.1016/j.ccm.2012.07.001.

Fisher J, Tait D, Garett-Mayer E, et al (2020). Cetuximab in patients with breast cancer, non small cell lung cancer and ovarian cancer without KRAS, NRAS or BRAF mutations. Results from the targeted agents and profiling utilization registry (TAPUR) study. *Targeted Oncol*. 15,733-741.

Fleuchacker M, Rolke H, Oerding C, et al (2015). Invitro and invivo application of the GILUPI Cellcollector system for the isolation and characterization of circulatory tumour cells (CTC's) in lung cancer patients. *Eur Resp Journal v*ol 46 issue suppl 59 pA526: doi 10.1183/13993003 congress-2015PA526.

Foss KM, Sima C, Ugolini D, et al (2011). MiR-1254 and miR-574-5p: serum-based microRNA biomarkers for early-stage non-small cell lung cancer. *J Thorac Oncol.;* 6:482–8. https://doi.org/10.1097/ JTO.0b013e318208c785.

Fogh J and Trempe G (1975). New human tumor cell lines. In: J. Fogh (ed.). Human Tumor Cells in Vitro, pp. 115-141. New York: Plenum Press,

Frega S, Lorenzi M, Fassan M, et al (2017). Clinical features and treatment outcome of non-small cell lung cancer (NSCLC) patients with uncommon or complex epidermal growth factor receptor (EGFR) mutations. *Oncotarget*, 8, 32626.

Fu M, Zhang W, Shen L et al (2014). Mutation status of somatic EGFR and KRAS genes in Chinese patients with prostrate cancer. *Virchows Arch: an international journal of Pathol*; 464(5):575-81.

Gatzemier U, Pluzanska A, Szczesna A, et al (2007). Phase III study of erlotinib in combination with cisplatin and gemcitabine in advanced non small cell lung cancer: The Tarceva Lung Cancer Investigation Trial. *J. clin Oncol.* April 20:25(12):1545-52.

Gerlinger M, Rowan AJ, Horswell S, et al (2012). Intratumor heterogeneity and branched evolution revealed by multiregion sequencing. *N Engl J Med; 366:883*-92.

Gheit T, Munoz J, Levicen J, et al (2012). Merkel cell polyomavirs in non small cell lung carcinoma from Chile. *Exp Mol pathol*: 93(1): 162-166.doi: 10.1016/j.exp.2012.04.008.

Giaccone G, Herbst RS, Manegold C, et al (2004). Gefitinib in combination with gemcitabine and cisplatin in advanced non-small-cell lung cancer: a phase III trial–INTACT 1. *J Clin Oncol* 22(5):777-784, 2004.

Gody-Oritz A, Sanchez-Munoz A, Chica Parrado M et al (2019). Deciphering HER2 breast cancer disease: Biological and Clinical Implications. *Front Oncol* Oct 29; (9):1124 doi:10.3389/fonc.2019.01124.

Gonzalez-Manzano R, Martinez-Navarro E, Eugenieva E et al (2008). A novel EGFR nonsense mutation in non small cell ling cancer (NSCLC) patient who did not derive any clinical benefit from combination with chemotherapy and erlotinib. *Clin Transl Oncol* Jul; 10(7):442-4.

Gote v, Nvokola A, Boka P et al (2021). Drug resistance in metastatic breast cancer. Tumour targeted nanomedicine to the rescue. *Int J mol Sci* 22(9):4673.

Goto K, Ichinose Y, Ohe Y, et al (2012). Epidermal growth factor receptor mutation status in circulating free DNA in serum: from IPASS, a phase III study of gefitinib or carboplatin/ paclitaxel in non-small cell lung cancer. *J Thorac Oncol* 7:115-21.

Graham RP, Treece AL, Lindeman NI, et al (2018). Worldwide frequency of commonly detected EGFR mutations. *Arch Pathol Lab Med*; 142:163–7

Gray M, Meehan J, Sullivian P et al (2019). A unique model to improve lung cancer research. *Front Oncol;*9:335doi: 10.3389/fonc.2019.00335.

Gridelli C, Rossi A, Carbone DP, et al (2015). Non-small-cell lung cancer. *Nat Rev Dis Primer* 2015; 1: 15009.

Grob TJ, Heilenkötter U, Geist S, et al (2012). Rare oncogenic mutations of predictive markers for targeted therapy in triple-negative breast cancer. *Breast Cancer Res Treat.;* 134:561–567

Guan X, Li C, Li Y et al (2021). Epithelial-Mesenchymal-transition like circulating tumour cell association white blood cells clusters as a prognostic biomarker in HER positive/HER2- negative breast cancer, *Front oncol*. https;//doi.org/10.3389/fonc 2021;662222

Gullick WJ, Marsden JJ, Whittle N, et al (1986). Expression of epidermal growth factor receptors on human cervical, ovarian, and vulval Carcinomas. *Cancer Res*., 46, 285–292.

Guo P, Pu T, Chen S, et al (2017). Breast cancers with EGFR and HER" co amplification favours distant metastasis and poor clinical outcomes. *Oncol Lett* 14(6):6562-6570.

Guo Y, Cao R, Zhang X, et al (2019). Recent progress in rare oncogenic drivers and targeted therapy for non small cell lung cancer. *Onco. Targets Ther.* Nov. 28;12: 10343-10360.

Gusterson B, Cowley G Smith J et al (1984). Cellular localisation of human epidermal growth factor receptor. *Cell biology reports* vol.8 iss.8 pg 649-658.

Habili Z, Al chama W, Saab R et al (2020). Circulatory tumour cell detection technologies and clinical utility: challenges and opportunities. *Cancers 12 1930;* doi; 10.3390/cancers 12071930.

Hardtstock F, Myers D, Li T, Cizova D, Maywald U, Wilke T, et al. (2020). Real-World Treatment and Survival of Patients with Advanced Non-Small Cell Lung Cancer: A German Retrospective Data Analysis. *BMC Cancer* 20(1):260

Han SE, Kim TY, Hwang PG, et al (2005). Predictive and prognostic impact of epidermal growth factor receptor mutation in non-small cell lung cancer patients treated with gefitinib. *J Clin Oncol* 23: 2493–2501.

Han J, Park K, Kim S et al (2012). First-SIGNAL first-line single agent Iressa versus gemcitabine and ciaplatin trial in never smokers with adenocarcinoma of the lung. *J clin Oncol.* April 1 30(10):1122-8.

Han X, Junyan W, Sun Y (2017). Circulating Tumor DNA as biomarkers for cáncer detection. *Genomics proteomics Bioinformatics* 15:59-72.

Han B, Tjulandin S, Hagiwara K, et al (2017). EGFR mutation prevalence in Asia-Pacific and Russian patients with advanced NSCLC of adenocarcinoma and non-adenocarcinoma histology: The IGNITE study. *Lung Cancer*. 113:37–44.

Hanjani M, Wilson G, Mcgraham N, et al (2017). Tracking the evolution of non-small cell lung cancer. *NEJM* vol 376 2109-21.

Hardstock F, Myers D, Li T, et al. (2020) Real-World Treatment and Survival of Patients with Advanced Non-Small Cell Lung Cancer: A German Retrospective Data Analysis. *BMC Cancer* 20(1):260

Hasegwa Y, Ando M, Kubo A, et al (2014). Human Papiloma virus in non small cell lung cáncer in never smokers a sytemic review of literatura. *Lung Cancer* 83;8-13.

Hashim A, Naz S, Hashim S et al (2019). Epidermal growth factor receptor over expression in triple negative breast cancer: association with clinico pathological features and prognostic parameters. *Surgical & experimental Pathol* 26. https://doi.org/10.1186/S4207-018-0029-0.

Hashimoto M., Barany F., Soper, S. A., (2006) *Biosens. Bioelect*, 21, 1915–1923

Heigener DF, Schumann C, Sebastian M, et al (2015). Afatinib in Non-Small Cell Lung Cancer Harboring Uncommon EGFR Mutations Pretreated with Reversible EGFR Inhibitors. *Oncologist* 20, 1167–1174.

Herbst R, Prager D, Herman R et al (2004). TRIBUTE- A phase III trial of erlotinib HCL (OSI-774) combined with carboplatin and paclitaxel (CP) chemotherapy in advanced non small cell lung cancer. *J clin Oncol* 22(14_suppl) 7011-7011 doi: 10.1200/jco2004 2214_suppl 7011.

Heitzer T, Auer M, Gasch C et al (2013). Complex tumour genomes inferred from simple circulating tumour cells by arrat CGH and next generation sequencing. *Cancer Res*. May 15:73 (10):2965-75

Hiley C, Quesne J, Santis G, et al (2016). Challenges in molecular testing in Non-Small Cell Lung Cancer patients with advanced disease. *The lancet,* vol 388 Sept 3 2016.

Hirose T, Murata Y, Oki T, et al (2012*).* Relationship of circulating tumor cells to the effectiveness of cytotoxic chemotherapy in patients with metastatic non-small-cell lung cancer *Oncol Res,* 20 (2012), pp. 131-137.

Ho C, Tong K, Ramsden K et al (2015). Histological classification of non small cell lung cancer over time reducing the rates of not otherwise specified. Curr Oncol June: 22(3): e164-e170.

Hong, C, Funk, C Whiteside T (2017), Isolation of biologically active exosomes from plasma of patients with cancer, *Meth. Mol. Biol.* 1633 257e265
Hosokwa M, Hayata T, Fukuda Y et al (2010). Size selective micro cavity array for rapid and efficient detection of circulatory tumour cells. *Anal Chem* Aug 1:82(15):6629-38.

Hou HW, Warkhiani ME, Khoo BL, et al (2013). Isolation and retrieval of circulating tumor cells using centrifugal forces. *Sci Rep.* https://doi.org/10.1038/srep01259.

Hsieh M, Fang Y, Chang W, et al (2006). Complex mutation patterns of epidermal growth factor receptor gene associated with variable responses to gefitinib treatment in patients with non small cell lung cancer. *Lung Cancer* 53,311-322.

Hsu J, Hung M (2016). The role of HER2, EGFR and other receptor tyrosine kinase in breast cancer. *Cancer metastasis rev* Dec; 35 (4):575-588.

Hsu L, Chu N, Kao S, et al (2017). Estrogen, Estrogen receptor & lung cancer. *Int. J Mol. Sci.* Aug 5; 18(8) E1713 doi: 10.3390 iijms 18081713.

Hu Y, Ren S, He Y, et al (2020). Possible oncogenic viruses associated with lung cancers. *Onco targets Ther* 13.10651-10666.

Huang Z, Wang Z, Bai H, et al (2012). The detection of EGFR mutation status in plasma is reproducible and can dynamically predict the efficacy of EGFR-TKI. *Thoracic Cancer;* 3:334-40.

Huang S, Liu H, Li L, et al (2004). High frequency of epidermal growth factor receptor mutation with complex pattern in non small cell lung cancer related to gefitinib responsiveness in Taiwan. *Clinical Cancer Res*. Vol 10 8195-8203.

Hubers A, Prinsen C, Sozzi G, et al (2013). Molecular sputum analysis for the diagnosis of lung cancer. Britsh Journal of cancer *109:530-537*

IARC Monographs on the Evaluation of Carcinogenic Risks to Humans. A review of human Carcinogens: Radiation. 2012;
vol.100D:341:http://monographs.iarc.fr/ENG/Mono
graphs/vol100D/mono100D-9.pdf.

Ignatidis M, Dawson S (2014). Circulating tumour cells and circulating tumour DNA for precisin medicine dream or reality. *Ann Oncol*. Dec 25 (12):2304-2313

Iliescu C, Taylor H, Avram M et al (2012). A practical guide for the fabrication of microfluidic deices using glass and silicon. *Biomicrofluidics* Mar 6; 6(1)16505-1650516

Inoue A, Suzuki T, Fukuhara T, et al (2006). Prospective Phase III study of gefitinib for chemotherapy naïve patients with advanced non small cell lung cancer with epidermal growth factor receptor gene mutations. *J clin Oncol.* Jul 20; 24(21) 3340-6.

Inoue A, Kobayashi K, Maemondo M et al (2013). Updated overall survival results from a randomized phase III trial comparing gefitinib with carboplatin paclitaxel for chemonaive non small cell lung cancer with sensitive EGFR gene mutations (NEJ 002). *Ann. Oncol*.Jan:24(1):54-9.

Ishii H, Azuma K, Sakai K, et al (2015). Digital PCR analysis of plasma cell-free DNA for non-invasive detection of drug resistance mechanisms in EGFR mutant NSCLC: Correlation with paired tumor samples. *Oncotarget 6,* 30850–30858.

Isobe K, Hata Y, Kobayashi K, et al (2012). Clinical significance of circulating tumor cells and free DNA in non-small cell lung cancer *Anticancer Res*, 32, pp. 3339-3344.

Jackman DM, Yeap BY, Sequist LV, *et al*. (2006). Exon 19 deletion mutations of epidermal growth factor receptor are associated with prolonged survival in non-small cell lung cancer patients treated with gefitinib or erlotinib. *Clin Cancer Res* 12: 3908–3914.

Jänne PA, Johnson BE. (2006). Effect of epidermal growth factor receptor tyrosine kinase domain mutations on the outcome of patients with non-small cell lung cancer treated with epidermal growth factor receptor tyrosine kinase inhibitors. *Clin Cancer Res* 12 (14 Suppl): 4416s–4420s.

Janne P, Wang X, Socinski M et al (2012). Randomized phase II trial or erlotinib alone or with carboplatin and paclitaxel in patients who were never or light former smokers with advanced lung adenocarcinoma. CALGB30406 trial. *J Clin Oncol.* Jun 10; 30(17):2063-9.

Jänne PA, Smith I, McWalter G, et al (2015). Impact of KRAS codon subtypes from a randomised phase II trial of selumetinib plus docetaxel in KRAS mutant advanced non-small-cell lung cancer. *Br J Cancer; 113:199*-203.

Ji H, Li D, Chen L et al (2006). The impact of human EGFR kinase domain on lung tumorigenesis and invivo sensitivity to EGFR targeted therapies. *Cancer cell Jun;* 9(6):485-95.

Ji J, Aredo JV, Piper-Vallillo A, et al (2020). Osimertinib in non-small cell lung cancer (NSCLC) with atypical EGFR activating mutations: A retrospective multicenter study. *J. Clin. Oncol.* Vol 38 issue 15 9570. DOI:10.1200/jco.2020.38.15_suppl9570.

Jiang W, Wang X, Zhang C et al (2020). Expression and clinical significance of MAPK& EGFR in triple negative breast cancer. *Oncol Lett* 19(3):1842-1848.

Jenkins S, Yang JC, Ramalingam SS, et al (2017). Plasma ctDNA analysis for detection of the EGFR T790M mutation in patients with advanced non-small cell lung cancer. *J Thorac Oncol*; 12(7):1061–70.

Juan O, Vidal J, Gisbert R, et al (2014). Prognostic significance of circulating tumor cells in advanced non-small cell lung cancer patients treated with docetaxel and gemcitabine. *Clin Transl Oncol; 16:637-43.*

Kadara, H, Scheet P, Wistuba I, et al. (2016). Early events in the Molecular Pathogenesis of Lung Cancer. *Cancer Prev. Res. (phila)* Jul; 9 (7):518-27.

Kalemkerian GP, Narula N, Kennedy EB, et al (2018). Molecular testing guideline for the selection of patients with lung cancer for treatment with targeted tyrosine kinase inhibitors: American Society of Clinical Oncology Endorsement of the College of American Pathologists/International Association for the Study of Lung Cancer/Association for Molecular Pathology Clinical Practice Guideline Update. *J Clin Oncol* 36:911–9. doi: 10.1200/JCO.2017.76.7293.

Kancha RK, Bubnoff NV, Peschel C, et al (2009). Functional Analysis of Epidermal Growth Factor Receptor (EGFR) Mutations and Potential Implications for EGFR Targeted Therapy. *Clin. Cancer Res.*, 15, 460–467.

Kancha, R.K.; Peschel, C.; Duyster, J et al (2011). The Epidermal Growth Factor Receptor-L861Q Mutation Increases Kinase Activity without Leading to Enhanced Sensitivity toward Epidermal Growth Factor Receptor Kinase Inhibitors. *J. Thoracic Oncol.* , 6, 387–392.

Karlovich C, Goldman JW, Sun JM, et al (2016). Assessment of EGFR mutation status in matched plasma and tumor tissue of NSCLC patients from a phase I study of rociletinib (CO-1686). *Clin Cancer Res*.; 22 (10):2386–95.

Kato T, Koriyama C, Khan N et al (2012). EGFR Mutations and Human Papiloma Virus in Lung Cancer. *Lung Cancer*: 78(2); 144-147.

Kamai, H, Akira I, Washiya K, et al (2005). Estrogen receptors α andβ are prognostic factors in Non small cell lung cancer. *Clin Cancer Res.* Jul 15:11(14):5084-9.

Kanagal-Shamanna R, Portier BP, Singh RR, et al (2014). Next-generationsequencing-based multi-gene mutation profiling of solid tumors using fine needle aspiration samples: promises and challenges for routine clinical diagnostics. *Mod Pathol* ; 27: 314–27.

Karachaliou N, Mayo-de las Casas C, Queralt C, et al (2015). Association of EGFR L858R Mutation in Circulating Free DNA with Survival in the EURTAC Trial. *JAMA Oncol; 1:149*-57.

Karachaliou, N, Sosa A, Molina M, Puiz M (2017). Possible application of circulatory free tumor DNA in non small cell lung cancer patients. *J thorac Dis; 9* (suppl13): S1364-S1372.

Karlovich, C., Goldman, J., Sun, J., et al (2016). Assessment of EGFR Mutation Status in Matched Plasma and Tumor Tissue of NSCLC Patients from a Phase I Study of Rociletinib (CO-1686). *Clin Cancer Res* 22, 2386–2395.

Kawai H, Ishii A, Washiya K, et al (2005). Estrogen receptors α andβ are prognostic factors in non small cell lung cancer. *Clinical cancer Res.* 11(14) 5084-5089.

Kawachi A, Colmet-Daie C, Dayris T et al (2019).1965P comparison of molecular profiles between primary tumour and matched metastasis in non-small cell lung cancer. *Annals of Oncology* vol 30 suppl 5 pg 789-790

Ke Z, Lin M, Chen J-F, et al (2014). Programming thermoresponsiveness of nanovelcro substrates enables effective purification of circulating tumor cells in lung cancer patients. *ACS Nano ;* 9, 62–70.

Keam B, Kim D-W, Park JH, et al (2013). Rare and complex mutations of epidermal growth factor receptor, and efficacy of tyrosine kinase inhibitor in patients with non-small cell lung cancer. *Int. J. Clin. Oncol* 19, 594–600.

Keup C, Benyaa K, Hauch S et al (2020). Targeted deep sequencing revealed variants in cell free DNA of hormone receptor positive metastatic breast cancer patients. *Cell Mol Life Sci.* Feb; 77(3):497-509.

Keup C, Kimmig R, Kasimi-Bauer S (2022). Multimodality in liquid biopsy: does a combination uncover insights undetectable in individual blood analytes. *Laboratorium medizini* https://doi.org/10.1515/labmed-2022-0009.

Khalili K, Del Valle L, Otte J, et al (2003). Human neurotropic polyomavirus, JCV, and its role in carcinogenesis. *Oncogene*. 22 (33):5181–5191.

Kim ST, Sung JS, Jo UH, et al (2013). Can mutations of EGFR and KRAS in serum be predictive and prognostic markers in patients with advanced non-small cell lung cancer (NSCLC)? *Med Oncol; 30:328.*

Kim Y, Kim J, Lee HD, et al (2013). Spectrum of EGFR gene copy number changes and KRAS gene mutation status in Korean triple negative breast cancer patients. *PLoS One.;* 8: e79014

Kim A, Jang M, Lee S et al (2017). Mutations of the epidermal growth factor receptor gene in triple negative breast cancer. *Journal of breast cancer*. June: 150-159

Kim H, Kim BH, Lee D et al (2019). Genomic alterations in signet ring and mucinous colorectal carcinoma. *Pathology research and practice* 215 (10):152566

Kim TH, Lim M, Park J, et al (2017). FAST: size-selective, clog-free isolation of rare cancer cells from whole blood at a liquid-liquid interface. *Anal Chem.; 89:1155*–62.

Kim EY, Cho EN, Park HS, et al (2016). Compound EGFR mutation is frequently detected with co- mutations of actionable genes and associated with poor clinical outcome in adenocarcinoma. *Cancer Bio Ther* Mar, 17(3); 237-245.

Kim H, Kim BH, Lee D et al (2019). Genomic alterations in signet ring and mucinous pattered colorectal carcinoma. *Pathol Res Prac* Oct 215(10):152566.

Klughammer, B., Brugger, W., Cappuzzo, F., et al (2016). Examining Treatment Outcomes with Erlotinib in Patients with Advanced Non–Small Cell Lung Cancer Whose Tumors Harbor Uncommon EGFR Mutations. *J. Thoracic Oncol.* , 11, 545–555.

Kobayashi S, Canepa HM, Bailey AS, et al (2013). Compound EGFR mutations and response to EGFR tyrosine kinase inhibitors. *J. Thorac. Oncol. , 8, 45–51.*

Kowalik A, Kowalewska M, Stanislaw G, (2017). Current approaches for avoiding the limitations of circulating tumor cells detection methods-implications for diagnosis and treatment of patients with solid tumors. *Translational Research* vol 185 pg59-84.

Koyi H, Johansson L, From J, et al (2015). Biopsy testing in an inoperable non small cell lung cancer population a retrospective real-life study in Sweden. *J thoracic Dis* 7 (12):2226-2233.

Krebs M, Hou T, Ward T, et al (2010). Circulating tumour cells: their utility in cancer management and predicting outcomes. *Ther. Adv Med Oncol* Nov: 2 (6):351-365

Krebs MG, Sloane R, Priest L, et al (2011). Evaluation and prognostic significance of circulating tumor cells in patients with non-small-cell lung cancer. *J Clin Oncol; 29:1556*-63.

Krebs M, Hou J, Sloane R et al (2012). Analysis of circulatory tumour cells in patients with non small cell lung cancer using epithelial marker dependent and independent approaches. *J of thorac. Oncol.* Vol.7 issue 2 pg 306-315.

Kuan F, Kuo L, Chen M, et al (2015). Overall survival benefits of first line EGFR tyrosine kinase inhibitors in EGFR mutated non small cell lung cancer. A systemic review and meta-analysis. *Br. Journal of Cancer* 113; 1519-1528.

Kukita Y, Uchida J, Oba S, et al (2013). Quantitative identification of mutant alleles derived from lung cancer in plasma cell-free DNA via anomaly detection using deep sequencing data. *PLoS ONE; 8*(11): e81468.

Kulasinghe A, Kapeliekis J, Cooper C et al (2019). Phenotypic characterization of circulating lung cancer cells for clinically actionable targets. *Cancers* 11 (3) 388 https://380:doi:10.3390/cancers11030380.

Kwak E, Sordella R, Bell D, et al (2005). Irreversible inhibitors of the EGF receptor may circumvent acquired resistance to gefitinib, *Proc Natl Acad Sci U.S.A.* May 24; 102(21) 7665-77670.

Kwak EL, Bang YJ, Camidge DR, et al (2010). Anaplastic lymphoma kinase inhibition in non-small-cell lung cancer. *N Engl J Med; 363:1693*-703.

Lalmahomed Z, Kram J, Grataeme J, et al (2010). Circulating tumor cells and sample size the more the better. *J clin Oncol*: 28: e288-9.

Lan D, Hsiung C, Matsuo K, et al (2012). Genome wide associated analysis. Identifies new lung cancer susceptibility loci in never smoking women in Asia. *Nat. Genet.* Dec 44(12):1330-1335.

Lancu G, Serban D, Badiu C, et al (2022). Tyrosine kinase inhibitors in breast cancer (Review). *Exp Ther Med*. Feb 23 (2):114 doi:10.3892/etm2021.11039.

Lasithiotaki I, Antonou K, Redas S et al (2013). The prescence of Merkel Cell Polyomavirus is associated with deregulated expression of BRAF & Bcl_2 gene in non small cell lung cancer. *Inter. J. Cancer.* 133(3); 604-611.

Lecharpentier A, Vielh P, Perez-Moreno P, Pet al., (2011). Detection of circulating tumour cells with a hybrid (epithelial/mesenchymal) phenotypein patients with metastatic non-small cell lung cancer. *Br. J. Cancer* 105, 1338–1341.

Leduc C, Merlio JP, Besse B, et al (2017). Clinical and molecular characteristics of non-small-cell lung cancer (NSCLC) harboring EGFR mutation: Results of the nationwide French Cooperative Thoracic Intergroup (IFCT) program. *Ann. Oncol.*, 28, 2715–2724

Lee W, Jiang Z, Liu J, et al. (2010). The mutation spectrum revealed by paired genome sequences from a lung cancer patient. *Nature 465:* 473–477

Lee JK, Shin J-Y, Kim S, et al (2013). Primary resistance to epidermal growth factor receptor (EGFR) tyrosine kinase inhibitors (TKIs) in patients with non-small-cell lung cancer harboring TKI-sensitive EGFR mutations: an exploratory study. *Ann Oncol; 24:2080*-7

Leone F, Cavalloni G, Pignochino Y et al (2006). Somatic mutations of epidermal growth factor receptor in bile duct and gall bladder carcinoma. *Clin Cancer Res.* Mar 15;12(6):1680-5

Leucke K, Gasiorowski L, Herold S, et al (2015). The GILUPI Cell collector an invivo tool for circulating tumour cells and molecular characterization in lung cancer patients. *Journal of Clinical Oncology* 33, no. 15_suppl
Levy M, Luvly C Pao, W (2012), Translating genomic information into clinical medicine Lung cancer as a paradigm. *Genome Res.* Nov.22 (11)2101-2108.

Li S, Choi U, Gong Z, et al (2016). Comprehensive characterization of oncogene drivers in Asian lung adenocarcinoma. *Journal of thoracic Oncology* vol 11 (12) 2129-2140.

Li Y, Cheng X, Chen Z, et al (2017). Circulating tumor cells in peripheral and pulmonary venous blood predict poor long-term survival in resected non-small cell lung cancer patients. *Sci. Rep.*, 7 p. 4971.

Lieber M, Mazetta J, Nelson-Rass, W. et al. (1975). "Establishment of a continuous tumor-cell line (PANC-1) from a human carcinoma of the exocrine pancreas". *Inter Journal of Cancer*. 15 (5): 741–747. *doi:*10.1002/ijc.2910150505

Lim M, Kim C, Sunkara V, et al (2018). Liquid biopsy in Lung cancer: Clinical applications of circulating biomarkers CTC's and ctDNA. *Micromachine* 9,100doi:10.3390 mi 9030100

Lim M, Park J, Lowe AC, et al (2020). A Lab-on-a-Disc Platform Enables Serial Monitoring of Individual CTCs Associated With Tumor Progression During EGFR-Targeted Therapy for Patients With NSCLC. *Theranostic* 10(12):5181–94. doi: 10.7150/thno.44693.

Lin D, Li C, Li Y et al (2021). Circulating tumour cells biology and clinical significance. *Signal transd, and targeted therapy* 6 404

Lindsay CR, Faugeroux V, Michiaels S, et al (2017). A prospective examination of circulating tumor cell profiles in non-small-cell lung cancer molecular subgroups. *Ann. Oncol.*, 28 (2017), pp. 1523-1531.

Lindelof B, Eklund G (2001). Analysis of hereditary component of cancer by use of a familial index by site. *Lancet.* ; 358:1696–1698. doi: 10.1016/S0140-6736(01)06721-6.

Lindeman NI, Cagle PT, Aisner DL, et al (2018). Updated molecular testing guideline for the selection of lung cancer patients for treatment with targeted tyrosine kinase inhibitors: guideline from the College of American Pathologists, the International Association for the Study of Lung Cancer, and the Association for Molecular Pathology. *Arch Pathol Lab Med.* 142:321–46. doi: 10.5858/arpa.2017-0388-CP.

Linnerth-Petrik N, Walsh S, Bogner P, et al (2014). Jagsiekete Sheep retrovirus detected in human lung tissue arrays. *BMC Res. Notes*; 7; 160.

Liu P, Morrison C, Wang L, et al (2012). Identification of somatic mutations in non-small cell lung carcinomas using whole exome sequencing. Carcinogenesis*; 33:1270*-6.

Liu M, Oxnard G, Klein E. et al (2020). Sensitive and specific muli cancer detection and localization using methylation signatures in cell free DNA

Liu J, Lian J, Chen Y et al (2021). Circulating tumour cells (CTC's): A unique model of cancer metastases and non-invasive biomarker of therapeutic response. Front.gene. httpps///: doi.org/10.3389/fgene.2021.734595

Loeb L, Kohrn B, Loubet-sereer K et al (2019). Extensive sub clonal mutational diversity in human colorectal cancer and its significance. *PNAS* 116(52), 26863-26872.

Lohinai Z, Hoda M, Fabian K (2015). Distinct epidiemology and clinical consequences of classic versus rare EGFR mutations in lung adenocarcinoma. *J of Thoracic Oncol* Vol. 10 Issue5 pg 738-746.

Lomas S, De Vito J, Lachance FB, et al (2016) Determination ofEGFR signaling output by opposing gradients of BMP and JAK/STAT activity, *Curr. Biol.* 26: 2572–2582.
Lv N, Xie X, Ge Q, et al (2011). Epidermal growth factor receptor in breast carcinoma: association between gene copy number and mutations. *Diagn Pathol.;* 6:118.

Lynch TJ, Bell DW, Sordella R., et al (2004). Activating mutations in the epidermal growth factor receptor underlying responsiveness of non–small-cell lung cancer to gefitinib. *N Engl J Med* ; 350 :2129-39.

Maheswaran S, Sequist LV, Nagrath S, et al (2008). Detection of mutations in *EGFR* in circulating lung cancer cells. *N Engl J Med* 359: 1–12.

Makarem M, Leigh N, (2020). Molecular testing for lung adenocarcinoma: is it time to adapt a plasma first approach. *Cancer* Vol. 126 issue 14 pg 3176-3180.

Malapelle U, Muscarella LA, Pisapia P, et al (2020). Targeting emerging molecular alterations in the treatment of non-small cell lung cancer: current challenges and the way forward. *Expert Opin Investig Drugs.* 29:363–72. doi: 10.1080/13543784.2020.1732922.

Maliza A, Egan J, Doran P, (2009). Il-4 increases CD21 dependent infection of pulmonary alveolar epithelium type II cells by EBV. *Mol immunol* May; 46 (8-9): 1905-10.doi:10.1016/j moliimm.2009.01.002 E pub 2009 Feb4.

Maly V, Maly O, Kolostova K, et al (2019). Circulating tumour cells in diagnosis and treatment of lung cancer. *Invivo* Jul-Aug; 33(4):1027-1037.

Marchetti A, Chen TH, Richards WG, et al (2011). Clinical features and outcome of patients with Non–small-cell lung cancer harboring BRAF mutations. *J Clin Oncol* ;29:3574-9.

Marchetti A, Del Grammastro M, Felicioni L, et al (2014). Assessment of EGFR mutations in circulating tumor cell preparations from NSCLC patients by next generation sequencing: Toward a real-time liquid biopsy for treatment. *PLoS One; 9:e103883.*

Martin V, Botta F, Zanellato E, et al (2012). Molecular characterization of EGFR and EGFR-downstream pathways in triple negative breast carcinomas with basal like features. *Histol Histopathol.* ; 27:785–792.

Martin J, Lehmann A, Klauschen F, et al (2019). Clinical impact of rare and compound mutations of epidermal growth factor receptor in patients with non-small-cell lung cancer. *Clin. Lung Cancer*, 20, 350–362.e4.

Masaoutis C, Mihailidou C, Tsourouflis G, et al (2018). Exosomes in lung cancer diagnosis and treatment. From the translating research into future clinical practice. *Biochime 252:27-36.*

Massarelli E, Johnson FM., Erickson HS, et al (2013). Uncommon Epidermal Growth Factor Receptor mutations in non-small cell lung cancer and their mechanisms of EGFR tyrosine kinase inhibitors sensitivity and resistance. *Lung Cancer*, 80, 235–241.

Matakidou A, Eisen T, Houston R et al (2005). Systemic review of the relationship between family history and lung cancer risk. *Br. J Cancer* Oct. 3; 93(7):825-833.

Matellan C, del Rio Hernandez A (2018). Cost effective rapid protyping and assembly of poly (methylmethacrylate) microfluidic devices. *Scientific reports* 8 article number 6971

Matsushima S, Ohtsuka K, Ohinishi H et al (2014). V843I, a lung cancer pre disposing EGFR mutation is responsible for resistance to EGFR tyrosine kinase inhibitors. *J thoracic Oncol* Sep; 9, 1377-84.

Mao L, Zhao W, Li X, et al (2021). Mutation Spectrum of EGFR from 21,324 Chinese Patients with Non-Small Cell Lung Cancer (NSCLC) Successfully Tested by Multiple Methods in a CAP-Accredited Laboratory. *Pathol. Oncol. Res*. 27, 602726.

Mayo-de-las-Casas C, jordana-Ariza N, Garzon-Ibanez M, et al. Large scale, prospective screening of EGFR mutations in the blood of advanced NSCLC patients to guide treatment decisions. *Ann Oncol 2017*; 28:2248-55.

Monot M, Erny A, Gineys B et al (2015). Early steps of Jaagsiekete Sheep retrovirus mediated cell transmission involve the interaction between ENV and the RALBP1 cellular protein *J virol*. 15: 89(16):8462-8473.

Mazières J, Peters S, Lepage B, et al (2013). Lung Cancer That Harbors an HER2 Mutation: Epidemiologic Characteristics and Therapeutic Perspectives. *J Clin Oncol; 31:1997-2003.*

Midha A, Dearden S, McCormack R, et al (2015). EGFR mutation incidence in non-small-cell lung cancer of adenocarcinoma histology: a systematic review and global map by ethnicity (mutMapII). Am J Cancer Res.; 5:2892–911.

Miller M, Robinson P, Wagner C, et al (2018). The Parsotrix cell separation system. A versatile liquid biopsy platform. *Cytometry A* Dec 93(12):1234-1237.

Mitchell PS, Parkin RK, Kroh EM, et al (2008). Circulating microRNAs as stableblood-based markers for cancer detection. *Proc Natl Acad Sci USA;* 105:10513–8.

Mitchell R, Lumor R, Burges A, (2018). Epidermal growth factor receptor: structure-function informing the design of anti cancer therapy. *Experimental cell research 371:1-13.*

Mitsudomi T (2014). Molecular epidemiology of lung cancer and geographic variations with special reference to EGFR mutations. *Transl Lung Cancer Res;* 3: 205e11.

Mitsudomi T, Morita S, Yatabe Y, et al (2010). Gefitinib versus cisplatin plus docetaxel in patients with non small cell lung cancer harbouring mutations of the epidermal growth factor (WJTOG 3405): an open label randomized phase III trial. *Lancet Oncol* Feb; 11(2) 121-8.

Mok TS, Wu YL, Thongprasert S, et al (2009). Gefitinib or carboplatin-paclitaxel in pulmonary adenocarcinoma. *N Engl J Med;* 361**:** 947–57.

Mok TS, To KF, Srimunimimit V, et al (2009b) Clinical outcomes of patients with epidermal growth factor receptor mutation in IPASS. *J Thorac Oncol* 4(Suppl 9): S351, 2009b.

Mok T, Wu YL, Lee JS, et al (2015). Detection and Dynamic Changes of EGFR Mutations from Circulating Tumor DNA as a Predictor of Survival Outcomes in NSCLC Patients Treated with First-line Intercalated Erlotinib and Chemotherapy. *Clin Cancer Res;* 21:3196-203.

Mok TS, Wu YL, Ahn MJ, et al (2017). Osimertinib or Platinum- Pemetrexed in EGFR T790M-Positive Lung Cancer. *N Engl J Med;* 376:629-40.

Monart M, Archer F, Gorres M et al (2015). Advances in the study of transmissible respiratory tumours in small ruminants. *Vet. Microbiol*.18 (1-2):170-177.

Moretti F, Dantona, P, Finardi E, et al (2017). Systemic review and citique of circulating miRNAs as biomarkers of stageI-II non small cell lung cancer. *Oncotargets* vol 8(58) pg 94980-94996.

Mukharjee T, Malik P, Hoidal J, (2021). The emerging role of oestrogen related receptor α in complications of Non small cell lung cancer (Review). *Oncology letters* (4) 1792-1082 https://doi-org//10.3892/01/2021.12519.

Muinelo-Romay L, Vieito M, Abalo A, et al (2014*).* Evaluation of circulating tumor cells and related events as prognostic factors and surrogate biomarkers in advanced

NSCLC patients receiving first-line systemic treatment *Cancers (Basel)*, 6 (2014), pp. 153-16.

Murlidhar V, Zeinali M, Grabauskiene S, et al (2014). A radial flow microfluidic device for ultra-high-throughput affinity-based isolation of circulating tumor cells. *Small;* 10: 4895–904. https://doi.org/10.1002/ smll.201400719.

Myung J, Hong S (2015). Microfluidic technologies to enrich and isolate circulatory tumour cells. *Lab on a chip* 09 Nov. (24):4500-4511

Nagini S (2017). Breast Cancer current molecular therapeutic targets and new players. *Anti cancer agents in medicinal chemistry* vol. 17 No 2 pg 152-163.

Nagrath S, Sequist LV, Maheswaran S, et al (2007). Isolation of rare circulating tumour cells in cancer patients by microchip technology. *Nature;* 450: 1235–9.

Nakamura H, Kawasaki N, Takaguchi M et al (2006). Survival impact of epidermal growth factor receptor over expression in patients with non small cell lung cancer. A meta-analysis. *Thorax Feb*; 61(2):140-145.

Nakajima H, Ishikawa Y, Furuya M, et al (2014). Protein expression, gene amplification, and mutational analysis of EGFR in triple-negative breast cancer. *Breast Cancer.;* 21:66–74.

Nalla L, Kalia K, and Khairnar A (2019). Self-renewal signaling pathways in breast cancer stem cells. *Int. J. Biochem. Cell Biol.* 107,140–153. doi: 10.1016/j.biocel.2018.12.017.

National Institute for Health and Care Excellence.https:// www.nice.org.uk, Accessed 26th April 2022.

Nedelijkovic M, Damjanovic J, (2019). Mechanisim of chemotherapy resistance in triple negative breast cancer how we can rise to the challenge. *Cells*: 8 (9):957 doi:10.3390/cells 8090957.

Ntzifa A, Kotsakis A, Georgoulias V, et al (2021). Detection of EGFR mutations in plasma cfDNA and paired CTC of NSCLC patients before and after Osimertinib therapy using crystal PCR. *Cancers (Basel)*. May 31; 13(11):2736. Doi 10.3390/cancers 13112736.

Ohtsuka K, Ohrishi H, Kurai D et al (2011). Familial lung adenocarcinoma caused by EGFR V843I germline mutation. *J. of clinical oncology*: 29(8): e191-e192.

Okami J, Taniguchi K, Hiyashiyama M et al (2007). Prognostic factors for geftinib treated post operative recurrence in non small cell lung cancer. *Oncology* 72: 234-242

Olaogun J, Omotayo J, Ige J et al (2020). Socio-demographic pattern of presentation and management outcome of breast cancer in a semi urban tertiary health institution. *Pan Afr Med J* Aug 28; 36:363 doi:10.11604/pamj.2020.36.363.17866

Olayioye M.A, Neve R.M, Lane HA, et al (2000**)**, The ErbB signaling network: Receptor heterodimerization in development and cancer. *EMBO J.* 19, 3159–3167.

Oxnard GR, Miller VA, Robson ME, et al (2012). Screening for germline EGFR T790M mutations through lung cancer genotyping. *J Thorac Oncol*; 7:1049-52. DOI: 10.1097/JTO.0b013e318250ed9.

Oxnard GR., Lo PC, Nishino M, et al (2013). Natural History and Molecular Characteristics of Lung Cancers Harboring EGFR Exon 20 Insertions. *J. Thoracic Oncol. , 8*, 179–184.

Oxnard GR, Thress KS, Alden RS, et al (2016). Association Between Plasma Genotyping and Outcomes of Treatment with Osimertinib (AZD9291) in Advanced Non-Small- Cell Lung Cancer. *J Clin Oncol;* 34:3375-82.

Paget (1889). The distribution of secondary growth of cancer of the breast. *Lancet: 133:571-3*

Pailler E, Adam J, Barthélémy A, et al (2013). Detection of circulating tumor cells harboring a unique ALK rearrangement in ALK-positive non-small-cell lung cancer. *J Clin Oncol; 31:2273*-81.

Pamme N (2007). Continous flow separations in microfluidic devices. *Lab chip* 2:1644-1659

Pantel K, Speicher M (2016). The biology of circulating tumor cells. *Oncogene,* 35, 1216–1224.

Pao W, Miller V, Zakowski M, et al (2004). EGF receptor gene mutations are common in lung cancers from "never smokers" and are associated with sensitivity of tumours to gefitinib and erlotinib. *Proc.Natl Acad Sci USA* Sep.7:101(36)13306-11 Doi:10.1073/pnas.0405220101.

Papadimitrakopoulou VA, Han JY, Ahn MJ, et al (2020). Epidermal growth factor receptor mutation analysis in tissue and plasma from the AURA3 trial: osimertinib versus platinum-pemetrexed for T790M mutation-positive advanced non-small cell lung cancer. *Cancer*; 126(2):373–80

Park HS, Jang MH, Kim EJ, et al (2014). High EGFR gene copy number predicts poor outcome in triple-negative breast cancer. *Mod Pathol.*; 27:1212–1222

Park SM, Wong DJ, Ooi CC, et al (2016). Molecular profiling of single circulating tumor cells from lung cancer patients. *Proc. Natl. Acad. Sci. USA*; 113, E8379–E8386
Park K, Tan E, O'Bryne K, et al (2016) Afatinib versus gefitinib as first-line treatment of patients with EGFR mutation-positive non-small-cell lung cancer (LUX-Lung 7): a phase 2B, open-label, randomised controlled trial. *Lancet Oncol.* 17:577-589

Passaro A, Prelaj A, Bonanno L, et al (2018). Activity of EGFR TKIs in Caucasian patients with NSCLC harboring potentially sensitive uncommon EGFR mutations. *Clin. Lung Cancer*, 20, e186–e194.

Passiglia F, Rizzo S, Di Maio M, et al (2018). The diagnostic accuracy of circulating tumor DNA for the detection of EGFR-T790M mutation in NSCLC: a systematic review and meta-analysis. *Sci Rep*.; 8(1):13379.

Petrelli F, Borgonovo K, Cabbidu M et al (2012). Efficacy of EGFR tyrosine kinase inhibitors in patients with EGFR mutated non-small cell lung cancer. A meta-analysis of 13 randomized trials. *Clin. Lung Cancer* vol 13; issue 2 pg 107-114

Patz E, Goodman P, Bepler G, (2000). Screening for lung cancer. *N. ENG.J. Med*.89:2334-44

Paweletz C, Sacher A, Raymond C, et al (2016). Bias-Corrected Targeted Next-Generation Sequencing for Rapid, Multiplexed Detection of Actionable Alterations in Cell-Free DNA from Advanced Lung Cancer Patients. *Clin Cancer Res* 22, 915–922.

Paz-Ares L, Sanchez JM, Garcia-Velasco B, (2006). A prospective phase II trial of erlotinib in advanced non-small cell lung cancer (NSCLC) patients (p) with mutations in the tyrosine kinase (TK) domain of the epidermal growth factor receptor (EGFR) (abstract). *J Clin Oncol* 24 (Suppl): 369s.

Penzel R, Sers C, Chen Y et al (2011). EGFR mutation detection in NSCLC—assesment of diagnostic application and reconmmendations of the German panel for mutation testing in NSCLC. *Virchow Arch* jan; 458(1):95-8.

Pinsky P, Church T, Izmirlian G, Kramer B (2013). The National lung screening trial. Results stratified by demographics, smoking, history and lung cancer histology. *Cancer* 119:3976-3983.

Piotrowska Z, Niederst MJ, Karlovich CA, et al (2015). Heterogeneity Underlies the Emergence of EGFRT790 Wild-Type Clones Following Treatment of T790M-Positive Cancers with a Third-Generation EGFR Inhibitor. *Cancer Discov;* 5:713-22.

Piotrowska Z, Sequist LV (2016). Treatment of EGFR-Mutant Lung Cancers after Progression in Patients Receiving First-Line EGFR Tyrosine Kinase Inhibitors: A Review. *JAMA Oncol*; 2:948-54.

Polyak K, Breast cancer: origins and evolution. *J clin. invest* Nov 1:117(11):3155-3163.

Prim N, Legrain M, Guerin E, et al (2014). Germ-line exon 21 EGFR mutations, V843I and P848L, in nonsmall cell lung cancer patients. *Eur Respir Rev; 23:390-2.*

Punnoose EA, Atwal S, Liu W, et al (2012). Evaluation of circulating tumor cells and circulating tumor DNA in non-small cell lung cancer: association with clinical endpoints in a phase II clinical trial of pertuzumab and erlotinib. *Clin Cancer Res; 18:2391*-401.

Qian H, Zhang Y, Xu J et al (2021). Progress and application of circulating tumour cells in non-small cell lung cancer. *Molecular therapy Oncolytics* vol 22 pg 72-84

Rao C, Chianese D, Doyle G, et al (2005). Expression of epithelial cell adhesion molecule in carcinoma cells present in blood and primary and metastatic tumors. *Int. J. Oncol. 27, 49–57.*

Reck M, Hagiwara K, Han B, et al (2016). ctDNA Determination of EGFR Mutation Status in European and Japanese Patients with Advanced NSCLC: The ASSESS Study. *J Thorac Oncol; 11:1682*-9.

Reckamp KL, Melnikova VO, Karlovich C, et al (2016). A highly sensitive and quantitative test platform for detection of NSCLC EGFR mutations in urine and plasma. *J Thorac Oncol*.; 11:1690–700.

Reis-Filho JS, Pinheiro C, Lambros MB, et al (2006). EGFR amplification and lack of activating mutations in metaplastic breast carcinomas. *J Pathol.;* 209:445–453.

Riess, JW, Gandara DR., Frampton GM, et al (2018). Diverse EGFR Exon 20 Insertions and Co-Occurring Molecular Alterations Identified by Comprehensive Genomic Profiling of NSCLC. *J. Thoracic Oncol.* 13, 1560–1568.

Richard J, Sainsbury C, Needham G et al (1987). Epidermal growth factor receptor status as predictor of early recurrence of and death from breast cancer. *The Lancet* vol 329 iss.8547 pg1398-1402.

Riley G, Pollitti K, Miller V, et al (2006). Update on epidermal growth factor receptor mutation in non small cell lung cancer. *Clinical Cancer Researh*; 12 (24).

Rittmeyer A, Barles F, Waterkemp D et al (2017). Atezolizumab versus docetaxed in patients with previously treated non small cell lung cancer (OAK) a phase 3 open label multi centre randomized controlled trial. *The lancet* vol 389 issue 10066 pg 255-265

Robichaux J, Le X, Vijaya R, et al (2021). Structural based classification predicts drug response in EGFR mutant NSCLC. *Nature*, 597; 732-737.

Romanidou O, Landi L, Capuzzo F et al (2016). Overcomming resistance to first- and second-generation epidermal growth factor receptor tyrosine kinase nhibitors and ALK inhibitors in oncogene addicted advanced non-small cell lung cancer. Ther. Adv. Med Oncol; 8 (3): 176-187

Rosell R, Carcereny E, Gervais R, et al (2012). Erlotinib versus standard chemotherapy as first-line treatment for European patients with advanced EGFR mutation-positive non-small-cell lung cancer (EURTAC): a multicentre, open-label, randomised phase 3 trial. *Lancet Oncol; 13*:239-46.

Rosell R, Karachaliou N. Large-scale screening for somatic mutations in lung cancer. *Lancet; 387:1354*-6.

Roskoski, R (2014). The ErbB/HER family of protein-tyrosine kinases and cancer. *Pharmacol. Res.* Jan: 79; 34-74 doi: 10.1016/j.phrs.2013:11:002 Epub 2013 Nov 20.

Rushton A, Nteliopolus G, Shaw J, et al (2021). A review of circulating tumour cell enrichment technologies. *Cancers* 13,970: https//doi.org/10.3990/cancers/13050970.

Russano M, Napoliteno A, Ribelli G, et al (2020). Liquid biopsy and tumour hetergenity in metastatic solid tumours: The potentiality of blood samples. *Journal of experimental& clinical res*. 39 No 95.

Russo A, Franchina T, Ricciardi G, et al (2019). Heterogenous responses to epidermal growth factor receptor (EGFR). Tyrosine Kinase inhibitors (TKI) in patients with uncommon EGFR mutations. New insights and future perspectives in this complex scenario. *Int J mol Sci* mar 21; 20 (6):143.

Sacher AG, Paweletz C, Dahlberg SE, et al (2016). Prospective Validation of Rapid Plasma Genotyping for the Detection of EGFR and KRAS Mutations in Advanced Lung Cancer. *JAMA Oncol; 2:1014-22*.

Sasaki H, Endo K, Takada M et al (2007). EGFR exon 20 insertion mutation in Japanese lung cancer. *Lung Cancer Vol.58 issue 3 pg 324-328.*

Scheumann N, Gorges T, Penkalla N et al (2015). Enumeration and molecular characterization of circulatory tumour cells in lung cancer patients using the GILUPI Cell Collector. *Annals of Oncol*. Vol 26 supplement 1https//doi.org/10.1093/annonc.

Schlessinger J (2000). Cell signalling by receptor tyrosine kinase *cell*: OCT 13;103(2):211-255.

Schwartz A, Prysak G Bock C Cote M (2006), the molecular epidemiology of lung cancer. *Carcinogenesis 28*(3):507-518.

Schwartzberg LS, Horinouchi H, Chan D, et al (2020). Liquid biopsy mutation panel for non-small cell lung cancer: analytical validation and clinical concordance. *NPJ Precis Oncol*. ; 4(1):15 doi: 10.1038/s41698-020-0118-x. ECollection 2020.

Scagliotti GV, Selvaggi G, Novello S, et al (2004) Hirsch FR. The biology of epidermal growth factor receptor in lung cancer. *Clin Cancer Res.; 10*(12 Pt 2):4227s–4232s.

Scott S, Ali Z (2021). Fabrication methods for microfluidic devices an overview. *Micromachines (Basel)*, Mar, 12 (3); 319

Secq V, Villeret J, Fina F, et al (2014). Triple negative breast carcinoma EGFR amplification is not associated with EGFR, Kras or ALK mutations. *Br J Cancer.* 110:1045–1052.

Selvaggi G, Novello S, Torri V et al (2004). Epidermal growth factor over expression correlates with a poor prognosis in completely resected non small cell lung cancer. *Ann Oncol* Jan. 15(1) 28-32 doi:10.1093/anon/mdholl.

Sequist LV, Joshi VA, Janne PA, et al (2006). Epidermal growth factor receptor mutation testing in the care of lung cancer patients. *Clin Cancer Res*; 12:4403s-8s. 10.1158/1078-0432.CCR-06-0099.

Sequist L, Nagrath S, Toner M et al (2009). The CTC chip an exciting tool to detect circulatory tumour cells in lung cancer patients. *J thorac Oncol.* Mar; 4(3): 281-283

Sequist LV, Heist RS, Shaw AT, et al (2011). Implementing multiplexed genotypingof non-small-cell lung cancers into routine clinical practice. *Ann Oncol*; 22:2616-24.

Shen J, Todd NW, Zhang H, Yu L, Lingxiao X, Mei Y, Guarnera M, Liao J, et al (2011). Plasma microRNAs as potential biomarkers for non-small-cell lung cancer. *Lab Invest. 2011; 91:579–87.* *https://doi.org/10.1038/labinvest.2010.194.*

Shepherd F, Pereira J, Ciuleau T et al (2005). Erlotinib in previously treated non small cell lung cancer BR 21 trials. *N Eng J med*:353:123-132.

Shigematsu H, Lin L, Takahashi T et al (2005a). Clinical and biological features associated with epidermal growth factor receptor gene mutations in Lung cancer. *J Natl Cancer Inst* Mar 2;97(5) 339-46 doi:10.1093/jnli/dji055.

Shigematsu H, Takahashi T, Nomura M, et al (2005b) Somatic mutations of the HER2 kinase domain in lung adenocarcinomas. *Cancer Res* **65**: 1642–1646.

Shih J, Gow C, Yu C, et al (2006). Epidermal growth factor receptor mutations in needle biopsy/aspiration samples predict response to gefitinib therapy and survival of patients with advanced non small cell lung cancer. *Int J cancer* 118, 963-968.

Shivalingaswamy S, Jayarag B, Mahesh P et al (2018). Epidermal growth factor receptor protein expression in lung cancer and survival analysis. *IJAM*. Vol.5 No.3 DOI:http://dx.doi.org/10.18203/2349-3933.ijam20182072.

Siegel RL, Miller KD, Jemal A (2016). Cancer statistics, 2016. *CA Cancer J Clin.;* 66:7–30. https://doi.org/10.3322/ caac.21332.

Siegel R, Miller K, Fuchs H, Jemal A (2021). Cancer Statistics 2021: *A cancer journal for clinicians. January/February 2021 pg 7-33 https:// doi.org//10.3322/caa.21617.*

Sienel W, Seen-Hibler R, Mutschler W, et al (2003). Tumour cells in the tumour draining vein of patients with non-small cell lung cancer: detection rate and clinical significance. *Eur J Cardiothorac Surg; 23:451*-6.

Sigsmund S, Avazato D Lanzetti L (2018), Emerging functions of EGFR in cancer. *Molecular Oncology* 12; 3-20.

Sinagra E, Raimondo D, Gall O et al (2017). JC virus and adenocarcinoma: fact or myth. *Anti cancer Research;* 37(6):3311-3314.

Singh G, Baspg J, Joshi S, et al (2020). Excellent response to erlotinib in breast carcinoma with rare EGFR mutation- a case report. *Ecancermedical science*; 14 10192 doi: 10.332/ecancer20201092.

Singh R (2020). Next generation sequencing in highly sensitive detection of mutations in tumours: challenges, advances and applications. *The journal of molecular dignostics* vol 22 iss 8 pg 994-1007

Siravegna G, Marsoni S, Siena S, et al (2017). Integrating liquid biopsies into the management of cancer. *Nat Rev Clin Oncol* Sep 14(9):531-548.

Smida T, Bruno T, Stabile L, (2020). Influence of estrogen on the NSCLC microenvironment. A comprehensive picture and clinical implications. *Front Oncol* 18 Feb. https://doi.org/10.3389//fonc2020.00137.

Soda M, Takada S, Takeuchi K, et al (2008). A mouse model for EML4-ALKpositiveung cancer. *Proc Natl Acad Sci USA; 105:19893*-7.

Sollier-Christen E, Renier E Kaplan T et al (2018). VTX-1 liquid biopsy system for fully automated and label free isolation of circulating tumour cells with automated enumeration by bioview platform. *Cytometry* Vol 93 issue 12 pg 1240-1245.

Soria J.C, Ohe Y, Vansteenkiste J, et al (2018). Osimertinib in Untreated EGFR-Mutated Advanced Non-Small-Cell Lung Cancer. *N. Engl. J. Med*.; 378:113–125. doi: 10.1056/NEJMoa1713137.

Sousa, AC, Silveira C, Janeiro A., et al (2020). Detection of rare and novel EGFR mutations in NSCLC patients: Implications for treatment-decision. *Lung Cancer, 139*, 35–40.

Sozzi G, Conte D, Leon M, et al (2003). Quantification of free circulating DNA as a diagnostic marker in lung cancer. *J Clin Oncol; 21:3902*-8.

Stott S, Hsu C, Tsukano D, et al (2010) Isolation of circulating tumour cells using a microvortex generating herringbone chip. *Applied bio-Sci.* 107(43) 18392-18397.

Strell B, Entschalden F, (2008). Extravasation of leucocytes in comparison to tumor cells
Cell common signal: 6:10.

Strille B, Yang L, Albarren J, et al (2016). Tumor cell induced endothelial cell receptors via death receptors promote metastasis. *Nature*; 536: 215-8.

Sun S, Schiler J, Gazdar A (2007). Lung cancer in never smokers a different disease. *Nat. Rev. Cancer:* 7;778-90.

Sunaga N, Tomizawa Y, Yanagatani N (2007). Phase II prospective study of the efficacy of gefitinib for the treatment of stage II/IV non small cell lung cancer with EGFR mutation irrespective of previous chemotherapy. *Lung cancer Vol 56*.iss.3 pg 383-389.

Sun Y, Guo W, Xu Y et al (2018). Circulating tumour cells from different vascular sites exhibit spatial hetergenity in epithelial and mesenchymal composition and distinct clinical significance in hepatocellular carcinoma. *Clin Cancer Res* 24(3):549-559.

Sung H, Ferlay J, Siegel R, Levesanne m et al (2021). Global cáncer statistics 2020: GLOBOCAN estimates of incidence and mortality worldwide for 36 cancers in 185 countries. *A cáncer Journal for clinicians* Volume 71 issue 3 pg 209-249.

Sundaresan, T. K., Sequist L, Heymach J, et al (2016). Detection of T790M, the Acquired Resistance EGFR Mutation, by Tumor Biopsy versus Noninvasive Blood Based Analyses. *Clin Cancer Res 22, 1103–1110.*

Suzawa K., Yamamoto H, Ohashi K, et al (2017). Optimal method for quantitative detection of plasma EGFR T790M mutation using droplet digital PCR system. *Oncol Rep*. 37; (5) 3100–3106. https://doi.org/10.3892/0r.2017.5567.

Takahama T, Sakai K., Takeda M., et al (2016). Detection of the T790M mutation of EGFR in plasma of advanced non-small cell lung cancer patients with acquired resistance to tyrosine kinase inhibitors (West Japan oncology group 8014LTR study). *Oncotarget 7, 58492–58499.*

Takano T, Ohe Y, Sakamotto H, *et al*. (2005). Epidermal growth factor receptor gene mutations and increased copy number predict gefitinib sensitivity in patients with recurrent non-small-cell lung cancer. *J Clin Oncol* 23: 6829–6837.

Takeda M, Nakagwa K (2019). First and second-generation EGFR TKI are all replaced to Osimertinib in chemo naïve EGFR mutation positive non small cell lung cancer. *Int J mol Sci* Jan 3; 20 (11):146.

Takeuchi K, Soda M, Togashi Y, et al. (2012). RET, ROS1 and ALK fusions in lung cancer. *Nature Med* 18: 378–381.

Takano N, Ariyasu R, Koyama J, et al. (2019) Improvement in the Survival of Patients with Stage IV Non-Small-Cell Lung Cancer: Experience in a Single Institutional 1995-2017. *Lung Cancer* 131:69–77

Tanaka F, Yoneda K, Kondo N, et al (2009). Circulating tumor cell as a diagnostic marker in primary lung cancer. *Clin Cancer Res; 15:6980*-6.

Tanaka Y, Terai Y, Tanabe A et al (2011). Prognostic effect of epidermal growth factor receptor gene mutation and the aberrant phosphorylation of AKT and ERK in ovarian cancer. *Cancer biology and therapy*; 11(1):50-7.

Taron M, Ichinose y, Rosell R et al (2005). Activating mutations in the tyrosine kinase domains of the epidermal growth factor receptor associated with improved survival in gefitinb treated chemorefractory lung adenocarcinoma. *Clin Cancer res.* Aug 15; 11(16); 58 78-85.

Teng YH, Tan WJ, Thike AA, et al (2011). Mutations in the epidermal growth factor receptor (EGFR) gene in triple negative breast cancer: possible implications for targeted therapy. *Breast Cancer Res.*; 13: R35.

Thatcher N, Chang A, Parikh P, et al (2005). Gefitinib plus best supportive care in previously treated patients with refractory advanced non-small-cell lung cancer: results from a randomised, placebo-controlled, multicentre study (Iressa Survival Evaluation in Lung Cancer). *Lancet;* 366: 1527–37.

Thompson J, Yee S, Toxel A et al (2016). Detection of therapeutically targetable driver and resistance mutations in lung cancer patients by next generation sequencing of cell free circulating tumour DNA. *Clin Cancer Res. Dec 1*:22(23):5772-5782.

Thress, K. S. Brant R., Hedley-Carr T., et al (2015). EGFR mutation detection in ctDNA from NSCLC patient plasma: A cross-platform comparison of leading technologies to support the clinical development of AZD9291. *Lung Cancer 90*, 509–515.

Tilch E, Seidens T, Cocciardi S, et al (2014). Mutations in EGFR, BRAF and RAS are rare in triple-negative and basal-like breast cancers from Caucasian women. *Breast Cancer Res Treat.* ; 143:385–392.

Tokumo M, Toyooka S, Kiura K, et al (2005). The relationship between epidermal growth factor receptor mutations and clinicopathologic features in non–small cell lung cancers. *Clin Cancer Res* 2; 11:1167-73.

Tong B, Xu Y, Zhao J, et al (2017). Prognostic significance of circulating tumor cells in non small cell lung cancer patients undergoing chemotherapy. *Oncotargets vol 8 (NO 49) pg: 86615-86624.*

Torre LA, Bray F, Siegel RL, et al (2015). Global Cancer Statistics, 2012. *CA Cancer J Clin; 65:87*-108.

Toyama T, Yamashita H, Kondo N et al (2008). Frequently increased epidermal growth factor receptor (EGFR) copy numbers and decreased BRCA1 mRNA expression in Japanese triple-negative breast cancers. *BMC Cancer; 8:309*

Tran H, Wu W, Lee N et al (2013). Ethanol and UV instantaneous bonding of PMMA assemblies and tunining bonding reversibility. *Sensors& Actuators B: Chemical* pg955-962.

Travis W, Brambila E, Nicholson A, et al (2015). The 2015 World Health Organisation Classification of Lung Tumors Impact of Genetic Clinical Radiological Advances since 2004 Classification. *J thorac Oncol*. 10:1243-1260.

Tsao MS, Sakurada A, Cutz JC, et al (2005) l. Erlotinib in lung cancer - molecular and clinical predictors of outcome. *N Engl J Med* 353(2):133-144.

Tsuji K, Hayata Y (1989). Riken cell bank. Cellbank.brc@rike.jp RCB4455.PC9

Tzankou E, Markou A, Politak E et al (2019). PIK3CA hot spot mutations in circulating tumour cells and paired tumour DNA in breast cancer: a direct comparison study. *Mol Oncol*.13 (12):2515-2530.

Ullrich A, Cousseus L, Hayflick J, et al (1984). Human epidermal growth factor receptor cDNA sequence and aberrant expression of the amplified gene in A431 epidermoid carcinoma cells. *Nature* 309; 418-425.

Uribe M, Marroco I, Yosef Y (2021). EGFR in cancer signalling mechanisim drugs and acquired resistance. Cancers (Basel); 13(11):2748.

Vander-aurewa I, Elst H, Van Laure S, (2009). The prescence of circulating total DNA and methylated gas is associated with circulatory tumor cells in blood from breast cancer patients. *Br J cancer;*100:1277-86.

VanderLaan PA, Roy-Chowdhuri S (2020). Current and future trends in non-small cell lung cancer biomarker testing: the American experience. *Cancer Cytopathol*. 128:629–36. doi: 10.1002/cncy.22313.

Van Noesel J, van der Ven WH, van Os TA, et al (2013). Activating germline R776H mutation in the epidermal growth factor receptor associated with lung cancer with squamous differentiation. *J Clin Oncol* 2013; 31: e161-4. 10.1200/JCO.2012.42.1586.

Vaishnavi A, Capelletti M, Le AT, et al (2013). Oncogenic and drug-sensitive NTRK1 rearrangements in lung cancer. *Nat Med; 19:1469*-72.

Vasan N, Baselga J., Hyman D.M. (2019) A View on Drug Resistance in Cancer. *Nature.*; 575:299–309. doi: 10.1038/s41586-019-1730-1.

Veale, D., Ashcroft, T., Marsh, C. et al (1987) Epidermal growth factor receptors in non-small cell lung cancer. *Br. J. Cancer*, 55, 513–516.
Vu H, Xinh P, Ngoc Ha H et al (2016). Spectrum of EGFR gene mutations in Vietnamese patients with non small cell lung cancer. *Asia Pac J clin oncol*. Mar 12 (1) 86-90.

Wang L, Hu H, Pan Y, et al (2014). PIK3CA mutations frequently coexist with EGFR/KRAS mutations in non-small cell lung cancer and suggest poor prognosis in EGFR/KRAS wildtype subgroup. *PLoS One; 9: e88291*.

Wang S & Wang Z (2014). EGFR mutations in patients with non-small cell lung cancer from mainland China and their relationship with clinic-pathologicall features: A meta-analysis. *Int J Clin Exp Med*; 7 (8): 1967-1968

Wang L, Wu C, Qiao L, et al (2017). Clinical significance of folate receptor-positive circulating tumor cells detected by ligand-targeted polymerase chain reaction in lung cancer. *J Cancer. ; 8: 104–110. https://doi.org/10.7150/jca.16856*.

Wang Q, Zhao L, Han L et al (2019). The discordance of gene mutations between circulating tumour cells and primary/metastatic tumours. Molecular therapy Oncoly. Vol 15 pg 21-29

Warkhani M.E, Khoo B.L, Wu L, et al (2016). Ultra-fast, label-free isolation of circulating tumor cells from blood using spiral microfluidics. *Nat. Protocols 11*, 134–148.

Wee P, Wang Z, (2017). Epidermal growth factor receptor cell proliferation signalling pathways. *Cancers (Basel).* May17; 9(5) 52.doi:10.3390/cancers9050052.

Weber F, Fukino K, Sawada T, et al (2005). Variability in organ specific EGFR mutational spectra in tumour epithelium and stroma may be the biological basis for different responses to tyrosine kinase inhibition. *Br J of cancer* 92:1922-1926.

Weinberg F, Peckys D, Jonge N, (2020). EGFR expression in HER 2 driver breast cancer cells. *Int J mol sci* 21(23) 9008.

Welter L, Xu L, Mckinley D et al (2020). Treatment response and tumour evolution: Lessons from an extended series of multi analyte breast cancer patient. *Cold spring harb mol case study* 6; a005819

White M, Khallil K (2005). Expression of JC virus regulatory protein in human cancer potential mechanisim for tumorigenesis. *Eur j Cancer*; 41(16):2537-2548.

Wonk K Spruck C (2020). Triple negative breast cancer therapy. Current and future perspective (Review*). Int.J Oncol*. Dec: 57(6);1245-1261.

World Health Organization [webpage on the Internet]. *Cancer. Fact Sheet*. 2021. Available from: http://www.who.int/mediacentre/factsheets/fs297/en/. March, 2022.

Wu C-T, Chang Y-T, Shin J-Y, et al. (2005). The significance of estrogen receptors β in 301 surgically treated non small cell lung cancer. *Journal of thoracic and cardiovascular surg.* Vol 130 iss.4 pg979-986.

Wu M-F, Cheng Y-W, Lai J-C, et al (2005). Frequent p16INK4a promoter hypermethylation in human papillomavirus-infected female lung cancer in Taiwan. *Int j Cancer*. 2005; 113(3):440–445. doi: 10.1002/ijc.20597.

Wu JY, Wu SG, Yang CH, et al (2008). Lung cancer with epidermal growth factor receptor exon 20 mutations is associated with poor gefitinib treatmentresponse. *Clin Cancer Res; 14:4877*-82.

Wu DW, Liu WS, Wang J, et al (2011). Reduced p21 (WAF1/CIP1) via alteration of p53-DDX3 pathway is associated with poor relapse-free survival in early-stage human papillomavirus-associated lung cancer. *Clin Cancer Res; 17(7):1895–1905.*

Wu YL, Sequist LV, Hu CP, et al (2017). EGFR mutation detection in circulating cell-free DNA of lung adenocarcinoma patients: analysis of LUX-Lung 3 and 6. *Br J Cancer; 116:175*-85.

Wu YL, Zhou C, Liam CK, et al (2015). First-line erlotinib versus gemcitabine/cisplatin in patients with advanced EGFR mutation-positive non-small-cell lung cancer: analyses from the phase III, randomized, open-label, ENSURE study. *Ann Oncol; 26:1883*-9.

Wu YL, Jenkins S, Ramalingam S, et al (2017). MA08.03 Osimertinib vs Platinum-Pemetrexed for T790M-Mutation Positive Advanced NSCLC (AURA3): Plasma ctDNA Analysis. *J Thorac Oncol; 12: S386*.

Wu SG, Yu CJ, Yang JC, et al (2020). The effectiveness of afatinib in patients with lung adenocarcinoma harboring complex epidermal growth factor receptor mutation. *Adv. Med. Oncol.*, 12, 175883592094615.

Wu S, Liu Y, Tsai M et al (2016). The mechnaisim of acquired resistance to irreversible EGFR tyrosine kinase inhibitor afatinib in Lung adenocarcinoma patients. *Oncotargets Mar* 15 ;(11):12404-13.

Wu Y, Cheng Y, Zhou X et al (2017). Dacomitinib versus gefitinib as first line treatment for patients with EGFR mutation positive non small cell lung cancer (ARCHER 1050). A randomized open label phase 3 trial. *Lancet Oncol* Nov: 18(11):1454-1466.

Xu F., Jabasini M., Baba Y., (2002) *Electrophoresis*, 23, 3608–3614

Xu J, Jin B, Chu T et al (2016). EGFR tyrosine kinase inhibitor (TKI) in patients with advanced non small cell lung cancer (NSCLC) harbouring uncommon EGFR mutations: A real world study. *Lung cancer* Jun; 96:87-92.

Xu JM, Han Y, Duan HQ, et al (2009). EGFR mutations and HER2/3 protein expression and clinical outcome in Chinese advanced non-small cell lung cancer patients treated with gefitinib. *Journal of cancer research and clinical oncology*; 135(6):771-82.

Xu H, Zong H, Ma C et al (2017). Epidermal growth factor receptor in glioblastoma. *Oncol Lett* Jul; 14(1):512-516.

Yagi S, Koh Y, Akamatsu H, et al. (2017) Development of an automated size-based filtration system for isolation of circulating tumor cells in lung cancer patients. *PLoS ONE* 12(6): e0179744. https://doi.org/10.1371/journal.pone.0179744.

Yang J, Shih J, Su w, et al (2012). Afatinib for patients with lung adenocarcinoma and epidermal growth factor receptor mutations (Lux-Lung 2): a phase 2 trial. *Lancet Oncol.* May 13(5): 539-48.

Yang JC, Wu YL, Schuler M, et al (2015). Afatinib versus cisplatin-based chemotherapy for EGFR mutation-positive lung adenocarcinoma (LUX-Lung 3 and LUX-Lung 6): analysis of overall survival data from two randomised, phase 3 trials. *Lancet Oncol;* 16**:** 141–51.

Yang J, Ahn M, Kim D et al (2017). Osimertinib in pre treated T790M positive advanced non small cell lung cancer: AURA study phase II extension component. *Journal of Clinical Oncol 35* no 12 1288-1296

Yang B, Qin A, Zhang K., et al (2017). Circulating tumor cells predict prognosis following tyrosine kinase inhibitor treatment in EGFR-mutant non-small-cell lung cancer patients *Oncol. Res.*, 25 (9), pp. 1601-1606

Yang Y, Giret T, Cole R (2021). Circulating tumour cells from enumeration to analysis: current challenges and future opportunities. *Cancers*, 13:2723 https//doi.org/10.3390/cancers/3112723

Yang F, Zhang W, Shang A et al (2022). Comparison of the efficacy and safety of first line treatments based on clinicopathological characteristics for patients with advanced epidermal growth factor receptor mutated non small cell lung cancer. A systemic review a network meta-analysis. *Critical review in oncology/haematology* vol 177 103760

Yasuda H, Park E, Yun, CH. et al (2013). Structural, Biochemical, and Clinical Characterization of Epidermal Growth Factor Receptor (EGFR) Exon 20 Insertion Mutations in Lung Cancer. *Sci. Transl. Med.* 5, 216ra177.

Yeh Y, Kao H, Lee K, et al (2019). Episten-Barr virus associated pulmonary carcinoma. *Am J. Surg. Pathol*.; 43(2); 211-219. Doi.10.1097/pas.000000001173.

Yeo, T., Tan, S.J., Lim, C.L., et al (2016). Microfluidic enrichment for the single cell analysis of circulating tumor cells. *Sci. Rep.*, 6, article number 22076.

Yip PY, Yu B, Cooper WA, et al (2013). Patterns of DNA mutations and ALKrearrangement in resected node negative lung adenocarcinoma. *J ThoracOncol; 8:408*-14.

Yoshida, H., Kim, Y., Ozasa, H et al (2017). EGFR T790M detection in circulating tumor DNA from non-small cell lung cancer patients using the PNALNA Clamp Method. *Anticancer Res* 37, 2721–2725.

Yu Y, Xu G, Cao J et al (2013). Combination of four gene markers to detect circulating tumour cells in the peripheral blood of patients with advanced lung adenocarcinoma using real time PCR. *Oncology letters* http://doi.org/10.3892/0l2013 pg 1400-1408

Yu Na, Zhou J, Fang C, et al (2015). Circulating tumor cells in lung cancer: Detection methods and clinical applications. *Lung* (193):157-171.

Yu S, Li A, Lin Q et al (2017). Chimeric antigen receptor T cells a novel therapy for solid tumour. *Journal of haematology and oncology* 10 No. 78.

Zhang E, Feng X, Liu F, et al (2014) Roles of PI3K/Akt and c-Jun signaling pathways in human papillomavirus type 16 oncoprotein-induced HIF-1alpha, VEGF, and IL-8 expression and in vitro angiogenesis in non-small cell lung cancer cells. *PLoS One*. ; 9(7):e103440.

Zhang YL, Yuan JQ, Wang KF, et al (2016). The prevalence of EGFR mutation in patients with non-small cell lung cancer: a systematic review and meta-analysis. Oncotarget. 7:78985–93.

Zhang Y, Wang Z, Hao X, et al (2017) Clinical characteristics and response to tyrosine kinase inhibitors of patients with non-small cell lung cancer harboring uncommon epidermal growth factor receptor mutations. *Chin. J. Cancer Res*, 29, 18–24.

Zhang, B., Wang, S., Qian, J., et al (2018). Complex epidermal growth factor receptor mutations and their responses to tyrosine kinase inhibitors in previously untreated advanced lung adenocarcinomas. *Cancer,* 124:2399–2406.

Zhang Q, Nong J, Wang J et al (2019). Isolation of circulatory tumour cells and detection of epidermal growth facror receptor gene mutations in patients with non small cell lung cancer. *Oncol lett* April 17(4):3799-3807.

Zheng M (2016): Classification and pathology of lung cancer. *Surg Oncol Clin N AM.* Pg Jul; 25(3):447-468.

Zheng D, Ye X, Zhang MZ, et al (2016). Plasma EGFR T790M ctDNA status is associated with clinical outcome in advanced NSCLC patients with acquired EGFR-TKI resistance. *Sci Rep.* Feb.12. 6(1): 20913.doi.10.1038/srep 20913.

Zheng Q, Zhang M, Zhou F et al (2021). The breast cancer stem cells traits and drug resistance. *Front Pharmacol*.https://doi.org/10.3389/fphar.2020599965.

Zhou W, Ercan D, Chen L, (2009) et al. Novel mutant-selective EGFR kinase inhibitors against EGFR T790M. *Nature; 462:1070*-4.

Zhou C, Wu Y, Chen G, et al (2011). Erlotinib versus chemotherapy as first line treatment for patients with advanced EGFR mutation positive non smallcell lung cancer (Optimal; CTONG-0802): a multi centre open label randomized phase 3 study. *Lancet Oncol.* Aug: 12 (8):735-42

Zhou C, Wu Y Chen G et al (2015). Final overall survival results from a randomised, phase III study of erlotinib versus chemotherapy as first-line treatment of EGFR mutation-positive advanced non-small-cell lung cancer (OPTIMAL, CTONG-0802). *AnnOncol; 26:1877–* 83.doi:10.1093/annonc/mdv276.

Zhou J, Dong, F. Cui F, et al (2017) the role of circulating tumor cells in evaluation of prognosis and treatment response in advanced non-small-cell lung cancer *Cancer Chemother. Pharmacol*, 79 (2017), pp. 825-833.

Zhou C, Ramalingam S, Kim T et al. (2021), Treatment outcomes and safety of mobocertinib in platinum-pretreated patients with EGFR exon 20 insertion–positive metastatic non–small celllung cancer: A phase 1/2 open-label nonrandomized clinical trial, JAMA Oncol. 7
(12), e21476

Zou D, Cui D (2018). Advances in isolation and detection of circulatory tumour cells based on microfluidics. *Cancer Bio Med*, Nov; 15(4):335-353

Appendix

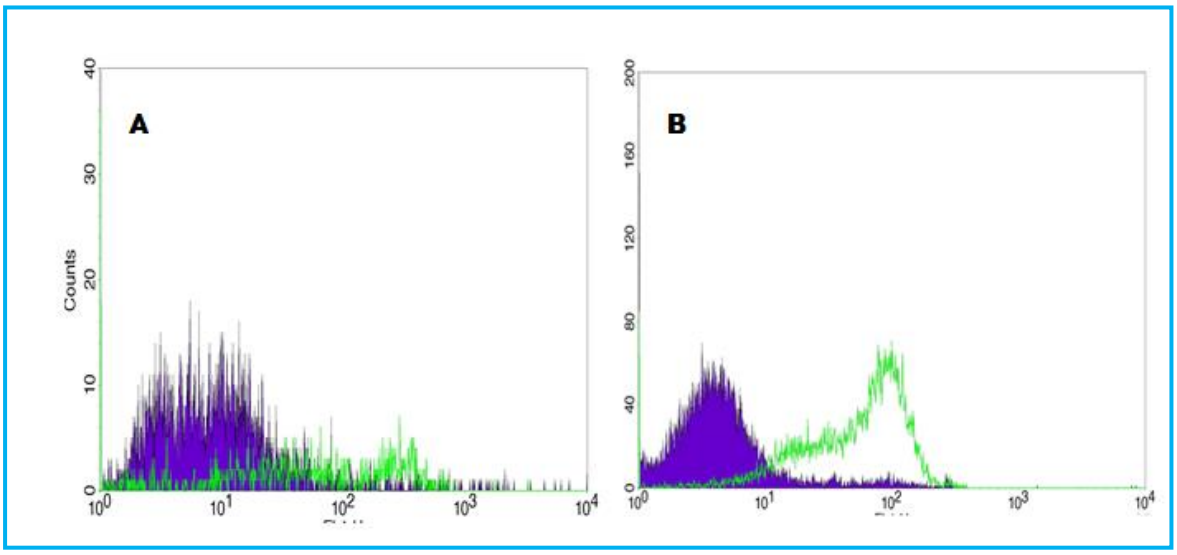

Appendix 1A and B is representative of data obtained from 2 experiments evaluating EpCAM expression in PC9 cell lines shown in **Figure 3.5**

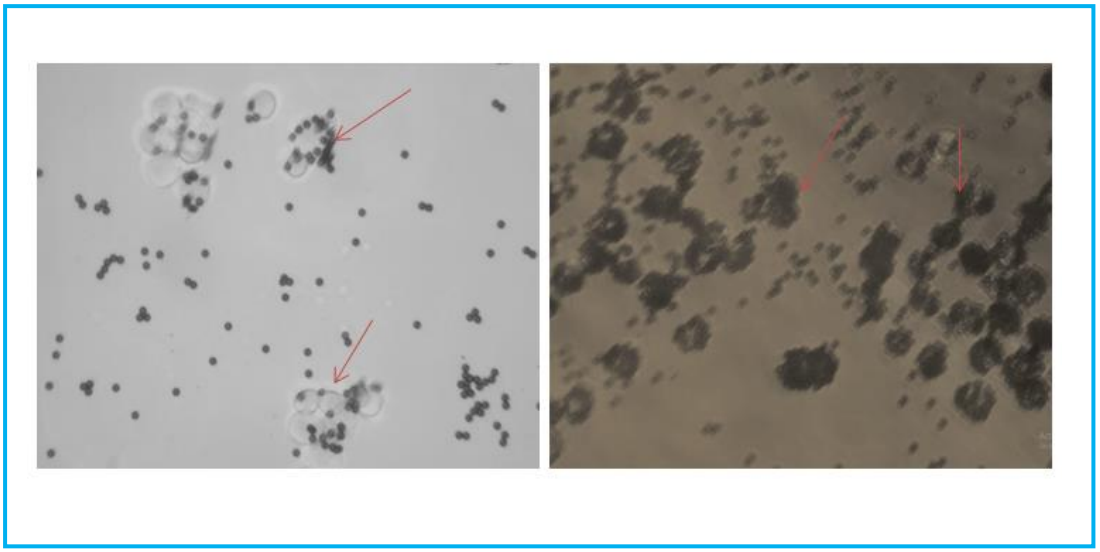

Appendix 2 represents data from two experiments in proof-of-concept experiments showing Lung Card Microfluidic device can isolate EpCAM positive PC9 cell lines shown in **Figure 3.6**. (Red arrows depicts capture of cells by beads)

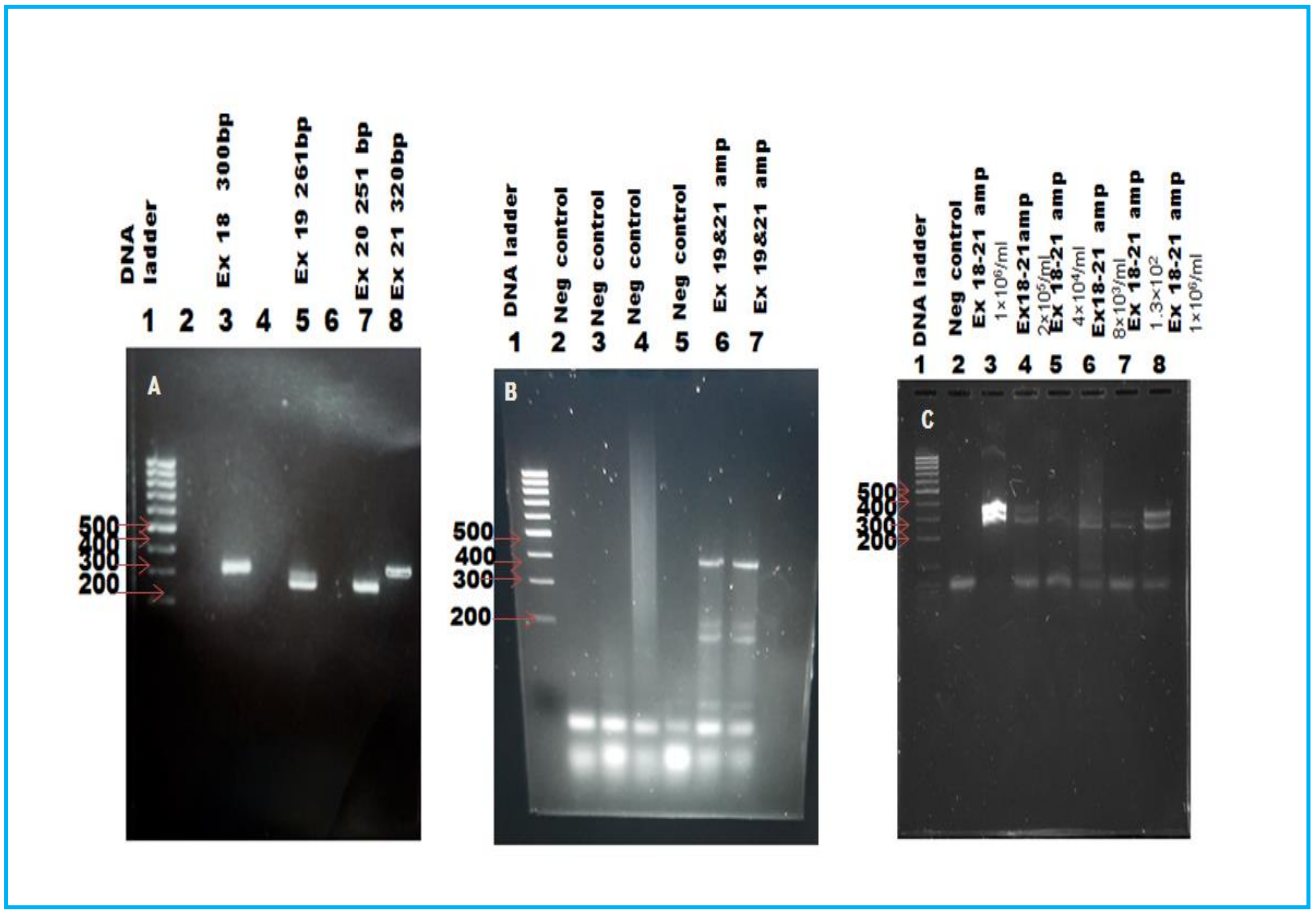

Appendix 3- represents data (**Figure 3.6**) from gel electrophoresis experiments showing that EpCAM positive cells isolated using the Lung card microfluidic device can be used for downstream analysis to determine EGFR mutations. **A**-represents amplification of exon 18-21 regions SV primers, **B**-represents detection of exon 21 L858R mutation, exon 19 deletion and exon 19 WT using UOH primers **C**-represents amplification of exon 18 -21 regions of the EGFR gene from PC9 cell lines from a range of concentrations.

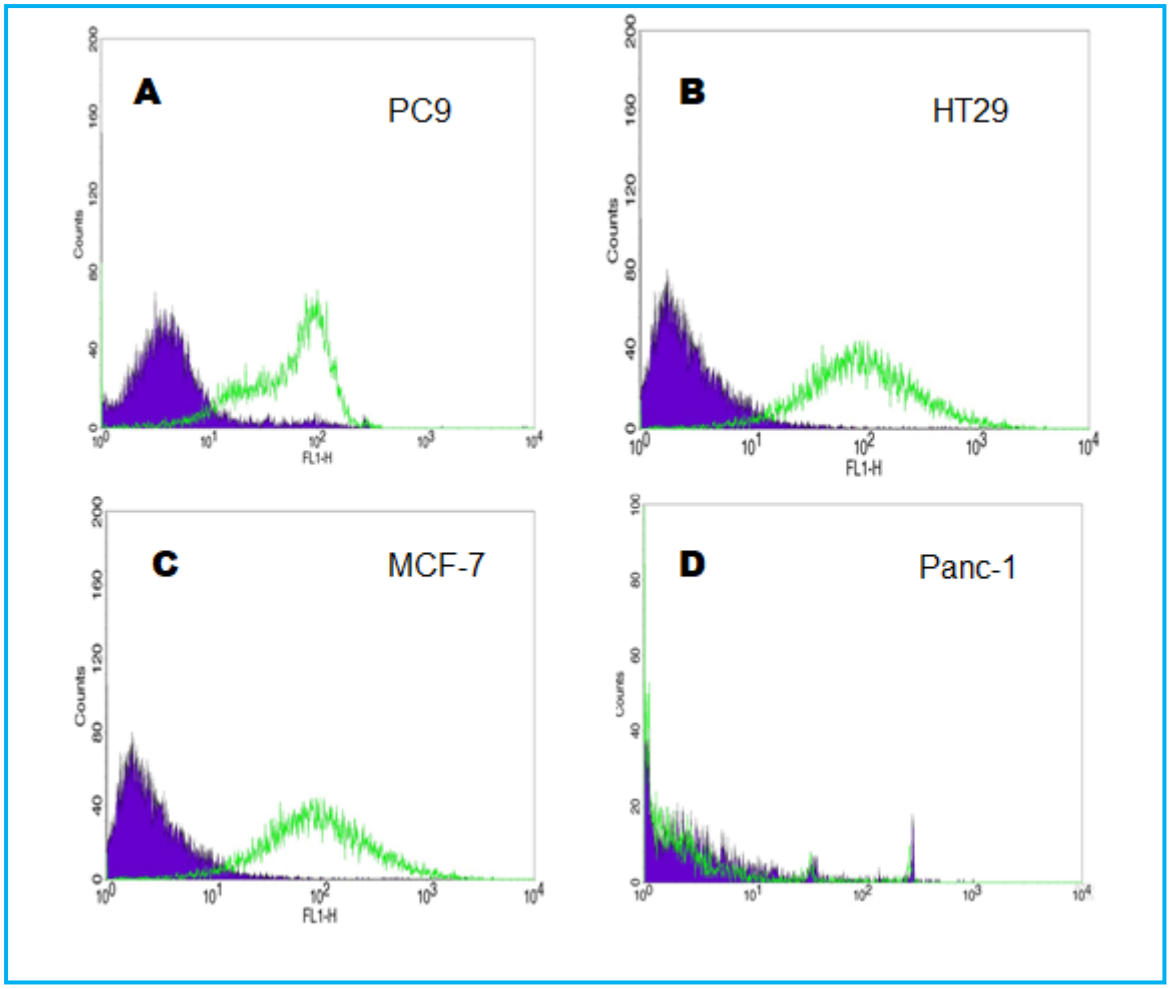

Appendix 4 represents data from one of two experiment shown in **Figure 4.1** that evaluated expression of EpCAM in the following cell lines PC9, HT29, MCF-7 and PANC-1 using flowcytometry

Appendix 5 Capture Efficiency of device for PC9 cell lines (**Spiking experiments in media**)

Cell Concentration spiked	Exp1 cells isolated	Exp2 cells isolated	Exp3 cells isolated	Exp1 efficiency	Exp2 Efficiency	Exp3 efficiency (%)
1×10^6	8.9×10^5	9.2×10^5	8.9×10^5	89	92	88
2×10^5	1.62×10^5	1.78×10^5	1.71×10^5	81	89	85.5
4×10^4	3.3×10^4	3.2×10^4	3.2×10^4	82.5	81.25	85
8×10^3	6.6×10^3	6.4×10^3	6.8×10^3	82.5	80	85

Appendix 6 Capture Efficiency of device for HT-29 cell lines (**Spiking experiments in media**)

Cell Concentration spiked	Exp1 cells isolated	Exp2 cells isolated	Exp3 cells isolated	Exp1 efficiency	Exp2efficiency	Exp3 efficiency (%)
1×10^6	8.8×10^5	8.6×10^5	8.4×10^5	88	86	84
2×10^5	1.62×10^5	1.7×10^5	1.65×10^5	81	85	82.5
4×10^4	3.25×10^4	3.2×10^4	3.2×10^4	81	80	80
8×10^3	6.45×10^3	6.35×10^3	6.5×10^3	80	81	80

Appendix 7 Capture Efficiency of device for MCF-7 cell lines (**Spiking experiments in media**)

Cell Concentration spiked	Exp1 cells isolated	Exp2 cells isolated	Exp3 cells isolated	Exp1 efficiency	Exp2efficiency	Exp3 efficiency (%)
1×10^6	9.2×10^5	9.34×10^5	9.3×10^5	91.5	90.8	92.6
2×10^5	1.7×10^5	1.72×10^5	1.65×10^5	85	88	82.5
4×10^4	3.4×10^4	3.2×10^4	3.2×10^4	84	80	80
8×10^3	6.5×10^3	6.6×10^3	6.5×10^3	81	82	81

Appendix 8 Capture Efficiency of device for PANC-1 cell lines (**Spiking experiments in media**)

Cell Concentration spiked	Exp1 cells isolated	Exp2 cells isolated	Exp3 cells isolated	Exp1 efficiency	Exp2 efficiency	Exp3 efficiency (%)
1×10^6	4.5×10^5	5.0×10^5	4.0×10^5	45	50	40
2×10^5	9×10^4	8.5×10^4	6.5×10^4	45	44	32
4×10^4	1.5×10^4	1.2×10^4	1.6×10^4	38	30	40

Appendix 9 Capture Efficiency of device for PC9 cell lines (**Spiking experiments in blood**)

Cell Concentration spiked	Exp1 cells isolated	Exp2 cells isolated	Exp3 cells isolated	Exp1 efficiency (%)	Exp2 efficiency (%)	Exp3 efficiency (%)
1×10^6	7.34×10^5	7.8×10^5	8.2×10^5	80	78	82
2×10^5	1.48×10^5	1.51×10^5	1.55×10^5	74	75.5	77.5
4×10^4	2.8×10^4	3.0×10^4	2.75×10^4	70	75	69
8×10^3	5.1×10^3	5.3×10^3	5.1×10^3	64	67	64

Appendix 10 Capture Efficiency of device for HT-29 cell lines (**Spiking experiments in blood**)

Cell Concentration spiked	Exp1 cells isolated	Exp2 cells isolated	Exp3 cells isolated	Exp1 efficiency	Exp2efficiency	Exp3 efficiency (%)
1×10^6	7.5×10^5	8.0×10^5	7.8×10^5	75	80	77
2×10^5	1.35×10^5	1.48×10^5	1.54×10^5	67	74	77
4×10^4	2.8×10^4	3.0×10^4	2.8×10^4	70	75	70
8×10^3	5.0×10^3	4.8×10^3	4.8×10^3	67	64	64

Appendix 11 Capture Efficiency of device for MCF-7 cell lines (**Spiking experiments in blood**)

Cell Concentration spiked	Exp1 cells isolated	Exp2 cells isolated	Exp3 cells isolated	Exp1 efficiency	Exp2efficiency	Exp3 efficiency (%)
1×10^6	7.45×10^5	8.0×10^5	8.4×10^5	75.5	80	84
2×10^5	1.5×10^5	1.45×10^5	1.7×10^5	75	72	85
4×10^4	3.2×10^4	3.0×10^4	2.8×10^4	80	75	70
8×10^3	5.0×10^3	6×10^3	5.5×10^3	67	75	69

Appendix 12 Capture Efficiency of device for PANC-1 cell lines (**Spiking experiments in blood**)

Cell Concentration spiked	Exp1 cells isolated	Exp2 cells isolated	Exp3 cells isolated	Exp1 efficieny	Exp2 efficiency	Exp3 efficiency (%)
1×10^6	4.0×10^5	4.3×10^5	3.8×10^5	40	43	38
2×10^5	7.5×10^4	7.0×10^4	8.2×10^4	38	35	41
4×10^4	1.5×10^4	1.4×10^4	1.25×10^4	38	35	32

Appendix 13 Purity of PC9 cell lines spiked in media with PBMC

Cell concentration/ ml	CTC: PBMC Exp1	Purity (%) Exp1	CTC: PBMC Exp2	Purity (%) Exp2	CTC: PBMC Exp3	Purity (%) Exp3
1×10^6	2,010:75	97	1,836:26	98.6	2,150:20	99
2×10^5	1,100:30	97.3	800:10	98.7	1,300:40	97
4×10^4	505:30	96.2	473:10	97.9	301:5	98.3
8×10^3	55:2	96.5	60:1	98.3	65:2	97.1
1.3×10^2	5:0	100	8:1	88.5	3:0	100

Appendix 14 Purity of HT-29 cell lines spiked in media with PBMC

Cell concentration	CTC: PBMC Exp1	Purity (%) Exp1	CTC: PBMC Exp2	Purity (%) Exp2	CTC: PBMC Exp3	Purity (%) Exp3
1×10^6	1,910:62	96.8	1,715:16	99	2,205:23	98.9
2×10^5	950:15	98.4	885:12	98.6	1,010:14	98.6
4×10^4	500:13	97.4	450:5	98.9	289:2	99.3
8×10^3	65:3	98.5	50:1	98.	67:2	97
1.3×10^2	5:0	100	9:1	89.5	3:0	100

Appendix 15 Purity of MCF-7 cell lines spiked in media with PBMC

Cell concentration	CTC: PBMC Exp1	Purity (%) Exp1	CTC: PBMC Exp2	Purity (%) Exp2	CTC: PBMC Exp3	Purity (%) Exp3
1×10^6	2,500:81	96.8	2,710:30	97	2,111:40	98.1
2×10^5	1,350:47	96.6	983:19	98.9	1,107:20	98.2
4×10^4	559:18	96.8	482:8	98.3	433:2	99.5
8×10^3	72:2	98.5	57:0	100	68:2	97
1.3×10^2	5:0	100	10:1	90	4:0	100

Appendix 16 Purity of PANC-1 cell lines spiked in media with PBMC

Cell concentration	CTC: PBMC Exp1	Purity (%) Exp1	CTC: PBMC Exp2	Purity (%) Exp2	CTC: PBMC Exp3	Purity (%) Exp3
1×10^6	300:10	96.7	215:5	97.7	175:2	98.8
2×10^5	81:3	96.4	42:1	97.7	38:0	100
4×10^4	10:1	90	7:0	100	5:0	100

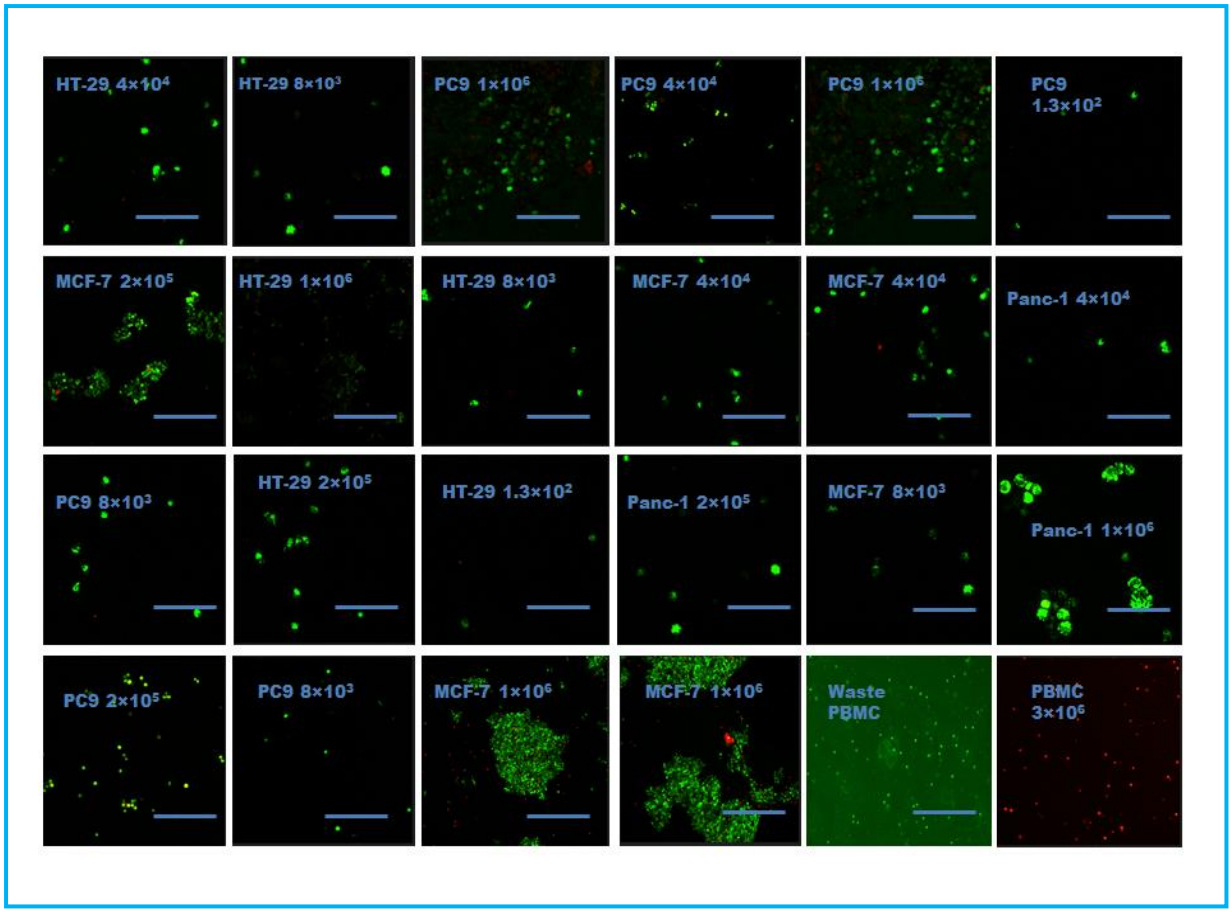

Appendix 17 represents data from purity experiments shown in **Figure 4.7**

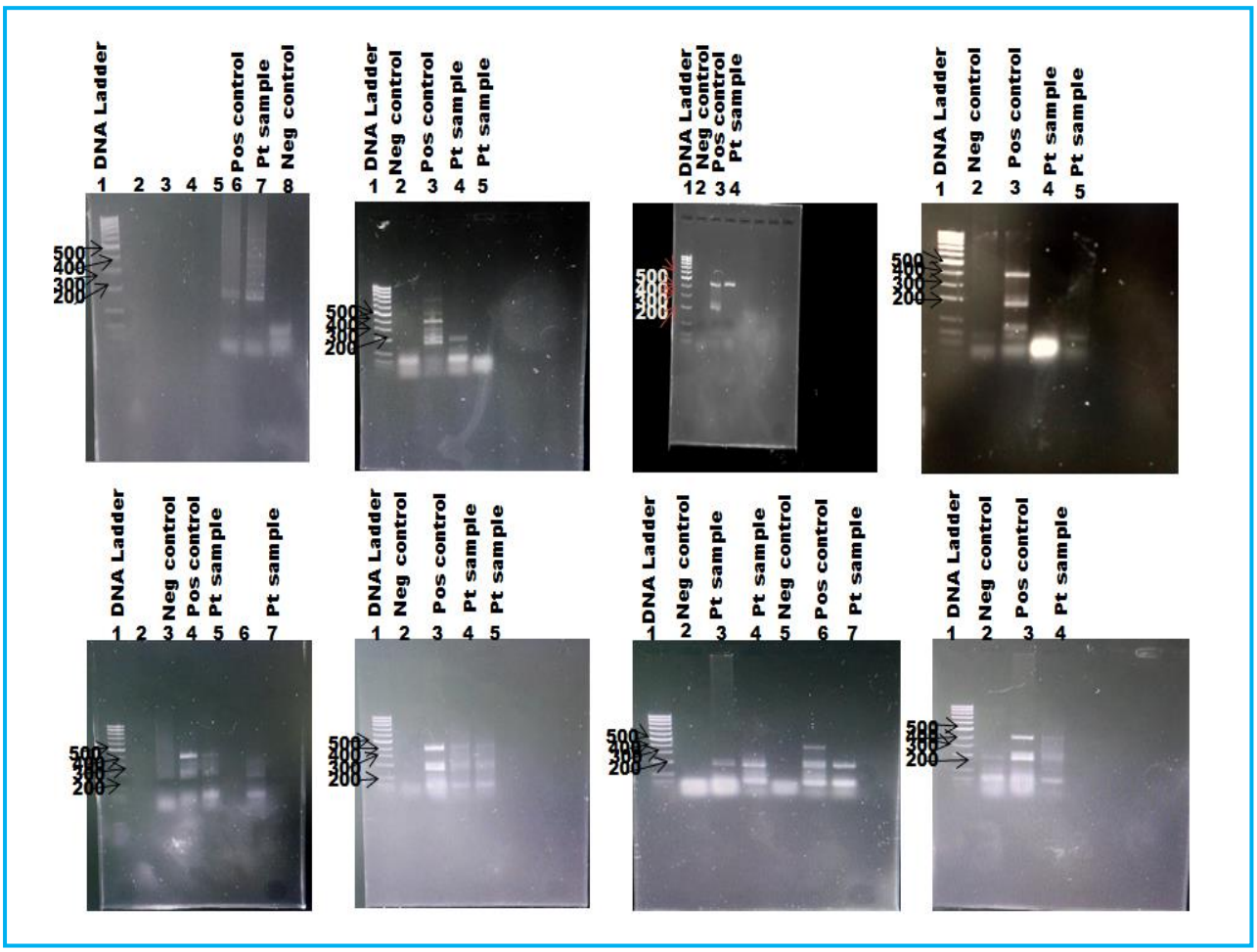

Appendix 18 Representative data of end point PCR to detect exon 19 deletion , and L858R mutation using UOH primers on CTC enriched samples obtained from patients with NSCLC to test for exon 19 deletion-172bp, L858R mutation- 388bp

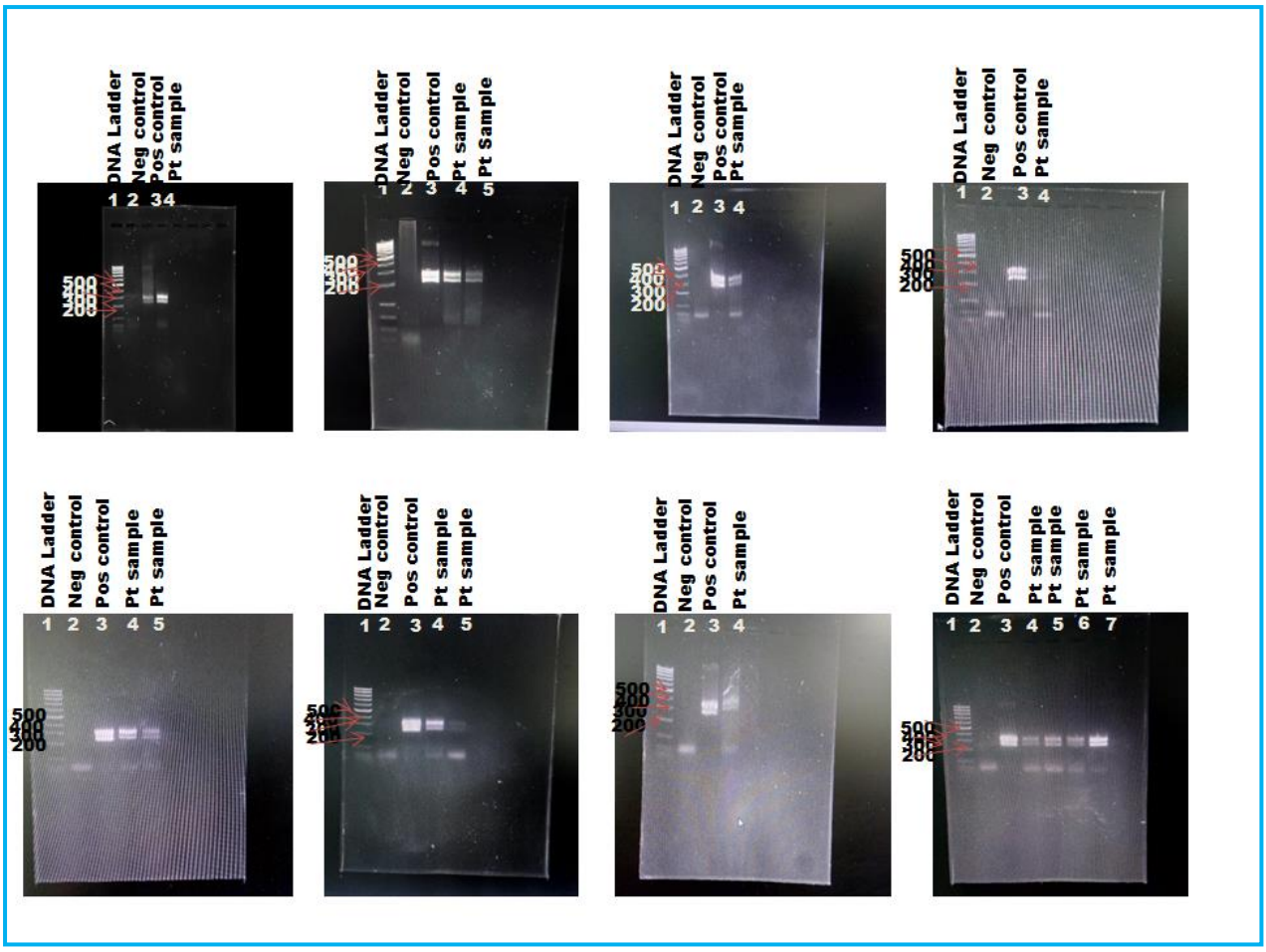

Appendix 19 Representative data of end point PCR for amplification of exon 18-21 segment of EGFR gene on CTC enriched samples obtained from patients with NSCLC using SV primers